

Some pages of this thesis may have been removed for copyright restrictions.

If you have discovered material in AURA which is unlawful e.g. breaches copyright, (either yours or that of a third party) or any other law, including but not limited to those relating to patent, trademark, confidentiality, data protection, obscenity, defamation, libel, then please read our [Takedown Policy](#) and [contact the service](#) immediately

Novel Imprinted Polymers as Artificial Enzymes

Stephen Whetton
Doctor of Philosophy

The University of Aston in Birmingham

July 2001

This copy of the thesis has been supplied on condition that anyone who consults it is understood to recognise that its copyright rests with its author and that no quotation from the thesis and no information derived from it may be published without proper acknowledgement.

The University of Aston in Birmingham

Novel Imprinted Polymers as Artificial Enzymes

Stephen Whetton

Submitted for the Degree of Doctor of Philosophy

July 2001

Summary

Derivatives of L-histidine were investigated as suitable models for the Asp-His couple found in the catalytic triad of serine proteases. A combination of molecular dynamics and ^1H NMR spectroscopy suggested that the most populous conformations of N-acetyl-L-histidine and the N-acetyl-L-histidine anion were predominated by those in which the carboxylate group was gauche to the imidazole ring overcoming steric and electrostatic repulsion, suggesting there is an interaction between the carboxylate group and the imidazole ring.

Kinetic studies, using imidazole, N-acetyl-L-histidine and the N-acetyl-L-histidine anion showed that in a DMSO/H₂O 9:1 v/v solution, the N-acetyl-L-histidine anion catalysed the hydrolysis of *p*-nitrophenyl acetate at a greater rate than using either imidazole or N-acetyl-L-histidine as catalyst. This indicates that the carboxylate group affects the nucleophilicity of the unprotonated imidazole ring.

^{31}P MAS NMR spectroscopy was investigated as a new technique for the study of the template molecule environment within the polymer networks. It was found that it was possible to distinguish between template associated with the polymer and that which was precipitated onto the surface, though it was not possible to distinguish between polymer within imprinted cavities and that which was not.

Attempts to study the effect of the carboxylate group/imidazole ring interaction in the imprinted cavity of a molecularly imprinted polymer network were hindered by the method used to follow the reaction. It was found though that in a pH 8.0 buffered solution the presence of imprinted cavities increased the rate of reaction for those polymers derived from L-histidine.

Some preliminary investigations into the design and synthesis of an MIP which would catalyse the oxy-Cope rearrangement were carried out but the results were inconclusive.

Keywords: Serine protease, Histidine, Phosphonate ester template, Hydrolysis, Oxy-Cope

Acknowledgements

Firstly, I would like to thank my supervisor Chris StPourçain for all the help and guidance he has given me over the period of my studies.

Next, I would like to thank Dr. Mike Perry for all the hard work he has put in on my NMR samples and all the mental torture he has made me endure with his jokes. I would also like to thank Denise Ingram for letting me invade the teaching labs and lending me copious amounts of chemicals.

Finally, I would like to thank my partner Claire for putting up with me during this time.

Contents

| | |
|---|----|
| Novel Imprinted Polymers as Artificial Enzymes | 1 |
| Summary | 2 |
| Acknowledgements | 3 |
| Contents | 4 |
| List of Figures | 9 |
| List of Tables | 13 |
| List of Equations | 15 |
| List of Abbreviations | 16 |
| Chapter 1 Introduction | 17 |
| 1.0 Introduction..... | 18 |
| 1.1 Enzymes..... | 18 |
| 1.1.1 The Lock and Key Model..... | 18 |
| 1.1.2 The Induced Fit Model..... | 19 |
| 1.1.3 Michaelis Menten Kinetics..... | 20 |
| 1.1.4 Reactions Catalysed by Enzymes..... | 22 |
| 1.1.5 Limitations of Enzymes..... | 22 |
| 1.2 The Serine Proteases..... | 23 |
| 1.3 Serine Protease Mimics..... | 26 |
| 1.3.1 Polymeric Serine-protease Mimics..... | 28 |
| 1.4 Molecularly Imprinted Polymers (MIP's)..... | 30 |
| 1.4.1 Properties of MIP's..... | 33 |
| 1.4.2 Applications of MIP's..... | 33 |
| 1.4.2.1 Separation..... | 33 |
| 1.4.2.2 Sensors..... | 36 |
| 1.4.2.3 Catalysis..... | 38 |
| 1.5 Synthesis of a Serine-protease Mimic using MIP's..... | 50 |
| 1.6 L-Histidine as the Basis for Models of the Catalytic Triad..... | 53 |
| 1.7 Aim and Scope..... | 54 |

| | | |
|---|--|-----------|
| 1.7.1 | Study of the Carboxylate Group/Imidazole Ring Interaction in Histidine Derivatives..... | 54 |
| 1.7.2 | The Carboxylate Group/Imidazole Ring Interaction in L-Histidine Based MIP's..... | 55 |
| 1.7.3 | Environment of the Template Molecule..... | 56 |
| 1.7.4 | Pericyclic Reactions..... | 57 |
| Chapter 2 Molecular Modeling of Amino Acid Derivatives..... | | 58 |
| 2.0 | Molecular Modelling of Amino Acid Derivatives..... | 59 |
| 2.1 | The Conformations of <i>N</i> -Acetyl-L-histidine..... | 59 |
| 2.2 | Dependency of Coupling Constants on Conformation Population..... | 62 |
| 2.3 | Calculation of $\alpha\beta$ and $\alpha\beta'$ Coupling Constants using ^1H NMR Spectroscopy.... | 65 |
| 2.3.1 | Choice of Molecules..... | 65 |
| 2.3.2 | Association of Molecules in Solution..... | 65 |
| 2.3.3 | Vicinal Coupling Constants..... | 67 |
| 2.4 | Calculation of Dihedral Angles using Molecular Modeling..... | 70 |
| 2.4.1 | Molecular Modeling..... | 70 |
| 2.4.2 | Conformational Searches..... | 70 |
| 2.4.3 | Molecular Dynamics Calculations..... | 74 |
| 2.4.4 | Calculation of Mole Fractions..... | 76 |
| Chapter 3 Hydrolysis Studies – Small Molecules..... | | 78 |
| 3.0 | Hydrolysis Studies - Small Molecules..... | 79 |
| 3.1 | Hydrolysis in pH 7.0, 7.6 and 8.0 Buffer Solutions..... | 79 |
| 3.1.1 | Calibration..... | 79 |
| 3.1.2 | Hydrolysis of <i>p</i> -Nitrophenyl Acetate Without Catalyst..... | 80 |
| 3.1.3 | Hydrolysis of <i>p</i> -Nitrophenyl Acetate in Aqueous Buffer Solution..... | 81 |
| 3.2 | Hydrolysis of <i>p</i> -Nitrophenyl Acetate in DMSO/H ₂ O 9:1 v/v Solution..... | 89 |
| 3.3 | Synthesis of Anions..... | 90 |
| 3.3.1 | Calibration..... | 90 |
| 3.3.2 | Hydrolysis of <i>p</i> -Nitrophenyl Acetate in DMSO/H ₂ O 9:1 v/v Solution..... | 91 |
| Chapter 4 Hydrolysis Studies - Molecularly Imprinted Polymers...97 | | |
| 4.0 | Hydrolysis Studies - Molecularly Imprinted Polymers..... | 98 |
| 4.1 | MIP's as Enzyme Mimics..... | 98 |
| 4.2 | Synthesis of Monomers and the Transition State Mimic..... | 99 |

| | | |
|------------------|--|------------|
| 4.3 | Synthesis of Polymers. | 100 |
| 4.3.1 | Difficulties of Using MIP's. | 102 |
| 4.4 | Hydrolysis in pH 8.0 Buffer Solution..... | 103 |
| 4.4.1 | Calculation of Masses of Polymer..... | 103 |
| 4.4.2 | Hydrolysis in pH 8.0 Buffer Solution..... | 103 |
| 4.5 | Hydrolysis in DMSO/H ₂ O 9:1 v/v Solution. | 108 |
| Chapter 5 | NMR Study of the Environment of the Template..... | 117 |
| 5.0 | NMR Study of the Environment of the Template. | 118 |
| 5.1 | The Use of ³¹ P MAS NMR to Study the Template Molecule. | 122 |
| 5.1.1 | A ³¹ P MAS NMR Study of the Initial Imprinted Polymer | 123 |
| 5.1.2 | A ³¹ P MAS NMR Study of Washed Polymer Ground Up with <i>p</i> -Nitrophenyl Methylphosphonate. | 125 |
| 5.1.3 | A ³¹ P MAS NMR Study of Washed Polymer Stirred with <i>p</i> -Nitrophenyl Methylphosphonate for 24 Hours then Filtered..... | 127 |
| 5.1.4 | A ³¹ P MAS NMR Study of Washed Polymer Stirred with <i>p</i> -Nitrophenyl Methylphosphonate for 24 hours..... | 130 |
| 5.1.5 | A ³¹ P MAS NMR Study of Washed Polymer Stirred with <i>p</i> -Nitrophenyl Methylphosphonate for an Hour..... | 133 |
| Chapter 6 | Artificial Enzymes for the Oxy-Cope Rearrangement... 138 | |
| 6.0 | Artificial Enzymes for the Oxy-Cope Rearrangement. | 139 |
| 6.1 | The Oxy-Cope Rearrangement..... | 140 |
| 6.2 | Oxy-Cope Rearrangement of 1,5-Hexadien-3-ol. | 141 |
| Chapter 7 | Conclusions and Further Work..... 144 | |
| 7.0 | Conclusions. | 145 |
| 7.1 | Further Work. | 146 |
| Chapter 8 | Experimental..... 148 | |
| 8.0 | Experimental..... | 149 |
| 8.1 | Reagents..... | 149 |
| 8.2 | Formation of pH 7.0, 7.6 and 8.0 Buffer Solutions..... | 150 |
| 8.3 | Methods of Analysis..... | 151 |
| 8.4 | Synthesis of Imidazole Derivatives..... | 152 |
| 8.4.1 | Synthesis of 4(5)-vinylimidazole..... | 152 |

| | | |
|---------|--|-----|
| 8.4.1.1 | Synthesis of N-Triptyl-4-imidazolecarboxaldehyde..... | 152 |
| 8.4.1.2 | Synthesis of 4-Vinyl-1-tritylimidazole..... | 152 |
| 8.4.1.3 | Synthesis of 4(5)-vinylimidazole..... | 153 |
| 8.5 | Synthesis of Amino-Acid Derivatives..... | 153 |
| 8.5.1 | Synthesis of <i>N</i> -Methacryloyl-L-histidine..... | 153 |
| 8.5.2 | Synthesis of <i>N</i> -Acetyl-L-histidine Salts..... | 154 |
| 8.5.3 | Synthesis of <i>N</i> -Acetyl-L-phenylalanine Salts..... | 154 |
| 8.6 | Synthesis of Template Molecules..... | 154 |
| 8.6.1 | Synthesis of <i>p</i> -Nitrophenyl Methylphosphonate..... | 154 |
| 8.7 | Polymer Synthesis..... | 155 |
| 8.7.1 | Synthesis of an Acrylamide Based MIP..... | 155 |
| 8.7.2 | Synthesis of an EDMA Based MIP..... | 156 |
| 8.7.3 | Synthesis of a Methyl Methacrylate Based MIP..... | 156 |
| 8.7.4 | Synthesis of an <i>N</i> -Methacryloyl-L-histidine Based MIP..... | 156 |
| 8.7.5 | Synthesis of a 4(5)-vinylimidazole Based MIP..... | 157 |
| 8.7.6 | Treatment of <i>N</i> -Methacryloyl-L-histidine Imprinted and Non-imprinted Polymers with Sodium Hydroxide and Tetra- <i>n</i> -butylammonium Hydroxide..... | 157 |
| 8.8 | Kinetic Studies..... | 157 |
| 8.8.1 | Hydrolysis of <i>p</i> -Nitrophenyl Acetate..... | 157 |
| 8.8.2 | Hydrolysis of <i>p</i> -Nitrophenyl Acetate in Buffer Solution, Small Molecules as Catalyst..... | 158 |
| 8.8.3 | Hydrolysis of <i>p</i> -Nitrophenyl Acetate in a DMSO/H ₂ O 9:1 v/v Solution, Small Molecules as Catalyst..... | 158 |
| 8.8.4 | Hydrolysis of <i>p</i> -Nitrophenyl Acetate in pH 8.0 Buffer Solutions, MIP's as Catalyst..... | 159 |
| 8.8.5 | Hydrolysis of <i>p</i> -Nitrophenyl Acetate in DMSO/H ₂ O 9:1 v/v Solution, MIP's as Catalyst..... | 159 |
| 8.9 | Study of the Conformations of <i>N</i> -Acetyl-L-histidine, <i>N</i> -Acetyl-L-phenylalanine and their Salts..... | 160 |
| 8.9.1 | Association of <i>N</i> -Acetyl-L-histidine and its Salts..... | 160 |
| 8.9.2 | Association of <i>N</i> -Acetyl-L-phenylalanine and its Salts..... | 160 |
| 8.10 | Study of the Environment of the Template in MIP's using ³¹ P MAS NMR..... | 160 |
| 8.10.1 | Study of the Environment of the Template in MIP using ³¹ P MAS NMR – Initial Imprinted Polymer..... | 160 |

| | | |
|--------------------------|--|-----|
| 8.10.2 | Study of the Environment of Template in MIP's using ^{31}P MAS NMR – Ground with <i>p</i> -Nitrophenyl Methylphosphonate..... | 161 |
| 8.10.3 | Study of the Environment of Template in MIP's using ^{31}P MAS NMR – Stirred with <i>p</i> -Nitrophenyl Methylphosphonate for an Hour. | 161 |
| 8.10.4 | Study of the Environment of Template in MIP's using ^{31}P MAS NMR – Stirred with <i>p</i> -Nitrophenyl Methylphosphonate for Twenty-four Hours. | 161 |
| 8.10.5 | Study of the Environment of Template in MIP's using ^{31}P MAS NMR – Stirred with <i>p</i> -Nitrophenyl Methylphosphonate for an Hour and Filtered..... | 161 |
| 8.10.6 | Study of the Environment of Template in MIP's using ^{31}P MAS NMR – Stirred with <i>p</i> -Nitrophenyl Methylphosphonate for Twenty-four Hours and Filtered. . | 162 |
| 8.11 | Oxy-Cope Rearrangement. | 162 |
| 8.11.1 | Polymer Synthesis | 162 |
| 8.11.2 | Catalysis..... | 162 |
| 8.12 | Molecular Mechanics and Molecular Dynamics..... | 162 |
| 8.12.1 | Molecular Mechanics..... | 162 |
| 8.12.2 | Molecular Dynamics..... | 163 |
| Appendices. | | 164 |
| References. | | 196 |

List of Figures

| | | |
|-----------|--|----|
| Figure 1 | The Lock and Key Model..... | 19 |
| Figure 2 | The Induced Fit Model..... | 20 |
| Figure 3 | The Serine Protease Mechanism – Charge Relay Mechanism..... | 24 |
| Figure 4 | The Serine Protease Mechanism – Charge Stabilisation Mechanism..... | 25 |
| Figure 5 | Serine Protease Mimic for Intramolecular Deacylation..... | 26 |
| Figure 6 | Serine Protease Mimic for the Hydrolysis of an Anilide..... | 27 |
| Figure 7 | Cyclodextrin Based Serine Protease Mimic..... | 28 |
| Figure 8 | <i>N</i> -Methylacrylohydroxamate and 4(5)-vinylimidazole based Serine-protease Mimic..... | 28 |
| Figure 9 | Tetrapeptide Serine-protease Mimic..... | 29 |
| Figure 10 | α -Helical Peptide based Serine-protease Mimic..... | 29 |
| Figure 11 | Retention of Spatial Arrangement through Cross-linking..... | 30 |
| Figure 12 | The Formation of MIP's..... | 31 |
| Figure 13 | Covalently Bound Template Molecule for the Resolution of Racemates..... | 31 |
| Figure 14 | Non-Covalently Bound Template Molecule for the Resolution of Racemates..... | 32 |
| Figure 15 | 2,6-Diaminoanthroquinone..... | 34 |
| Figure 16 | Formation of an Imprinted Polymer for the Resolution of Enantiomers..... | 35 |
| Figure 17 | Release of Proton on Binding of Glucose..... | 38 |
| Figure 18 | Phosphonate Ester as a Model for Ester Transition State..... | 39 |
| Figure 19 | Transition State Analog and Substrate for an Immunoglobulin..... | 39 |
| Figure 20 | Hapten and Substrate for a Catalytic Antibody..... | 40 |
| Figure 21 | Serine-protease Mimic for the Hydrolysis of an L-Phenylalanine Ester..... | 41 |
| Figure 22 | Water Soluble Polymer for Ester Hydrolysis..... | 41 |
| Figure 23 | Template Molecule and Substrate for an Ester Hydrolysing Imprinted Polymer..... | 42 |
| Figure 24 | Reduced Schiffs Base, <i>N</i> -pyridoxyl-L-phenylalanineanilide..... | 42 |
| Figure 25 | Formation of a Schiffs Base..... | 43 |
| Figure 26 | Transition State Analogue for the α -elimination of HF..... | 44 |
| Figure 27 | Imprinted Polymer for the α -elimination of HF..... | 45 |
| Figure 28 | Transition State Analogue for the Formation of an Imprinted Polymer for an Aldol Condensation..... | 45 |

| | | |
|-----------|---|----|
| Figure 29 | Imprinted Polymer Catalysed Aldol Condensation of Acetophenone and Benzaldehyde..... | 46 |
| Figure 30 | The Diels-Alder reaction between tetrachlorothiophene and maleic anhydride and its Transition State Analogue..... | 46 |
| Figure 31 | Isomerisation of Benzisoxazole..... | 47 |
| Figure 32 | Transition State Mimics for the Isomerisation of Benzisoxazole..... | 47 |
| Figure 33 | Diethyl(4-nitrobenzyl)phosphonate, 21, and Paraoxon, 22..... | 48 |
| Figure 34 | Hydride Transfer Reduction..... | 48 |
| Figure 35 | Formation of an Imprinted Polymer for the Hydride Transfer Reduction of Benzophenone..... | 48 |
| Figure 36 | Imprinted Polymer with a Rhodium Complex for a Hydride Transfer Reduction..... | 49 |
| Figure 37 | Silica Based Imprinted Polymer..... | 50 |
| Figure 38 | Transition State Analogue and Substrate used in the Formation of a Serine-protease Mimic..... | 51 |
| Figure 39 | The Hydrolysis of <i>p</i> -Nitrophenyl Acetate and its Transition State Analogue..... | 51 |
| Figure 40 | Complex Formation for an Ester Hydrolysing Imprinted Polymer..... | 52 |
| Figure 41 | Polymerisable Derivatives of L-Histidine..... | 53 |
| Figure 42 | Models for Small Molecule Hydrolysis Studies..... | 54 |
| Figure 43 | Nucleophilic Hydrolysis Mechanism of <i>p</i> -Nitrophenyl Esters..... | 55 |
| Figure 44 | Models for the MIP Hydrolysis Studies..... | 56 |
| Figure 45 | <i>p</i> -Nitrophenyl Methylphosphonate..... | 56 |
| Figure 46 | Newman Projections of the Three Conformations of <i>N</i> -Acetyl-L-Histidine..... | 59 |
| Figure 47 | Tautomers of <i>N</i> -Acetyl-L-Histidine Anion..... | 61 |
| Figure 48 | Diagram for the Calculation of Electronegativity Values..... | 64 |
| Figure 49 | Association of <i>N</i> -Acetyl-L-Histidine and its Salts..... | 66 |
| Figure 50 | Association of <i>N</i> -Acetyl-L-Phenylalanine Sodium salt..... | 67 |
| Figure 51 | ¹ H NMR Spectrum of <i>N</i> -Acetyl-L-histidine Sodium Salt in D ₂ O at 0.45 M..... | 68 |
| Figure 52 | <i>N</i> -Acetyl-L-histidine Zwitterion and Unprotonated Forms..... | 71 |
| Figure 53 | Hydrolysis in pH 7.0 Buffer Solution, Imidazole as Catalyst..... | 82 |
| Figure 54 | Hydrolysis in pH 7.0 Buffer Solution, <i>N</i> -Acetyl-L-histidine as Catalyst..... | 82 |
| Figure 55 | Hydrolysis in pH 7.6 Buffer Solution, Imidazole as Catalyst..... | 83 |
| Figure 56 | Hydrolysis in pH 7.6 Buffer Solution, <i>N</i> -Acetyl-L-histidine as Catalyst..... | 84 |
| Figure 57 | Hydrolysis in pH 8.0 Buffer Solution, Imidazole as Catalyst..... | 85 |

| | | |
|-----------|---|-----|
| Figure 58 | Hydrolysis in pH 8.0 Buffer Solution, <i>N</i> -Acetyl-L-histidine as Catalyst..... | 85 |
| Figure 59 | Rates of Reaction for Small Molecules in Buffer Solutions..... | 86 |
| Figure 60 | Imidazolium Ion. | 87 |
| Figure 61 | Nucleophilic Catalysis..... | 88 |
| Figure 62 | Dissociation of <i>N</i> -Acetyl-L-histidine. | 88 |
| Figure 63 | Hydrolysis in DMSO/H ₂ O 9:1 v/v Solution, Imidazole as Catalyst..... | 91 |
| Figure 64 | Hydrolysis in DMSO/H ₂ O 9:1 v/v Solution, <i>N</i> -Acetyl-L-histidine as Catalyst. | 92 |
| Figure 65 | Hydrolysis in DMSO/H ₂ O 9:1 v/v Solution, <i>N</i> -Acetyl-L-histidine Sodium Salt as Catalyst. | 92 |
| Figure 66 | Hydrolysis in DMSO/H ₂ O 9:1 v/v Solution, <i>N</i> -Acetyl-L-histidine Tetra- <i>n</i> -butylammonium Salt as Catalyst..... | 93 |
| Figure 67 | Rates of Reaction for Small Molecules in DMSO/H ₂ O 9:1 v/v Solution..... | 95 |
| Figure 68 | Synthesis of 4(5)-vinylimidazole..... | 99 |
| Figure 69 | Synthesis of <i>N</i> -Methacryloyl-L-histidine. | 99 |
| Figure 70 | Synthesis of <i>p</i> -Nitrophenyl Methylphosphonate. | 100 |
| Figure 71 | Interaction of the Template Molecule with Polymer..... | 100 |
| Figure 72 | Hydrolysis in pH 8.0 Buffer Solution, Imprinted 4(5)-vinylimidazole MIP as Catalyst. | 104 |
| Figure 73 | Hydrolysis in pH 8.0 Buffer Solution, Non-Imprinted 4(5)-vinylimidazole MIP as Catalyst..... | 105 |
| Figure 74 | Hydrolysis in pH 8.0 Buffer Solution, Imprinted <i>N</i> -Methacryloyl-L-histidine MIP as Catalyst..... | 105 |
| Figure 75 | Hydrolysis in pH 8.0 Buffer Solution, Non-Imprinted <i>N</i> -Methacryloyl-L-histidine MIP as Catalyst..... | 106 |
| Figure 76 | Hydrolysis in DMSO/H ₂ O 9:1 v/v Solution, Imprinted 4(5)-vinylimidazole MIP as Catalyst..... | 109 |
| Figure 77 | Hydrolysis in DMSO/H ₂ O 9:1 v/v Solution, Non-Imprinted 4(5)-vinylimidazole MIP as Catalyst..... | 109 |
| Figure 78 | Hydrolysis in DMSO/H ₂ O 9:1 v/v Solution, Imprinted <i>N</i> -Methacryloyl-L-histidine MIP as Catalyst..... | 110 |
| Figure 79 | Hydrolysis in DMSO/H ₂ O 9:1 v/v Solution, Non-Imprinted <i>N</i> -Methacryloyl-L-histidine MIP as Catalyst..... | 110 |
| Figure 80 | Hydrolysis in DMSO/H ₂ O 9:1 v/v Solution, Imprinted <i>N</i> -Methacryloyl-L-histidine MIP Treated with Sodium Hydroxide as Catalyst..... | 111 |

| | | |
|-----------|---|-----|
| Figure 81 | Hydrolysis in DMSO/H ₂ O 9:1 v/v Solution, Non-Imprinted <i>N</i> -Methacryloyl-L-histidine MIP Treated with Sodium Hydroxide as Catalyst..... | 111 |
| Figure 82 | Hydrolysis in DMSO/H ₂ O 9:1 v/v Solution, Imprinted <i>N</i> -Methacryloyl-L-histidine MIP Treated with Tetra- <i>n</i> -butylammonium Hydroxide as Catalyst... | 112 |
| Figure 83 | Hydrolysis in DMSO/H ₂ O 9:1 v/v Solution, Non-Imprinted <i>N</i> -Methacryloyl-L-histidine MIP Treated with Tetra- <i>n</i> -butylammonium Hydroxide as Catalyst... | 112 |
| Figure 84 | Template Molecule Covalently Bound to Functional Monomers. | 119 |
| Figure 85 | Covalently Bound Template for the Study of Rebinding. | 120 |
| Figure 86 | MIP for the Study of Rebinding, Template Removed. | 120 |
| Figure 87 | Theophylline and Caffeine | 121 |
| Figure 88 | ³¹ P MAS NMR Spectra of Unwashed MIP's. | 124 |
| Figure 89 | ³¹ P MAS NMR Spectra of MIP's Ground Up with <i>p</i> -Nitrophenyl Methylphosphonate. | 126 |
| Figure 90 | ³¹ P MAS NMR Spectra of MIP's Stirred with <i>p</i> -Nitrophenyl Methylphosphonate for 24 Hours then Filtered. | 128 |
| Figure 91 | ³¹ P MAS NMR Spectra of MIP's Stirred with <i>p</i> -Nitrophenyl Methylphosphonate for 24 Hours. | 130 |
| Figure 92 | ³¹ P MAS NMR Spectra of MIP's Stirred with <i>p</i> -Nitrophenyl Methylphosphonate for an Hour..... | 133 |
| Figure 93 | ³¹ P MAS NMR Spectra of MIP's Stirred with <i>p</i> -Nitrophenyl Methylphosphonate for an Hour then Filtered. | 135 |
| Figure 94 | The Oxy-Cope rearrangement. | 140 |
| Figure 95 | Effect of Polymer on the Rate of Formation of the Higher Boiling Point Product. | 142 |
| Figure 96 | Potential Catalysts Containing an Imidazole Ring and Hydroxyl Group..... | 146 |
| Figure 97 | Monomer for an Ester Hydrolysing MIP..... | 147 |
| Figure 98 | Oxy-Cope Rearrangement..... | 147 |

List of Tables

| | | |
|----------|---|-----|
| Table 1 | Substituent electronegativity values | 64 |
| Table 2 | Coupling Constants for H _α , H _β and H _{β'} Protons of Amino Acid Derivatives. | 69 |
| Table 3 | Average Coupling Constants for H _α , H _β and H _{β'} Protons of Amino Acid Derivatives..... | 70 |
| Table 4 | Conformations of L-Histidine and L-Phenylalanine Derivatives in the Gas Phase. | 72 |
| Table 5 | Overall Mole Fractions..... | 73 |
| Table 6 | Conformational Dihedral Angles..... | 75 |
| Table 7 | Calculated Mole Fractions..... | 76 |
| Table 8 | Hydrolysis Rates for Uncatalysed Reactions..... | 81 |
| Table 9 | Rates of Reaction in pH 7.0 Buffer Solution..... | 83 |
| Table 10 | Rates of Reaction in pH 7.6 Buffer Solution..... | 84 |
| Table 11 | Rates of Reaction in pH 8.0 Buffer Solution..... | 86 |
| Table 12 | Rate Constants for Imidazole and <i>N</i> -Acetyl-L-histidine in Buffer Solutions. | 87 |
| Table 13 | Rates of Reaction in DMSO/H ₂ O 9:1 v/v Solution. | 94 |
| Table 14 | Rate Constants for all Catalysts in DMSO/H ₂ O 9:1 v/v Solution. | 95 |
| Table 15 | Reactivity Ratios for 4(5)-vinylimidazole Polymers in pH 8.0 Buffer Solution. | 107 |
| Table 16 | Reactivity Ratios for <i>N</i> -Methacryloyl-L-histidine Polymers in pH 8.0 Buffer Solution..... | 107 |
| Table 17 | Mean Reactivity Ratios and Standard Deviations for the Hydrolysis in pH 8.0 Buffer Solution. | 108 |
| Table 18 | Reactivity Ratios for 4(5)-vinylimidazole Polymers in DMSO/H ₂ O 9:1 v/v Solution..... | 113 |
| Table 19 | Reactivity Ratios for <i>N</i> -Methacryloyl-L-histidine Polymers in DMSO/H ₂ O 9:1 v/v Solution..... | 113 |
| Table 20 | Reactivity Ratios for <i>N</i> -Methacryloyl-L-histidine Polymers Treated with Sodium Hydroxide in DMSO/H ₂ O 9:1 v/v Solution. | 114 |
| Table 21 | Reactivity Ratios for <i>N</i> -Methacryloyl-L-histidine Polymers Treated with Tetra- <i>n</i> -butylammonium Hydroxide in DMSO/H ₂ O 9:1 v/v Solution. | 114 |

| | | |
|----------|--|-----|
| Table 22 | Mean Reactivity Ratios and Standard Deviations for the Hydrolysis in DMSO/H ₂ O 9:1 v/v Solution..... | 115 |
| Table 23 | ³¹ P MAS NMR Data of the Initial MIP's..... | 125 |
| Table 24 | ³¹ P MAS NMR Data of MIP's Ground Up with <i>p</i> -Nitrophenyl Methylphosphonate..... | 127 |
| Table 25 | ³¹ P MAS NMR Data of MIP's Stirred with <i>p</i> -Nitrophenyl Methylphosphonate for 24 Hours then Filtered..... | 129 |
| Table 26 | ³¹ P MAS NMR Data of MIP's Stirred with <i>p</i> -Nitrophenyl Methylphosphonate for 24 Hours..... | 132 |
| Table 27 | ³¹ P MAS NMR Data of MIP's Stirred with <i>p</i> -Nitrophenyl Methylphosphonate for an Hour..... | 135 |
| Table 28 | ³¹ P MAS NMR Data of MIP's Stirred with <i>p</i> -Nitrophenyl Methylphosphonate for an Hour then Filtered..... | 137 |
| Table 29 | Rates of Reaction for the Formation of the Higher Boiling Point Product..... | 142 |

List of Equations

| | | |
|-------------|---|-----|
| Equation 1 | Relationship of the $J_{\alpha\beta}$ and Individual $^1\text{H} - ^1\text{H}$ Coupling Constants..... | 62 |
| Equation 2 | Relationship of the $J_{\alpha\beta'}$ and Individual $^1\text{H} - ^1\text{H}$ Coupling Constants..... | 62 |
| Equation 3 | The Karplus Equation ($0^\circ \geq \phi \geq 90^\circ$)..... | 63 |
| Equation 4 | The Karplus Equation ($90^\circ \geq \phi \geq 180^\circ$)..... | 63 |
| Equation 5 | Expression for the $\alpha\beta$ Vicinal Coupling Constants..... | 63 |
| Equation 6 | Expression for the $\alpha\beta'$ Vicinal Coupling Constants..... | 63 |
| Equation 7 | Boltzmann Distribution..... | 71 |
| Equation 8 | Rate Equation for the Hydrolysis of <i>p</i> -Nitrophenol..... | 80 |
| Equation 9 | Gibbs Free Energy..... | 98 |
| Equation 10 | Relationship of the Chemical Shift to the Nuclear Shielding..... | 122 |

List of Abbreviations

| <u>Abbreviation</u> | <u>Description</u> |
|---------------------|--|
| AIBN | 2,2'-azobisisobutyronitrile |
| Asp | Aspartic acid |
| CTABr | cetyltrimethylammonium bromide |
| CP/MAS NMR | Cross-Polarisation / Magic Angle Spinning Nuclear Magnetic Resonance |
| DMF | <i>N,N</i> -dimethylformamide |
| DMSO | dimethyl sulfoxide |
| EDMA | ethylene glycol dimethacrylate |
| FTIR | Fourier Transform Infra-Red |
| GC | Gas Chromatography |
| Gly | Glycine |
| His | Histidine |
| HPLC | High Performance Liquid Chromatography |
| MAS NMR | Magic Angle Spinning Nuclear Magnetic Resonance |
| MIP | Molecularly Imprinted Polymer |
| NMR | Nuclear Magnetic Resonance |
| Phe | Phenylalanine |
| Ser | Serine |
| TEA | triethylamine |
| THF | tetrahydrofuran |
| TSA | Transition State Analogue |

Chapter 1 Introduction.

1.0 Introduction.

1.1 Enzymes.

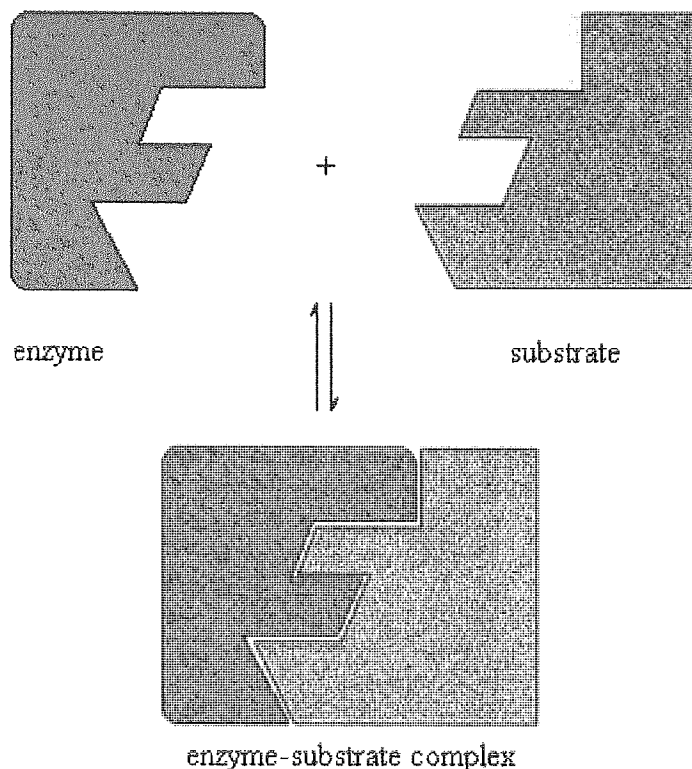
Enzymes are protein molecules that act as biological catalysts. Enzymes, like all catalysts, do not alter the equilibrium of a reaction but provide an alternative, lower energy path for the reaction. The reactants of enzyme catalysed reactions are known as substrates. Enzymes are very efficient catalysts,¹ accelerating reactions by a factor of 10^8 - 10^{10} compared to non-enzymatic methods, and sometimes exceeding a value of 10^{12} . They catalyse a wide range of reactions, there being an enzyme-catalysed process equivalent to almost every type of organic reaction² and they exhibit a high substrate tolerance by accepting a wide variety of unnatural substances even in organic media. They display chemoselectivity-often acting on a single type of functional group; regioselectivity³-distinguishing between functional groups which are situated in different regions of the same substrate molecule and enantioselectivity-being made up from L-amino acids they are chiral catalysts. They are completely degradable in the environment and they act under mild conditions, generally in a pH range of 5-8 and in a temperature range of 20-40 °C.

Consequently, enzymes are being used in a wide variety of ways. The types of reaction that enzymes are used to catalyse in industry include oxidation, reduction, inter- and intramolecular transfer of groups, hydrolysis, cleavage of covalent bonds by elimination, addition of groups to double bonds and isomerisation.⁴

1.1.1 The Lock and Key Model.

It was suggested by Fischer⁵ in 1894 that the reason for the high specificity of enzymes was that there are complementary structural features in the enzyme and the substrate, see Figure 1. The substrate is thought of as fitting into the active site of the enzyme like a key fitting into the lock. According to this model the enzyme combines with the substrate to form an enzyme-substrate complex. The substrate is modified and then the products are released from the enzyme. Alternatively the enzyme-substrate complex can dissociate back to the enzyme and the substrate. In this model, a substrate whose structure does not complement the active site is not bound.

Figure 1 The Lock and Key Model.



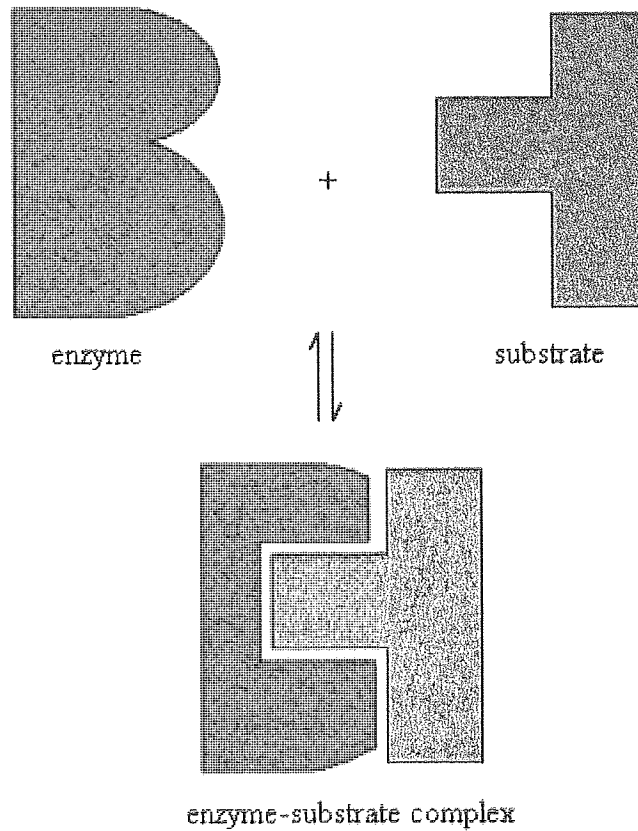
The substrate is held in the active site by intermolecular forces. These interactions explain the stereochemical specificity shown by enzymes. Binding sites link to specific groups on the substrate ensuring that the enzyme and the substrate are held in a fixed orientation with each other. This orientation holds the reactive groups of the substrate in the vicinity of the catalytic sites.

The lock and key model is somewhat simplistic as it assumes a rigid enzyme structure and is not able to explain why the enzyme is able to act on large substrates but does not act on smaller similar substrates. It also does not explain why enzymes are able to accept molecules that are not their natural substrates. In order to account for these observations an alternative model, the Induced Fit Model, was proposed.⁶

1.1.2 The Induced Fit Model.

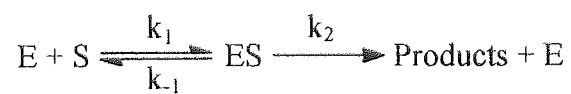
In this model the substrate and the enzyme do not precisely complement each other. However, the enzyme is able to deform via small conformational changes. This explains the ability of enzymes to accept a wide variety of substrates, see Figure 2.

Figure 2 The Induced Fit Model.



1.1.3 Michaelis Menten Kinetics.

Enzyme catalysed reactions often follow Michaelis-Menten kinetics.⁷



Where E = Enzyme

S = Substrate

ES = Enzyme-Substrate complex

An expression has been derived to explain the effect of substrate concentration on the rate of reaction. The concentration of free enzyme in the system at equilibrium is all of the original enzyme that is not complexed, $[E]-[ES]$. The substrate concentration $[S]$ is usually greatly in excess of $[E]$, so that its equilibrium concentration is essentially equal to its initial concentration $[S]$.

Therefore the dissociation constant K of $[ES]$ is:

$$K = \frac{([E]-[ES])[S]}{[ES]}$$

$$[ES] = \frac{[E][S]}{K + [S]}$$

It is assumed that the rate of product formation is so slow that it does not alter the position of equilibrium, therefore the rate of reaction (v) is that of the second reaction.

$$v = k_2[ES]$$

$$= \frac{k_2[E][S]}{K + [S]}$$

The maximum reaction rate (v_{\max}) is reached when all of the enzyme is complexed, i.e. $[ES] = [E]$.

$$v_{\max} = k_2[E]$$

Substitution of v_{\max} gives the Michaelis-Menten equation with K being known as the Michaelis-Menten constant.

$$v = \frac{v_{\max}[S]}{K + [S]}$$

The Michaelis-Menten constant can be related to the individual rate constants through the following equation.

$$K = \frac{(k_{-1} + k_2)}{k_1}$$

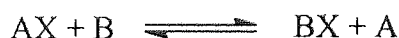
A Lineweaver-Burk plot of $1/v$ against $1/[S]$ gives a y-intercept of K/v_{\max} and a slope of K/v_{\max} from which the Michaelis-Menten constant K can be calculated. In Michaelis-Menten kinetics K reflects the affinity of an enzyme for a particular substrate. The lower the value of K the higher the affinity.

1.1.4 Reactions Catalysed by Enzymes.

Enzymes are classified into 6 main classes according to the reactions they catalyse.⁸

Class 1 are the oxidoreductases and they catalyse the transfer of H atoms, O atoms or electrons from one substrate to another.

Class 2 are the transferases, and they catalyse reactions of the type:



excluding oxidoreductase and hydrolase reactions.

Class 3 are the hydrolases, and they catalyse hydrolytic reactions of the form:



Class 4 are the lyases, and they catalyse the non-hydrolytic removal of groups from substrates, often leaving double bonds.

Class 5 are the isomerases, and they catalyse isomerisation reactions.

Class 6 are the ligases, and they catalyse the synthesis of new bonds, coupled to the breakdown of ATP or other nucleoside triphosphates and are of the form:



1.1.5 Limitations of Enzymes.

Despite the remarkable properties of enzymes there are limits to the conditions under which they can be used. Enzymes are usually active only between 20-40 °C and between pH 5-8.

Conditions outside of these ranges often lead to irreversible denaturation. In addition, only those enzymes that occur naturally are available as catalysts. Reactions for which there are no naturally occurring enzymes or that are carried out under more extreme conditions must be catalysed using an alternative catalyst.

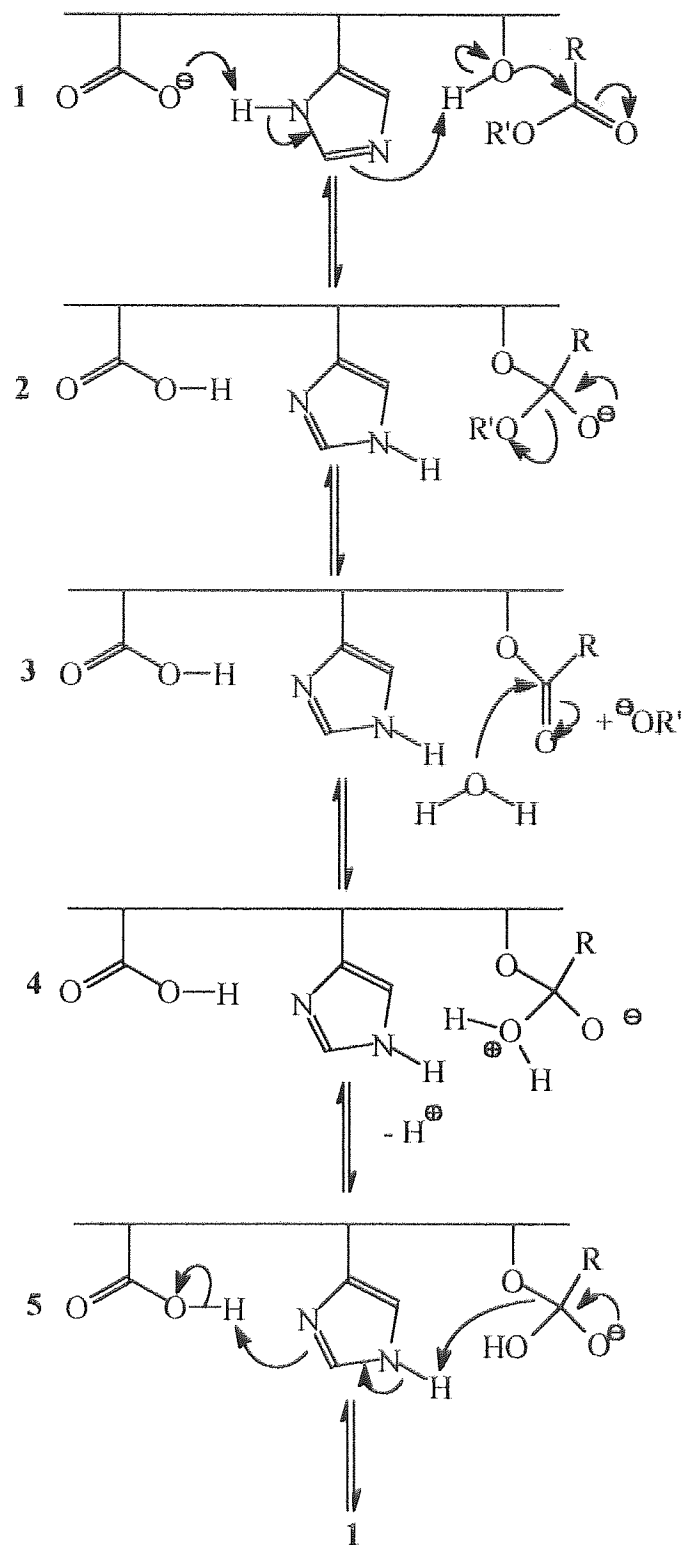
1.2 The Serine Proteases.

The serine proteases, such as chymotrypsin, trypsin and elastase, are endopeptidases that catalyse the hydrolysis of the peptide bonds in the middle of polypeptides. All of these enzymes contain the same catalytic triad of amino acid residues within their active sites and consequently operate by the same mechanism.⁹ This catalytic triad consists of serine, histidine and aspartic acid residues, although sometimes a glutamic acid residue replaces the aspartic acid.

Chymotrypsin has been the most widely studied of these enzymes and although many aspects of its catalysis are understood it is still the subject of intense controversy. Over 30 years ago it was reported¹⁰ that Asp-102 was hydrogen bonded to His-57. This led to the development of the charge relay mechanism in which, in the transition state, Asp-102 acts as a general base, together with the imidazole ring of His-57, to deprotonate the hydroxyl group of Ser-195 thereby increasing the nucleophilicity of the OH group,¹¹ see Figure 3.

Figure 3

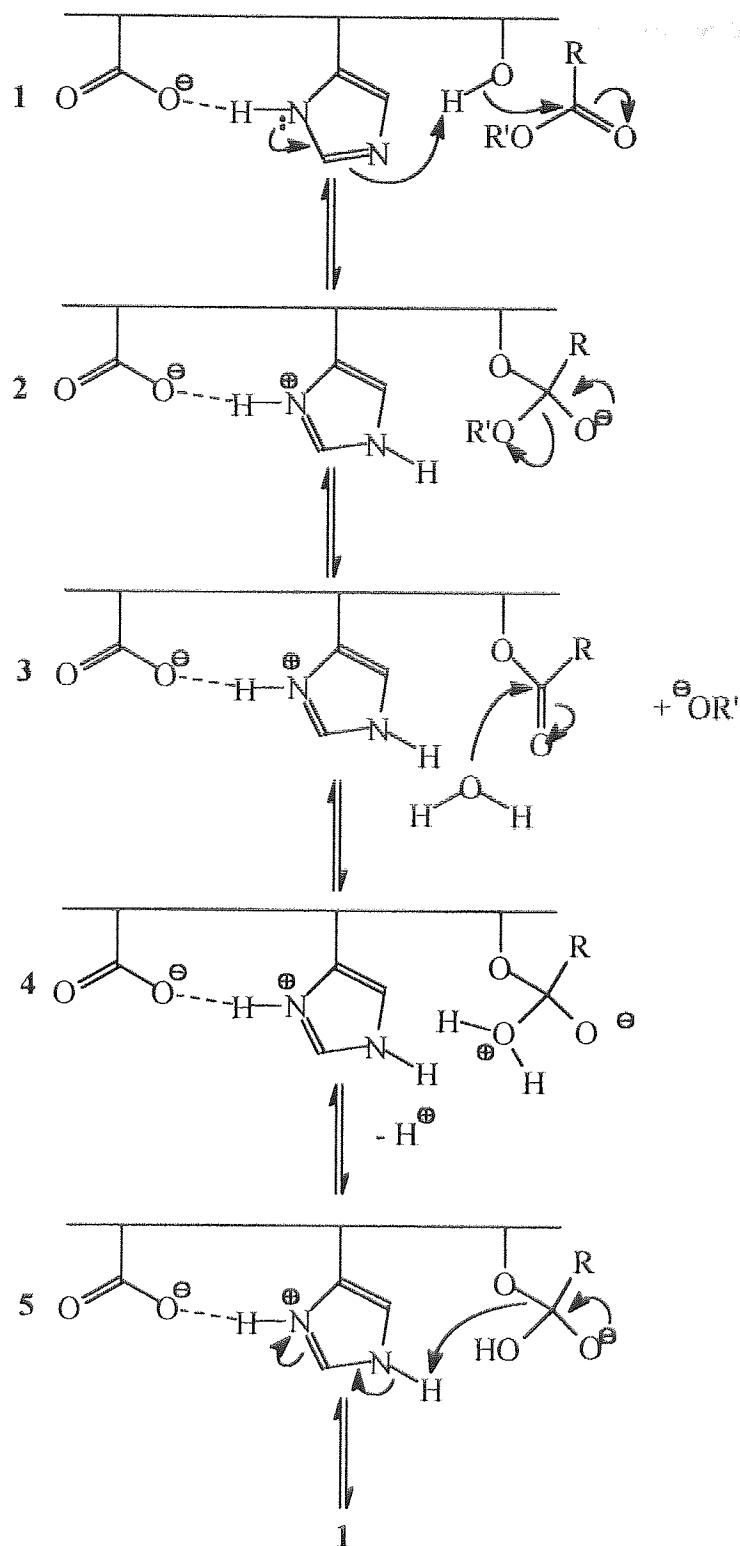
The Serine Protease Mechanism – Charge Relay Mechanism



An alternative mechanism¹² has been proposed, in which the proton from Ser-195 is transferred to His-57 whilst the carboxylate group of Asp-102 stabilises the developing charge on the imidazole ring, see Figure 4.

Figure 4

The Serine Protease Mechanism – Charge Stabilisation Mechanism.



Other suggestions for the role of the carboxylate group in Asp-102 have included a) it holds the imidazole in the correct tautomeric form,¹² and b) it anchors the histidine group in the correct orientation.¹² In recent years it has been suggested that a low barrier hydrogen bond is present between Asp-102 and His-57 and that the strength of this bond is a significant factor

in stabilizing the transition state and consequently for the activity of the enzyme.¹³ This idea has been strongly criticized¹⁴ and indeed recent work has even suggested that low-barrier hydrogen bonds are unable to exist in condensed phases.¹⁵

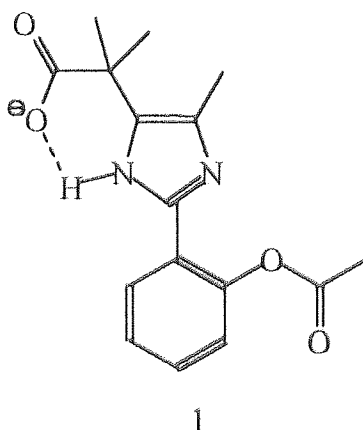
In addition, it has been suggested that unnatural substrates are hydrolysed by different mechanisms to natural substrates. For example the mechanism for the hydrolysis by chymotrypsin of an unnatural ester substrate such as *p*-nitrophenyl acetate first involves the *N*-acylation of the histidine group quickly followed by rapid acyl transfer to the serine hydroxyl group rather than initial attack by the serine hydroxyl group.^{16,17}

Despite having no sequence homology, bacterial and mammalian serine proteases contain identical catalytic triads. The imidazole rings of a histidine residue hydrogen bonded to a carboxylate of aspartate or glutamate (the Asp-His couple) have been found in the active sites of zinc containing enzymes¹⁸, glutathione reductase¹⁹, lipases²⁰, maleate and lactate dehydrogenase²¹, DNAse I²², and all serine proteases.^{23,24} Although its function is different in some of these enzymes its widespread occurrence suggests that significant catalytic benefit arises from the Asp-His couple. In order to study these complex enzyme mechanisms and to determine the exact role of the Asp-His couple in each enzyme, model systems have great potential.

1.3 Serine Protease Mimics.

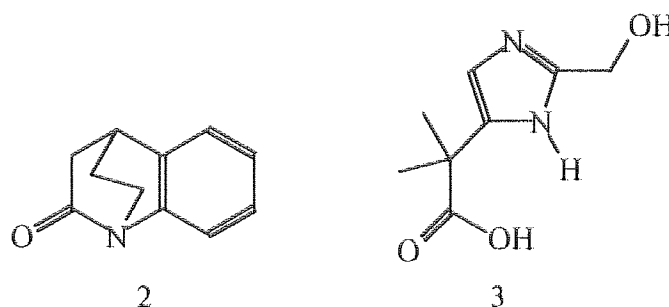
The syntheses of small molecules that mimic the serine proteases have been reported. Rogers and Bruice²⁵ studied the deacylation of compound 1 shown in Figure 5.

Figure 5 Serine Protease Mimic for Intramolecular Deacylation.



The presence of the carboxylate group gave only a 3-fold rate increase over a molecule without the carboxylate functional group. This was taken as evidence against the charge relay model. Brown et al²⁶ showed that in the hydrolysis of compound **2**, shown in Figure 6, the use of compound **3** as catalyst showed only a small rate enhancement and fitted onto a Brønsted plot, indicating that the role of the carboxylate group was to increase the basicity of the imidazole ring.

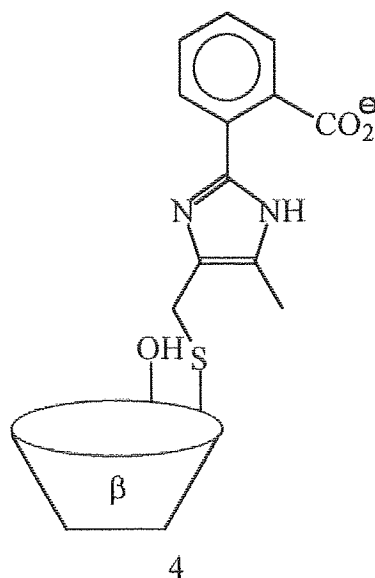
Figure 6 Serine Protease Mimic for the Hydrolysis of an Anilide



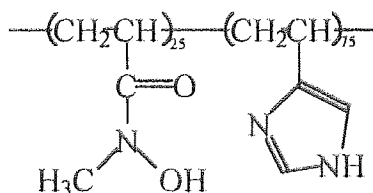
Zimmerman et al²⁷ studied the effect of several molecules containing carboxylate groups and imidazole rings with *syn*- and *anti*- oriented carboxylates. They found that there was no general base catalysis occurring in either orientation. They also found that the rate enhancement due to the carboxylate group in all models was less than 10-fold, and limited to the increase in pK_a of the imidazole ring. It appears that in small molecule serine protease mimic studies the rate enhancements appear to be small and due entirely to the increase in the pK_a of the imidazole ring. In order to obtain greater rate enhancements it may be necessary to mimic other properties of the enzymes such as the binding site.

One method for the formation of a binding site mimic has been the use of cyclodextrins. It has been shown²⁸ that cyclodextrin can provide a hydrophobic binding site, such as that found in chymotrypsin. Bender et al²⁹ attached *o*-(4(5)-mercaptomethyl-4(5)-methylimidazol-2-yl) benzoate, to the secondary hydroxyl groups of cycloheptamylose (β -cyclodextrin) forming molecule **4**, which contained a binding site and a catalytic site within the same molecule, see Figure 7. When compared with α -chymotrypsin at their optimum pHs, 7.9 for α -chymotrypsin and 10.7 for the artificial enzyme, the hydrolysis of *m-t*-butylphenyl acetate by the artificial enzyme was catalysed at a rate more than twice that of α -chymotrypsin.

Figure 7

Cyclodextrin Based Serine Protease Mimic.**1.3.1 Polymeric Serine-protease Mimics.**

Attempts to synthesize serine protease mimics using soluble vinyl polymers containing pendant catalytically active functional groups have been reported. Overberger et al.³⁰ synthesized a copolymer of 4(5)-vinylimidazole and 4-vinylphenol for use as a catalyst in the hydrolysis of *p*-nitrophenyl acetate. The hydrolysis in the presence of the copolymer showed a rate of hydrolysis at pH 9.1 approximately 10 times greater than that obtained in the presence of poly-4(5)-vinylimidazole or imidazole. A concerted effect between the hydroxyl and imidazole functional groups was also noted in the work of Kunitake and Okahata³¹ using an *N*-methylacrylohydroxamate, 4(5)-vinylimidazole copolymer, see Figure 8, as a catalyst in the hydrolysis of *p*-nitrophenyl acetate.

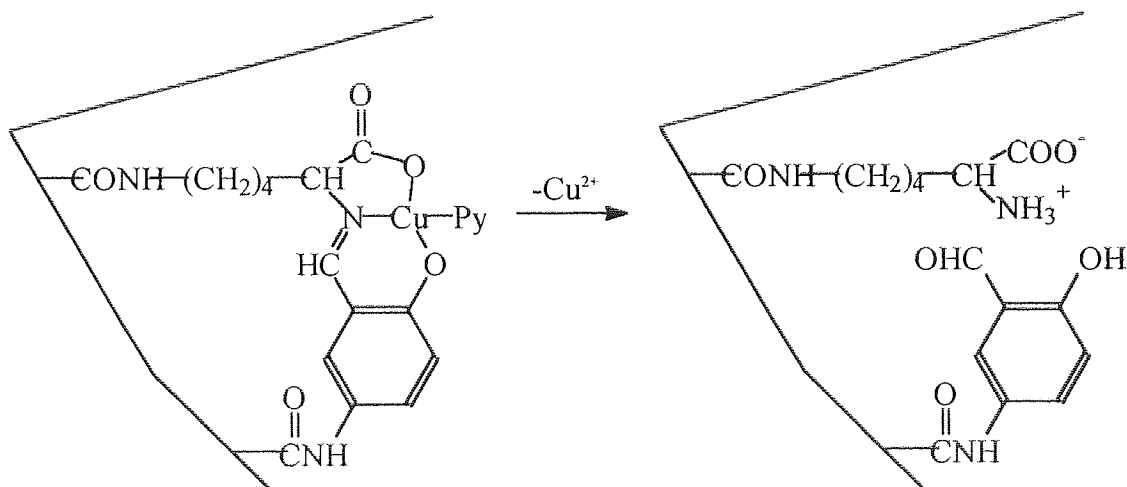
Figure 8 *N*-Methylacrylohydroxamate and 4(5)-vinylimidazole based Serine-protease Mimic

chymotrypsin for the hydrolysis of acetyltyrosine ethyl ester. This was still an effective catalyst as the rate of reaction was approximately 10^5 times greater than the non-catalysed reaction.

From these studies it is evident that any design of a serine-protease mimic needs to include a mechanism whereby the catalytic groups can be brought into the vicinity of one another in the correct orientation.

It is possible to bring catalytic monomers into close contact with one another by the formation of metal ion coordination complexes before polymerization. The spatial arrangement of the catalytic groups can be retained even after the removal of the metal ion by the use of cross-linking. Belekou et al³⁴ formed a copolymer of (*N*^α-5-methacryloylamino-salicylidene-*N*^ε-methacryloyl-(*S*)-lysinate)(pyridine)copper(II) with acrylamide and *N,N'*-methylenebis(acrylamide), see Figure 11.

Figure 11 Retention of Spatial Arrangement through Cross-linking



After removal of the $\text{Cu}^{(II)}$ ions, see Figure 11, the lysine and salicylaldehyde moieties retained their special arrangements in both cross-linked and gel like polymers. This study though was unable to produce polymers which acted as an intramolecular catalyst. An alternative approach is the use of molecularly imprinted polymers.

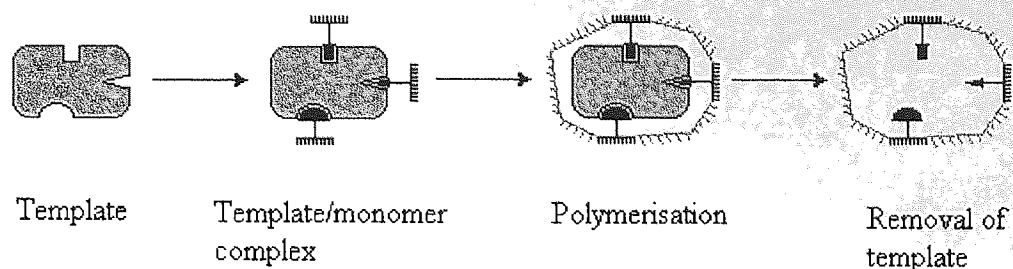
1.4 Molecularly Imprinted Polymers (MIP's).

The formation of MIP's involves the formation of a highly crosslinked polymer network around a template molecule. Removal of the template results in the formation of a cavity

which corresponds to the shape and chemical functionality of the template molecule, see Figure 12.

Figure 12 The Formation of MIP's.

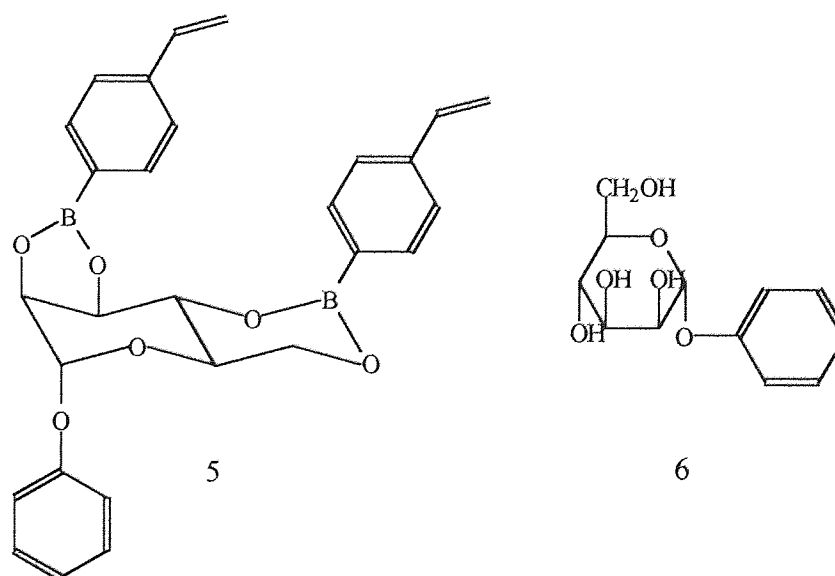
Redrawn from ref 35



After removal of the template, the imprinted polymer possesses a memory for the print molecule and is able to rebind the template in preference to other molecules.

The basic concept for the formation of an MIP, i.e. formation of a highly cross-linked polymer around a template molecule, is the same for most MIP's. The major difference that arises is the decision of what type of template molecule to use. Initially template molecules covalently bound to the monomers were used. Wulff et al^{36,37} radically copolymerised monomer **5** with large amounts of ethyleneglycol dimethacrylate (EDMA) in the presence of an inert solvent, see Figure 13.

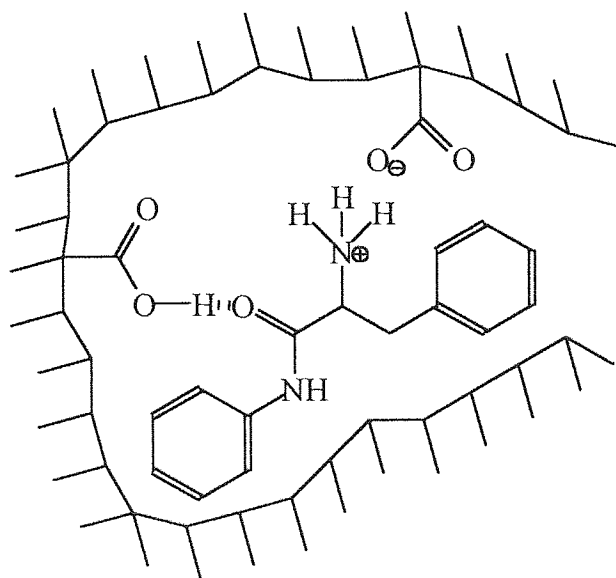
Figure 13 Covalently Bound Template Molecule for the Resolution of Racemates.



Removal of up to 95% of the template by treatment with methanol and water yielded an MIP capable of chiral discrimination that could achieve baseline separation of racemates of phenyl α -D-mannopyranose mannoside, **6**, when used as the stationary phase in HPLC.

The usefulness of the process increased when Mosbach et al³⁸ achieved an effective imprinting effect using exclusively non-covalent interactions. L-Phenylalanine anilide was used as template molecule in a polymer formed from methacrylic acid and EDMA. It was thought that one methacrylic acid moiety forms an electrostatic bond with the template and another forms a hydrogen bond as shown in Figure 14.

Figure 14 Non-Covalently Bound Template Molecule for the Resolution of Racemates.



The process was extensively optimized and achieved selectivities for the resolution of racemates of L-phenylalanine anilide that were similar to those obtained using covalently bound template.

Since these early examples, very many substances have been used as templates to form MIP's. Examples of these are, sugars and sugar derivatives,^{36,37} diols and polyols,³⁹ hydroxycarboxylic acids,⁴⁰ amino acid derivatives,³⁸ peptides,⁴¹ proteins,^{42,43} nucleosides and nucleotides,^{44,45} purine derivatives,^{44,46} steroids,^{47,48} basic drugs,^{49,50} acidic drugs,⁵¹ dialdehydes,⁵² diketones,⁵³ dicarboxylic acids,⁵³ disulfides,⁵⁴ dyes,⁵⁵ coenzyme analogues,³⁴ basic condensed aromatics,⁵⁶ bisimidazoles^{57,58} and phosphonate esters.^{59,60}

1.4.1 Properties of MIP's.

The structure of the polymer matrix is crucial to the properties of the MIP. Therefore the polymer should have the following properties.

- a) Stiffness of the polymer structure enables the cavities to retain their shape after removal of the template molecule.
- b) High flexibility of the polymer works against the above property but is essential for rapid equilibration with the substrate to be embedded.
- c) Good accessibility of as many cavities as possible in the polymer structure.
- d) The polymer must have good mechanical stability when used in high pressure applications or in a stirred reactor.
- e) The polymer must have good thermal stability when used in an application for which a raised temperature is required.

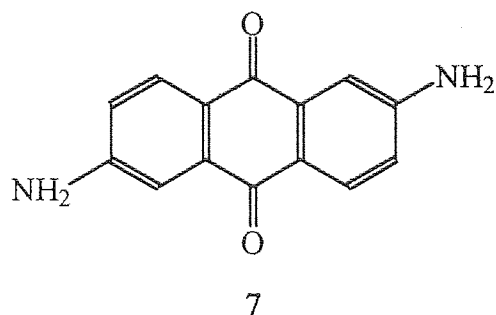
Although several different monomers have been studied for the formation of MIP's, EDMA has been used most widely as polymers derived from this monomer have many of the above properties.

1.4.2 Applications of MIP's.

1.4.2.1 Separation.

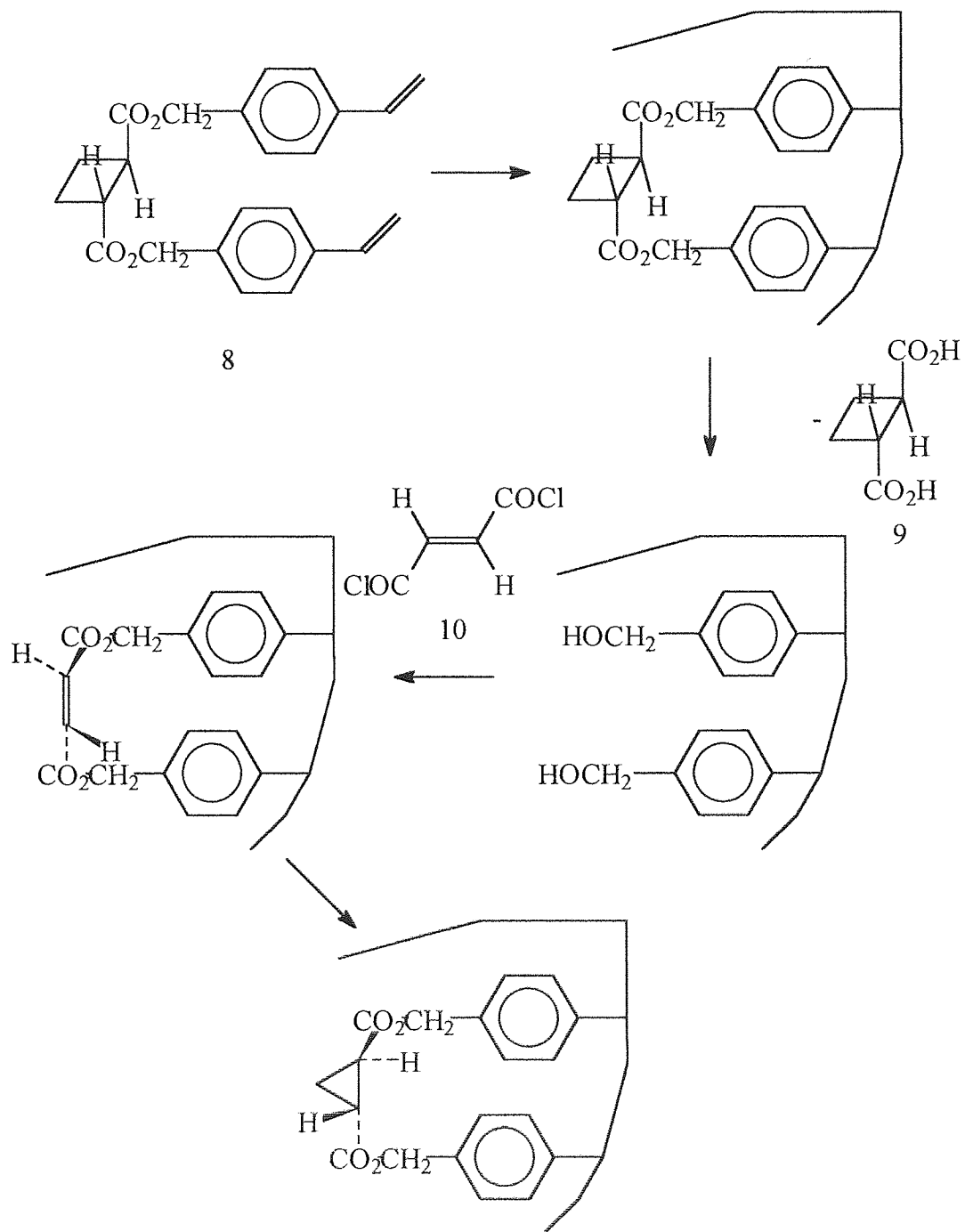
One of the major uses for MIP's is for separation purposes. Arshady and Mosbach⁵⁵ imprinted polymers with various dye molecules. The imprinted polymer showed selectivity in rebinding of the imprinted dye over other molecules. Shea et al⁴⁴ formed a polymer from methacrylic acid, cross-linked with EDMA and *N,N'*-1,3-phenylenebis(2-methyl-propenamide) around the template molecule 9-ethyladenine, a nucleotide base. The imprinted polymers showed affinity for derivatives of adenine over other substrates. Mosbach et al⁴⁶ synthesised methacrylic acid/EDMA polymers imprinted with theophylline and diazepam for use as drug assays in human serum. The polymers showed selectivity for the imprint drug but showed reduced selectivity when tested with derivatives of the imprint drug. Sherrington et al⁵⁶ found that an imprinted polymer containing sulfonic acid groups formed shape selective cavities for the rebinding of 2,6-diaminoanthroquinone, 7, see Figure 15.

Figure 15 2,6-Diaminoanthroquinone.



It is also possible to use MIP's for the resolution of enantiomers. They are particularly suited to this because imprinting with one enantiomer leaves a chiral cavity. Shea and Thompson⁶¹ proposed that a polymer imprinted with a chiral template would exhibit a 'memory' for the asymmetry of the template molecule. To investigate this they formed a cross-linked polymer from divinylbenzene and bis(vinylbenzyl)*trans*-1,2-cyclobutanedicarboxylate, **8**, see Figure 16.

Figure 16 Formation of an Imprinted Polymer for the Resolution of Enantiomers



Removal of molecule 9, see Figure 16, by hydrolysis yielded a polymer containing cavities capable of chiral discrimination. The prochiral alkene 10, see Figure 16, was then covalently bound into the cavity. Methylene transfer to this molecule would result in either *cis* or *trans*-cyclopropane dicarboxylic acid. If racemic template was used in the formation of the polymer methylenation and hydrolysis would result in racemic cyclopropane dicarboxylic acid being formed. When *(-)*-*trans*-1,2-cyclobutanedicarboxylic acid was used as the template molecule,

methylenation and hydrolysis resulted in the synthesis of a mixture with 0.05% enantiomeric excess.

Wulff and Minarik³⁷ formed an imprinted system where α -phenylmannoside was covalently bound to the polymer as the template molecule. After polymerization the covalent bond was broken and the polymer was packed into an HPLC column and used to separate a racemic mixture of α - and β -phenylmannoside. The separation was poor using normal techniques but baseline separation and 99% enantiomeric purity was obtained using gradient elution.

It has also been shown that enantiomeric separation can be obtained using polymers that have been imprinted using template molecules bound using non-covalent interactions. Mosbach et al³⁸ prepared polymers derived from EDMA and methacrylic acid imprinted with L-phenylalanine derivatives. The polymers were packed into chromatographic columns through which racemic mixtures of the print molecules were run. The polymers showed pronounced enantioselectivity as well as substrate selectivity for their complementary substrate. Use of the complementary substrate as the mobile phase resulted in nearly baseline separation of the enantiomers.

It was then shown by Andersson and Mosbach⁶² that it was possible to synthesise an imprinted polymer that exhibits both enantiomeric separation and catalytic activity. Imprinting an EDMA and methacrylic acid based polymer with the reduced Schiff's base, *N*-pyridoxyl-L-phenylalanineanilide resulted in a MIP which would resolve the enantiomers of the template molecule. The polymer was also used to catalyse the condensation reaction of phenylalanineanilide and pyridoxal. It was found that the imprinted polymer catalysed the condensation reaction approximately 9 times faster than the non-imprinted polymer or no polymer at all.

1.4.2.2 Sensors.

A second application of imprinted polymers is that of supramolecular sensors. The same general principles that apply to biosensors also apply to sensors formed from MIP's.⁶³ A signal is generated when the analyte is bound to a recognition element. Properties of the analyte or changes in the properties of the polymer system upon analyte binding are used for detection.

Mass-sensitive acoustic transducers such as the surface-acoustic wave (SAW) oscillator^{64,65}, the Love-wave oscillator⁶⁶ or the quartz crystal microbalance (QCM)^{64,65,67,68,69,70} have been used for sensors based on MIP's. Polyurethane based polymers have been formed on the

surface of SAW and QCM oscillators in the presence of certain organic solvents.⁶⁴ The polymers preferentially take up the imprinting solvent in preference to other solvents. The uptake of this solvent can be quantified by the change in the oscillation frequency resulting from the mass change at the oscillator surface. QCM/imprinted polymer type sensor systems have been used to rebind a variety of molecules. These sensors have demonstrated that the selectivities are similar to those obtained in other applications of MIP's, such as enantioselectivity.⁶⁸

Detection principles such as ellipsometry or surface plasmon resonance have also been used to detect mass accumulation in MIP based sensors.

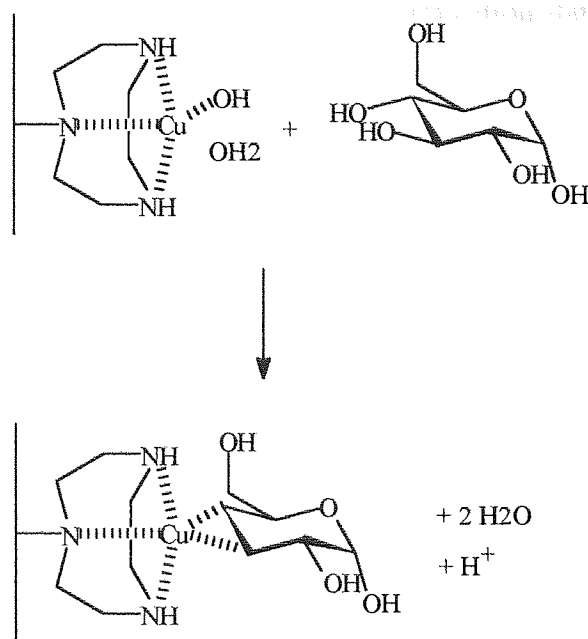
Sensors have been designed based on conductometric transducers.^{71,72,73,74} Two electrodes are separated by an imprinted membrane. When the analyte binds to the polymer, its conductivity is changed which translates to an electronic signal. Piletsky et al^{75,76} have investigated the development of sensors based on imprinted polymers prepared from (2-diethylaminoethyl)methacrylate and ethylene dimethacrylate imprinted with adenosine monophosphate, amino acids, cholesterol or atrazine by non-covalent interactions. Electro dialysis showed that these membranes were selectively permeable.

An analyte which exhibits fluorescence or electrochemical activity can be used in the formation of MIP based sensors.^{65,77} The fluorescence of these systems has been measured using fiber optics⁷⁷ and flow systems.⁶⁵ A problem arising from this fluorescence based system can be the presence of imprint molecule within the polymer which can cause a high background signal resulting in decreased sensitivity.

A competitive or displacement sensor may also be used.^{78,79,80,81,82} A radio-labeled analyte derivative is allowed to compete with the analyte for binding sites in the MIP. Alternatively the labeled analyte derivative is allowed to bind completely in the MIP and is then displaced by the analyte.

The signal can also be generated by the polymer itself.⁸³ An example of this is a glucose-sensing polymer which works in a ligand exchange mode. A polymerisable copper chelate and methylglucoside complex was used to prepare the polymer. The copper and methylglucoside was extracted followed by reloading of the copper to yield the active form of the polymer. Addition of glucose resulted in coordination to the metal accompanied by proton release, see Figure 17.

Figure 17 Release of Proton on Binding of Glucose



The proton release was a function of analyte concentration and could be quantified by pH measurement.

Optical sensing systems have also been described where fluorescent reporter groups incorporated into the MIP have their properties altered upon analyte binding.^{84,85,86}

Marx-Tibbon and Willner⁸⁷ demonstrated a system where the imprinted functions of a polymer containing photoisomerisable functional groups could be switched on and off by bathing the polymer in UV and visible light respectively. This resulted in a polymer membrane that could transport or block the flow of the imprint molecule tryptophan.

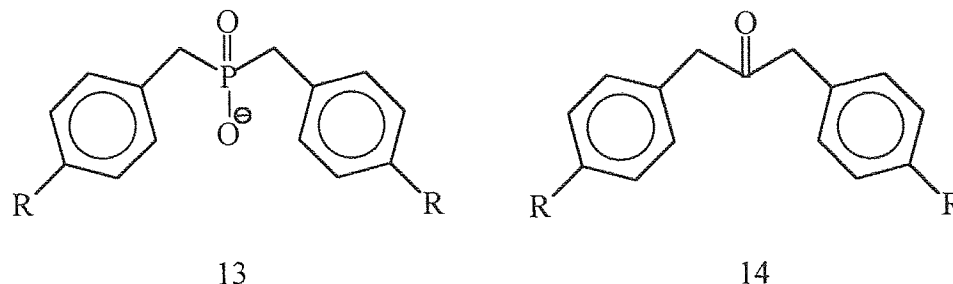
Sherrington et al⁸⁸ synthesised macroporous imprinted polymers as completely transparent monoliths. Irradiation of the template molecules bound to the polymer with polarized light resulted in those template molecules lying in the direction of the excitation to react with the polymer matrix. The polymers show a pronounced dichroism in UV light, which promises the development of chemical sensors.

1.4.2.3 Catalysis.

Careful design of the groups binding the template molecule to the polymer can upon removal of the template leave groups that will make the cavity catalytically active. These systems have great potential, yet only a small number have been reported.^{59,60,62,89,90,91,92,93,94,95,96,97,98,99,100,101,102,103,104,105,106,107}

site. Tramontano, Janda and Lerner¹¹⁴ produced antibodies for which the phosphonate ester **13**, see Figure 20, had been used as hapten.

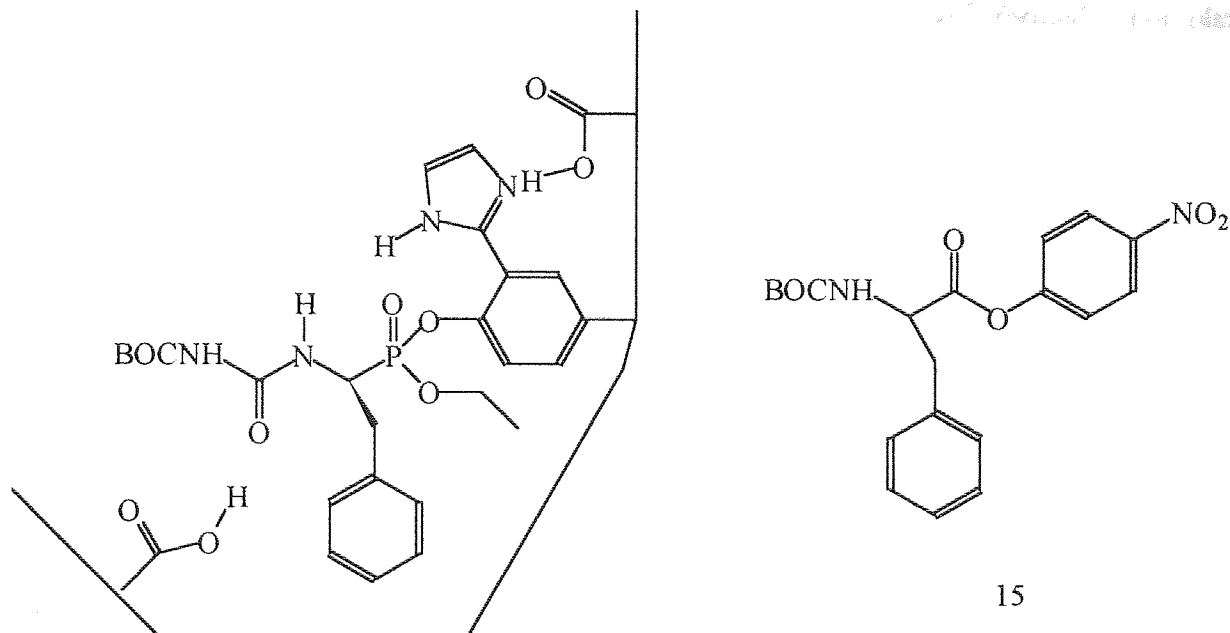
Figure 20 Hapten and Substrate for a Catalytic Antibody



Tramontano et al¹¹⁴ found that esters that were similar to the structure of the phosphonate esters were accepted by the antibody in a catalytic process that exhibited many of the characteristics of an enzyme. The chromatographic profiles obtained during the hydrolysis of these esters were found to be the same as that obtained when hog liver esterase was used as catalyst. They eventually obtained a rate of hydrolysis of ester **14**, see Figure 20, that was 960 times greater than that of the uncatalysed reaction.

Similar transition state mimics have been used to prepare MIP's for the hydrolysis of esters. MIP's have been synthesized which show some α -chymotrypsin-like activity in that they hydrolyse amino acid derivatives. Sellergren and Shea⁹⁰ synthesized a polymer containing hydroxyl, imidazole and carboxylate functional groups imprinted with a phosphonate ester derivative of L-phenylalanine, see Figure 21.

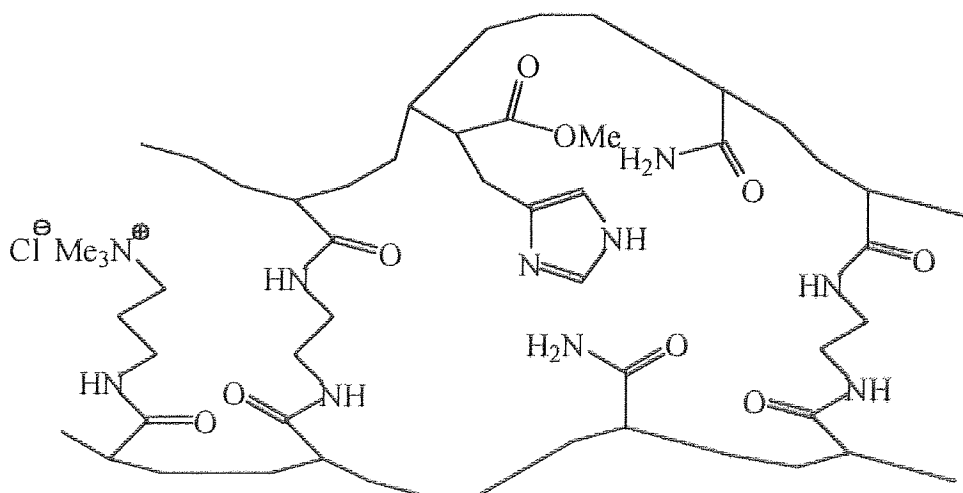
Figure 21 Serine-protease Mimic for the Hydrolysis of an L-Phenylalanine Ester



When used as catalyst for the hydrolysis of the L-phenylalanine ester **15**, see Figure 21, the polymer produced a 10-fold rate enhancement over the monomer in solution. In a further study,⁹¹ they showed that the polymer gave a rate enhancement of 2.5 when compared with that obtained using a non-imprinted control polymer.

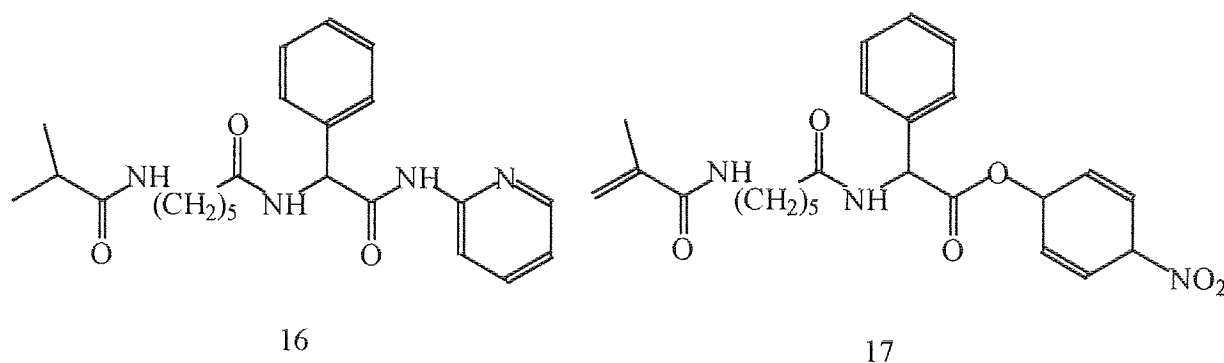
Ohkubo et al⁹² formed a water soluble acrylamide and methyl *N*-acryloyl-L-histidinate cross-linked copolymer imprinted with a phosphonate ester analogue of an L-leucine derivative, see Figure 22.

Figure 22 Water Soluble Polymer for Ester Hydrolysis



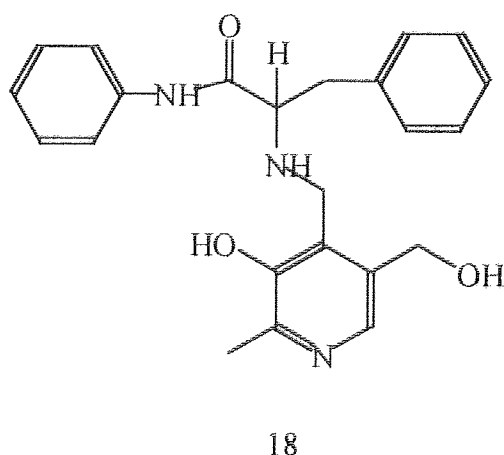
When the imprinted polymer was used to catalyse the hydrolysis of the analogous ester a rate enhancement of approximately 10-fold was obtained. Kulkarni et al⁹⁴ formed a complex comprising of *N*-methacryloyl-L-histidine, methacrylic acid, template molecule **16**, see Figure 23, and CoCl₂. The complex was diluted with 2-hydroxyethyl methacrylate and cross-linked with EDMA. After removal of the imprint molecule, it was reported that the reaction containing the polymer showed a rate of hydrolysis similar to that obtained using α -chymotrypsin for the hydrolysis of molecule **17**, see Figure 23.

Figure 23 Template Molecule and Substrate for an Ester Hydrolysing Imprinted Polymer.



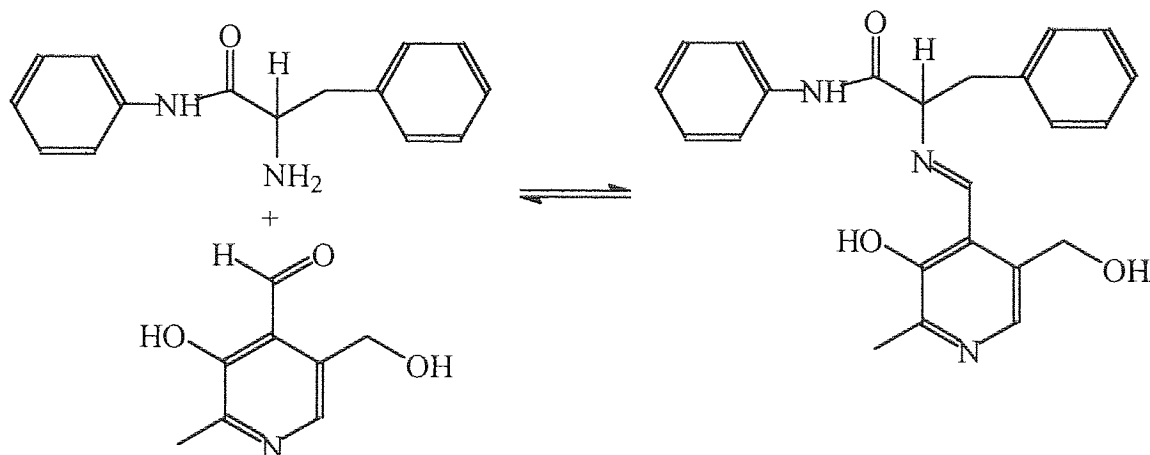
MIP's have also been formed that catalyse the reaction of a coenzyme with an amino acid to form a Schiff's base.⁶² Andersson and Mosbach synthesised an imprinted polymer from EDMA and methacrylic acid imprinted with the reduced Schiff's base, *N*-pyridoxyl-L-phenylalanineanilide **18**, see Figure 24.

Figure 24 Reduced Schiff's Base, *N*-pyridoxyl-L-phenylalanineanilide



The polymer was used to catalyse the condensation reaction of phenylalaninamide and pyridoxal, the first step in many pyridoxal catalysed reactions, see Figure 25.

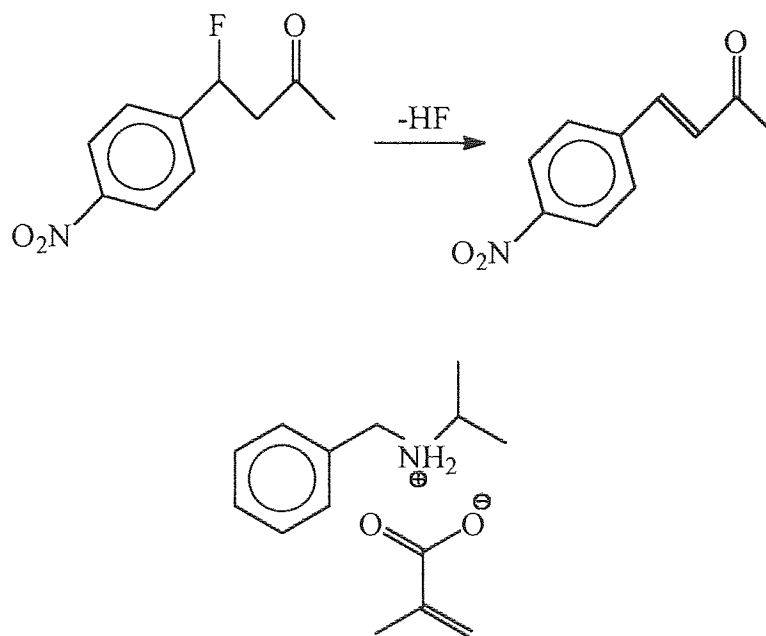
Figure 25 Formation of a Schiff's Base



It was found that the rate of reaction in the presence of imprinted polymer was approximately 9 times faster than that in the presence of non-imprinted polymer or no polymer at all.

Muller, Andersson and Mosbach⁹⁶ attempted to catalyse the β -elimination of HF from 4-fluoro-4-(*p*-nitrophenyl)-2-butanone, see Figure 26, using polymers imprinted with a range of template molecules including *N*-benzylisopropylamine in methacrylic acid/EDMA copolymers, see Figure 26.

Figure 26 Transition State Analogue for the β -elimination of HF

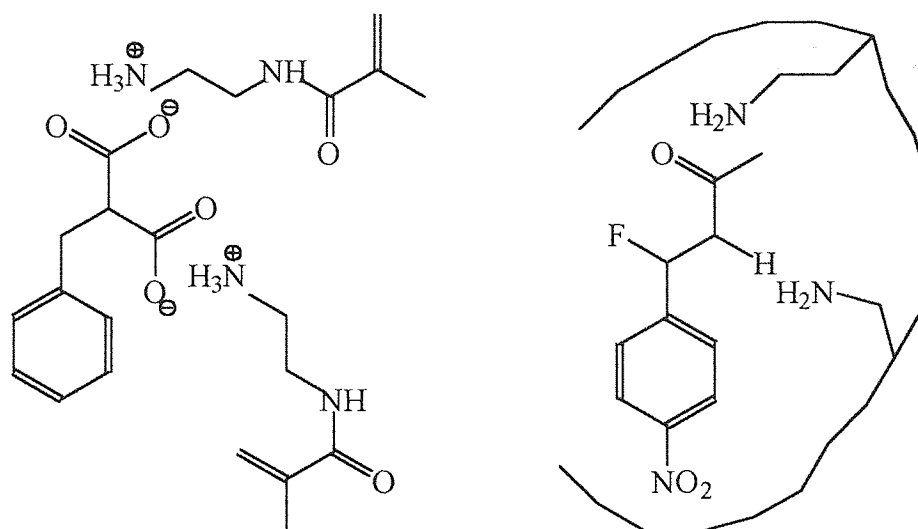


The template molecule was held in the correct orientation by hydrogen bonding with the carboxylate functional group of the methacrylic acid. Removal of the template molecule left cavities able to rebind substrates of similar structure to the imprint and which contained a carboxylate moiety positioned to effect the elimination reaction. The rate of reaction in the presence of imprinted polymers was greater than that for non-catalysed reactions and in the presence of non-imprinted analogues. The polymer imprinted with *N*-benzylisopropylamine showed greater rate enhancement than those polymers imprinted with molecules not resembling the transition state.

Brüggeman⁹⁷ used this reaction to investigate the use of methacrylic acid based MIP's in different kinds of chemical reactors. He carried out the reaction in batch reactors, fixed bed reactors and membrane reactors. Using a batch reactor, he achieved a greater catalytic effect than that obtained by Mosbach et al.⁹⁶ Using a fixed bed reactor, the substrate concentration was shown to decrease after having been pumped through the reactor. A steady state was reached after 90 minutes that continued for a further 30 minutes showing that the decrease in substrate concentration was not caused by the absorptive effects of the catalyst.

This reaction has also been studied by Beach and Shea.⁹⁷ They used a polymer formed from *N*-(2-aminoethyl)-methacrylamide/methyl methacrylate/EDMA copolymer imprinted with benzylmalonic acid, the carboxylate groups being used to hold the acrylamide groups in the correct orientation, see Figure 27.

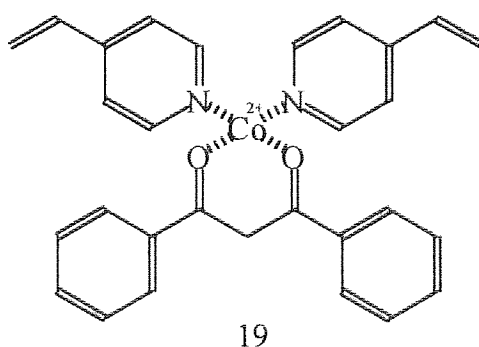
Figure 27 Imprinted Polymer for the β -elimination of HF



The presence of the imprinted polymer gave an increase in the rate of reaction for the β -elimination reaction of HF from 4-fluoro-4-(*p*-nitrophenyl)-2-butanone 3.2 times the rate obtained using the control polymer.

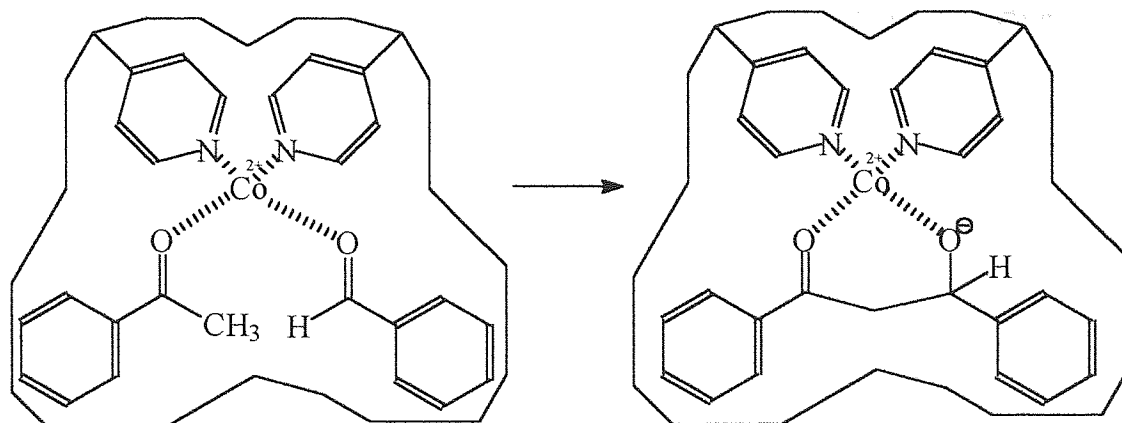
The Aldol condensation has also been studied using imprinted polymers. Mosbach et al⁹⁹ have designed a polymer where the template molecule is held in the correct orientation through co-ordination with a Co^{II} ion **19**, see Figure 28.

Figure 28 Transition State Analogue for the Formation of an Imprinted Polymer for an Aldol Condensation



Removal of the template and introduction of acetophenone and benzaldehyde results in them being in the correct orientation for an aldol condensation to take place, see Figure 29.

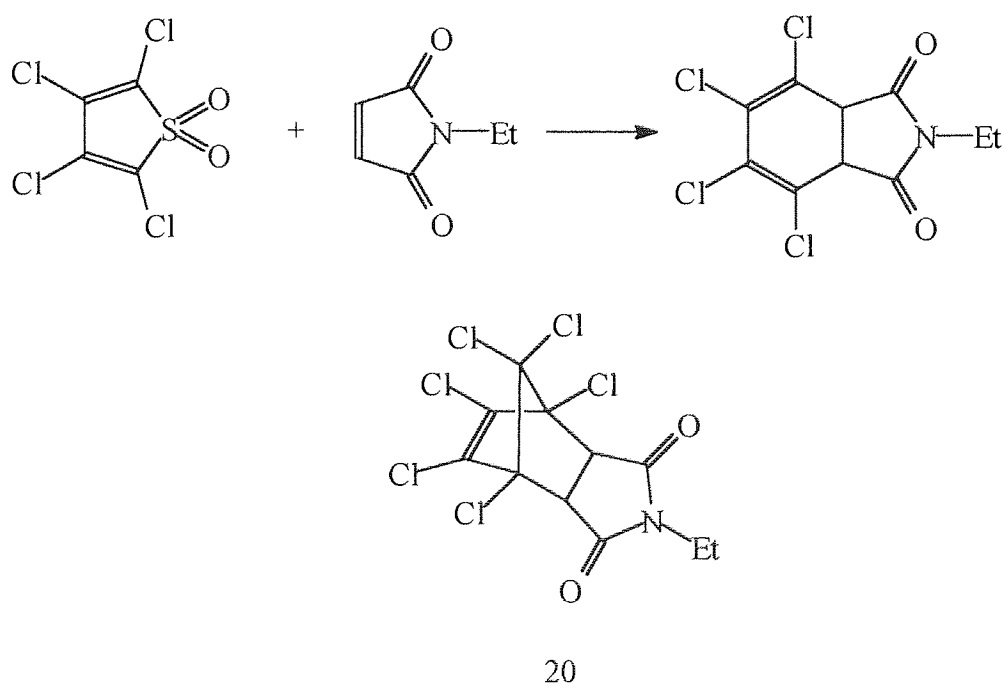
Figure 29 Imprinted Polymer Catalysed Aldol Condensation of Acetophenone and Benzaldehyde



The imprinted polymer gave an 8-fold rate increase for the condensation over that for solution phase Co^{II} and twice that for the non-imprinted analogue.

Catalytic antibodies imprinted with transition state mimics have been used to catalyse the Diels-Alder reaction.^{115,116} In an analogous approach Liu and Mosbach¹⁰⁰ formed a methacrylic acid/EDMA copolymer imprinted with chlorendic anhydride, **20**, see Figure 30, for use in the Diels-Alder reaction between tetrachlorothiophene and maleic anhydride, see Figure 30.

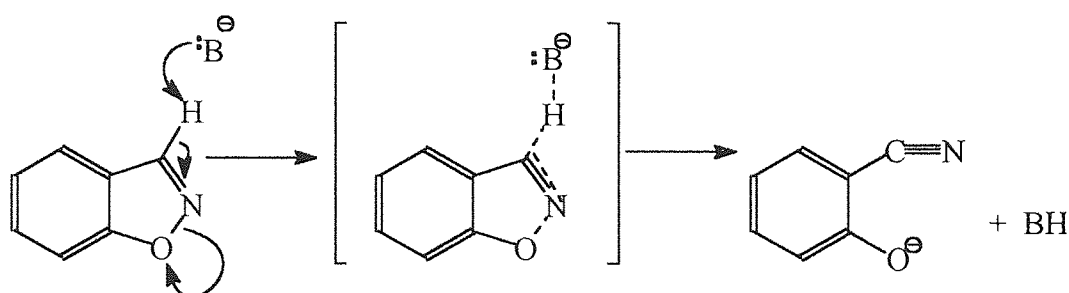
Figure 30 The Diels-Alder reaction between tetrachlorothiophene and maleic anhydride and its Transition State Analogue



The imprinted polymer showed substrate selectivity over a non-imprinted analogue and gave a rate enhancement of 270-fold greater than that obtained by an uncatalysed reaction.

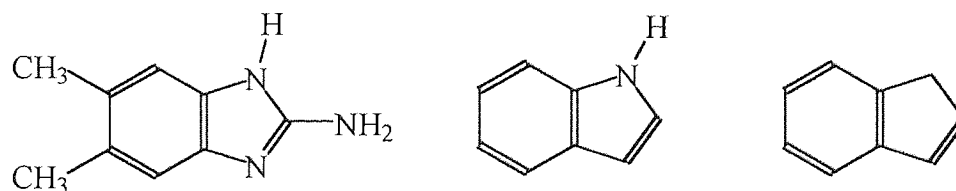
MIP's have also been designed to catalyse the isomerisation of molecules. Liu and Mosbach¹⁰² have shown that it is possible to catalyse the isomerisation of benzisoxazole using MIP's, as shown in Figure 31.

Figure 31 Isomerisation of Benzisoxazole.



A 4-vinylpyridine, EDMA copolymer was synthesized and imprinted with molecules designed to mimic the transition state, see Figure 32.

Figure 32 Transition State Mimics for the Isomerisation of Benzisoxazole

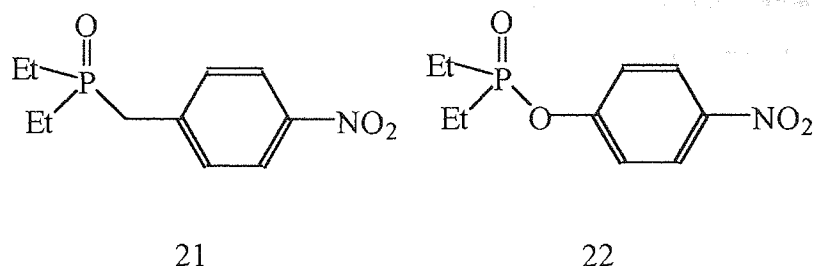


The polymer imprinted with indole when used as a catalyst gave a rate enhancement for the isomerisation over the non-imprinted analogues, and a rate enhancement over the uncatalysed reaction of 4.04×10^4 .

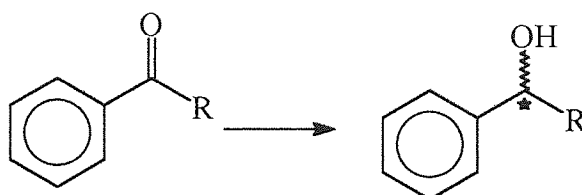
The active site of the enzyme phosphotriesterase is composed primarily of two Co^{2+} ions coordinated mainly to histidine residues. Yamazaki et al¹⁰³ synthesised imprinted polymers containing Co^{2+} -imidazole complexes to attempt to mimic the catalytic activity of the phosphotriesterase. The polymer imprinted with diethyl(4-nitrobenzyl)phosphonate, **21**, catalysed the hydrolysis of paraoxon, **22**, at a rate of 1.5 times greater than the control polymers prepared without template, see Figure 33.

Figure 33

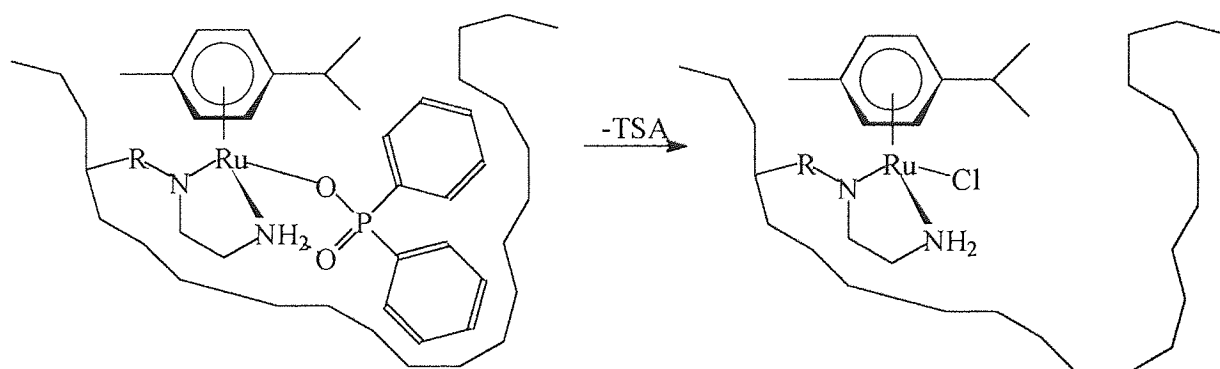
Diethyl(4-nitrobenzyl)phosphonate, 21, and Paraoxon, 22



Imprinted polymers have also been synthesized to catalyse a hydride transfer reduction, see Figure 34.

Figure 34 Hydride Transfer Reduction

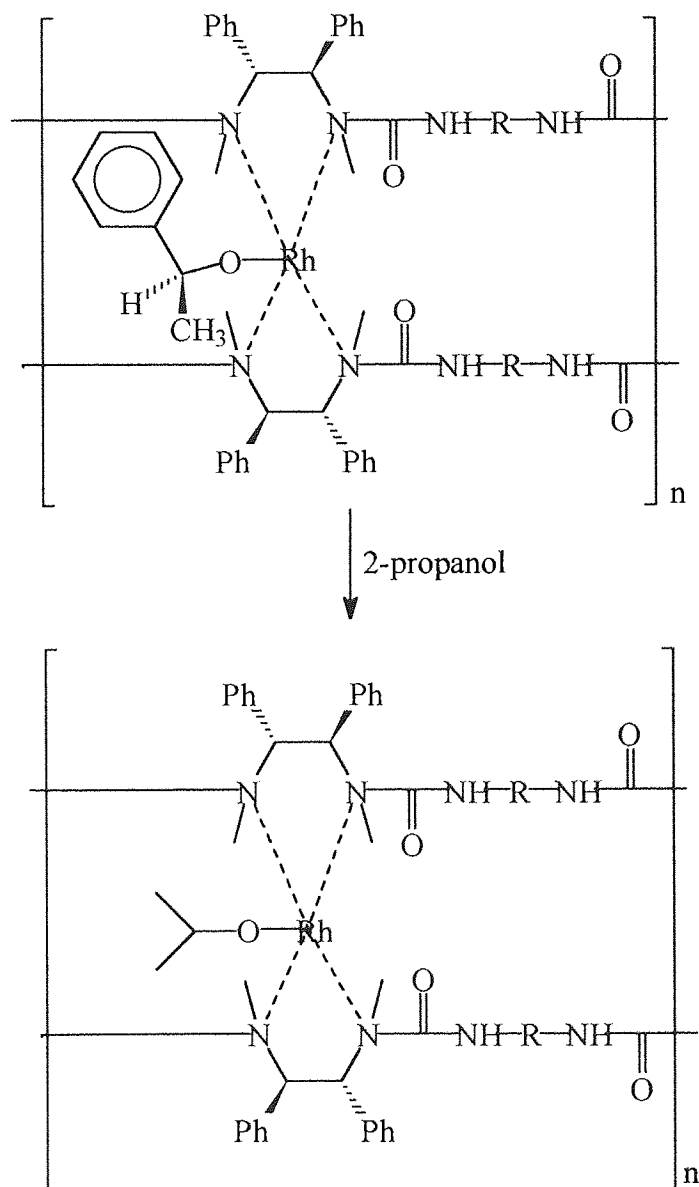
Polborn and Severin¹⁰⁴ designed a polymer containing a ruthenium catalyst bound to a transition state analogue for the hydride transfer mediated reduction of benzophenone, see Figure 35.

Figure 35 Formation of an Imprinted Polymer for the Hydride Transfer Reduction of Benzophenone

The phosphinato ligand was then cleaved and the polymer used as a catalyst in the reduction of benzophenone. The reaction containing the imprinted polymer gave a rate enhancement when compared with a non-imprinted analogue of a factor of three.

Lemaire et al¹⁰⁵ prepared an imprinted polymer containing a rhodium complex for use as a catalyst in hydride transfer reduction. The polymer was prepared using optically pure 1-(s)-phenylethanol as template which was removed by washing with an excess of 2-propanol, Figure 36.

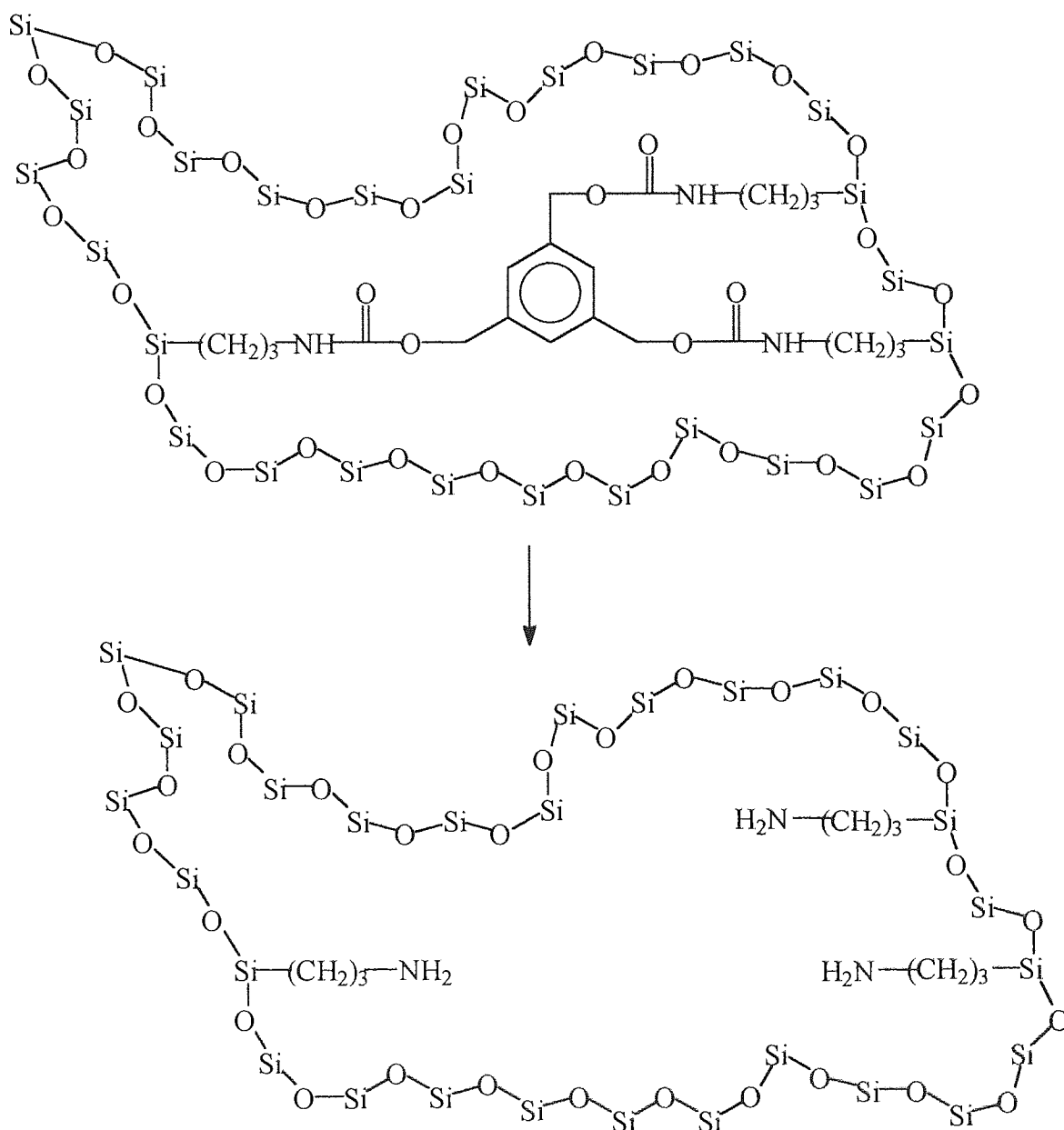
Figure 36 Imprinted Polymer with a Rhodium Complex for a Hydride Transfer Reduction



The washed polymer was found to catalyse a hydride transfer mediated reduction and the nature of the template had an effect on the enantiomeric excesses of the products formed. Imprinted polymers have also been synthesized using silica. Katz and Davis¹⁰⁶ formed an imprinted polymer from bulk amorphous silica, see Figure 37.

Figure 37 Silica Based Imprinted Polymer

Application in the Formation of a Serine



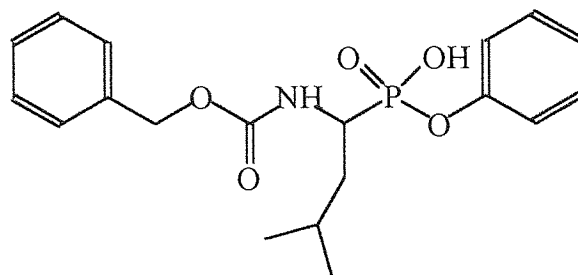
The polymer was found to be a catalyst for the Knoevenagel condensation reaction of malonitrile and isophthalaldehyde.

1.5 Synthesis of a Serine-protease Mimic using MIP's.

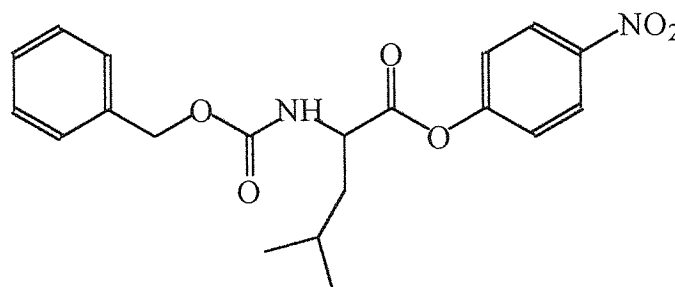
Okhubo et al¹¹⁷ designed a water soluble polymer imprinted with transition state analogue **23**, for the hydrolysis reaction of *p*-nitrophenyl ester **24**, in the presence of Co^{II} ions, see Figure 38.

Figure 38

Transition State Analogue and Substrate used in the Formation of a Serine-protease Mimic



23

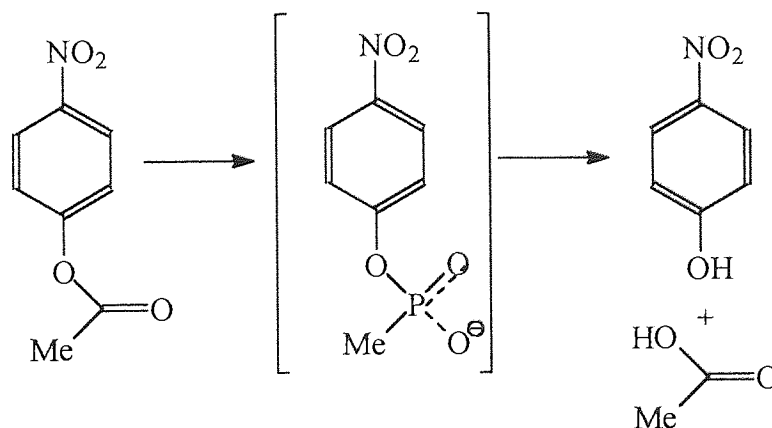


24

The imprinted polymer gave an 8.7 fold rate increase over the uncatalysed reaction but showed only a small substrate specificity. Robinson and Mosbach⁹⁵ synthesized a similar insoluble system from 4(5)-vinylimidazole and Cu^{II} ions to catalyse the hydrolysis of *p*-nitrophenyl acetate, see Figure 39.

Figure 39

The Hydrolysis of *p*-Nitrophenyl Acetate and its Transition State Analogue

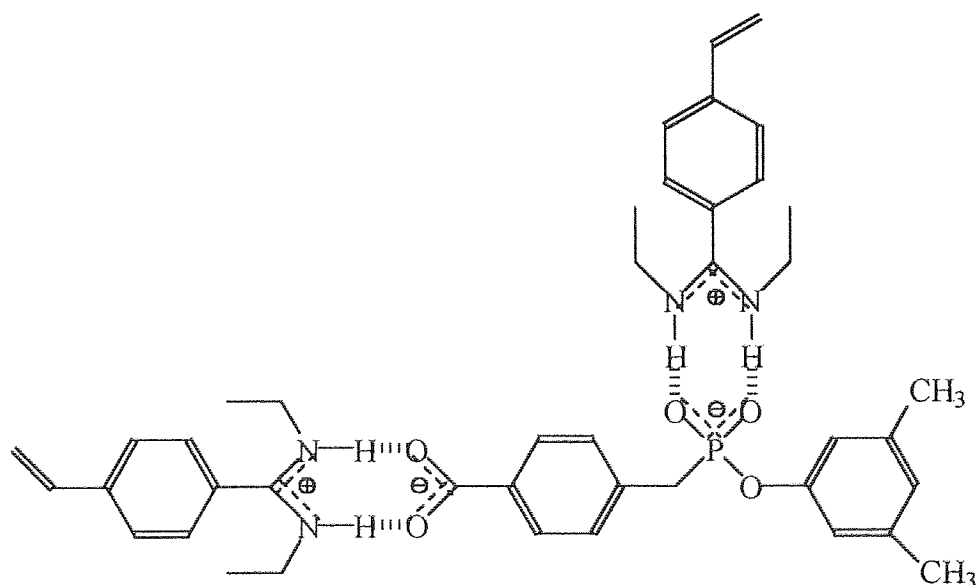


The system showed an increase in the rate of reaction that was inhibited by the presence of the print molecule showing that the catalytic activity was most enhanced by the presence of the imprinted cavities.

Kawanami et al¹⁰⁴ synthesised a polymer from 4(5)-vinylimidazole and divinylbenzene imprinted with *p*-nitrophenyl acetate. The catalytic activity of the imprinted polymer was found to be two times higher than a non-imprinted control polymer and 85 times higher than an uncatalysed reaction for the hydrolysis of *p*-nitrophenyl acetate. The hydrolytic activity of the imprinted polymer was inhibited by the presence of the template suggesting the transition state of the hydrolysis reaction is stabilized by the catalytic site.

Hydrogen bonding of the template molecule to the catalytic groups of the monomers has also been used to form an arranged cavity. Wulff et al¹⁰¹ formed a polymer containing amidine groups in the catalytic cavity. The *N,N'*-diethyl(4-vinylphenyl)amidine molecules had been shown to form complexes with the phosphonate ester template molecule, see Figure 40.

Figure 40 Complex Formation for an Ester Hydrolysing Imprinted Polymer



The catalytic groups were held in the correct spatial position to facilitate the corresponding ester hydrolysis. The rate increase over an uncatalysed reaction was found to be 100-fold.

Another method of ensuring that the catalytic groups are in the correct arrangement around an imprinted cavity is by covalently binding the template molecule to the catalytic functional group. Removal of the template results in the formation of the cavity with catalytic groups in the correct spatial arrangement. As described previously Sellergren and Shea⁹⁰ used this

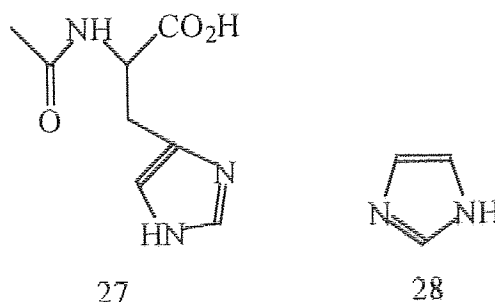
Another study that also suggests an attractive interaction between the carboxylate group and the imidazole ring was carried out by Weinkam and Jorgensen.¹²¹ They used the vicinal coupling constants of the α and β protons of L-histidine derivatives and the Karplus equation to determine which of the three conformations of histidine was most prevalent. They showed that the most populous conformations were the ones in which the carboxylate function was gauche to the imidazole ring. This suggested that the carboxylate group/imidazole ring interactions were the most important factors when determining the conformation of L-histidine derivatives. Komber¹²², using a similar system, showed that an intramolecular hydrogen bond could overcome steric hindrance to form non-staggered conformers of racemic 2,3-dimethylsuccinic acid and 2,3-diethylsuccinic acid. These promising results suggested that MIP's based on L-histidine might be effective catalysts for ester hydrolysis.

1.7 Aim and Scope.

1.7.1 Study of the Carboxylate Group/Imidazole Ring Interaction in Histidine Derivatives.

With the advent of good molecular modeling packages, it is now possible to model the conformational properties of histidine derivatives. This data could then be combined with NMR studies similar to those carried out by Weinkam and Jorgensen¹²¹ to determine if the carboxylate group/imidazole ring interaction is present. Since there is evidence that the rate of hydrolysis is increased by the presence of a carboxylate group it would also be possible to use the molecules modeled as the catalyst for the hydrolysis of esters to corroborate the modeling studies. *N*-Acetyl-L-histidine, 27, is a molecule that would lend itself to these studies, see Figure 42.

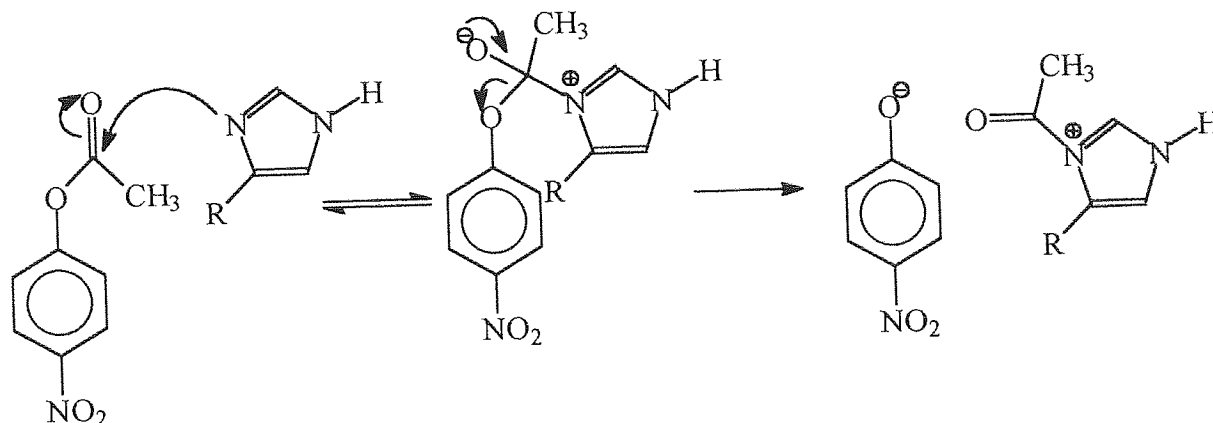
Figure 42 Models for Small Molecule Hydrolysis Studies.



It would then be necessary to compare the results for *N*-acetyl-L-histidine to those obtained using a molecule without a carboxylate group. The molecule that lends itself to this is imidazole, **28**.

p-Nitrophenyl acetate is a molecule that has been used extensively for kinetic studies of ester hydrolysis and the nucleophilic hydrolysis mechanism is well understood, see Figure 43.

Figure 43 Nucleophilic Hydrolysis Mechanism of *p*-Nitrophenyl Esters.

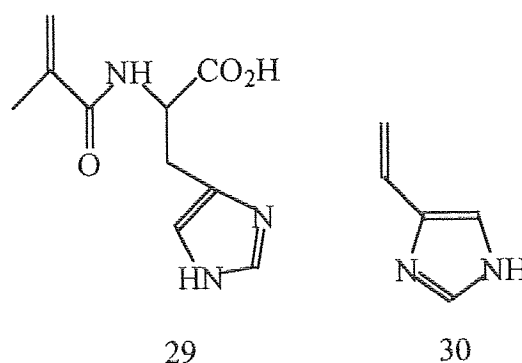


As the nucleophile approaches the ester, a bond begins to form and a positive charge develops on the imidazole ring. Anything that stabilises this charge will lead to an increase in the rate of reaction. The negatively charged carboxylate group on **27** should be able to stabilise the positively charged ring and therefore increase the rate of reaction. The reactions are also easily followed using UV spectrometry to follow the formation of the *p*-nitrophenolate ion.

1.7.2 The Carboxylate Group/Imidazole Ring Interaction in L-Histidine Based MIP's.

To study whether there is any interaction between the carboxylate group and imidazole ring in an L-histidine based MIP, it would be necessary to form polymerisable derivatives of molecules **27** and **28**. The synthesis of the monomers, *N*-methacryloyl-L-histidine, **29**, and 4(5)-vinylimidazole, **30**, see Figure 44, have been reported.^{123,124}

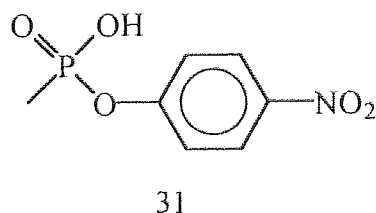
Figure 44 Models for the MIP Hydrolysis Studies.



As the experiment being studied is a hydrolysis reaction, the presence of any water in the polymerisation solution will hydrolyse the template, causing the polymer to be imprinted by molecules other than the template molecule. Therefore, the polymerisation solution needs to be free from water so all solvents and reagents must be anhydrous.

The MIP's are to be studied when being used as catalysts for the hydrolysis of *p*-nitrophenyl acetate. The phosphonate ester that mimics the transition state of *p*-nitrophenyl acetate is *p*-nitrophenyl methylphosphonate, **31**, see Figure 45. The synthesis of this molecule has been reported.¹²⁵ This is the molecule that will be used in the imprinting step to form the MIP's.

Figure 45 *p*-Nitrophenyl Methylphosphonate.



1.7.3 Environment of the Template Molecule.

Since this study will use *p*-nitrophenyl methylphosphonate it is possible to use ³¹P MAS NMR spectroscopy to study the imprinted molecule within the polymer. It was thought that ³¹P NMR would provide information about the environments that *p*-nitrophenyl methylphosphonate is in within the polymer matrix. It was therefore an aim of this work to obtain ³¹P MAS NMR spectra for polymers imprinted with *p*-nitrophenyl methylphosphonate both containing and not containing template molecule. It was hoped that this would enable us to discover the number and types of environments in which the template molecule is found.

1.7.4 Pericyclic Reactions.

As MIP's have been synthesised which were effective catalysts for the Diels-Alder reaction,¹⁰⁰ the synthesis of an MIP that can be used to catalyse other pericyclic reactions was considered. Since there was no enzyme available for the catalysis of oxy-Cope rearrangements and the rearrangement takes place at high temperatures, it would be of interest to synthesise a polymer that could reduce the temperature at which these rearrangements occur.

Chapter 2 Molecular Modeling of Amino Acid Derivatives.

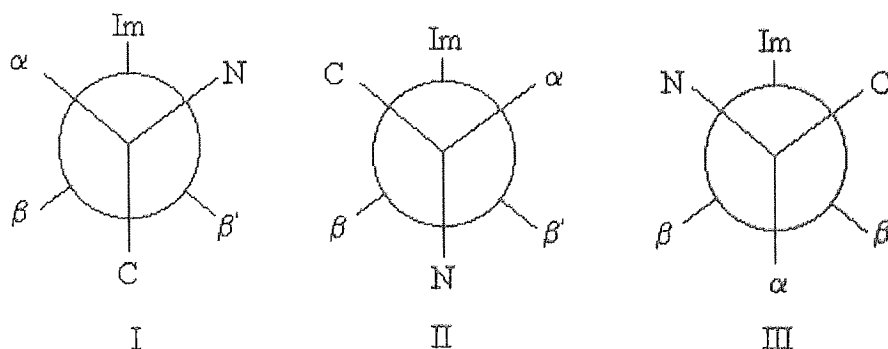
2.0 Molecular Modelling of Amino Acid Derivatives.

One of the principle aims of this research was the design and synthesis of a MIP that contained within its active site, catalytic functionalities that would mimic the arrangement of the histidine, serine and aspartic acid residues found in the active site of the serine proteases. The first step in the design of such a polymer was to identify a suitable compound that would mimic these functionalities. Derivatives of L-histidine seemed to be promising molecules since there was the potential for a hydrogen bond to form between the N-H of the imidazole ring and the carboxylate group and *N*-methacryloyl-L-histidine appeared to be a suitable radically polymerisable monomer. The effectiveness of histidine derivatives as mimics for the aspartate-histidine couple in serine proteases depends on their conformational properties. *N*-acetyl-L-histidine is a readily available compound and its conformational properties could be studied by both NMR spectroscopy and molecular modeling to determine whether there was hydrogen bond formation between the imidazole ring and the carboxylate group.

2.1 The Conformations of *N*-Acetyl-L-histidine.

A molecule of *N*-acetyl-L-histidine can adopt three staggered conformations when viewed along the $C_{\alpha} - C_{\beta}$ bond. The higher energy eclipsed conformations can be discounted. These three conformations are shown in Figure 46.

Figure 46 Newman Projections of the Three Conformations of *N*-Acetyl-L-Histidine.
Redrawn from Ref 121.



Where Im is the imidazole ring, C is the carboxylate group, N is the amide and α , β and β' are hydrogen atoms on the α and β carbon atoms.

In two conformations (II and III) the imidazole ring and the carboxylate group are gauche and in the third conformation (I), these groups are anti to each other.

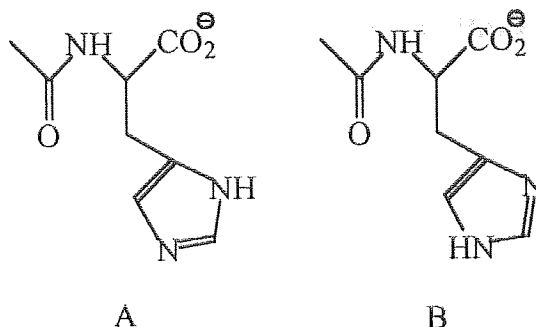
Conformations (I and II) both have one gauche interaction whilst conformation III has two gauche interactions. The amide group has a larger steric requirement than the carboxylate group and so in the absence of any interactions other than steric ones the order of stability would be expected to be II>I>III.

If there was an attractive interaction (e.g. hydrogen bond) between the imidazole ring and carboxylate group, in the absence of steric factors, conformations II and III would be expected to be of similar energy as the carboxylate and imidazole groups are gauche to each other and such an interaction could occur. In conformation I these groups are anti to each other and no attractive interaction could occur. The stability order would then be expected to be II \approx III>I.

If both an attractive interaction and steric factors were present conformation II would be expected to be the most stable as it has the possibility for a carboxylate group/imidazole ring interaction and only one gauche interaction. It is unclear whether conformation I with only one gauche interaction but no possibility of a carboxylate group/imidazole ring interaction or conformation III with the possibility of a carboxylate group/imidazole ring interaction but two gauche interactions will be the most stable. For this reason the stability order is expected to be II>I \approx III

The effectiveness of *N*-acetyl-L-histidine derivatives as catalysts in ester hydrolysis requires the imidazole ring to be unprotonated. Consequently the conformational properties of the anion of *N*-acetyl-L-histidine also need to be studied. Although *N*-acetyl-L-histidine exists in only one form, the anion has two different tautomers, see Figure 47. In tautomer A it is possible to have this interaction between the carboxylate group and the imidazole ring. In tautomer B, although it is possible to have rotation about the C_{α} - C_{β} bond such an interaction is not possible.

Figure 47

Tautomers of *N*-Acetyl-L-Histidine Anion.

The conformational properties of tautomer A in which a hydrogen bond between the imidazole ring and the carboxylate group is possible, would be expected to have similar conformational properties to *N*-acetyl-L-histidine itself. However, no such hydrogen bond is possible in tautomer B and the conformations of tautomer B should principally be governed by steric factors. This tautomer is expected to have similar conformational properties as *N*-acetyl-L-phenylalanine.

Whilst it is possible to model the two different tautomers, it is not possible to study them by experiment. In order to determine if there is hydrogen bonding between the imidazole ring and the carboxylate group in these molecules it is necessary to determine the mole fraction of each conformation. One previous attempt to deal with the problem used the vicinal $^1\text{H} - ^1\text{H}$ coupling constants and the application of the Karplus equation.¹²¹ This study suggested that there was an interaction between the carboxylate and imidazole groups in both the zwitterionic and anionic forms of the carboxylate carbon. However, the results of this study were greatly affected by the assignment of the H_β and H_β' protons in the ^1H NMR spectrum. A sufficiently wide range of histidine derivatives were studied in which the magnitude of the mole fraction of each conformation could only be rationalised if $J_{\alpha\beta} > J_{\alpha\beta'}$. An alternative study¹²⁶ claimed that the $^{13}\text{C} - ^1\text{H}$ coupling constants of the carboxylate carbon could provide an extra set of equations which could resolve the ambiguity in assignment of the H_β and H_β' protons. This study showed an approximate reversal in the mole fractions for rotamers I and II. In this study, it was assumed that there was no effect on the dihedral angles due to either an electronic interaction or steric factors thus all the dihedral angles were assigned as being multiples of 60° greatly simplifying the relationship between the average coupling constants and the conformation populations. In order to calculate conformation populations using $^{13}\text{C} - ^1\text{H}$ coupling constants it was necessary to calculate conformation populations using $^1\text{H} - ^1\text{H}$ coupling constants. During these calculations it was also assumed that the dihedral angles

were 60 °, which made the calculations 'semi quantitative'. Additionally, the assignment of the H_β and H_β' protons, the problem which Espersen and Bruce Martin were attempting to solve, was necessary for the calculation of conformation populations using ¹H – ¹H coupling constants and this affected the results of the ¹³C – ¹H coupling constant study.

The approach of Weinkam and Jorgensen had one major drawback, the assumptions made when assigning the dihedral angles. The possible interactions between the carboxylate and imidazole groups could have a large influence on the dihedral angles. Molecular modelling can now be carried out quite easily and it was decided that modelling of the conformations might give more accurate dihedral angles and hence a more accurate determination of the mole fractions using the equations of Weinkam and Jorgensen.

2.2 Dependency of Coupling Constants on Conformation Population.

The magnitude of the average vicinal coupling constants observed for each of the three staggered conformations of a C_αHXY-C_βHH'Z molecule are dependent upon the individual coupling constants and the mole fractions of these conformations as shown in Equations 1 and 2.

Equation 1 Relationship of the $J_{\alpha\beta}$ and Individual ¹H – ¹H Coupling Constants.

$$J_{\alpha\beta} = n_I J_I + n_{II} J_{II} + n_{III} J_{III}$$

Equation 2 Relationship of the $J_{\alpha\beta}'$ and Individual ¹H – ¹H Coupling Constants.

$$J_{\alpha\beta}' = n_I J_I' + n_{II} J_{II}' + n_{III} J_{III}'$$

Where $J_{\alpha\beta}$ and $J_{\alpha\beta}'$ are the average vicinal coupling constants, n_I , n_{II} and n_{III} are the mole fractions of the three conformations and J_I , J_{II} and J_{III} and J_I' , J_{II}' and J_{III}' are the $\alpha\beta$ and $\alpha\beta'$ coupling constants for the individual conformations.

The individual vicinal coupling constants are dependent upon the C_αH_α-C_βH_β and C_αH_α-C_βH_β' dihedral angles, the electronegativity of X, Y and Z and the orientation of these substituents. The angular dependence of the vicinal coupling constant for a C_αH_αXY-C_βH_βH_β'Z fragment is described by the Karplus equation as shown in Equations 3 and 4.

Equation 3 The Karplus Equation ($0^\circ \geq \phi \geq 90^\circ$).

$$J_{HH'} = A + B_1 \cos^2 \phi$$

Equation 4 The Karplus Equation ($90^\circ \geq \phi \geq 180^\circ$).

$$J_{HH'} = A + B_2 \cos^2 \phi$$

Where A, B₁ and B₂ are constants and ϕ is the dihedral angle.

Weinkam and Jorgensen¹²¹ modified the Karplus equation to obtain an expression for the $\alpha\beta$ and $\alpha\beta'$ vicinal coupling constants containing terms for the dihedral angle, substituent electronegativity and substituent orientation as shown in Equations 5 and 6.

Equation 5 Expression for the $\alpha\beta$ Vicinal Coupling Constants.

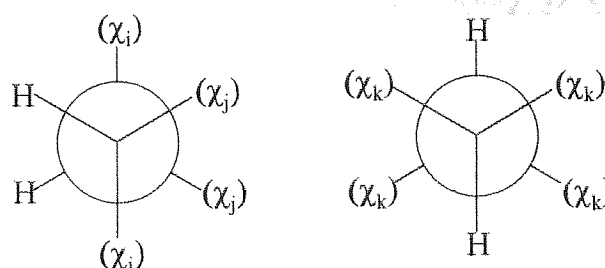
$$J_{\alpha\beta} = n_I(1 + a\Delta\chi_i^I + b\Delta\chi_j^I)(B_1^u \cos^2 \phi_{\alpha\beta}^I) + n_{II}(1 + c\Delta\chi_k^{II})(B_2^u \cos^2 \phi_{\alpha\beta}^{II}) + n_{III}(1 + a\Delta\chi_i^{III} + b\Delta\chi_j^{III})(B_1^u \cos^2 \phi_{\alpha\beta}^{III})$$

Equation 6 Expression for the $\alpha\beta'$ Vicinal Coupling Constants.

$$J_{\alpha\beta'} = n_I(1 + c\Delta\chi_k^I)(B_2^u \cos^2 \phi_{\alpha\beta'}^I) + n_{II}(1 + a\Delta\chi_i^{II'} + b\Delta\chi_j^{II'})(B_1^u \cos^2 \phi_{\alpha\beta'}^{II'}) + n_{III}(1 + a\Delta\chi_i^{III'} + b\Delta\chi_j^{III'})(B_1^u \cos^2 \phi_{\alpha\beta'}^{III'})$$

Where n_I, n_{II} and n_{III} are the mole fractions for the conformations I, II and III and the sum of the mole fractions, (n_I + n_{II} + n_{III}) is equal to one. B₁^u and B₂^u are the constants from the Karplus equation uncorrected for electronegativity effects and have values of B₁^u = 13.2Hz and B₂^u = 17.4Hz. The parameters a=0.13, b=-0.35 and c=-0.06 are derived from the equations of Pachler and weigh the effect of the electronegativity differences of substituents gauche to a gauche HCCH unit ($\Delta\chi_i$), anti to a gauche HCCH unit ($\Delta\chi_j$) and gauche to an anti HCCH unit ($\Delta\chi_k$) as shown in Figure 48.

Figure 48 Diagram for the Calculation of Electronegativity Values.



The electronegativity differences are calculated from the values given in Table 1.

Table 1 Substituent electronegativity values

Calculated using Refs 121, 127 and 128

| Substituent | Group electronegativity | Δ_x |
|------------------------------|-------------------------|------------|
| H | 2.15 | 0 |
| NH ₂ | 2.91 | 0.76 |
| NH ₃ ⁺ | 3.66 | 1.51 |
| COOH | 2.60 | 0.45 |
| COO ⁻ | 2.48 | 0.33 |
| Im | 2.55 | 0.40 |
| ImH ⁺ | 2.73 | 0.58 |

In order to be able to calculate the mole fractions of the three rotamers of *N*-acetyl-L-histidine and its anion, it is necessary to insert values for the $\alpha\beta$ and $\alpha\beta'$ vicinal coupling constants and the dihedral angles ($\phi_{\alpha\beta}$ and $\phi_{\alpha\beta'}$) for each conformation in to Equations 5 and 6 and solve them for n_I , n_{II} and n_{III} using $n_I + n_{II} + n_{III} = 1$ as the third simultaneous equation. The vicinal coupling constants can be obtained from the ¹H NMR spectrum. The biggest influence on the vicinal coupling constant is the dihedral angle whilst electronegativity effects are relatively minor by comparison.¹²¹ Since there were no suitable methods available for determining the average dihedral angles at the time of their study, Weinkam and Jorgensen made assumptions for the dihedral angles based on the possibility of interaction between the carboxylate and imidazole groups. Any error in the assumed values could significantly alter the calculated conformer populations. Good molecular modelling techniques are now available and it is possible to obtain more realistic values for the dihedral angles in each conformation.

2.3 Calculation of $\alpha\beta$ and $\alpha\beta'$ Coupling Constants using ^1H NMR Spectroscopy.

2.3.1 Choice of Molecules.

The aim of this study was to determine the conformational properties of the zwitterion and anion of *N*-acetyl-L-histidine. In both the zwitterion and tautomer A of the anion there is the possibility of forming a hydrogen bond between the N-H of the imidazole ring and the carboxylate group, see Figure 47. In tautomer B of the anion this hydrogen bond is not able to form. The anion of *N*-acetyl-L-phenylalanine differs from tautomer B in the substitution of a phenyl ring for the imidazole ring. Since these two groups have similar steric requirements and no possibility of hydrogen bond formation with the carboxylate group these two compounds should have similar conformational properties. Although all four of these compounds can be readily modelled it is not possible to study tautomers A and B experimentally. However, *N*-acetyl-L-histidine and *N*-acetyl-L-phenylalanine can be studied experimentally and used as models for tautomers A and B respectively.

In order to determine the mole fraction of each staggered conformation from the Karplus equation discussed in the previous section, ^1H NMR spectra were required for *N*-acetyl-L-histidine and the corresponding sodium and tetra-*n*-butylammonium salts. Two different cations were studied as the formation of intimate ion pairs could significantly alter the conformational properties of the anion. It was expected that intimate ion pairs would play a much smaller role for the tetra-*n*-butylammonium salt because of the large size of the alkyl groups. Similarly the ^1H NMR spectra of the sodium and tetra-*n*-butylammonium salts of *N*-acetyl-L-phenylalanine were also needed.

2.3.2 Association of Molecules in Solution.

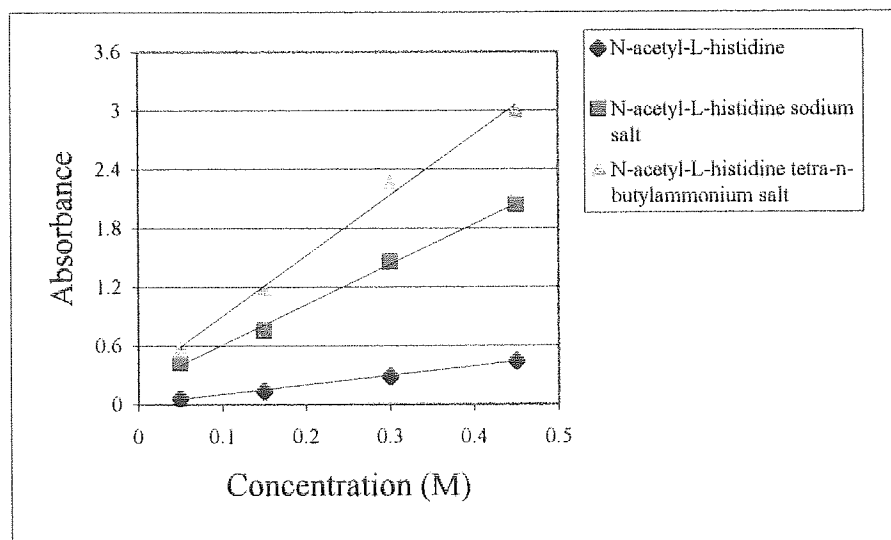
In order to study the interaction between the carboxylate group and imidazole ring it is necessary to ensure that the molecules being studied are monomeric in solution. Therefore it must be determined at what concentrations the relationship between molecule concentration and UV absorbance is linear. A plot of concentration against absorbance in the UV spectrum will show a linear relationship if there is no association.

Aqueous solutions of *N*-acetyl-L-histidine and its sodium and tetra-*n*-butylammonium salts were measured on the UV spectrometer at 260.0 nm for *N*-acetyl-L-histidine, 390.4 nm for *N*-

acetyl-L-histidine sodium salt and 285.0 nm for *N*-acetyl-L-histidine tetra-*n*-butylammonium salt.

The results are shown in Figure 49.

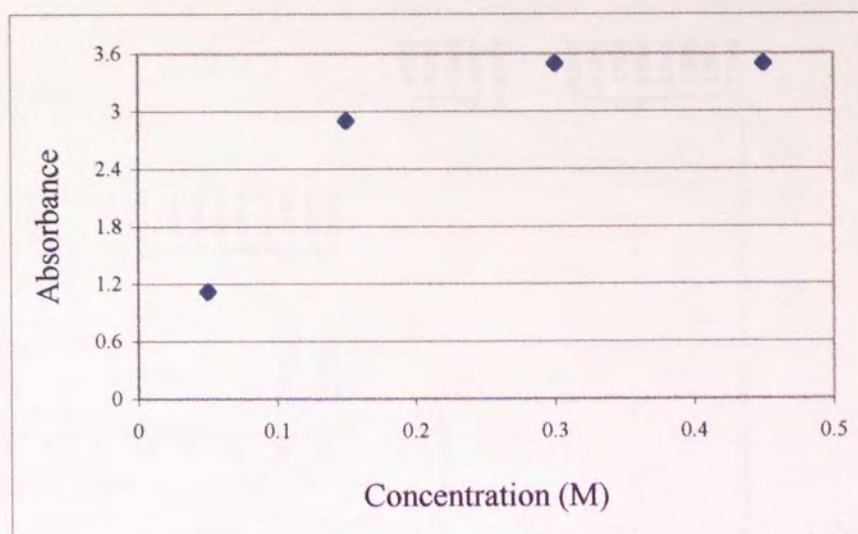
Figure 49 Association of *N*-Acetyl-L-Histidine and its Salts.



Since the absorbance for each of these molecules showed a linear dependence on concentration, it can be concluded that they are monomeric in aqueous solution at these concentrations.

In contrast *N*-acetyl-L-phenylalanine tetra-*n*-butylammonium salt would not dissolve in water at these concentrations and consequently could not be used for these studies. Aqueous solutions of *N*-acetyl-L-phenylalanine sodium salt were studied by UV spectroscopy at 257.6 nm at the concentrations used in the previous experiment. The results are shown in Figure 50.

Figure 50 Association of *N*-Acetyl-L-Phenylalanine Sodium salt.

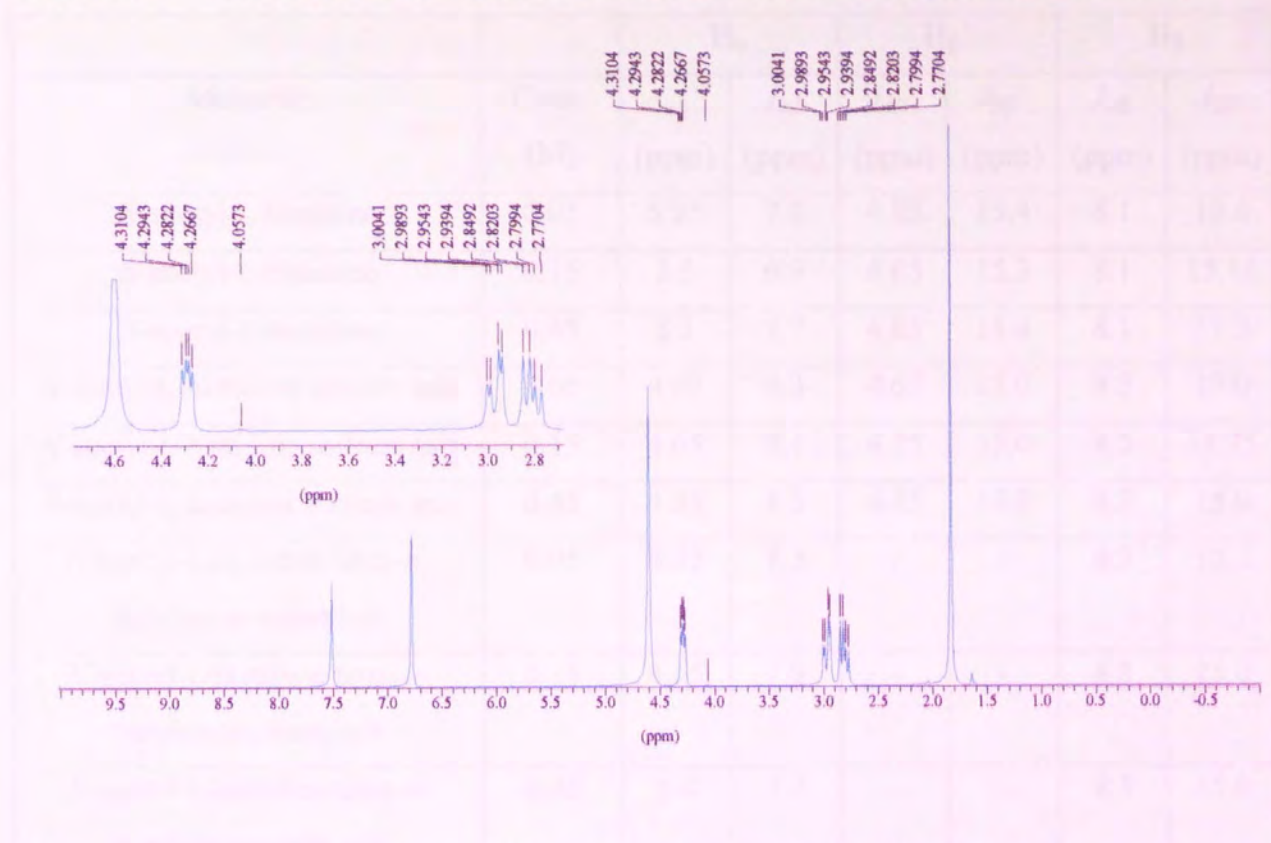


It is clear from Figure 50 that the sodium salt of *N*-acetyl-L-phenylalanine shows a non-linear dependence of absorbance with concentration. Consequently NMR studies of this molecule were not possible.

2.3.3 Vicinal Coupling Constants.

^1H NMR spectra were obtained for *N*-acetyl-L-histidine and the corresponding sodium and tetra-*n*-butylammonium salts in D_2O at concentrations of 0.05 M, 0.15 M and 0.45 M. All of the spectra were similar and a typical example is shown in Figure 51.

Figure 51 ^1H NMR Spectrum of *N*-Acetyl-L-histidine Sodium Salt in D_2O at 0.45 M.



Using the notation of Weinkam and Jorgensen, the double doublets at 4.3 ppm and the two double doublets at 2.8 and 3.0 ppm were assigned to the H_α , H_β' and H_β protons respectively. The $\alpha\beta$ and $\alpha\beta'$ coupling constants were determined by analysis of these signals. The other molecules were analysed in the same way.

The coupling constants calculated from these spectra are shown in Table 2.

Table 2 Coupling Constants for H_{α} , H_{β} and $H_{\beta'}$ Protons of Amino Acid Derivatives.

| Molecule | Conc. (M) | H_{α} | | $H_{\beta'}$ | | H_{β} | |
|--|--------------|-----------------------------|----------------------------|-----------------------------|----------------------------|----------------------------|----------------------------|
| | | $J_{\alpha\beta'}$ (ppm) | $J_{\alpha\beta}$ (ppm) | $J_{\alpha\beta'}$ (ppm) | $J_{\beta\beta'}$ (ppm) | $J_{\alpha\beta}$ (ppm) | $J_{\beta\beta'}$ (ppm) |
| <i>N</i> -acetyl-L-histidine | 0.05 | 5.25 | 7.5 | 4.85 | 15.4 | 8.1 | 15.4 |
| <i>N</i> -acetyl-L-histidine | 0.15 | 5.5 | 6.9 | 4.65 | 15.2 | 8.1 | 15.15 |
| <i>N</i> -acetyl-L-histidine | 0.45 | 5.3 | 7.7 | 4.85 | 15.4 | 8.1 | 15.2 |
| <i>N</i> -acetyl-L-histidine sodium salt | 0.05 | 4.65 | 8.3 | 4.65 | 15.0 | 8.5 | 15.0 |
| <i>N</i> -acetyl-L-histidine sodium salt | 0.15 | 4.65 | 8.1 | 4.25 | 15.0 | 8.5 | 14.75 |
| <i>N</i> -acetyl-L-histidine sodium salt | 0.45 | 4.85 | 8.5 | 4.45 | 15.0 | 8.7 | 15.0 |
| <i>N</i> -acetyl-L-histidine tetra- <i>n</i> -butylammonium salt | 0.05 | 4.85 | 8.3 | - | - | 8.5 | 15.2 |
| <i>N</i> -acetyl-L-histidine tetra- <i>n</i> -butylammonium salt | 0.15 | 4.65 | 7.9 | - | - | 8.5 | 15.0 |
| <i>N</i> -acetyl-L-histidine tetra- <i>n</i> -butylammonium salt | 0.45 | 4.4 | 7.7 | - | - | 8.5 | 15.0 |

In all spectra the signal assigned to H_{α} was only just resolved. It was possible to measure the vicinal coupling constants from this signal but the better resolved H_{β} and $H_{\beta'}$ signals are more likely to give accurate measurements. Where possible the vicinal coupling constants calculated from these signals were used in further calculations. Unfortunately, in the spectra obtained for the *N*-acetyl-L-histidine tetra-*n*-butylammonium salt, a signal at 3.0 ppm attributable to the tetra-*n*-butylammonium cation, covers part of the $H_{\beta'}$ signal. It was therefore necessary to derive the coupling constants from a combination of the H_{α} and H_{β} signals. The coupling constant with the value of approximately 15 Hz was attributed to the geminal coupling between the H_{β} and $H_{\beta'}$ protons.

There is no clear trend between the coupling constants and the change in concentration of the molecules being studied. The UV studies indicated that these molecules were monomeric at all of these concentrations and so the coupling constant was calculated from the average of the coupling constants at all three concentrations. The results are shown in Table 3.

Table 3 Average Coupling Constants for H_{α} , H_{β} and $H_{\beta'}$ Protons of Amino Acid Derivatives.

| Molecule | H_{α} | | $H_{\beta'}$ | | H_{β} | |
|--|--|---|--|------------------------------|---|-------------------------------|
| | $J_{\alpha\beta'}$ (ppm) | $J_{\alpha\beta}$ (ppm) | $J_{\alpha\beta'}$ (ppm) | $J_{\beta\beta'}$ (ppm) | $J_{\alpha\beta}$ (ppm) | $J_{\beta\beta'}$ (ppm) |
| <i>N</i> -acetyl-L-histidine | 5.35 (4.4 ^a , 5.0 ^b) | 7.4 (9.0 ^a , 8.5 ^b) | 4.8 (4.4 ^a , 5.0 ^b) | 15.3 (15.0 ^b) | 8.1 (9.0 ^a , 8.5 ^b) | 15.25 (15.0 ^b) |
| <i>N</i> -acetyl-L-histidine sodium salt | 4.7 (4.1 ^a , 4.6 ^b) | 8.3 (9.7 ^a , 8.7 ^b) | 4.45 (4.1 ^a , 4.6 ^b) | 15.0 (15.0 ^b) | 8.6 (9.7 ^a , 8.7 ^b) | 14.9 (15.0 ^b) |
| <i>N</i> -acetyl-L-histidine tetra- <i>n</i> -butylammonium salt | 4.6 | 8.0 | - | - | 8.5 | 15.1 |

a – value obtained from ref 121 at 0.15M in D₂O.

b – value obtained from ref 126 at 0.30M in D₂O.

It is clear from this table that the vicinal and geminal coupling constants are in good agreement with those reported previously and were particularly close to those reported by Espersen and Bruce-Martin.¹²⁶ It is clear from the close similarities of the data obtained for the sodium and tetra-*n*-butylammonium salts that the cation appears to play no significant role in determining the populated conformations.

2.4 Calculation of Dihedral Angles using Molecular Modeling.

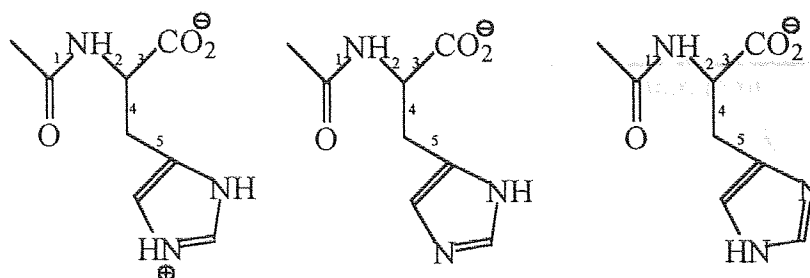
2.4.1 Molecular Modeling.

The molecular modeling was carried out using the AMBER forcefield, a forcefield that has been specifically designed for proteins and nucleic acids.

2.4.2 Conformational Searches.

The starting point for the molecular modeling studies was a thorough search of the conformational space for the molecules shown in Figure 52 using molecular mechanics calculations.

Figure 52 N-Acetyl-L-histidine Zwitterion and Unprotonated Forms.



These calculations were carried out using the AMBER forcefield using a random conformational search method in which random changes in the torsional angles around the single bonds 1-5 were used to generate new starting structures. Minima were assumed to have been reached when the gradient was below 0.01 kcal/Åmol. 5000 minimisations were carried out for each molecule. Each conformation within 2.4 kcalmol⁻¹ of the lowest energy conformation was found at least 12 times suggesting that the conformational space had been completely explored. Conformations more than 2.4 kcalmol⁻¹ above the lowest are insignificantly populated at room temperature and were not considered further. It is possible to calculate mole fractions from the calculated energies using the Boltzmann distribution.

Equation 7 Boltzmann Distribution.

$$N_i / N_j = e^{-(\epsilon_i - \epsilon_j)/kT}$$

Where N_i/N_j is the ratio of the numbers of particles i and j , ϵ_i and ϵ_j the energies of particles i and j , k is the Boltzmann constant and T is the thermodynamic temperature.

The NH and OH bond lengths and NO distance and the NHO bond angle were also analysed to identify the presence of any hydrogen bonds. The results of this study are shown in Table 4 along with the lowest energy examples of any conformations unpopulated at room temperature.

Table 4 Conformations of L-Histidine and L-Phenylalanine Derivatives in the Gas Phase.

| Molecule | Conformer | Energy (kcal/ mol) | Mole fraction | Interatomic distances (Å) | | | Bond angle (°) |
|---|-----------|--------------------------|------------------|------------------------------|------|------|-------------------|
| | | | | NH | HO | NO | NHO |
| <i>N</i> -acetyl-L-histidine | II | 0.00 | 0.55 | 1.03 | 1.64 | 2.56 | 147 |
| <i>N</i> -acetyl-L-histidine | III | 0.27 | 0.35 | 1.03 | 1.67 | 2.60 | 149 |
| <i>N</i> -acetyl-L-histidine | III | 1.01 | 0.10 | 1.03 | 1.71 | 2.56 | 137 |
| <i>N</i> -acetyl-L-histidine | I | 9.64 | - | - | - | - | - |
| <i>N</i> -acetyl-L-histidine anion, Tautomer A | II | 0.00 | 0.46 | 1.02 | 1.71 | 2.62 | 147 |
| <i>N</i> -acetyl-L-histidine anion, Tautomer A | III | 0.14 | 0.37 | 1.02 | 1.74 | 2.66 | 149 |
| <i>N</i> -acetyl-L-histidine anion, Tautomer A | III | 0.67 | 0.15 | 1.02 | 1.74 | 2.66 | 149 |
| <i>N</i> -acetyl-L-histidine anion, Tautomer A | III | 2.27 | 0.01 | 1.02 | 1.84 | 2.67 | 136 |
| <i>N</i> -acetyl-L-histidine anion, Tautomer A | II | 2.30 | 0.01 | 1.02 | 1.71 | 2.63 | 147 |
| <i>N</i> -acetyl-L-histidine anion, Tautomer A | I | 4.44 | - | - | - | - | - |
| <i>N</i> -acetyl-L-histidine anion, Tautomer B | III | 0.00 | 0.65 | - | - | - | - |
| <i>N</i> -acetyl-L-histidine anion, Tautomer B | II | 0.65 | 0.22 | - | - | - | - |
| <i>N</i> -acetyl-L-histidine anion, Tautomer B | II | 1.12 | 0.10 | - | - | - | - |
| <i>N</i> -acetyl-L-histidine anion, Tautomer B | I | 1.84 | 0.03 | - | - | - | - |
| <i>N</i> -acetyl-L- phenylalanine anion | III | 0.00 | 0.74 | - | - | - | - |
| <i>N</i> -acetyl-L- phenylalanine anion | I | 0.91 | 0.16 | - | - | - | - |

| | | | | | | | |
|--|----|------|------|---|---|---|---|
| <i>N</i> -acetyl-L-phenylalanine anion | II | 1.22 | 0.10 | - | - | - | - |
|--|----|------|------|---|---|---|---|

For all the molecules studied only the three staggered conformations were found to be populated at room temperature. Small conformational changes in the substituent groups were responsible for finding several minimum energy conformations for each of the basic conformations I-III. The overall mole fractions are shown in Table 5.

Table 5 Overall Mole Fractions.

| Molecule | Mole Fraction | | |
|---|----------------|-----------------|------------------|
| | Conformation I | Conformation II | Conformation III |
| <i>N</i> -Acetyl-L-histidine | 0.00 | 0.55 | 0.45 |
| <i>N</i> -Acetyl-L-histidine anion, Tautomer A | 0.00 | 0.47 | 0.53 |
| <i>N</i> -Acetyl-L-histidine anion, Tautomer B | 0.03 | 0.32 | 0.65 |
| <i>N</i> -Acetyl-L-phenylalanine anion | 0.16 | 0.10 | 0.74 |

For both *N*-acetyl-L-histidine and tautomer A of the corresponding anion conformation II was found to be the minimum energy conformation, with conformation III somewhat higher in energy. Significantly, the lowest energy arrangement for conformation I in each case was so high in energy that it would not be significantly populated at room temperature.

Another common feature of these two systems was that in all arrangements for conformations II and III the N-H, O-H and NO distances and the NHO bond angle were remarkably similar and well within the parameters required for hydrogen bond formation.¹²⁹

N-Acetyl-L-phenylalanine anion and tautomer B of *N*-acetyl-L-histidine also showed similarities in the conformations that are populated at room temperature. For both of these systems all three conformations were populated at room temperature. There was no evidence of hydrogen bond formation for tautomer B.

2.4.3 Molecular Dynamics Calculations.

Although the conformations found in the molecular mechanics studies could be used for obtaining the $H_{\alpha}-H_{\beta}$ and $H_{\alpha}-H_{\beta'}$ dihedral angles, this approach takes no account of the dynamic properties of the molecule. Also these calculations are essentially for molecules in the gas phase and no account is taken of the solvent. Molecular dynamics calculations can be used to model these properties. Since NMR spectroscopy only detects the average dihedral angle over the time of the experiment, molecular dynamics calculations of each of the conformations I-III in a periodic box of water can be used to calculate the average dihedral angles for these conformations.

The lowest energy arrangements for each of the conformations I-III obtained from molecular mechanics calculations were used for molecular dynamics simulations. Initially, the solute was placed within a periodic box filled with water molecules. There are two stages involved in obtaining data using molecular dynamics. The first is the equilibration phase, which involves bringing the system to equilibrium from the starting configuration. For an inhomogeneous system such as the system being studied in this work, the solvent alone is first subject to energy minimization with the solute kept in its initial conformation. The solvent is then allowed to evolve using molecular dynamics, with the solute again kept in its initial conformation. This equilibration should be long enough to allow the solvent to completely readjust to the potential field of the solute molecule. The equilibration should be longer than the relaxation time of the solvent (the time taken for a molecule to lose any 'memory' of its original orientation, which for water is about 10 ps).¹³⁰ After this, the entire system must be minimized. It is then possible to start the molecular dynamics calculations for the whole system. At the start of the production phase, the system is allowed to evolve.

During the equilibration phase the system was heated from 100-300 K over 1 ps then kept at 300 K for 15 ps in order for the water to lose its 'memory' of its initial orientation. During the production phase, the system was heated from 100-300 K over 0.1 ps and then kept at 300 K for 50 ps with a data point recorded every 0.0025 ps. This gave 20000 data points for the $\alpha\beta$ and $\alpha\beta'$ dihedral angles from which mean values for the 50 ps of the simulation could be calculated. The results are shown in Table 6.

Table 6 Conformational Dihedral Angles.

| Molecule | Conformer | Dihedral Angles (°) | |
|---|-----------|---------------------|----------------|
| | | $\alpha\beta$ | $\alpha\beta'$ |
| <i>N</i> -acetyl-L-histidine | I | 283 | 166 |
| <i>N</i> -acetyl-L-histidine | II | 190 | 73 |
| <i>N</i> -acetyl-L-histidine | III | 46 | 290 |
| <i>N</i> -acetyl-L-histidine anion, Tautomer A | I | 289 | 171 |
| <i>N</i> -acetyl-L-histidine anion, Tautomer A | II | 193 | 75 |
| <i>N</i> -acetyl-L-histidine anion, Tautomer A | III | 53 | 296 |
| <i>N</i> -acetyl-L-histidine anion, Tautomer B | I | 296 | 179 |
| <i>N</i> -acetyl-L-histidine anion, Tautomer B | II | 174 | 58 |
| <i>N</i> -acetyl-L-histidine anion, Tautomer B | III | 54 | 298 |
| <i>N</i> -acetyl-L-phenylalanine anion | I | 306 | 189 |
| <i>N</i> -acetyl-L-phenylalanine anion | II | 181 | 63 |
| <i>N</i> -acetyl-L-phenylalanine anion | III | 70 | 315 |

The dihedral angles used by Weinkam and Jorgensen were as follows. When steric requirements were thought to be important the dihedral angles were assigned as $\phi_{\alpha\beta}^I=295^\circ$, $\phi_{\alpha\beta}^{II}=185^\circ$, $\phi_{\alpha\beta}^{III}=60^\circ$, $\phi_{\alpha\beta'}^I=175^\circ$, $\phi_{\alpha\beta'}^{II}=65^\circ$, $\phi_{\alpha\beta'}^{III}=300^\circ$. When a carboxylate group/histidine ring interaction was thought to be most important the dihedral angles were assigned as $\phi_{\alpha\beta}^I=300^\circ$, $\phi_{\alpha\beta}^{II}=180^\circ$, $\phi_{\alpha\beta}^{III}=60^\circ$, $\phi_{\alpha\beta'}^I=180^\circ$, $\phi_{\alpha\beta'}^{II}=60^\circ$, $\phi_{\alpha\beta'}^{III}=300^\circ$.

The results from the modeling gave values for the dihedral angles $\alpha\beta$ and $\alpha\beta'$ which differed by up to 17° from those used by Weinkam and Jorgenson in their study. Consequently some differences in the mole fractions of conformation I-III can be expected when the dihedral angles obtained from this molecular modeling study are used. Another important observation from the molecular dynamics simulation was that all the hydrogen bonds identified in the initial conformations used remained intact throughout the simulation.

2.4.4 Calculation of Mole Fractions.

Inserting the average $\alpha\beta$ and $\alpha\beta'$ dihedral angles obtained for each conformation from the molecular modeling studies together with the $J_{\alpha\beta}$ and $J_{\alpha\beta}'$ coupling constants obtained from the ^1H NMR spectra into Equation 5 and Equation 6 allowed the mole fractions of conformations I-III for each molecule to be calculated. These results are shown in Table 7.

Table 7 Calculated Mole Fractions.

| Molecule | Salt | $J_{\alpha\beta'} > J_{\alpha\beta}$ | | | $J_{\alpha\beta} > J_{\alpha\beta}'$ | | |
|---|------|--|--|--|--------------------------------------|------------------------------|------------------------------|
| | | n_I | n_{II} | n_{III} | n_I | n_{II} | n_{III} |
| <i>N</i> -acetyl-L-histidine | - | 0.52 (0.50 ^a , 0.56 ^b) | 0.23 (0.15 ^a , 0.23 ^b) | 0.25 (0.35 ^a , 0.21 ^b) | 0.23 (0.13 ^a) | 0.41 (0.49 ^b) | 0.36 (0.38 ^b) |
| <i>N</i> -acetyl-L-histidine anion, Tautomer A | Na | 0.51 (0.54 ^a , 0.58 ^b) | 0.18 (0.13 ^a , 0.19 ^b) | 0.31 (0.33 ^a , 0.23 ^b) | 0.23 (0.09 ^b) | 0.47 (0.53 ^b) | 0.30 (0.38 ^b) |
| <i>N</i> -acetyl-L-histidine anion, Tautomer A | TBA | 0.51 (0.54 ^a , 0.58 ^b) | 0.18 (0.13 ^a , 0.19 ^b) | 0.31 (0.33 ^a , 0.23 ^b) | 0.24 (0.09 ^b) | 0.47 (0.53 ^b) | 0.29 (0.38 ^b) |
| <i>N</i> -acetyl-L-histidine anion, Tautomer B | Na | 0.46 | 0.12 | 0.42 | 0.13 | 0.42 | 0.45 |
| <i>N</i> -acetyl-L-histidine anion, Tautomer B | TBA | 0.46 | 0.13 | 0.41 | 0.14 | 0.41 | 0.45 |

a – value obtained from ref 121.

b – value obtained from ref 126.

Recorded in Table 7 are mole fractions calculated when $J_{\alpha\beta'} > J_{\alpha\beta}$ and $J_{\alpha\beta} > J_{\alpha\beta}'$. These are similar to those values obtained by Weinkam and Jorgensen. The mole fractions they obtained using the assumption that $J_{\alpha\beta'} > J_{\alpha\beta}$ were found to be in the order of $n_I > n_{II} > n_{III}$. This order did not fit those which should be obtained if a carboxylate group/imidazole ring interaction is the most important factor ($n_{II} \approx n_{III} > n_I$), steric and electrostatic repulsion are the most important factors ($n_{II} > n_I > n_{III}$) or a combination of a carboxylate group/imidazole ring interaction and steric factors ($n_{II} > n_I \approx n_{III}$). Similar results were obtained in this study when the dihedral angles were calculated using molecular modeling. These results discount $J_{\alpha\beta'} > J_{\alpha\beta}$ as a valid assumption.

The conformation order of $n_{II} > n_{III} > n_I$ that Weinkam and Jorgensen obtained for $J_{\alpha\beta} > J_{\alpha\beta}'$ allowed them to rule out steric and electrostatic repulsion as important factors in affecting the vicinal coupling constant and to claim that a carboxylate group/imidazole ring interaction is the dominant factor. The results obtained for the zwitterion and Tautomer A bear out these conclusions though there are some differences. The population of conformation I was found to be approximately twice that previously obtained. This would indicate that steric factors are more important in these molecules than was thought. These results also show that the *N*-acetyl-L-histidine zwitterion is a good model for Tautomer A of the *N*-acetyl-L-histidine anion.

The conformation populations obtained for Tautomer B ($n_{II} \approx n_{III} > n_I$) would indicate that the only factor affecting the conformation population is a carboxylate group/imidazole ring interaction. However, in this tautomer no interaction should be possible, so steric factors should be most dominant. The results for Tautomer B are difficult to rationalize if steric factors are important. The only explanation for these results are that for this molecule Tautomer B is not present in solution.

The results for both Tautomers A and B show that, as also seen in the coupling constants, the counterion of the salts of *N*-acetyl-L-histidine has little effect.

Chapter 3 Hydrolysis Studies – Small Molecules.

3.0 Hydrolysis Studies - Small Molecules.

The encouraging results obtained from the study of the conformations of *N*-acetyl-L-histidine and its anion suggested that there was an attractive interaction (probably a hydrogen bond) between the imidazole ring and the carboxylate group in both the zwitterion and anion. This study suggested that this interaction could enhance the catalytic ability of these molecules when they are used in the hydrolysis of *p*-nitrophenyl acetate.

It is necessary to look at the differences in the rate of hydrolysis between a catalyst containing just an imidazole group and then one containing both the imidazole and carboxylate functions in order to see if there is any interaction between them similar to that present in the serine protease catalytic triad.

3.1 Hydrolysis in pH 7.0, 7.6 and 8.0 Buffer Solutions.

All of the reactions were carried out in potassium dihydrogen phosphate/disodium phosphate buffer, ionic strength $\mu=0.1$ (KCl), at 25 ± 0.1 °C and are the average of three separate determinations. All of the hydrolysis experiments were carried out using the pseudo first order method used by Ihara et al.¹²⁰

3.1.1 Calibration.

p-Nitrophenyl acetate is commonly used in kinetic studies of ester hydrolysis and the hydrolysis can be easily followed by recording the UV absorbance at 410 nm. In order to conduct the kinetic experiments it is necessary that the variation of *p*-nitrophenol concentration with UV absorbance is linear. Conversion of absorbance into concentration enables calculation of the observed rate. The UV absorbance at 410 nm at varying concentrations of *p*-nitrophenol were measured in pH 7.0, 7.6 and 8.0 buffer solutions. The results of these calibrations showed that at pH 7.0, 7.6 and 8.0, the absorbance was proportional to the concentration of *p*-nitrophenol below a concentration of 4.0×10^{-4} M. Therefore it was possible to carry out the hydrolysis experiments in these solutions below this concentration.

The conformational studies were carried out for a single unassociated *N*-acetyl-L-histidine molecule. The imidazole ring carboxylate group interaction predicted by this study depended on the catalysts being in a monomeric unassociated form. Neuvonen and Neuvonen¹³¹ have

shown that in a similar system, *cis*-urocanic acid associated above a certain concentration. It was therefore necessary to discover if the catalysts in this study were associating in the buffered solution. In order to determine this, the UV absorbance of imidazole and *N*-acetyl-L-histidine were measured at varying catalyst concentrations. The absorbances were measured at 278.0 nm for imidazole and 224.8 nm for *N*-acetyl-L-histidine. The region of the plot in which the catalyst concentration was proportional to the absorbance were the concentrations at which the *N*-acetyl-L-histidine was in a monomeric form. The plots carried out in both pH 7.0 and pH 8.0 were identical and the linear range was found to be below 1.50×10^{-3} M. In summary, the calibration and association experiments indicated that the hydrolysis experiments should be carried out below a concentration of 4.0×10^{-4} M of *p*-nitrophenyl acetate, and a concentration of 1.50×10^{-3} M of catalyst.

3.1.2 Hydrolysis of *p*-Nitrophenyl Acetate Without Catalyst.

Since imidazole based catalysts for ester hydrolysis are known to act via a nucleophilic mechanism, the practice of previous studies has been to carry out the hydrolyses using pseudo first order kinetics. The method used was that described by Ihara et al¹²⁰ in the study of micellar systems using an excess of the catalyst over *p*-nitrophenyl acetate. The only modification was to change the concentrations of catalyst and substrate because of the results of the calibration experiments.

Equation 8 Rate Equation for the Hydrolysis of *p*-Nitrophenol.

$$\frac{d[p - NP]}{dt} = k[\text{Cat}]$$

Where *p* - NP = *p*-nitrophenol

Cat = catalyst

It was necessary to calculate the rates of hydrolysis when there was no catalyst present in order to see whether there was any effect due to the presence of catalyst. If the catalyst does have an effect the rate of reaction will be greater than that in which there is no catalyst.

A *p*-nitrophenyl acetate solution was added to pH 7.0, 7.6 or 8.0 buffer solutions and the *p*-nitrophenol UV absorbance measured every minute for twenty minutes. The hydrolyses were carried out in triplicate and the results averaged. The results are shown in Table 8.

Table 8 Hydrolysis Rates for Uncatalysed Reactions.

| Solvent | Hydrolysis Rate (molL ⁻¹ s ⁻¹) | R ² |
|------------------------|--|----------------|
| pH 7.0 buffer solution | 6.76x10 ⁻¹⁰ ±0.06x10 ⁻¹⁰ | 0.987 |
| pH 7.6 buffer solution | 5.30x10 ⁻⁹ ±1.95x10 ⁻⁹ | 0.978 |
| pH 8.0 buffer solution | 1.26x10 ⁻⁸ ±0.06x10 ⁻⁸ | 0.973 |

The results show that the initial rate increased with increasing pH, and for all three pHs the initial rate of hydrolysis varied linearly with time. The rate of reaction can easily be determined by calculating the slope of concentration against time.

3.1.3 Hydrolysis of *p*-Nitrophenyl Acetate in Aqueous Buffer Solution.

Imidazole was used as a comparison to *N*-acetyl-L-histidine as its reactivity depends only on the imidazole ring. Any difference in the reactions catalysed by imidazole and *N*-acetyl-L-histidine can therefore be attributed to the presence of the carboxylate group in *N*-acetyl-L-histidine.

A *p*-nitrophenyl acetate solution was added to a catalyst solution. The UV absorbance of *p*-nitrophenol was then measured every minute for an hour. The experiment was repeated for both catalysts at five catalyst concentrations at pH 7.0, 7.6 and 8.0. All experiments were carried out in triplicate and the results averaged. The results are plotted in the following figures.

Figure 53 Hydrolysis in pH 7.0 Buffer Solution, Imidazole as Catalyst.

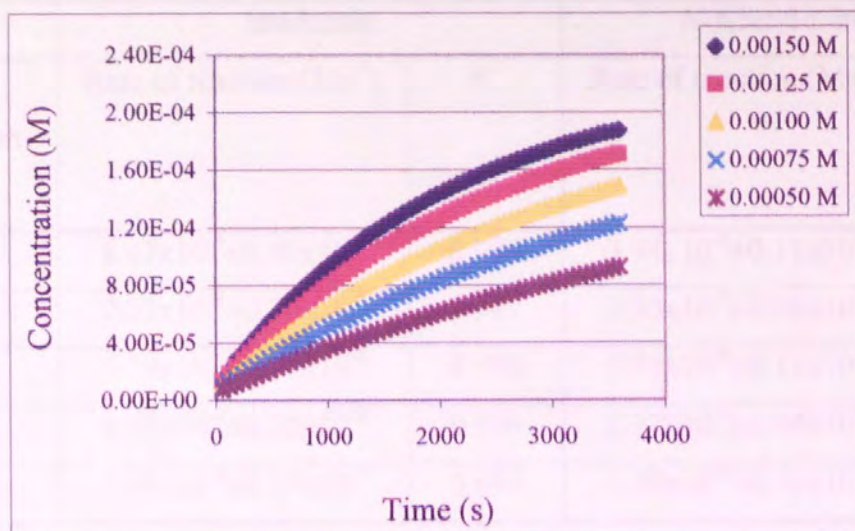
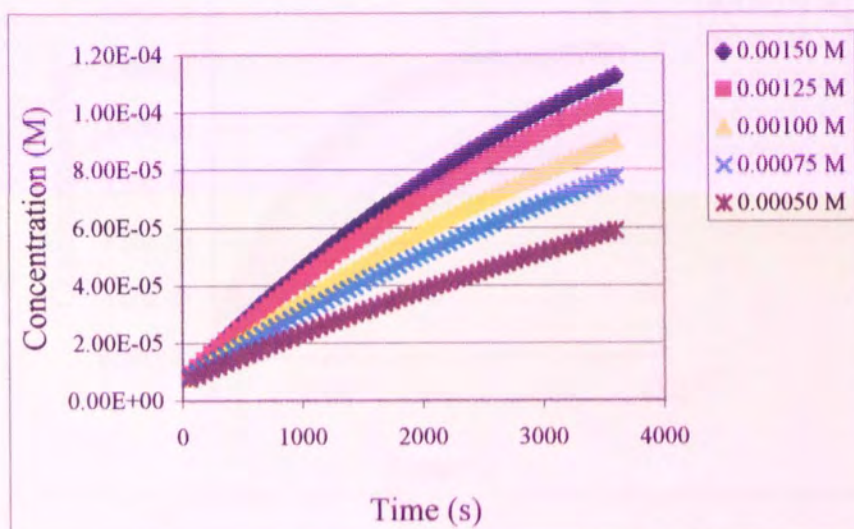


Figure 54 Hydrolysis in pH 7.0 Buffer Solution, *N*-Acetyl-L-histidine as Catalyst.



Below 900 seconds all these curves were linear and the slopes of these plots were used to calculate the initial rate of formation of *p*-nitrophenol, see Table 9.

Table 9 Rates of Reaction in pH 7.0 Buffer Solution.

| Catalyst concentration (M) | Imidazole | | N-Acetyl-L-histidine | |
|----------------------------|--|----------------|--|----------------|
| | Rate of reaction (Ms ⁻¹) | R ² | Rate of reaction (Ms ⁻¹) | R ² |
| 1.50x10 ⁻³ | 8.47x10 ⁻⁸ ±0.40x10 ⁻⁸ | 0.996 | 3.94x10 ⁻⁸ ±0.11x10 ⁻⁸ | 0.999 |
| 1.25x10 ⁻³ | 7.22x10 ⁻⁸ ±0.30x10 ⁻⁸ | 0.997 | 3.55x10 ⁻⁸ ±0.08x10 ⁻⁸ | 0.999 |
| 1.00x10 ⁻³ | 5.79x10 ⁻⁸ ±0.31x10 ⁻⁸ | 0.998 | 3.92x10 ⁻⁸ ±0.11x10 ⁻⁸ | 0.999 |
| 0.75x10 ⁻³ | 4.43x10 ⁻⁸ ±0.32x10 ⁻⁸ | 0.999 | 2.37x10 ⁻⁸ ±0.04x10 ⁻⁸ | 0.999 |
| 0.50x10 ⁻³ | 3.06x10 ⁻⁸ ±0.15x10 ⁻⁸ | 0.999 | 1.68x10 ⁻⁸ ±0.11x10 ⁻⁸ | 0.999 |

Figure 55 Hydrolysis in pH 7.6 Buffer Solution, Imidazole as Catalyst.

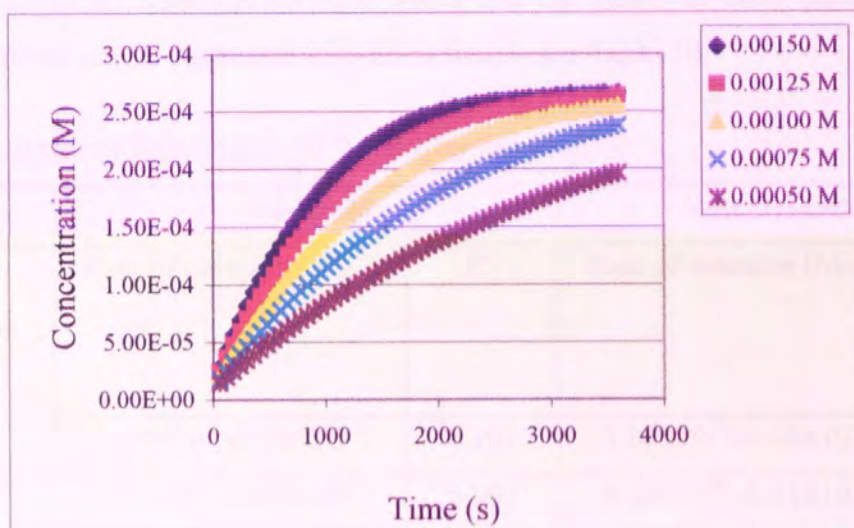
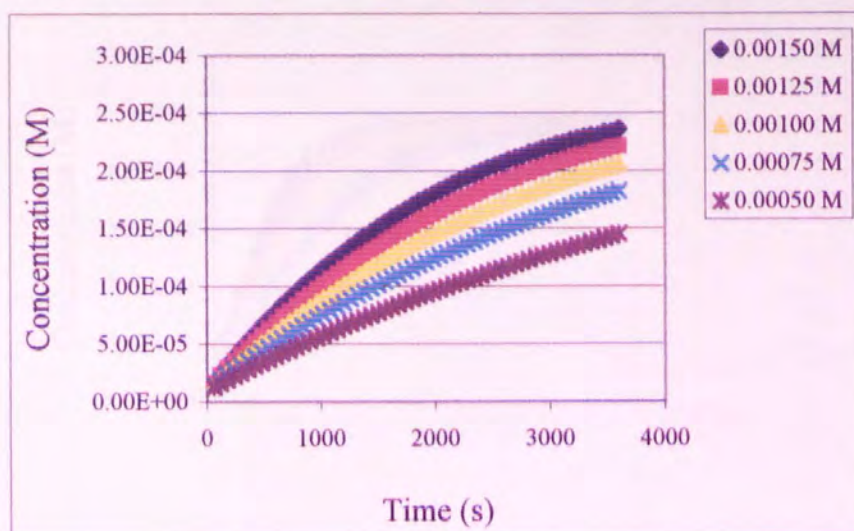


Figure 56 Hydrolysis in pH 7.6 Buffer Solution, *N*-Acetyl-L-histidine as Catalyst.



Below 900 seconds all these curves were linear and the slopes of these plots were used to calculate the initial rate of formation of *p*-nitrophenol, see Table 10.

Table 10 Rates of Reaction in pH 7.6 Buffer Solution.

| Catalyst concentration (M) | Imidazole | | <i>N</i> -Acetyl-L-histidine | |
|----------------------------|--|----------------|--|----------------|
| | Rate of reaction (Ms ⁻¹) | R ² | Rate of reaction (Ms ⁻¹) | R ² |
| 1.50x10 ⁻³ | 1.75x10 ⁻⁷ ±0.09x10 ⁻⁷ | 0.991 | 1.05x10 ⁻⁷ ±0.03x10 ⁻⁷ | 0.997 |
| 1.25x10 ⁻³ | 1.56x10 ⁻⁷ ±0.09x10 ⁻⁷ | 0.993 | 9.20x10 ⁻⁸ ±0.41x10 ⁻⁸ | 0.998 |
| 1.00x10 ⁻³ | 1.31x10 ⁻⁷ ±0.11x10 ⁻⁷ | 0.996 | 7.95x10 ⁻⁸ ±0.32x10 ⁻⁸ | 0.998 |
| 0.75x10 ⁻³ | 1.04x10 ⁻⁷ ±0.06x10 ⁻⁷ | 0.997 | 6.52x10 ⁻⁸ ±0.36x10 ⁻⁸ | 0.999 |
| 0.50x10 ⁻³ | 7.39x10 ⁻⁸ ±0.49x10 ⁻⁸ | 0.999 | 4.77x10 ⁻⁸ ±0.33x10 ⁻⁸ | 0.999 |

Figure 57 Hydrolysis in pH 8.0 Buffer Solution, Imidazole as Catalyst.

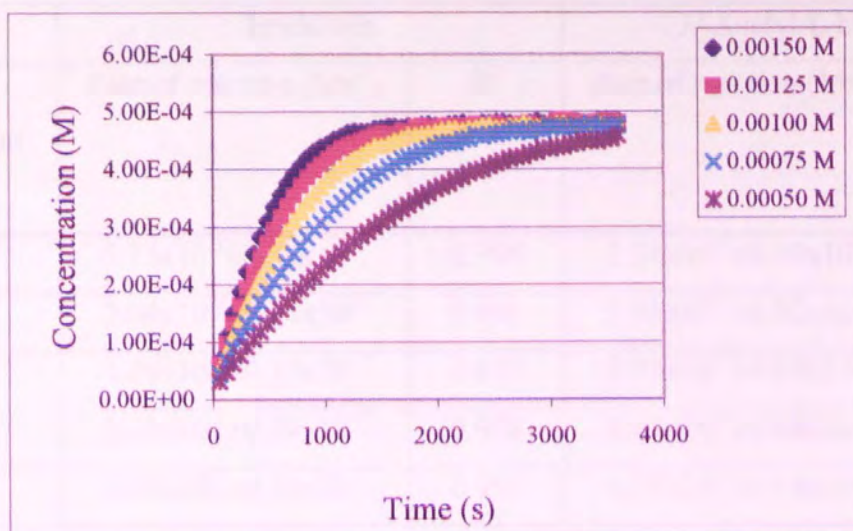
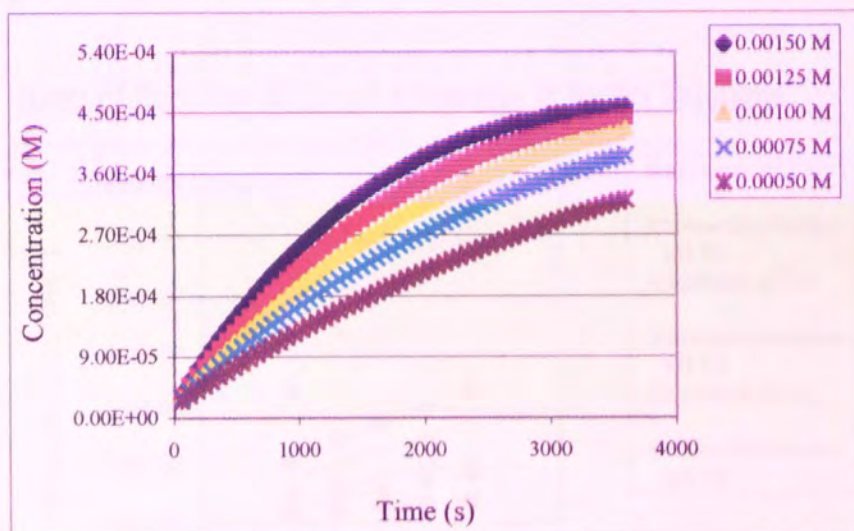


Figure 58 Hydrolysis in pH 8.0 Buffer Solution, *N*-Acetyl-L-histidine as Catalyst.



Below 480 seconds all these curves were linear and the slopes of these plots were used to calculate the initial rate of formation of *p*-nitrophenol, see Table 11.

Table 11 Rates of Reaction in pH 8.0 Buffer Solution.

| Catalyst concentration (M) | Imidazole | | N-Acetyl-L-histidine | |
|----------------------------|--|----------------|--|----------------|
| | Rate of reaction (Ms ⁻¹) | R ² | Rate of reaction (Ms ⁻¹) | R ² |
| 1.50x10 ⁻³ | 5.73x10 ⁻⁷ ±0.35x10 ⁻⁷ | 0.994 | 2.34x10 ⁻⁷ ±0.10x10 ⁻⁷ | 0.996 |
| 1.25x10 ⁻³ | 5.04x10 ⁻⁷ ±0.14x10 ⁻⁷ | 0.996 | 2.03x10 ⁻⁷ ±0.02x10 ⁻⁷ | 0.997 |
| 1.00x10 ⁻³ | 4.29x10 ⁻⁷ ±0.15x10 ⁻⁷ | 0.997 | 1.77x10 ⁻⁷ ±0.07x10 ⁻⁷ | 0.998 |
| 0.75x10 ⁻³ | 3.41x10 ⁻⁷ ±0.29x10 ⁻⁷ | 0.998 | 1.47x10 ⁻⁷ ±0.08x10 ⁻⁷ | 0.999 |
| 0.50x10 ⁻³ | 2.37x10 ⁻⁷ ±0.16x10 ⁻⁷ | 0.999 | 1.11x10 ⁻⁷ ±0.04x10 ⁻⁷ | 0.999 |

The rates of reaction from all of these experiments when plotted against the catalyst concentration gives the plot shown in Figure 59.

Figure 59 Rates of Reaction for Small Molecules in Buffer Solutions.

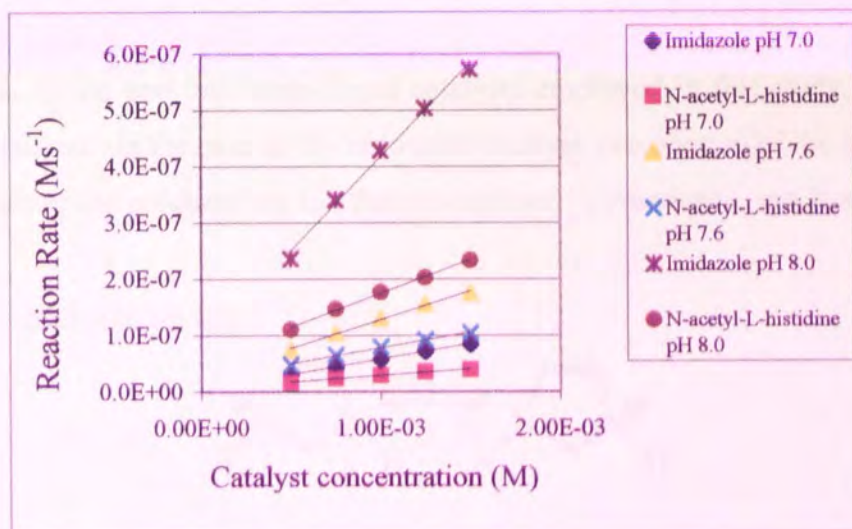


Figure 59 shows that there is a linear dependence of the rate of reaction on the concentration of catalyst. This means that the reaction fits the rate equation, and is first order with respect to the catalyst concentration. This means that the slope of the above plots corresponds to the rate constant, *k*. The rate constants are shown in Table 12.

Table 12 Rate Constants for Imidazole and *N*-Acetyl-L-histidine in Buffer Solutions.

| Buffer | Imidazole | | <i>N</i> -Acetyl-L-histidine | |
|--------|-------------------------------------|----------------|-------------------------------------|----------------|
| | Rate constant (s ⁻¹) | R ² | Rate constant (s ⁻¹) | R ² |
| pH 7.0 | 5.44x10 ⁻⁵ | 0.999 | 2.28x10 ⁻⁵ | 0.993 |
| pH 7.6 | 1.02x10 ⁻⁴ | 0.993 | 5.66x10 ⁻⁵ | 0.995 |
| pH 8.0 | 3.34x10 ⁻⁴ | 0.993 | 1.21x10 ⁻⁴ | 0.997 |

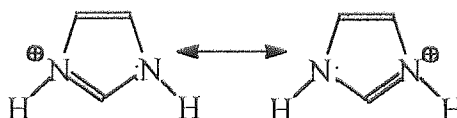
As can be seen from the values of the rate constant in Table 12 at all pHs the rate constant for imidazole is greater than that for *N*-acetyl-L-histidine and this can be explained by the differences in pK_a.

The experiments were carried out in buffered aqueous solution, so the carboxylic acid group would exist as a carboxylate anion. The pK_a of imidazole¹³² is 6.93 and that of *N*-acetyl-L-histidine¹³³ is 7.26. An acid dissociation in aqueous solution has the form:



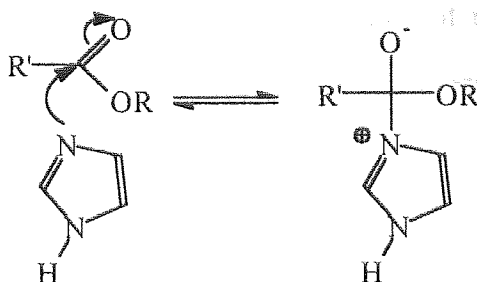
Below the pK_a of the two imidazole based catalysts employed in this study, the protonated form is predominant. In the case of the imidazole catalyst, protonation of the molecule results in the formation of the imidazolium ion that is stabilised by resonance, see Figure 60.

Figure 60 Imidazolium Ion.



As the pH of the medium becomes more acidic, the imidazolium ions predominate. The imidazole ring takes part in the nucleophilic catalysis of the hydrolysis of esters by attacking the electron deficient carbonyl carbon as shown in Figure 61.

Figure 61 Nucleophilic Catalysis.

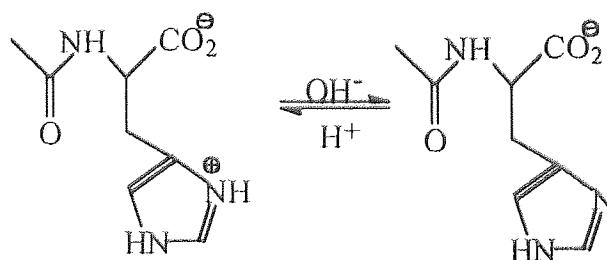


In order to act as a nucleophile, the imidazole ring needs the nitrogen (N-3) to possess a lone pair of electrons. Protonation of the imidazole ring to form the imidazolium ion means that the lone pair of electrons is involved in forming a bond to the proton, in effect deactivating the catalyst. Decreasing the alkalinity of the solution, increases the concentration of imidazolium ions and consequently decreases the efficiency of the catalyst.

The pK_a of imidazole at 25°C in aqueous solution is equal to 6.93. The reaction carried out at pH 7.0 would have an imidazole concentration roughly equal to the concentration of imidazolium ions. At higher pHs the concentration of imidazolium ions is lower and the concentration of the catalytically active imidazole molecules is higher. Consequently the rate of reaction increases with increasing pH of the solution.

The *N*-acetyl-L-histidine catalyst also has an imidazole functional group that is able to act as a nucleophile in ester hydrolysis. This means that the increase in the rate of reaction with increase in pH is also found for this catalyst.

Figure 62 Dissociation of *N*-Acetyl-L-histidine.



The pK_a of *N*-acetyl-L-histidine¹³³ is 7.26. At pH 7.0, the equilibrium will lie towards the protonated imidazole ring and the majority of catalyst molecules will be protonated. As the pH of the solution is increased the proportion of molecules with a protonated imidazole ring decreases, see Figure 62.

Protonated imidazole, having a lower pK_a than *N*-acetyl-L-histidine, is the stronger acid and at a given pH for the medium will have a higher proportion of the unprotonated form. The protonated form of both catalysts are deactivated as the lone pair of electrons on the ring is not free to form a bond to the substrate. So the more of this protonated form the less active the catalyst will be. Consequently *N*-acetyl-L-histidine would be expected to be a less effective catalyst than imidazole.

The conformational studies described in Chapter 2 suggested that in aqueous solution there is an attractive interaction between the carboxylate group and the imidazole ring in *N*-acetyl-L-histidine and the corresponding anion. Although an interaction between the carboxylate group and the imidazole ring of *N*-acetyl-L-histidine might be occurring in aqueous solution, its effect on the stabilisation of the transition state is clearly very small or even completely absent. Studies of ester hydrolysis with variety of imidazole systems^{26,27}, both with and without carboxylate groups have been found to lie on the same Brønsted plots indicating that the reaction mechanism depends entirely on the pK_a of the imidazole functional group. Water is polar and will form hydrogen bonds to polar and charged groups solvating the carboxylate group and imidazole ring and so weakening or even destroying the interaction between these groups.

3.2 Hydrolysis of *p*-Nitrophenyl Acetate in DMSO/H₂O 9:1 v/v Solution.

Clearly in aqueous solution the carboxylate group has little if any effect on the rate of reaction. In order to increase the magnitude of the stabilising effect that the carboxylate group has on the imidazole ring it is necessary to work in a less polar solvent. It was expected that a decrease in solvent polarity would lead to stronger H-bonding and electrostatic interactions between the carboxylate group and the imidazole ring. A DMSO/H₂O 9:1 v/v solution was chosen as a suitable solvent system to determine whether the carboxylate group/imidazole ring interaction occurs in a less polar solvent.

As it is not operating in a buffered system, *N*-acetyl-L-histidine will exist in a protonated form so it should be a poor catalyst. The *N*-acetyl-L-histidine anions synthesised for the conformational studies would have unprotonated imidazole rings and so should be better catalysts.

3.3 Synthesis of Anions.

Sodium salt

N-Acetyl-L-histidine was stirred overnight with an equimolar amount of 1.0 M aqueous sodium hydroxide solution. The solvent was removed and the salt dried using Dean and Stark apparatus.

Tetra-*n*-butylammonium salt

N-Acetyl-L-histidine was stirred overnight with an equimolar amount of 1.2 M aqueous tetra-*n*-butylammonium solution. The solvent was removed and the salt dried using Dean and Stark apparatus.

3.3.1 Calibration.

As in the case of the hydrolyses carried out in buffered aqueous solutions, it was necessary to ensure there was a linear relationship between the absorbance and concentration of *p*-nitrophenol.

The hydrolysis of *p*-nitrophenyl acetate produces a carboxylic acid and *p*-nitrophenol. As these experiments are carried out in an unbuffered system and the catalysts present are bases there will be a change in the proportion of the *p*-nitrophenolate ion. It is necessary to make sure that the relationship between the absorbance and concentration of *p*-nitrophenolate is linear in the presence of the catalysts.

The UV absorbance of *p*-nitrophenol at various concentrations were measured at 424.8 nm in the presence of imidazole. The same calibrations were carried out using *N*-acetyl-L-histidine, *N*-acetyl-L-histidine sodium salt and *N*-acetyl-L-histidine tetra-*n*-butylammonium salt. The results showed a linear relationship between the UV absorbance and the *p*-nitrophenol concentration in the presence of the catalysts.

As in the case with the buffered solutions it was necessary to discover if there was any association of the catalyst molecules in the solvent being used. In order to determine this, the UV absorbance of imidazole, *N*-acetyl-L-histidine and the *N*-acetyl-L-histidine salts were measured at a variety of catalyst concentrations. The absorbances of the catalysts were then measured. The results were found to give linear plots showing that for all molecules at the concentrations being used the catalysts were not associating, so it was then possible to carry out the hydrolysis experiments at these concentrations.

3.3.2 Hydrolysis of *p*-Nitrophenyl Acetate in DMSO/H₂O 9:1 v/v Solution.

It was necessary to carry out a hydrolysis without catalyst to ensure that the catalyst molecules increase the rate of reaction. A *p*-nitrophenyl acetate solution was added to a DMSO/H₂O 9:1 v/v solution and the *p*-nitrophenol UV absorbance measured every minute for an hour. No observable increase in the concentration of *p*-nitrophenol was measured over 1 hour.

A *p*-nitrophenyl acetate solution was added to a catalyst solution in DMSO/H₂O 9:1 v/v solution and the UV absorbance measured every minute for an hour. The experiment was repeated for all catalysts at five catalyst concentrations. The experiment was carried out in triplicate and the results averaged.

The results are plotted in the following figures.

Figure 63 Hydrolysis in DMSO/H₂O 9:1 v/v Solution, Imidazole as Catalyst.

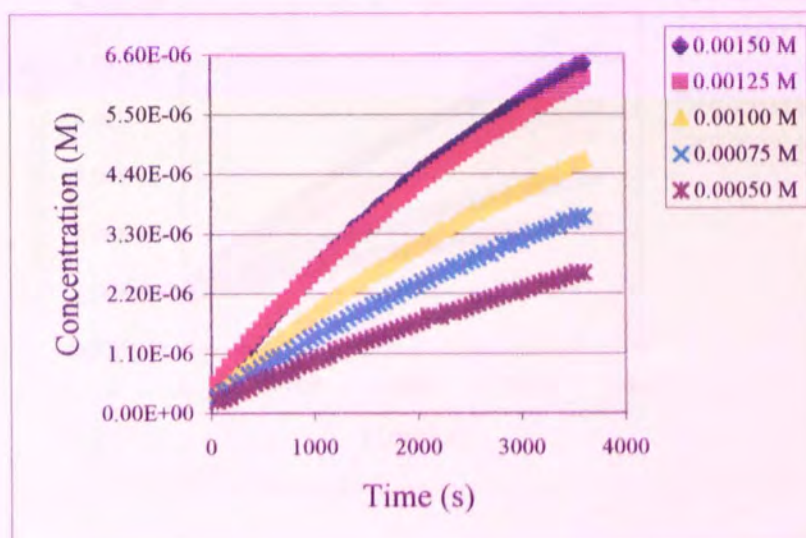


Figure 64 Hydrolysis in DMSO/H₂O 9:1 v/v Solution, *N*-Acetyl-L-histidine as Catalyst.

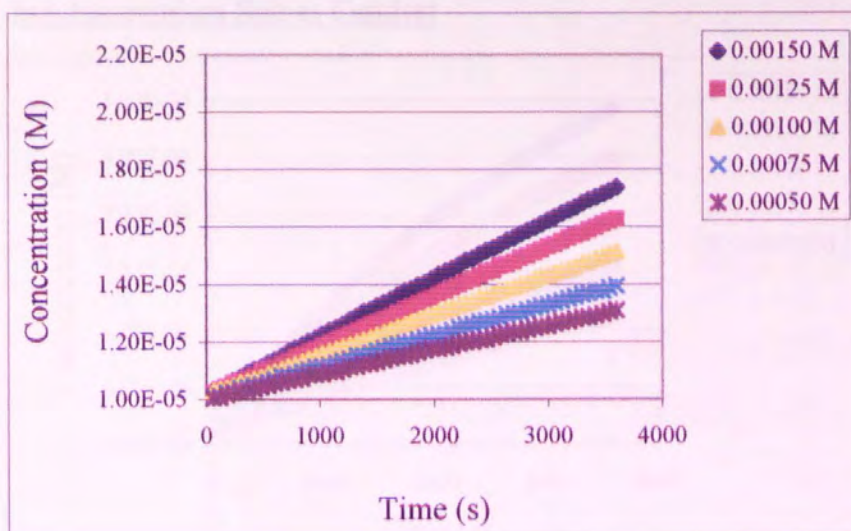


Figure 65 Hydrolysis in DMSO/H₂O 9:1 v/v Solution, *N*-Acetyl-L-histidine Sodium Salt as Catalyst.

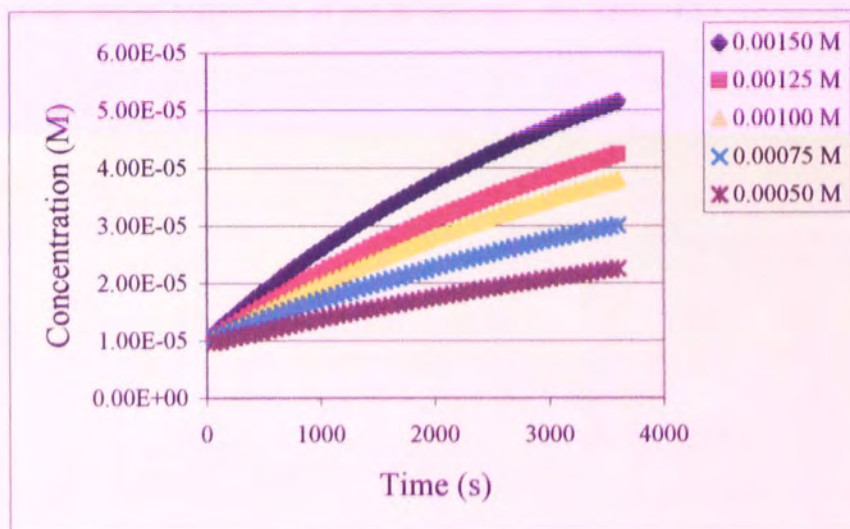
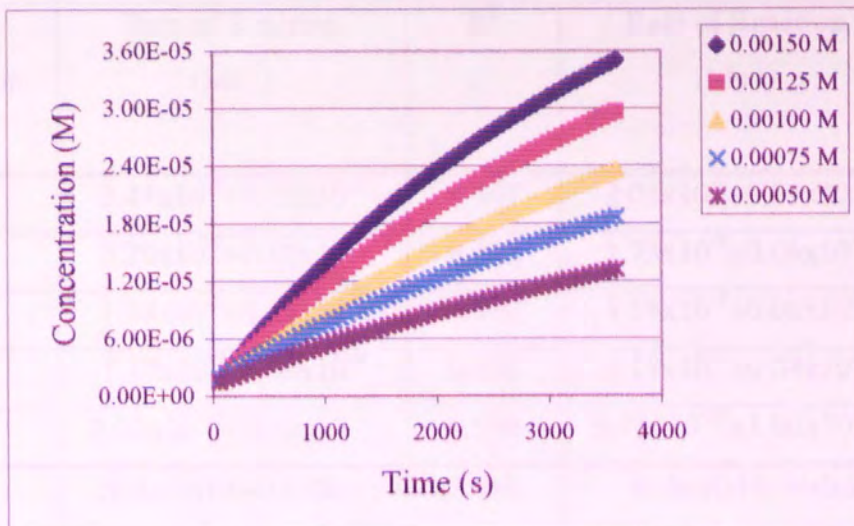


Figure 66 Hydrolysis in DMSO/H₂O 9:1 v/v Solution, *N*-Acetyl-L-histidine Tetra-*n*-butylammonium Salt as Catalyst



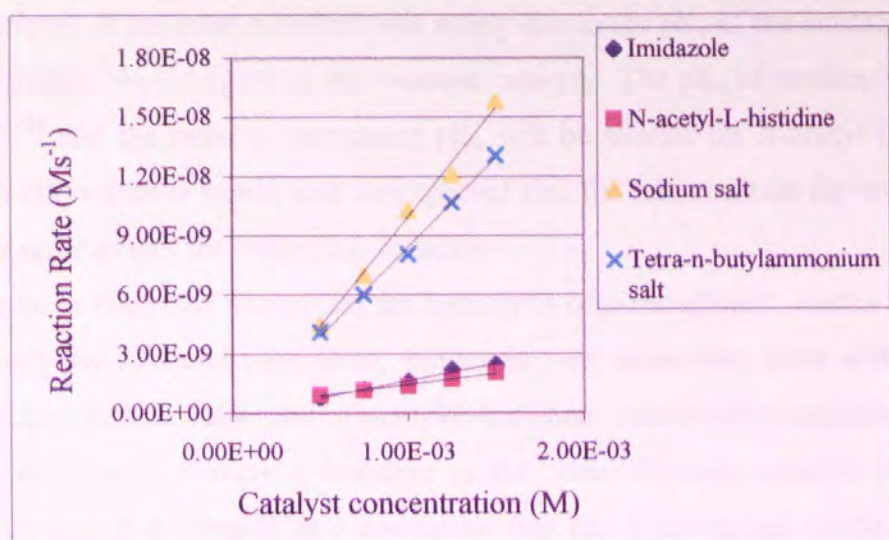
Below 900 seconds all these curves were linear and the slopes of these plots were used to calculate the initial rate of formation of *p*-nitrophenol, see Table 13.

Table 13 Rates of Reaction in DMSO/H₂O 9:1 v/v Solution.

| Catalyst Concentration (M) | Imidazole | | <i>N</i> -Acetyl-L-histidine | |
|--|---|----------------|--|----------------|
| | Rate of Reaction (Ms ⁻¹) | R ² | Rate of Reaction (Ms ⁻¹) | R ² |
| 1.50x10 ⁻³ | 2.44x10 ⁻⁹ ±0.12x10 ⁻⁹ | 0.997 | 2.05x10 ⁻⁹ ±0.03x10 ⁻⁹ | 0.999 |
| 1.25x10 ⁻³ | 2.20x10 ⁻⁹ ±0.17x10 ⁻⁹ | 0.997 | 1.73x10 ⁻⁹ ±0.06x10 ⁻⁹ | 0.998 |
| 1.00x10 ⁻³ | 1.58x10 ⁻⁹ ±0.11x10 ⁻⁹ | 0.998 | 1.36x10 ⁻⁹ ±0.06x10 ⁻⁹ | 0.997 |
| 0.75x10 ⁻³ | 1.17x10 ⁻⁹ ±0.06x10 ⁻⁹ | 0.996 | 1.14x10 ⁻⁹ ±0.04x10 ⁻⁹ | 0.997 |
| 0.50x10 ⁻³ | 8.02x10 ⁻¹⁰ ±0.10x10 ⁻¹⁰ | 0.996 | 9.11x10 ⁻¹⁰ ±1.00x10 ⁻¹⁰ | 0.993 |
| | <i>N</i> -Acetyl-L-histidine sodium salt | | <i>N</i> -Acetyl-L-histidine tetra- <i>n</i> -butylammonium salt | |
| Catalyst Concentration (molL ⁻¹) | Rates of Reaction (molL ⁻¹ s ⁻¹) | R ² | Rates of Reaction (molL ⁻¹ s ⁻¹) | R ² |
| 1.50x10 ⁻³ | 1.58x10 ⁻⁸ ±0.05x10 ⁻⁸ | 0.999 | 1.31x10 ⁻⁸ ±0.03x10 ⁻⁸ | 0.999 |
| 1.25x10 ⁻³ | 1.21x10 ⁻⁸ ±0.06x10 ⁻⁸ | 0.999 | 1.07x10 ⁻⁸ ±0.06x10 ⁻⁸ | 0.999 |
| 1.00x10 ⁻³ | 1.03x10 ⁻⁸ ±0.01x10 ⁻⁸ | 0.999 | 8.06x10 ⁻⁹ ±0.17x10 ⁻⁹ | 0.999 |
| 0.75x10 ⁻³ | 7.01x10 ⁻⁹ ±0.29x10 ⁻⁹ | 0.999 | 6.00x10 ⁻⁹ ±0.59x10 ⁻⁹ | 0.999 |
| 0.50x10 ⁻³ | 4.46x10 ⁻⁹ ±0.11x10 ⁻⁹ | 0.999 | 4.11x10 ⁻⁹ ±0.12x10 ⁻⁹ | 0.999 |

The rates of hydrolysis catalysed by all molecules in DMSO/H₂O 9:1 v/v solution are all greater than those which were found for the hydrolysis of *p*-nitrophenyl acetate without catalyst. This shows that the catalysts being used in this study do affect the rate of hydrolysis. A plot of catalyst concentration against rate of reaction gives the graph shown in Figure 67.

Figure 67 Rates of Reaction for Small Molecules in DMSO/H₂O 9:1 v/v Solution.



As the plots are linear, there is a first order relationship between the rate of reaction and the catalyst concentration. It is therefore possible to calculate the rate constant from the slope of the plots. The results are shown in Table 14.

Table 14 Rate Constants for all Catalysts in DMSO/H₂O 9:1 v/v Solution.

| Catalyst | Rate constant (s ⁻¹) | R ² |
|--|----------------------------------|----------------|
| Imidazole | 1.72x10 ⁻⁶ | 0.986 |
| <i>N</i> -Acetyl-L-histidine | 1.15x10 ⁻⁶ | 0.988 |
| <i>N</i> -Acetyl-L-histidine sodium salt | 1.11x10 ⁻⁵ | 0.992 |
| <i>N</i> -Acetyl-L-histidine tetra- <i>n</i> -butylammonium salt | 9.07x10 ⁻⁶ | 0.996 |

The rate constants for the reactions carried out in DMSO/H₂O 9:1 v/v solution are lower than the corresponding reactions carried out in aqueous buffer because of the difference in solvent polarity. The catalytic action of imidazole derivatives in the hydrolysis of *p*-nitrophenyl acetate involves a charged transition state. Polar solvents are able to stabilise charged species more effectively than non-polar solvents so the transition state is more stable in polar solvents. These results are in accord with the work carried out by Brown et al²⁶ who showed that the rate of hydrolysis of an anilide by 2-(hydroxymethyl)imidazoles was decreased when going from H₂O to ethanol as solvent.

There is clearly an observable effect from the change in functional group on the rate constants of these reactions. If the catalytic effect was solely due to the pK_a of the imidazole group, the *N*-acetyl-L-histidine should again be the weakest catalyst. The pK_a of imidazole in DMSO is 18.6 at 25°C¹³⁴ and the trend of increasing pK_a will be similar for *N*-acetyl-L-histidine. If there was no interaction it would also be expected that the rate constant for both of the salts would be the same as that for *N*-acetyl-L-histidine.

The plot shown in Figure 67 shows that the hydrolysis of *p*-nitrophenyl acetate was catalysed least effectively by *N*-acetyl-L-histidine, imidazole was somewhat more effective and *N*-acetyl-L-histidine sodium salt and *N*-acetyl-L-histidine tetra-*n*-butylammonium salt were much more effective. *N*-acetyl-L-histidine is the least effective catalyst because in an unbuffered solution it is present as a zwitterion that has a protonated imidazole ring. As discussed previously the protonation of the imidazole functional group deactivates the catalyst as there is no longer any free lone pair of electrons to attack the ester and form the transition state. The rate constants for the salts of *N*-acetyl-L-histidine are larger than for imidazole. This indicates that stabilisation by the carboxylate group is taking place.

If there was no stabilising interaction between the carboxylate group and the imidazole ring in the transition state, a change in counterion should have no effect. A small difference in reaction rate was observed for the sodium and tetra-*n*-butylammonium salts of *N*-acetyl-L-histidine. Initially it might be expected that the tetra-*n*-butylammonium salt would be the best catalyst, since the tetra-*n*-butylammonium counterion has large hydrophobic groups and the formation of intimate ion pairs would be more difficult than for the much smaller sodium ion. However, the hydrolysis studies in DMSO/H₂O 9:1 v/v solution show that the sodium salt is the more effective catalyst. Presumably the sodium ion is solvated readily by the polar DMSO molecules and this solvation reduces the ability of the sodium ions to form intimate ion pairs.

Chapter 4 Hydrolysis Studies - Molecularly Imprinted Polymers.

4.0 Hydrolysis Studies - Molecularly Imprinted Polymers.

The hydrolysis experiments carried out in solution showed that in buffered aqueous solution both imidazole and *N*-acetyl-L-histidine were effective catalysts for the hydrolysis of *p*-nitrophenyl acetate and that the rate of reaction increased with increasing pH. There was no evidence for the carboxylate group in *N*-acetyl-L-histidine enhancing the reaction rate in aqueous solution. In contrast, in DMSO/H₂O 9:1 v/v solution, both the sodium and tetra-*n*-butylammonium salts of *N*-acetyl-L-histidine were more effective catalysts than imidazole itself. This suggested that in a medium of lower polarity than water the carboxylate group was responsible for enhancing the rate of reaction via interaction with the imidazole ring. In light of these encouraging results, methods for the incorporation of a suitable L-histidine derivative into an MIP were sought.

4.1 MIP's as Enzyme Mimics.

One of the most important factors in enzyme catalysis is entropy, and its effect on the Gibbs free energy of activation (ΔG^\ddagger). The effect of entropy is related to the Gibbs free energy of activation through the following equation:

Equation 9 Gibbs Free Energy.

$$\Delta G^\ddagger = \Delta H^\ddagger - T\Delta S^\ddagger$$

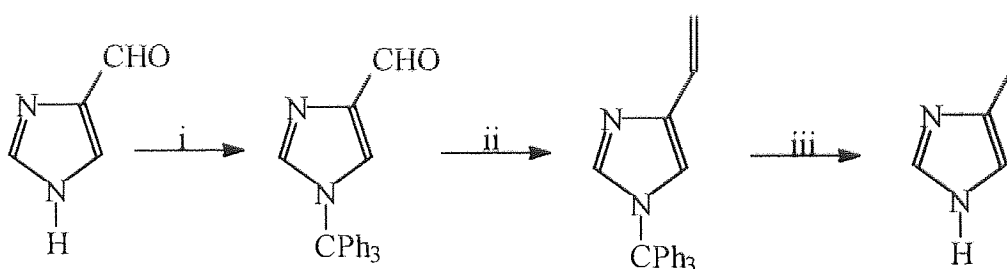
During a catalysed reaction in solution there is a large decrease in entropy as bringing together the catalyst and substrate(s) to form the transition state results in a considerable loss of freedom. In an enzyme catalysed reaction the initial step is the binding of the substrate(s) into the active site. This step is accompanied by a substantial decrease in entropy. The actual reaction of the substrate(s) to form products involves the bound substrate(s) and consequently the entropy change on going from bound substrate(s) to product is very much smaller than for the same reaction in the absence of enzyme. This leads to a much lower value of ΔG^\ddagger and consequently an increase in the rate of reaction. It is this preorganisation by the enzyme that is thought to be the main reason for the effectiveness of enzymes as catalysts. Since MIP's imprinted with a transition state mimic should also be able to exhibit a similar preorganising effect, these materials should also be good models for enzymes.

The principle aim of this study of MIP's was to determine whether the carboxylate group would interact with the imidazole ring when in an imprinted cavity thereby resulting in an increase in the rate of ester hydrolysis. Success in this study would confirm the suitability of L-histidine derivatives as models for the Asp-His couple of serine proteases and consequently the suitability of this MIP system as the basis for a model for the catalytic triad of serine proteases.

4.2 Synthesis of Monomers and the Transition State Mimic.

In order to study the hydrolysis of *p*-nitrophenyl acetate by MIP's, it was necessary to prepare polymerisable analogues of the catalysts used in the solution phase experiments. The molecules that were chosen were 4(5)-vinylimidazole and *N*-methacryloyl-L-histidine. 4(5)-Vinylimidazole was prepared using the method described by Kokosa et al.¹²⁴

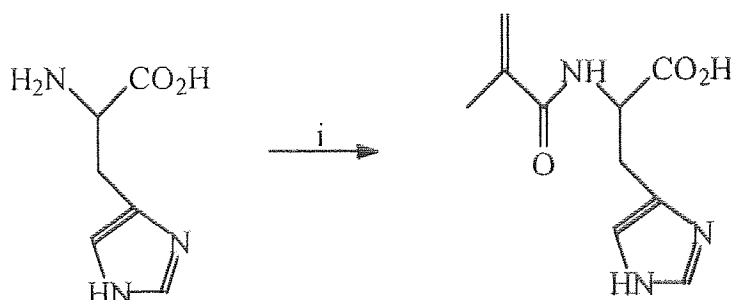
Figure 68 Synthesis of 4(5)-vinylimidazole.



i) $\text{Ph}_3\text{CCl}/\text{DMF}/\text{TEA}$; ii) $70^\circ\text{C}/4.5\text{h}$; iii) $\text{HCl}/\text{THF}/\text{reflux}$

N-Methacryloyl-L-histidine was prepared using the method described by Yoshihara et al.¹²³

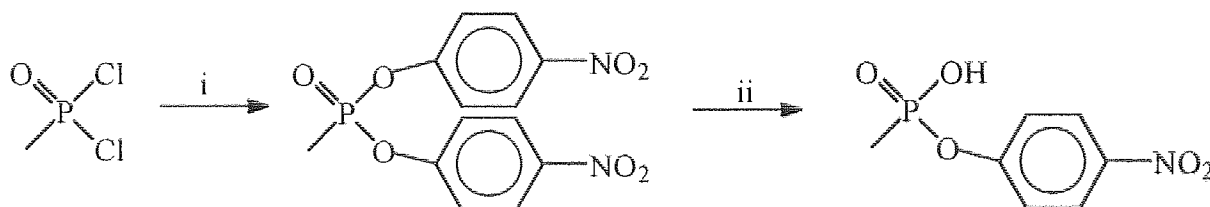
Figure 69 Synthesis of *N*-Methacryloyl-L-histidine.



i) 2M-NaOH/CH₃C(CH₂)C(O)Cl/DCM

p-Nitrophenyl methylphosphonate was prepared using the method described by Edwards et al.¹²⁵

Figure 70 Synthesis of *p*-Nitrophenyl Methylphosphonate.

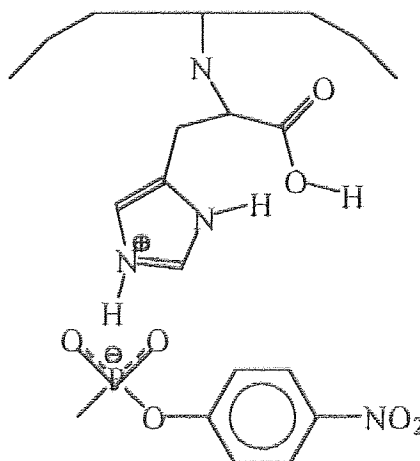


i) HO(C₆H₄)NO₂/160°C/4h; ii) 0.3M-NaOH/reflux

4.3 Synthesis of Polymers.

Several attempts to prepare MIP's based on imidazole derivatives as catalysts for ester hydrolysis have been reported.^{90,92,94,95} Clearly in order to be effective, the catalytic imidazole groups must be within the imprinted cavity. This requires the imidazole ring and the template molecule (in all cases phosphonate esters) to be closely associated during the polymerization step. Previous successful methods to achieve this have used Co^{II} ions⁹⁵, hydrogen bonding/electrostatic interactions¹⁰¹ and the formation of ion pairs.^{38,90} As the system developed in the work described here relied on imprinting the polymer with *p*-nitrophenyl methylphosphonate, a transition state mimic for the hydrolysis of *p*-nitrophenyl acetate, the third approach was selected as the most appropriate. This method relies on the protonation of the histidine moiety by the acidic phosphonate and the formation of an ion pair, see Figure 71.

Figure 71 Interaction of the Template Molecule with Polymer.



Using DMSO as the porogen for the imprinting process should ensure that the ion pairs remain closely associated during the polymerization reaction. Even so, the position of the template molecule may not result in an optimum position for the transition state with respect to the imidazole ring. However, previous studies using this technique have demonstrated that the interaction is sufficient to show a rate increase over the non-imprinted analogues.^{90,95}

Ethyleneglycol dimethacrylate (EDMA) has been used in the synthesis of several effective catalytic MIP's^{90,96,97,100,101,102} and was used as the basis for the synthesis of MIP's in this study. An alternative cross-linker, ethylene bisacrylamide, was also considered as a suitable monomer, as the amide groups would be effective hydrogen bond donors. It has been suggested that hydrogen bonds stabilize the transition state in the serine proteases¹³⁵ and it was anticipated that MIP's prepared from this monomer might be more efficient catalysts than those based on EDMA. Unfortunately, ethylene bisacrylamide was not sufficiently soluble in DMSO to allow the synthesis of MIP's. Whilst this monomer would be more soluble in more polar solvents such as methanol, it was not possible to use these solvents as they are powerful hydrogen bond donors and acceptors and would attenuate the carboxylate group/imidazole ring interaction upon which the effectiveness of these histidine based MIP's depends.

Polymers were synthesized from EDMA and 16 mol% of either 4(5)-vinylimidazole, *N*-methacryloyl-*L*-histidine, methyl methacrylate or acrylamide and 4 mol% of the transition state analogue, *p*-nitrophenyl methylphosphonate. A series of analogues were prepared in the absence of the template molecule for use as controls. The effectiveness of imidazole rings as the basis for a catalytic system for ester hydrolysis relies on the imidazole ring being unprotonated. *N*-Methacryloyl-*L*-histidine exists as a zwitterion with the imidazole ring protonated. It was therefore desirable that polymers also be made from the corresponding anion in which the imidazole ring was unprotonated. Unfortunately neither the sodium salt nor the tetra-*n*-butylammonium salts of *N*-methacryloyl-*L*-histidine were sufficiently soluble to be used. To overcome this difficulty the reactions of the imprinted polymers were studied in aqueous solution buffered to pH 8.0. At this pH a significant proportion of the imidazole rings should be unprotonated. Although water is a powerful hydrogen bonding solvent that might be expected to disrupt the interaction between the imidazole ring and the carboxylate group, the polymer was synthesized in DMSO and consequently the two groups should remain fixed in the necessary positions for an effective interaction after polymerisation. Also the serine protease enzymes function in aqueous solution. Binding of the substrate

necessitates the removal of water molecules from the active site and it was hoped that a similar process might occur with the imprinted polymers.

Since the solution phase reactions described in Chapter 3 suggested that the presence of a carboxylate group enhances the catalytic activity of the imidazole ring in ester hydrolysis in DMSO/H₂O 9:1 v/v solution, the activity of the polymers was also investigated in this solvent system. It was therefore necessary to form polymerisable derivatives of those molecules used in the solution phase reactions, as these seem to be good models. As the histidine system contained a protonated ring and it was not possible to prepare imprinted polymers directly from the corresponding sodium and tetra-*n*-butylammonium salts, the polymers derived from *N*-methacryloyl-L-histidine were soaked overnight in 1.11 M NaOH in methanol or 1.20 M tetra-*n*-butylammonium hydroxide in methanol to deprotonate the imidazole rings and the solvent then removed. Although the hydroxide ion is small the tetra-*n*-butylammonium cation is large and it was thought that whilst the hydroxide ion would be able to enter the imprinted cavity and deprotonate the imidazole ring, the large cation would be unable to enter and therefore not be able to form an intimate ion pair with the anion. In contrast, the smaller sodium cation would be able to form an intimate ion pair. Consequently the carboxylate group/imidazole ring interaction should be much stronger for the tetra-*n*-butylammonium system and should therefore be a more effective catalyst than the sodium analogue.

The polymers containing methyl methacrylate and acrylamide were synthesized as these materials contain no catalytic functional groups and their activity relies solely upon the shape of the imprinted cavities for their catalytic action. The acrylamide system contained hydrogen bond donors that were absent in the methyl methacrylate system. The formation of hydrogen bonds to the imprint molecule in the acrylamide system could assist in the orientation of the template molecule within the imprinted cavity and consequently lead to stabilization of the transition state through hydrogen bonding.

After polymerization, the polymers were ground using a pestle and mortar and the resulting particles washed using methanol in a Soxhlet extractor. The polymer was then dried and sieved with a 38 μm sieve to allow isolation of particulate polymeric material greater than 38 μm in diameter.

4.3.1 Difficulties of Using MIP's.

When carrying out the hydrolysis reactions in solution, it was possible to monitor the reaction taking place in the cuvette within the UV spectrometer. When carrying out the analogous

polymer catalysed reactions it was not possible to do this as the suspended polymer interfered with the measurements. It was therefore necessary to develop an alternative technique to monitor these reactions. The reaction was carried out in a flask and samples taken every 6 minutes. These samples had to be filtered before the UV spectrum could be recorded. The first problem encountered with this approach was that taking samples would affect the relative proportions of polymer in the reaction. In order to minimize this it was necessary to remove very small samples. Since the reaction mixture consisted of a suspension of the polymer, the reaction was stirred rapidly in order that the samples taken were homogenous, and the relative proportions of polymer to solution remained unchanged. The second problem that arose was the filtration of the samples. Initially a syringe was used to remove the sample and the mixture filtered through a 0.2 μm , nylon membrane syringe filter. This was found to be impractical as the syringe needles were prone to blocking and the syringe filters blocked up rapidly with fine particles of polymer, making it impossible to consistently obtain a suitable filtered sample. It was therefore necessary to use a filter that wouldn't block with the fine polymer particles. An alternative was to filter the sample through a pasteur pipette containing a layer of cotton wool, a layer of celite and another layer of cotton wool. Whilst this system allowed the polymer to be filtered off, the system allowed fine particles to pass through the celite. In order to remedy this, after grinding, the polymer was separated by a 38 μm sieve, the particles being collected by the sieve were used in the hydrolysis experiments. Despite these precautions samples occasionally appeared to contain a slight haze.

4.4 Hydrolysis in pH 8.0 Buffer Solution.

4.4.1 Calculation of Masses of Polymer.

The masses of polymer were calculated to contain the same number of moles of catalytic groups as used in the solution phase experiments.

4.4.2 Hydrolysis in pH 8.0 Buffer Solution.

The hydrolysis of *p*-nitrophenyl acetate using MIP's as catalysts in pH 8.0 buffer solutions were carried out using acrylamide, EDMA, methyl methacrylate, 4(5)-vinylimidazole and *N*-

methacryloyl-L-histidine imprinted and non-imprinted polymers using the method described by Mosbach et al.¹⁴⁹ The polymer was filtered instead of using the centrifuge.

p-Nitrophenyl acetate solution was added to a stirred mixture of polymer in a buffered solution. Samples were taken every six minutes, filtered and the UV absorbance measured. The hydrolyses were carried out for all imprinted and non-imprinted polymers at 5 different masses. All experiments were carried out in triplicate and the results averaged. The results are shown in the following plots.

Figure 72 Hydrolysis in pH 8.0 Buffer Solution, Imprinted 4(5)-vinylimidazole MIP as Catalyst.

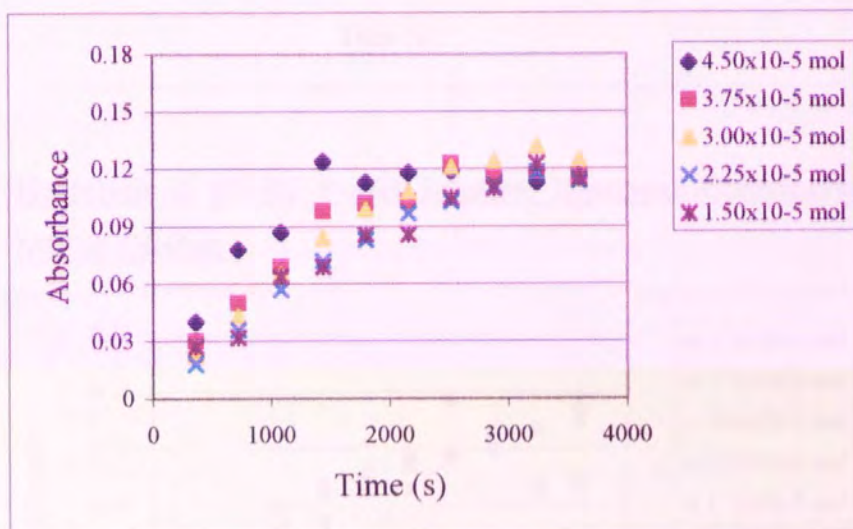


Figure 73 Hydrolysis in pH 8.0 Buffer Solution, Non-Imprinted 4(5)-vinylimidazole MIP as Catalyst.

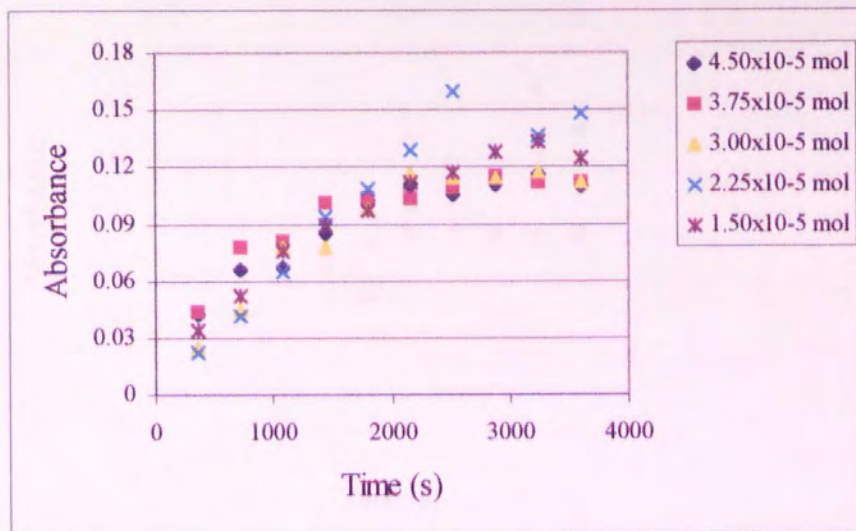


Figure 74 Hydrolysis in pH 8.0 Buffer Solution, Imprinted *N*-Methacryloyl-L-histidine MIP as Catalyst.

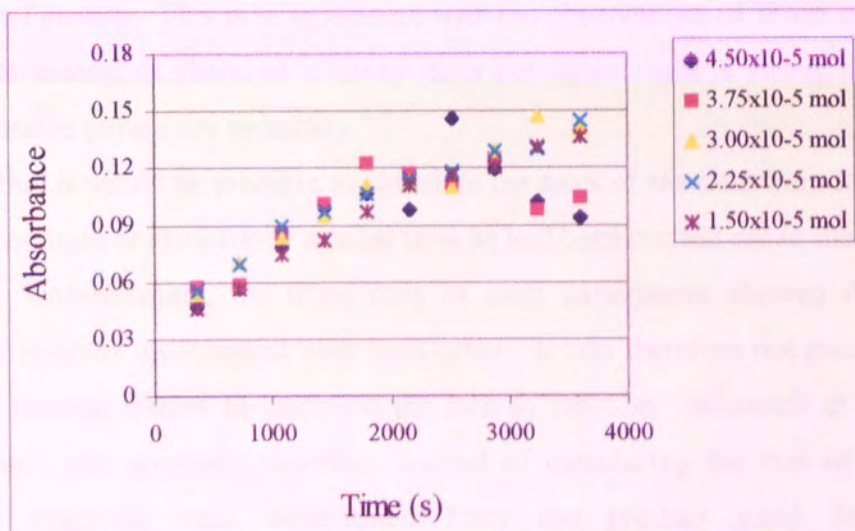
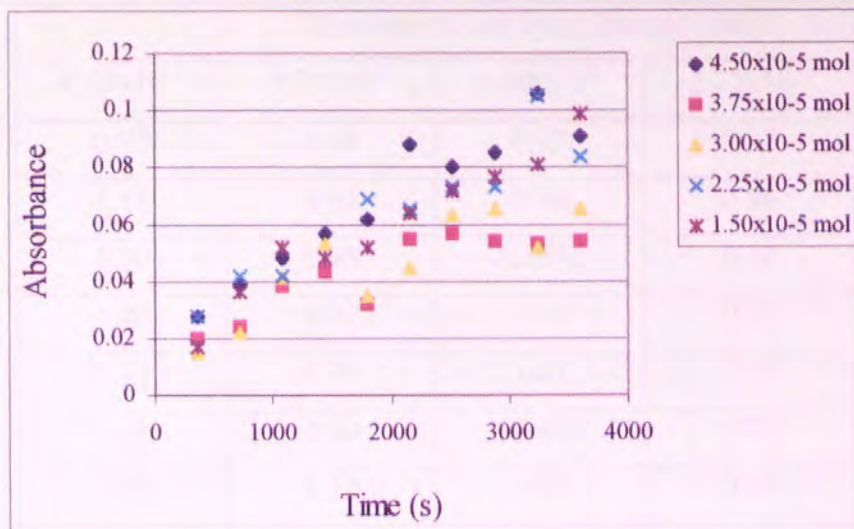


Figure 75 Hydrolysis in pH 8.0 Buffer Solution, Non-Imprinted *N*-Methacryloyl-L-histidine MIP as Catalyst.



It was found that the MIP's derived from acrylamide, methyl methacrylate and EDMA showed in pH 8.0 buffer solution no detectable rate enhancement when used in the hydrolysis of *p*-nitrophenyl acetate. This is in agreement with the observations of Wulff et al¹⁰¹ that "the transition state analogous shape of a cavity does not alone cause a strong catalytic effect, additional effective groups are necessary."

It was hoped that it would be possible to calculate the rates of reaction from the slopes of the plots of concentration or absorbance against time as had been carried out in the solution phase experiments. Unfortunately, the three runs of each experiment showed that the values obtained were at times inconsistent with each other. It was therefore not possible to use the slopes of the average values to calculate the rate of reaction. Mosbach et al⁹⁹ were also unable to obtain rate constants therefore instead of calculating the rate of reaction, they calculated a reactivity ratio determined from the product yield from imprinted polymer/product yield from non-imprinted polymer.

It is possible using the results from this study to calculate the reactivity ratios at a wide range of timepoints and using different effective catalyst concentrations. It is not possible however to convert the absorbances measured into concentrations as some of the *p*-nitrophenol will be absorbed into the polymer. Imprinted and non-imprinted analogues of the same polymer could absorb the *p*-nitrophenol to similar extents, but the level of absorbance between different types of polymer are likely to be different. Therefore it is only possible to compare imprinted and non-imprinted analogues of the same polymer and not different polymer types. The results for all points are shown in Tables 15 and 16.

Table 15 Reactivity Ratios for 4(5)-vinylimidazole Polymers in pH 8.0 Buffer Solution.

| Time (s) | Number of Catalytic Groups (mol) | | | | |
|----------|----------------------------------|-----------------------|-----------------------|-----------------------|-----------------------|
| | 4.50×10^{-5} | 3.75×10^{-5} | 3.00×10^{-5} | 2.25×10^{-5} | 1.50×10^{-5} |
| 360 | 0.93 | 0.68 | 0.92 | 0.82 | 0.79 |
| 720 | 1.18 | 0.64 | 0.96 | 0.86 | 0.62 |
| 1080 | 1.30 | 0.85 | 0.83 | 0.88 | 0.84 |
| 1440 | 1.46 | 0.97 | 1.08 | 0.77 | 0.77 |
| 1800 | 1.11 | 0.99 | 1.01 | 0.76 | 0.89 |
| 2160 | 1.06 | 1.00 | 0.93 | 0.75 | 0.77 |
| 2520 | 1.13 | 1.13 | 1.06 | 0.64 | 0.90 |
| 2880 | 1.05 | 1.01 | 1.09 | 0.87 | 0.86 |
| 3240 | 0.97 | 1.05 | 1.13 | 0.87 | 0.92 |
| 3600 | 1.05 | 1.03 | 1.12 | 0.77 | 0.92 |

Table 16 Reactivity Ratios for N-Methacryloyl-L-histidine Polymers in pH 8.0 Buffer Solution.

| Time (s) | Number of Catalytic Groups (mol) | | | | |
|----------|----------------------------------|-----------------------|-----------------------|-----------------------|-----------------------|
| | 4.50×10^{-5} | 3.75×10^{-5} | 3.00×10^{-5} | 2.25×10^{-5} | 1.50×10^{-5} |
| 360 | 1.68 | 2.90 | 3.53 | 1.96 | 2.71 |
| 720 | 1.44 | 2.46 | 3.18 | 1.64 | 1.56 |
| 1080 | 1.65 | 2.24 | 2.02 | 2.14 | 1.44 |
| 1440 | 1.74 | 2.35 | 1.79 | 2.02 | 1.71 |
| 1800 | 1.73 | 3.81 | 3.17 | 1.55 | 1.87 |
| 2160 | 1.11 | 2.13 | 2.51 | 1.75 | 1.73 |
| 2520 | 1.83 | 1.96 | 1.75 | 1.62 | 1.61 |
| 2880 | 1.40 | 2.31 | 1.98 | 1.77 | 1.56 |
| 3240 | 0.96 | 1.85 | 2.83 | 1.24 | 1.62 |
| 3600 | 1.03 | 1.93 | 2.17 | 1.73 | 1.37 |

The mean reactivity ratios and standard deviations are shown in Table 17.

Table 17 Mean Reactivity Ratios and Standard Deviations for the Hydrolysis in pH 8.0 Buffer Solution.

| | Mean Reactivity Ratio | Standard Deviation |
|------------------------------------|-----------------------|--------------------|
| 4(5)-vinylimidazole | 0.94 | 0.17 |
| <i>N</i> -Methacryloyl-L-histidine | 1.96 | 0.60 |

The polymers derived from 4(5)-vinylimidazole give results that show that there is very little difference between the imprinted and non-imprinted polymers in this solvent. The results for *N*-methacryloyl-L-histidine consistently give reactivity ratios greater than one. The mean reactivity ratio and the standard deviation suggest that the presence of the cavity is having an effect on the rate of hydrolysis of *p*-nitrophenyl acetate for this polymer, though it is impossible using this system to tell if there is any interaction between the carboxylate group and the imidazole ring.

4.5 Hydrolysis in DMSO/H₂O 9:1 v/v Solution.

The hydrolysis of *p*-nitrophenyl acetate using imprinted polymers in DMSO/H₂O 9:1 v/v solution was carried out using acrylamide, EDMA, methyl-methacrylate, 4(5)-vinylimidazole, *N*-methacryloyl-L-histidine, *N*-methacryloyl-L-histidine treated with sodium hydroxide and *N*-methacryloyl-L-histidine treated with tetra-*n*-butylammonium hydroxide based imprinted polymers as catalysts. The method used for the hydrolyses was the same as that employed for the reactions in pH 8.0 buffer solution.

p-Nitrophenyl acetate solution was added to a stirred mixture of polymer in DMSO/H₂O 9:1 v/v. Samples were taken every six minutes, filtered and the UV absorbance measured. The hydrolyses were carried out for all imprinted and non-imprinted polymers at 5 different masses. All experiments were carried out in triplicate and the results averaged. The experimental results gave the following plots.

Figure 76 Hydrolysis in DMSO/H₂O 9:1 v/v Solution, Imprinted 4(5)-vinylimidazole MIP as Catalyst.

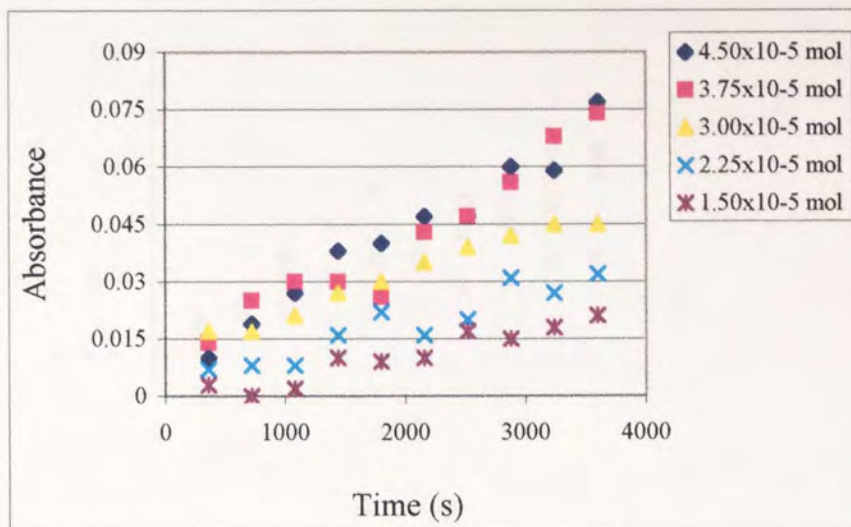


Figure 77 Hydrolysis in DMSO/H₂O 9:1 v/v Solution, Non-Imprinted 4(5)-vinylimidazole MIP as Catalyst.

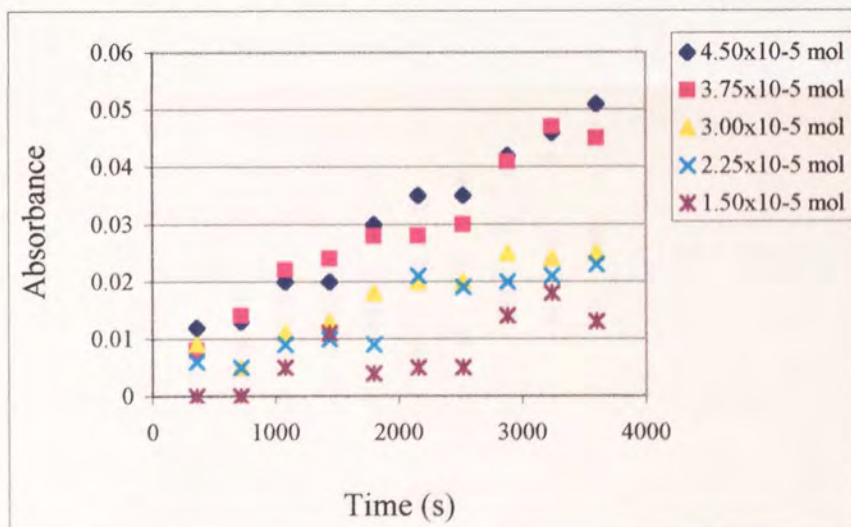


Figure 78 Hydrolysis in DMSO/H₂O 9:1 v/v Solution, Imprinted *N*-Methacryloyl-L-histidine MIP as Catalyst.

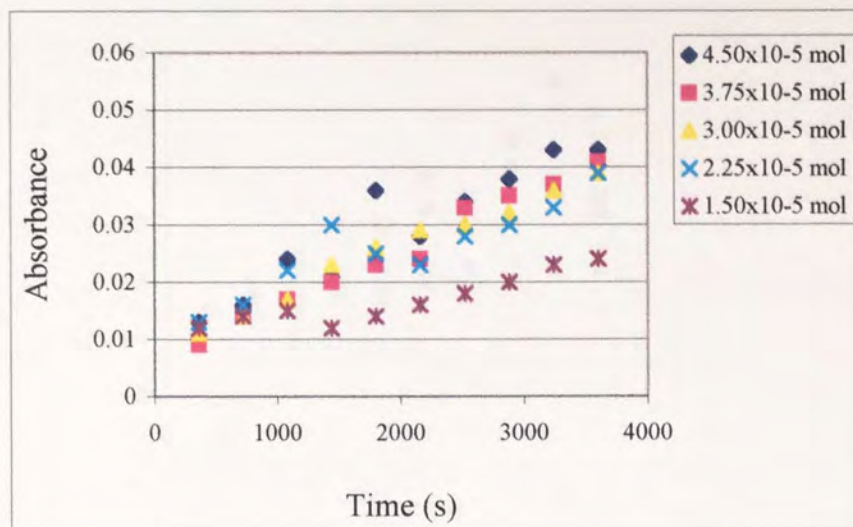


Figure 79 Hydrolysis in DMSO/H₂O 9:1 v/v Solution, Non-Imprinted *N*-Methacryloyl-L-histidine MIP as Catalyst.

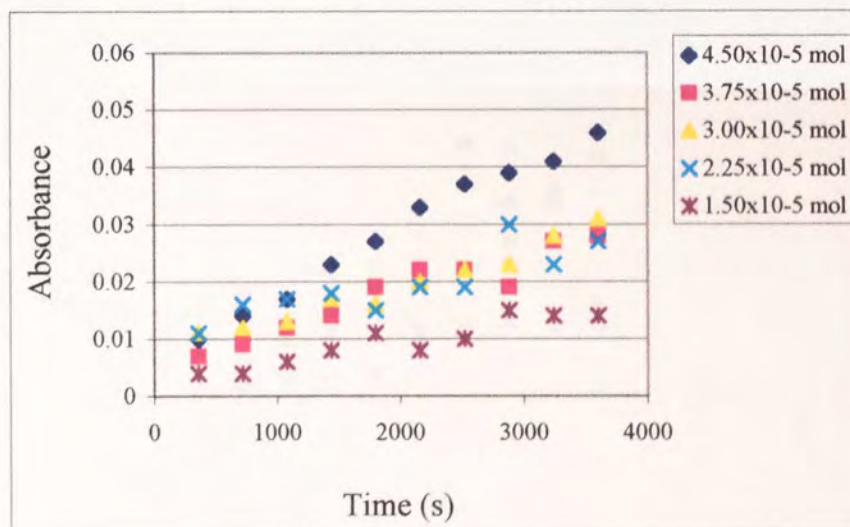


Figure 80 Hydrolysis in DMSO/H₂O 9:1 v/v Solution, Imprinted *N*-Methacryloyl-L-histidine MIP Treated with Sodium Hydroxide as Catalyst.

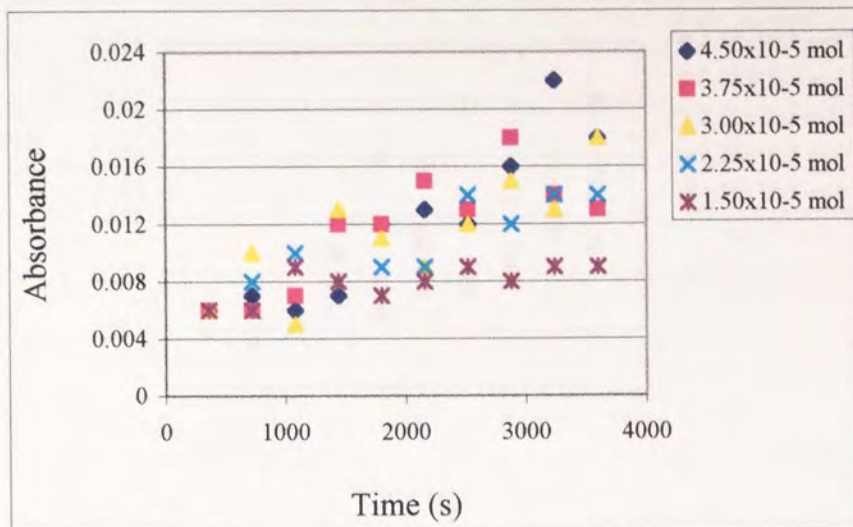


Figure 81 Hydrolysis in DMSO/H₂O 9:1 v/v Solution, Non-Imprinted *N*-Methacryloyl-L-histidine MIP Treated with Sodium Hydroxide as Catalyst.

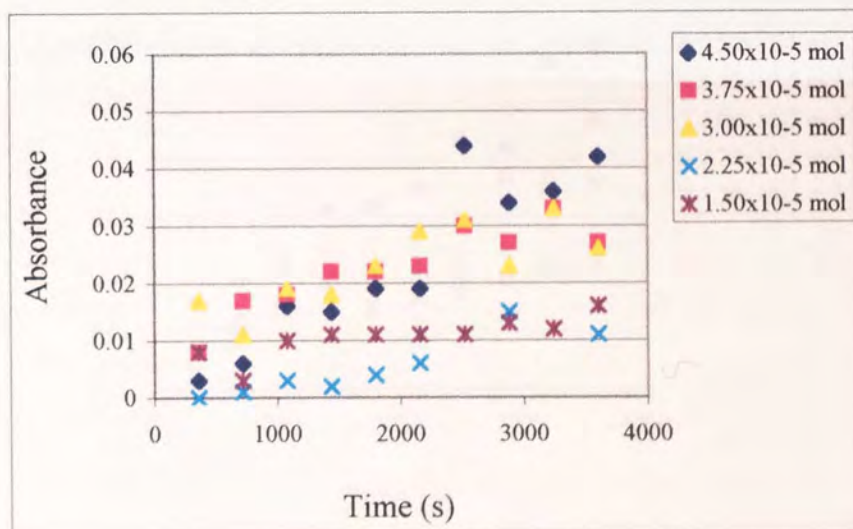


Figure 82 Hydrolysis in DMSO/H₂O 9:1 v/v Solution, Imprinted *N*-Methacryloyl-L-histidine MIP Treated with Tetra-*n*-butylammonium Hydroxide as Catalyst.

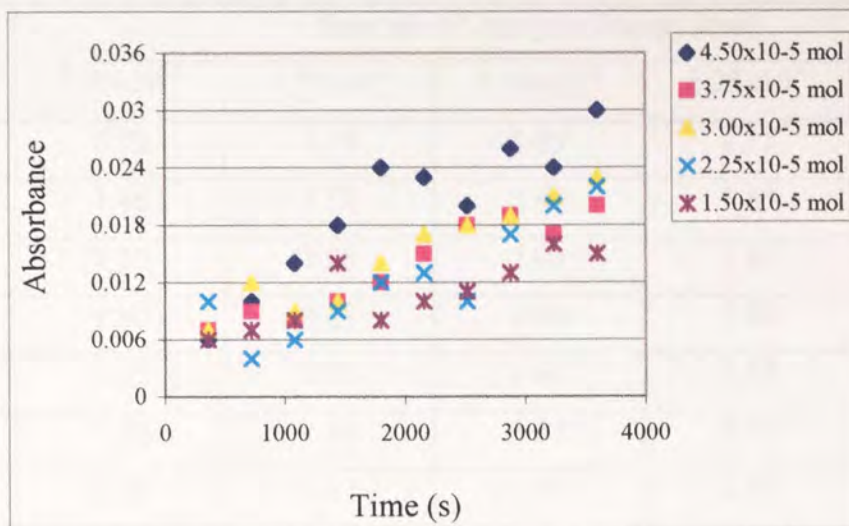
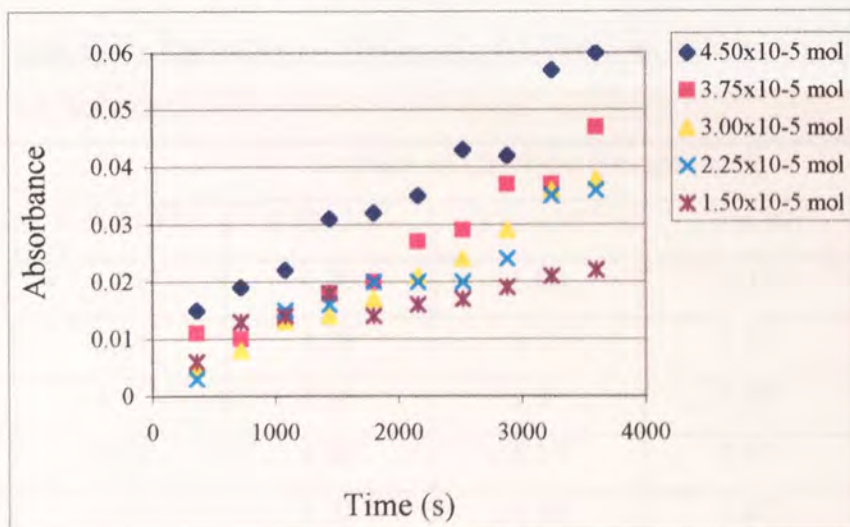


Figure 83 Hydrolysis in DMSO/H₂O 9:1 v/v Solution, Non-Imprinted *N*-Methacryloyl-L-histidine MIP Treated with Tetra-*n*-butylammonium Hydroxide as Catalyst



The trends of the above plots show that there is an increase in the rate of reaction as the mass of the polymer is increased both for the imprinted and non-imprinted systems. Unfortunately, as in the case of those experiments carried out in pH 8.0 buffer solution, the consistency of the three runs is poor for certain sample times. It is therefore necessary to again use the reactivity ratio method. The results for all points are shown in the following tables.

Table 18 Reactivity Ratios for 4(5)-vinylimidazole Polymers in DMSO/H₂O 9:1 v/v Solution.

| Time (s) | Number of Catalytic Groups (mol) | | | | |
|----------|----------------------------------|-----------------------|-----------------------|-----------------------|-----------------------|
| | 4.50×10^{-5} | 3.75×10^{-5} | 3.00×10^{-5} | 2.25×10^{-5} | 1.50×10^{-5} |
| 360 | 0.83 | 1.75 | 1.89 | 1.17 | - |
| 720 | 1.46 | 1.79 | 3.40 | 1.60 | - |
| 1080 | 1.35 | 1.36 | 1.91 | 0.89 | 0.40 |
| 1440 | 1.90 | 1.25 | 2.08 | 1.60 | 0.91 |
| 1800 | 1.33 | 0.93 | 1.67 | 2.44 | 2.25 |
| 2160 | 1.34 | 1.54 | 1.75 | 0.76 | 2.00 |
| 2520 | 1.34 | 1.57 | 1.95 | 1.05 | 3.40 |
| 2880 | 1.42 | 1.37 | 1.68 | 1.55 | 1.07 |
| 3240 | 1.28 | 1.45 | 1.88 | 1.29 | 1.00 |
| 3600 | 1.51 | 1.64 | 1.80 | 1.39 | 1.62 |

Table 19 Reactivity Ratios for N-Methacryloyl-L-histidine Polymers in DMSO/H₂O 9:1 v/v Solution.

| Time (s) | Number of Catalytic Groups (mol) | | | | |
|----------|----------------------------------|-----------------------|-----------------------|-----------------------|-----------------------|
| | 4.50×10^{-5} | 3.75×10^{-5} | 3.00×10^{-5} | 2.25×10^{-5} | 1.50×10^{-5} |
| 360 | 1.30 | 1.29 | 1.00 | 1.18 | 3.00 |
| 720 | 1.14 | 1.56 | 1.17 | 1.00 | 3.50 |
| 1080 | 1.41 | 1.42 | 1.31 | 1.29 | 2.50 |
| 1440 | 0.91 | 1.43 | 1.35 | 1.67 | 1.50 |
| 1800 | 1.33 | 1.21 | 1.63 | 1.67 | 1.27 |
| 2160 | 0.85 | 1.09 | 1.45 | 1.21 | 2.00 |
| 2520 | 0.92 | 1.50 | 1.36 | 1.47 | 1.80 |
| 2880 | 0.97 | 1.84 | 1.39 | 1.00 | 1.33 |
| 3240 | 1.05 | 1.37 | 1.29 | 1.43 | 1.64 |
| 3600 | 0.94 | 1.46 | 1.26 | 1.44 | 1.71 |

Table 20 Reactivity Ratios for *N*-Methacryloyl-L-histidine Polymers Treated with Sodium Hydroxide in DMSO/H₂O 9:1 v/v Solution.

| Time (s) | Number of Catalytic Groups (mol) | | | | |
|----------|----------------------------------|-----------------------|-----------------------|-----------------------|-----------------------|
| | 4.50×10^{-5} | 3.75×10^{-5} | 3.00×10^{-5} | 2.25×10^{-5} | 1.50×10^{-5} |
| 360 | 2.00 | 0.75 | 0.35 | - | 0.75 |
| 720 | 1.17 | 0.35 | 0.91 | 8.00 | 2.00 |
| 1080 | 0.38 | 0.39 | 0.26 | 3.33 | 0.90 |
| 1440 | 0.47 | 0.55 | 0.72 | 4.00 | 0.73 |
| 1800 | 0.63 | 0.55 | 0.48 | 2.25 | 0.64 |
| 2160 | 0.68 | 0.65 | 0.31 | 1.50 | 0.73 |
| 2520 | 0.27 | 0.43 | 0.39 | 1.27 | 0.82 |
| 2880 | 0.47 | 0.67 | 0.65 | 0.80 | 0.62 |
| 3240 | 0.61 | 0.42 | 0.39 | 1.17 | 0.75 |
| 3600 | 0.43 | 0.48 | 0.69 | 1.27 | 0.56 |

Table 21 Reactivity Ratios for *N*-Methacryloyl-L-histidine Polymers Treated with Tetra-*n*-butylammonium Hydroxide in DMSO/H₂O 9:1 v/v Solution.

| Time (s) | Number of Catalytic Groups (mol) | | | | |
|----------|----------------------------------|-----------------------|-----------------------|-----------------------|-----------------------|
| | 4.50×10^{-5} | 3.75×10^{-5} | 3.00×10^{-5} | 2.25×10^{-5} | 1.50×10^{-5} |
| 360 | 0.40 | 0.64 | 1.40 | 3.33 | 1.00 |
| 720 | 0.53 | 0.90 | 1.50 | 0.31 | 0.54 |
| 1080 | 0.64 | 0.62 | 0.69 | 0.40 | 0.57 |
| 1440 | 0.58 | 0.56 | 0.71 | 0.56 | 0.78 |
| 1800 | 0.75 | 0.60 | 0.82 | 0.60 | 0.57 |
| 2160 | 0.66 | 0.56 | 0.81 | 0.65 | 0.63 |
| 2520 | 0.47 | 0.62 | 0.75 | 0.50 | 0.65 |
| 2880 | 0.62 | 0.51 | 0.66 | 0.71 | 0.68 |
| 3240 | 0.42 | 0.46 | 0.58 | 0.57 | 0.76 |
| 3600 | 0.50 | 0.43 | 0.61 | 0.61 | 0.68 |

The mean reactivity ratios and standard deviations are shown in Table 22.

Table 22 Mean Reactivity Ratios and Standard Deviations for the Hydrolysis in DMSO/H₂O 9:1 v/v Solution.

| | Mean Reactivity Ratio | Standard Deviation |
|---|-----------------------|--------------------|
| 4(5)-vinylimidazole | 1.56 | 0.55 |
| <i>N</i> -Methacryloyl-L-histidine | 1.43 | 0.48 |
| <i>N</i> -Methacryloyl-L-histidine Treated with Sodium Hydroxide | 1.01 | 1.24 |
| <i>N</i> -Methacryloyl-L-histidine Treated with Tetra- <i>n</i> - butylammonium Hydroxide | 0.70 | 0.43 |

The solution catalysed experiments showed that there was an effect on the rate constant from the addition of the carboxylate functional group. Those experiments showed that there was an interaction between the carboxylate functional group and the imidazole ring increasing the catalytic ability of the molecules.

The next step was to see if incorporation of these functional groups within an imprinted cavity would increase the rate of reaction still further. It would demonstrate if the polymer was incorporating two facets of serine protease catalysed reaction. Firstly the interaction of the functional groups to increase the nucleophilicity of the imidazole ring and secondly the use of a specifically shaped cavity to hold the substrate in the correct position for hydrolysis to take place.

The monomers used to produce the imprinted polymers had different molecular weights. Therefore the masses of polymer used in the hydrolysis studies were calculated so that the number of catalytic sites in analogous experiments of different polymers would be equivalent. Due to the inconsistency of the technique used to measure the absorbance of *p*-nitrophenol it was not possible to use the gradients obtained from the absorbance against time plots, to calculate the rates of reaction. Instead a ratio of the absorbances of imprinted and non-imprinted polymers was used to enable their comparison. It is possible that polymers derived from different monomers will potentially absorb different amounts of *p*-nitrophenyl acetate and *p*-nitrophenol within the polymer matrix. Therefore it would not be possible to compare polymers derived from different monomers. It was therefore only possible to compare imprinted and non-imprinted polymers derived from the same monomer. Despite this the

polymers have been shown to be much more efficient for the ester hydrolysis of *p*-nitrophenyl acetate than in the uncatalysed reaction.

All of the mean reactivity ratios obtained in these experiments are within a standard deviation of a value of 1. This means that the hydrolyses catalysed by the imprinted and non-imprinted polymers may be occurring at the same rate. Clearly, a new method of following the rate of reaction must be devised to obtain more meaningful results than the ones obtained in the current study.

The easiest modification to make would be to centrifuge each sample before measuring the absorbance. Centrifugation would have to be carried out rapidly as the hydrolysis reaction would be ongoing. Alternatively quenching the reaction before centrifuging the sample would circumvent this potential problem.

Another method of following the reaction would be to use the polymer as the stationary phase on an HPLC column and to pass a *p*-nitrophenyl acetate solution through the column.

Unfortunately, due to time constraints, it was not possible to attempt any of these methods during the course of the current study.

Chapter 5 NMR Study of the Environment of the Template.

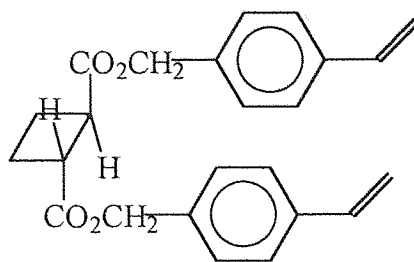
5.0 NMR Study of the Environment of the Template.

The performance of a molecularly imprinted polymer, whether in catalytic or separation applications, relies critically on the number and nature of imprinted cavities. The cavities within MIP's are polyclonal rather than monoclonal in nature and this will have an effect on the selectivity of the polymer.³⁶ The cavities are of different types, therefore some template molecules will be easily removed, some will be more difficult and some will not be able to be removed at all. When the imprinted polymer is being utilized some active sites will be easier to access than others. Because of this it is important to look at the number and nature of the accessible cavities and how they affect the selectivity of the polymer.

A simple method to determine the number of accessible sites is to calculate the amount of template that has been removed from the polymer during the washing process. The quantity of template present in the washings has been determined by HPLC¹⁰¹ and GC⁵³. This method can give a crude approximation of the proportion of removable template but provides no evidence of the environment that the template has been removed from. Similar information can be obtained using elemental analysis⁹⁶ of the polymer after removal of the template. This method allows calculation of the amount of template still resident within the polymer and from this value the amount removed can be determined. Again this gives no idea of the environment that surrounded the template that was removed.

Rather than determine the amount of template that has been removed from the polymer during washing it is more useful to look at the number of binding sites and whether the binding sites are accessible to the template. The main approach has been to study the number of active binding sites present within the polymer by attempting to reintroduce the template or another similar molecule. This technique has mainly been utilized with templates that are covalently bound to the polymer. Shea and Thompson⁶¹ produced an imprinted polymer by copolymerising molecule **8**, see Figure 84, with divinylbenzene.

Figure 84 Template Molecule Covalently Bound to Functional Monomers.

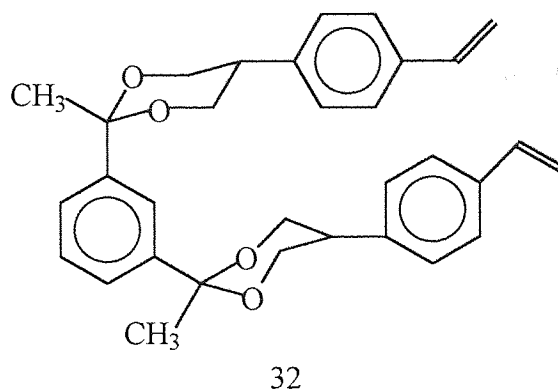


8

They firstly verified the presence of the covalently bound template as the infrared spectrum of the polymer exhibits an ester peak at 1736 cm^{-1} . The template was then removed by hydrolysis to leave imprinted cavities containing two polymer bound benzyl alcohol groups. The presence of these functionalities was verified by the introduction of trifluoroacetic anhydride. Binding of this molecule resulted in a new infrared absorption at 1788 cm^{-1} which was assigned to the trifluoromethylacetate group. Attempts to bind trifluoroacetic anhydride with unhydrolysed polymer which still contained template, did not lead to the appearance of this new absorption. Fumaryl chloride, a reagent of similar geometry to the template, was reintroduced into the hydrolysed polymer and the change in intensity in the carbonyl region of the IR spectrum suggested that new ester linkages between polymer and fumarate group are formed. This method can indicate if rebinding occurs within the imprinted sites, but cannot give a quantitative value for the number of active sites. However, upon hydrolysis of this polymer fumaric acid was liberated, and the change from fumaryl chloride to fumaric acid can be followed to give a quantitative value for the number of active sites. It was found that 80% of sites had covalently bound the fumaryl chloride. This method can only be used with imprinted polymers which rely on covalent binding.

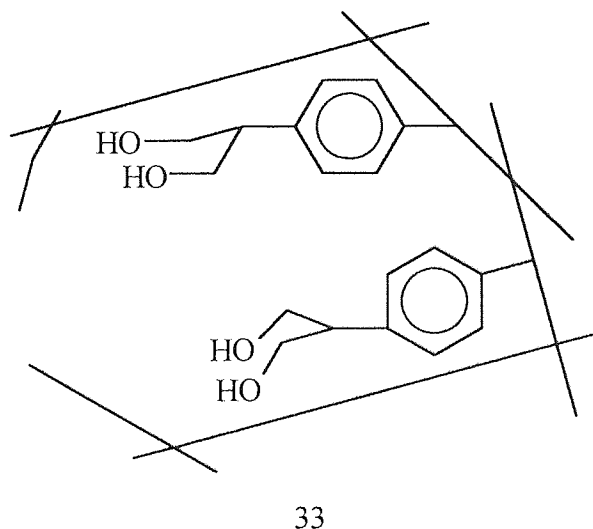
Shea and Sasaki⁵³ used a similar method complemented by ^{13}C CP/MAS NMR. They formed an imprinted polymer by copolymerising monomer **32** with styrene and *m*-diisopropenylbenzene, see Figure 85.

Figure 85 Covalently Bound Template for the Study of Rebinding.



Hydrolysis of the imprinted polymer removed the template to leave cavities like **33**, shown in Figure 86.

Figure 86 MIP for the Study of Rebinding, Template Removed.



Rebinding of $^{13}\text{C}=\text{O}$ -labeled 1,3-diacetylbenzene could result in one or two-point rebinding. One point rebinding would introduce a ketal and a ketone group, whereas two-point rebinding would introduce two ketal groups. Determination of which peaks were due to the ketal and the ketone functions was possible and by integration of the relevant ^{13}C NMR signals the concentration of ketal and ketone per gram of polymer was determined. It was then possible to calculate percentages of one and two point rebinding and the amount of rebinding that occurs. This technique is not generally applicable as it can only be used when employing a covalently bound template and the ^{13}C nucleus is a poor nucleus to study as it has only 1% abundance, though this was overcome using ^{13}C -labelling. However, ^{13}C -labelling is an

87, using IC₅₀ values. These values showed that the polymer demonstrated a significant selectivity for the template molecule.

Binding isotherms have also been used in the study of binding within imprinted polymers. Information about the binding can be estimated from the binding isotherms [B(concentration of bound guest) versus F(concentration of free guest)] using various mathematical models. MIP's have been studied in which the binding isotherm corresponds to a Langmuir type absorption¹³⁷, the Bi-Langmuir model¹³⁸ and the Freundlich isotherm.^{138,139}

Shimizu et al¹³⁹ found that a methacrylic acid, EDMA copolymer imprinted with ethyl adenine-9-acetate had an adsorption isotherm which obeyed the Freundlich isotherm and claimed that this isotherm was generally applicable in modeling the adsorption isotherms of non-covalently imprinted polymers. The implications of this isotherm with respect to MIP's were an exponential distribution of binding sites and a simplification of the experimental and calculation of the binding parameters in MIP's along with greater accuracy and repeatability.

The aim of this study was to develop a new system to study the polyclonality of imprinted polymers.

5.1 The Use of ³¹P MAS NMR to Study the Template Molecule.

The purpose of this project was to develop catalytically active polymers imprinted with *p*-nitrophenyl methylphosphonate. Since ³¹P has an abundance of 100% and it is the only phosphorous atom present in both the template and the polymer it seemed that it might be possible to study the template environment in imprinted polymers by ³¹P MAS NMR.

The chemical shift of a particular nucleus within a sample is defined as the nuclear shielding divided by the applied field.¹⁴⁰ The chemical shift is a function of the nucleus and its environment and is given by the equation:

Equation 10 Relationship of the Chemical Shift to the Nuclear Shielding.

$$\delta = \frac{(B_{\text{reference}} - B_{\text{sample}})}{B_{\text{reference}}} \times 10^6 \text{ ppm}$$

where B_{reference} is the magnetic field experienced by the nucleus of reference material and B_{sample} is the magnetic field experienced by the nucleus of the sample material.

The shielding of the nucleus is affected by its surrounding environment and each different environment alters the magnetic field at the nucleus. Therefore it is possible to distinguish between environments by looking at the different chemical shifts.

Three systems polymerised in the presence of *p*-nitrophenyl methylphosphonate were prepared.

A highly crosslinked EDMA system. This system has no groups capable of hydrogen bonding to the template.

An EDMA system containing 16.7 mol% methyl methacrylate. This system is less cross-linked than the EDMA system but does not introduce any groups capable of hydrogen bonding to the template

An EDMA system containing 16.7 mol% acrylamide. Again this is less cross-linked than the EDMA system and also introduces hydrogen bond donors that might form H-bonds to the template possibly increasing binding and selectivity.

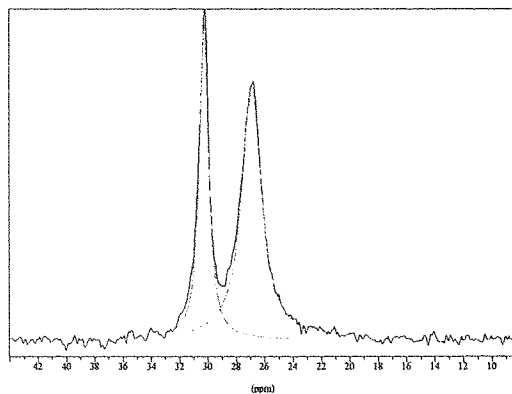
All ^{31}P MAS NMR spectra were obtained using 121.5 Hz proton high power, MAS decoupling with a rotor speed of 6500 MHz and using 88 % phosphoric acid as reference.

5.1.1 A ^{31}P MAS NMR Study of the Initial Imprinted Polymer

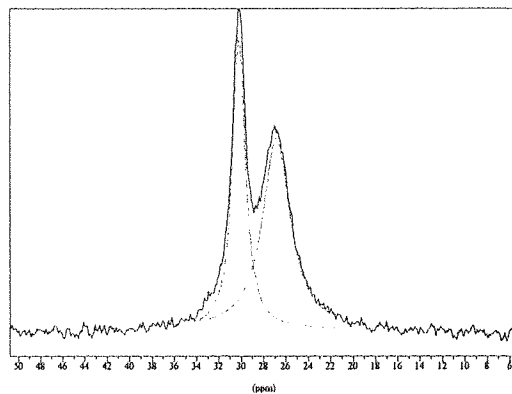
EDMA, methyl methacrylate and acrylamide were copolymerised with EDMA using *p*-nitrophenyl methylphosphonate as a template. The polymerisations were initiated with AIBN and heated at 60 °C for 72 hrs. They were then ground and sieved using a 38 μm sieve. The particles that were retained by the sieve were used for all further studies. The ^{31}P solid state NMR spectra for these polymers are shown in Figure 88.

Figure 88 ^{31}P MAS NMR Spectra of Unwashed MIP's.

a) EDMA



b) Acrylamide



c) Methyl methacrylate

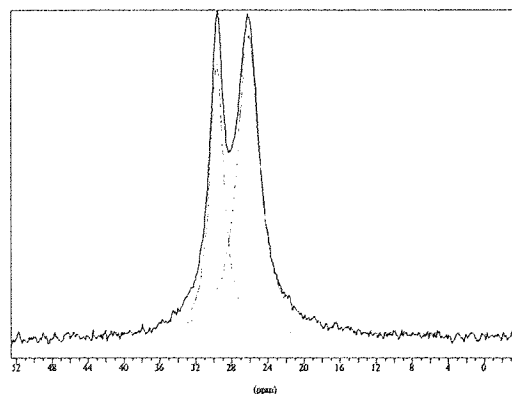


Table 23 ^{31}P MAS NMR Data of the Initial MIP's.

| Polymer | Chemical Shift (ppm) | Integral(rel.) Peak 1 | Chemical Shift (ppm) | Integral(rel.) Peak 2 |
|---------------------|-------------------------|--------------------------|-------------------------|--------------------------|
| EDMA | 30.28 | 37 | 26.91 | 63 |
| Acrylamide | 30.20 | 41 | 26.85 | 59 |
| Methyl methacrylate | 29.63 | 37 | 26.12 | 63 |

The spectra show that the template exists in two distinct environments in each of these polymer systems. There were several possible environments for the template molecule any two of which might account for the two signals observed in the NMR spectra.

- a) the template could be completely templated but different orientations of the template molecule to the polymer backbone might be possible.
- b) the template could be bound to the polymer by intermolecular forces but not be within a templated cavity. Again different orientations of the template molecule to the polymer backbone might be possible.
- c) the template molecule could be dissolved in bulk solvent within large pores within the polymer structure.

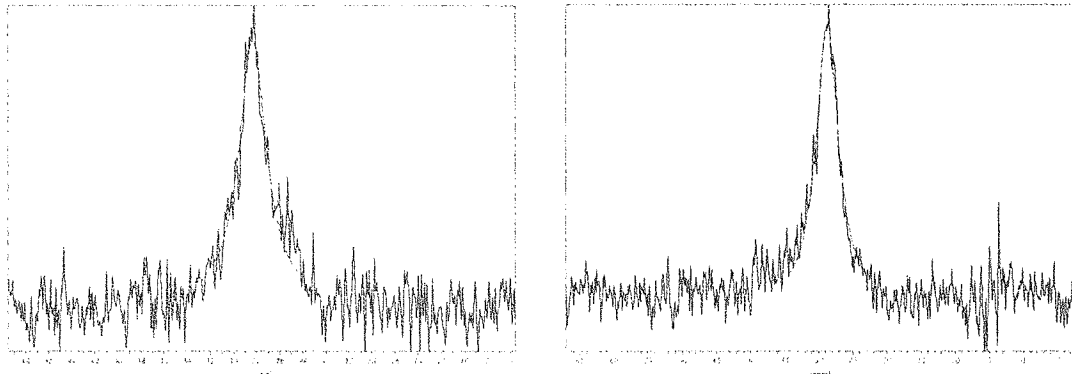
It was not clear from this initial study which of these possibilities corresponded to the peaks in the NMR spectra and further experiments were conducted to try to distinguish between these different environments.

5.1.2 A ^{31}P MAS NMR Study of Washed Polymer Ground Up with *p*-Nitrophenyl Methylphosphonate.

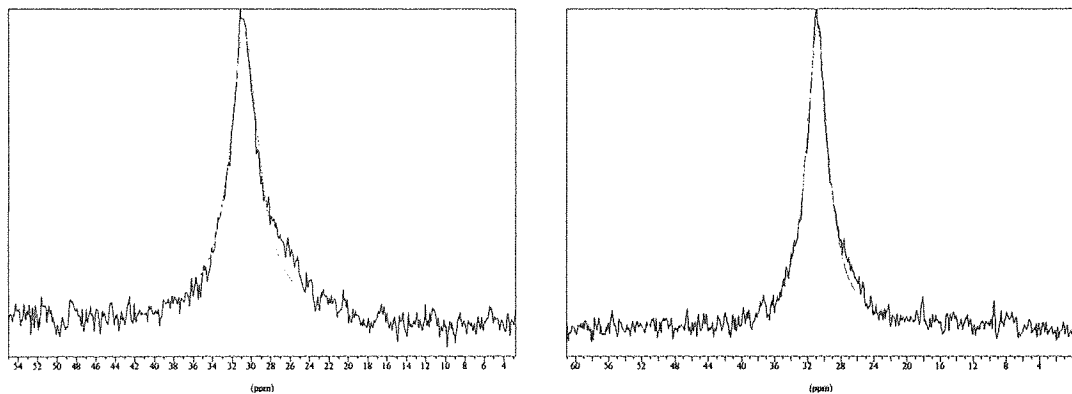
In order to distinguish between the different possibilities, the polymers prepared in the presence of template were studied together with the analogues prepared without template. To identify template that was not associated with the polymer in any way all polymer systems were extracted with methanol using a Soxhlet extractor and then dried in an oven at 60 ° for 24 hours. An amount of template equivalent to that which was used in the polymerisation step was then ground up with the polymer and a ^{31}P MAS NMR spectra obtained. Before reintroduction of the template, no ^{31}P MAS NMR signals could be found for any of the washed and dried polymers. The ^{31}P MAS NMR spectra for these materials are shown in Figure 89.

Figure 89 ³¹P MAS NMR Spectra of MIP's Ground Up with *p*-Nitrophenyl Methylphosphonate.

a) EDMA – Prepared With and Without Template



b) Acrylamide – Prepared With and Without Template



c) Methyl methacrylate – Prepared With and Without Template

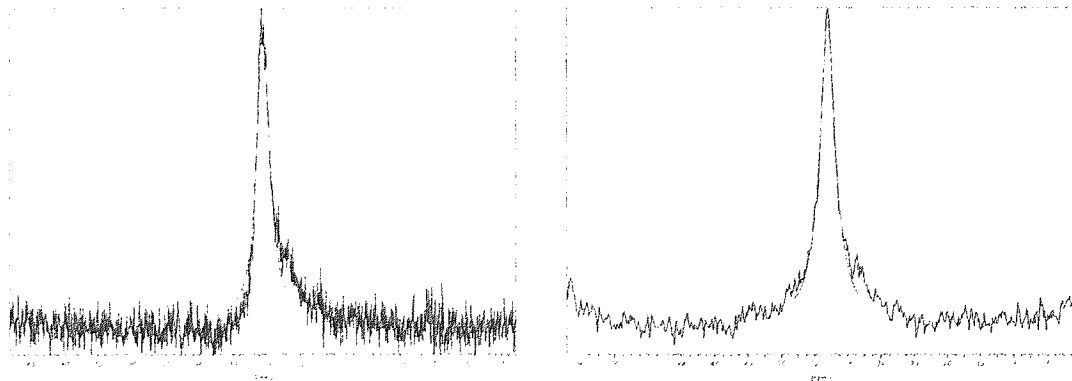


Table 24 ^{31}P MAS NMR Data of MIP's Ground Up with *p*-Nitrophenyl Methylphosphonate.

| Polymer | Chemical Shift (ppm) | Integral(rel.) |
|--|----------------------|----------------|
| EDMA (Prepared with Template) | 28.32 | 100 |
| EDMA (Prepared without Template) | 28.72 | 100 |
| Acrylamide (Prepared with Template) | 30.74 | 100 |
| Acrylamide (Prepared without Template) | 30.81 | 100 |
| Methyl methacrylate (Prepared with Template) | 30.43 | 100 |
| Methyl methacrylate (Prepared without Template) | 30.41 | 100 |

Although there is some difference in the chemical shift between the different polymer systems, there is close agreement between the chemical shifts of those polymers prepared with and without template. This would suggest that there is little difference in the environments of the template between the two types of polymer.

5.1.3 A ^{31}P MAS NMR Study of Washed Polymer Stirred with *p*-Nitrophenyl Methylphosphonate for 24 Hours then Filtered.

The previous study suggested that in each case the signal at higher chemical shift for each of the polymers, before template removal, might be caused by non-imprinted template molecules that were not associated with the polymer but were present in the solvent filled pores. Surprisingly the chemical shifts of the signal at lower frequency were similar to that of the solid *p*-nitrophenyl methylphosphonate ground with the washed polymer.

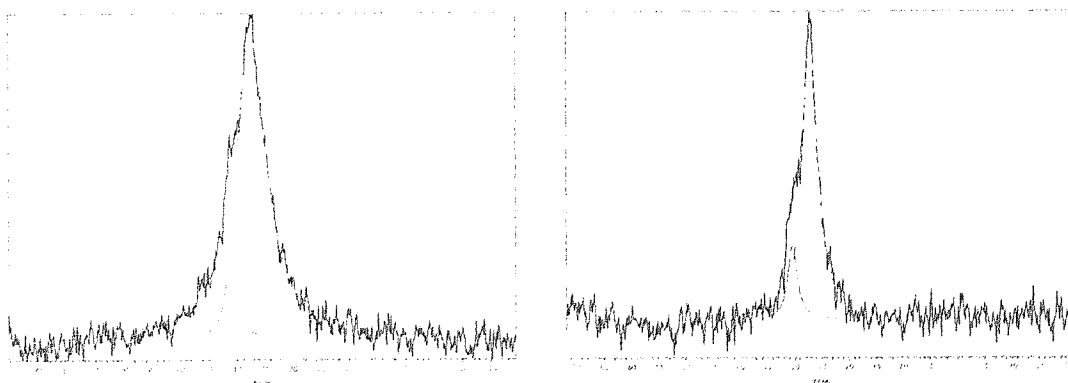
Experiments to reintroduce the template into systems prepared with and without template were expected to show a clear difference. It was expected that the polymers prepared without template would be unable to incorporate the template, except in the solvent filled pores and hence have ^{31}P spectra similar to those obtained for the physical mixture of polymer and

template. In contrast those systems prepared with template were expected to have signals arising from template within solvent filled pores and those bound into the active sites. It was also possible, in both imprinted and non-imprinted systems, that template might not be within an imprinted cavity and yet still be associated with the polymer.

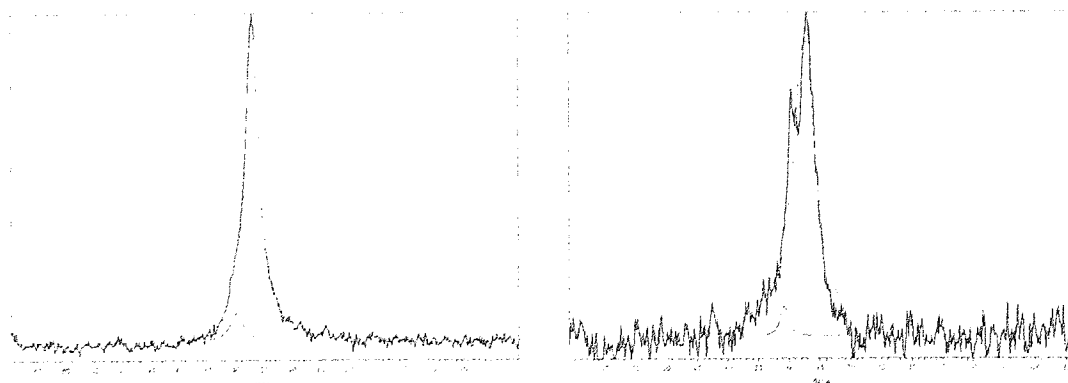
Each of the polymers was stirred in acetonitrile for 24 hours with an amount of template equivalent to that which was used in the polymerisation step. In order to remove template dissolved in bulk solvent, which would precipitate onto the surface of the polymer on solvent removal, the polymers were filtered and then dried in an oven at 60 °C. It was expected that signals arising from template rebound in active sites, or otherwise associated with the polymer and template in large pores within the polymer structure would be the only, or at least the major, signals. Template within the solvent filled pores would precipitate on removal of the solvent and should therefore have a similar chemical shift to the *p*-nitrophenyl methylphosphonate observed in the spectra of the physical mixtures of polymer and template. The ^{31}P spectra for these experiments are shown in Figure 90.

Figure 90 ^{31}P MAS NMR Spectra of MIP's Stirred with *p*-Nitrophenyl Methylphosphonate for 24 Hours then Filtered.

a) EDMA – Prepared With and Without Template



b) Acrylamide – Prepared With and Without Template



c) Methyl-methacrylate – Prepared With and Without Template

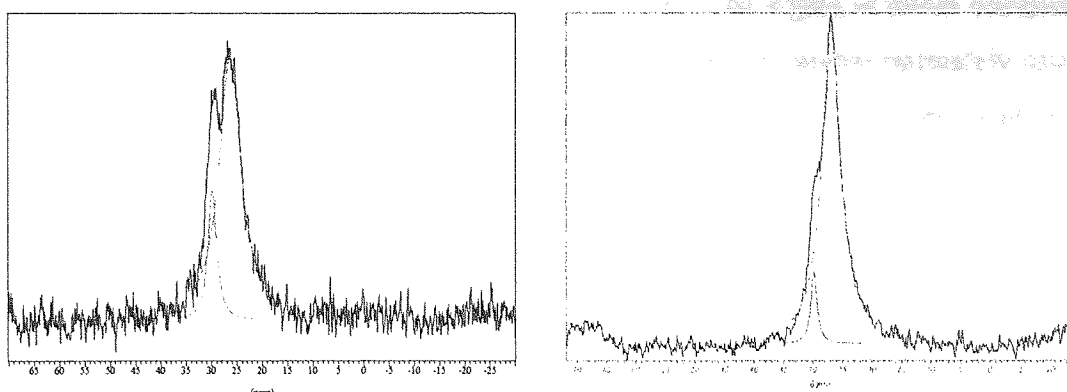


Table 25 ^{31}P MAS NMR Data of MIP's Stirred with *p*-Nitrophenyl Methylphosphonate for 24 Hours then Filtered.

| Polymer | Chemical Shift (ppm) | Integral(rel.) | Chemical Shift (ppm) | Integral(rel.) |
|---|----------------------|----------------|----------------------|----------------|
| EDMA (Prepared with Template) | 31.31 | 7 | 27.34 | 93 |
| EDMA (Prepared without Template) | 30.33 | 14 | 27.02 | 86 |
| Acrylamide (Prepared with Template) | 29.78 | 8 | 26.96 | 92 |
| Acrylamide (Prepared without Template) | 30.77 | 4 | 27.49 | 96 |
| Methyl methacrylate (Prepared with Template) | 29.83 | 16 | 26.30 | 84 |
| Methyl methacrylate (Prepared without Template) | 29.79 | 7 | 26.82 | 93 |

The results of these experiments are shown in Table 25. Surprisingly the spectra of the polymers prepared with template were very similar to those of their analogues prepared without template. The smaller signal at higher chemical shift occurred at a similar chemical shift to the *p*-nitrophenyl methylphosphonate/polymer physical mixture. This signal would

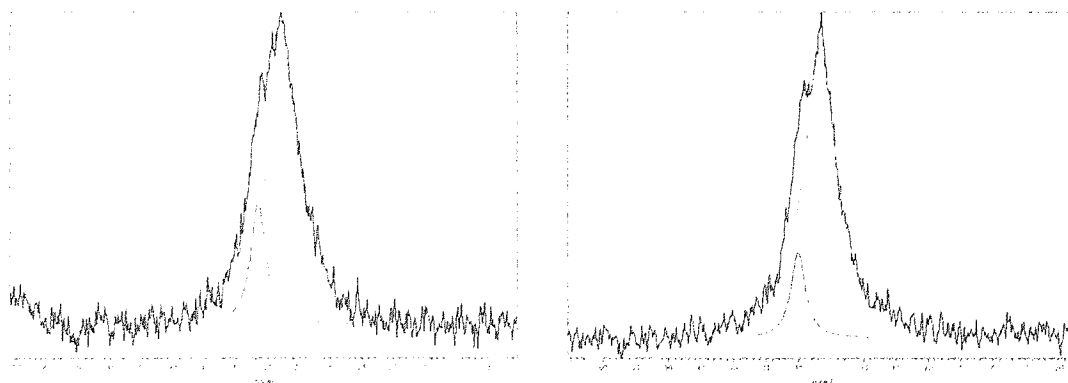
appear to be either template precipitated within the solvent cavities or template precipitated onto the surface of the polymer during the filtration step. The signal at lower chemical shift could be either template precipitated within solvent cavities or template intimately associated with the polymer through intermolecular bonds. If the signal at higher chemical shift was caused by template precipitated onto the surface of the polymer rather than within the cavities, the relative size of this signal should be larger if the solvent was simply evaporated rather than being filtered off.

5.1.4 A ^{31}P MAS NMR Study of Washed Polymer Stirred with *p*-Nitrophenyl Methylphosphonate for 24 hours.

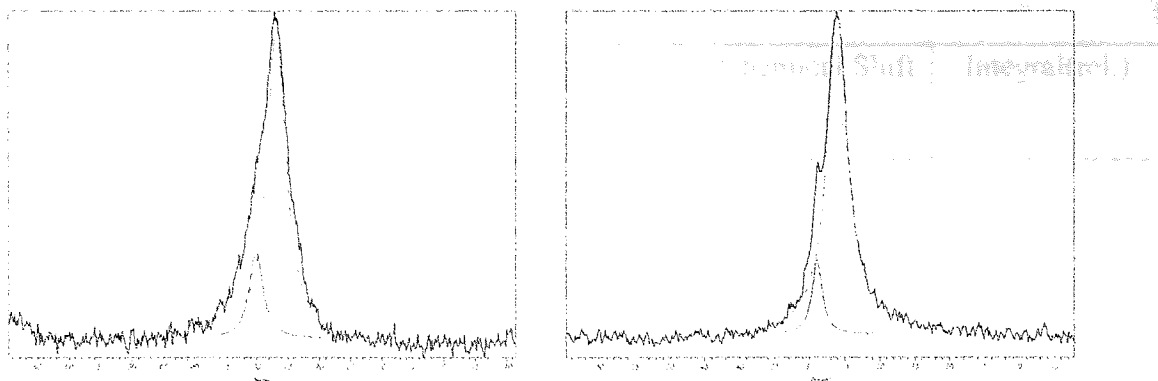
In order to determine if the signal at higher chemical shift was caused by template precipitated onto the surface of the polymer rather than within the large cavities, the reintroduction experiments were repeated but the samples were not filtered and the solvent was removed in an oven at 60 °C. The ^{31}P MAS NMR spectra for these experiments are shown in Figure 91.

Figure 91 ^{31}P MAS NMR Spectra of MIP's Stirred with *p*-Nitrophenyl Methylphosphonate for 24 Hours.

EDMA – Prepared With and Without Template



b) Acrylamide – Prepared With and Without Template



c) Methyl methacrylate – Prepared With and Without Template

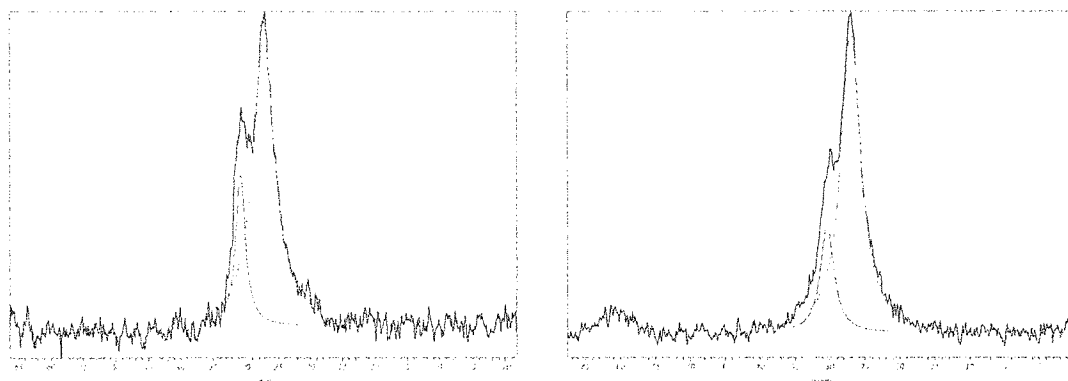


Table 26 ^{31}P MAS NMR Data of MIP's Stirred with *p*-Nitrophenyl Methylphosphonate for 24 Hours.

| Polymer | Chemical Shift (ppm) | Integral(rel.) | Chemical Shift (ppm) | Integral(rel.) |
|---|-------------------------|----------------|-------------------------|----------------|
| EDMA (Prepared with Template) | 31.47 | 18 | 27.66 | 82 |
| EDMA (Prepared without Template) | 30.06 | 11 | 26.64 | 89 |
| Acrylamide (Prepared with Template) | 30.10 | 17 | 26.80 | 83 |
| Acrylamide (Prepared without Template) | 28.94 | 10 | 25.97 | 90 |
| Methyl methacrylate (Prepared with Template) | 30.77 | 19 | 27.14 | 81 |
| Methyl methacrylate (Prepared without Template) | 30.41 | 20 | 26.98 | 80 |

The results of these experiments are shown in Table 26. They show that after the evaporation of the solvent there was an increase in the relative size of the signal at the higher chemical shift from approximately 5-10 % to approximately 10-20 %. This suggested that the template dissolved in the bulk solvent precipitates onto the surface of the polymer upon solvent removal and therefore contributes to the signal at higher chemical shift. The spectra of the initial polymers contained a signal at approximately 30 ppm which appeared to correspond to both template precipitated onto the surface of the polymers, in reintroduction experiments, and to solid *p*-nitrophenyl methylphosphonate. Since no precipitation should have occurred in the preparation of polymers formed in the presence of template, as they still contained solvent, it seemed that template molecules dissolved in solvent pores and those precipitated onto the polymer surface both gave signals in the ^{31}P MAS NMR spectra at approximately 30 ppm and were indistinguishable from one another. The lower chemical shift signal can be assigned to template molecules which are associated in some way with the polymer. It was

not possible to distinguish between template molecules within imprinted cavities and those simply bound to the polymer through intermolecular forces.

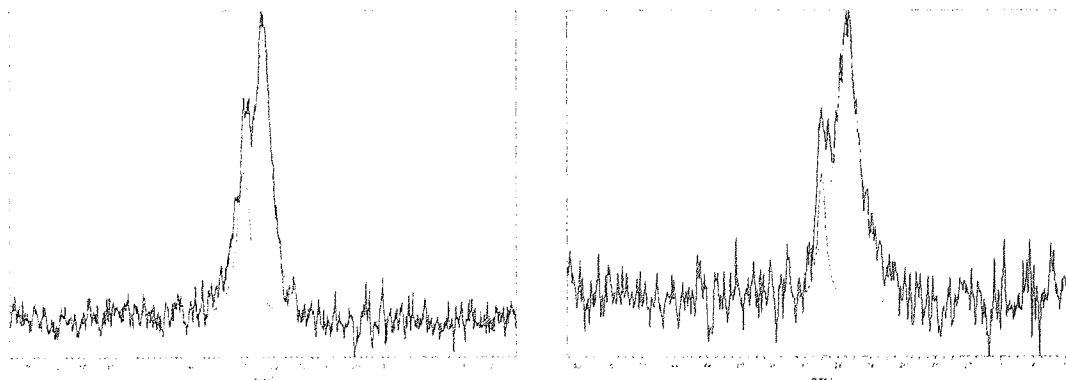
It can also be seen in those spectra that contain both signals, that the signal at lower chemical shift is broader than that at higher. This may indicate that the signal may be a composite of several environments.

5.1.5 A ^{31}P MAS NMR Study of Washed Polymer Stirred with *p*-Nitrophenyl Methylphosphonate for an Hour.

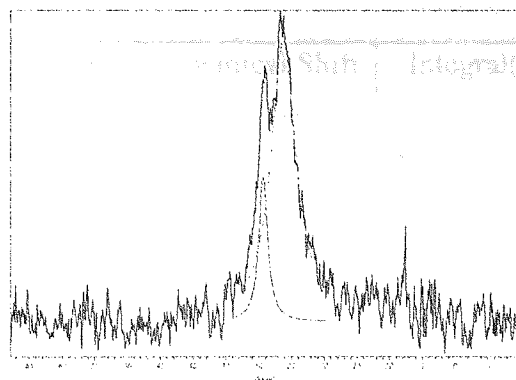
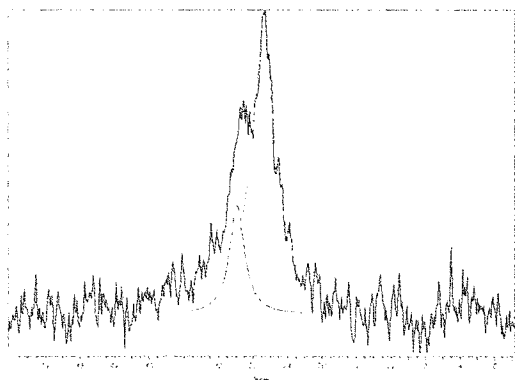
The EDMA system is more rigid than those containing methyl methacrylate and acrylamide and it was interesting to see if this made it more difficult for the template to become associated with the polymer. In order to determine this the template reintroduction experiments were carried out again, but the reaction stopped after one hour. The ^{31}P spectra for these experiments are shown in Figure 92.

Figure 92 ^{31}P MAS NMR Spectra of MIP's Stirred with *p*-Nitrophenyl Methylphosphonate for an Hour.

a) EDMA – Prepared With and Without Template



b) Acrylamide – Prepared With and Without Template with α -Nitrobenzyl Alcohol



c) Methyl methacrylate – Prepared With and Without Template

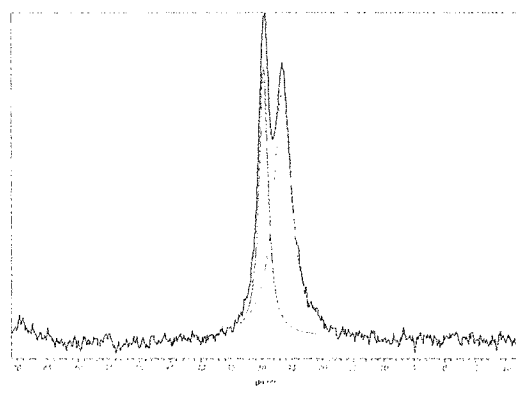
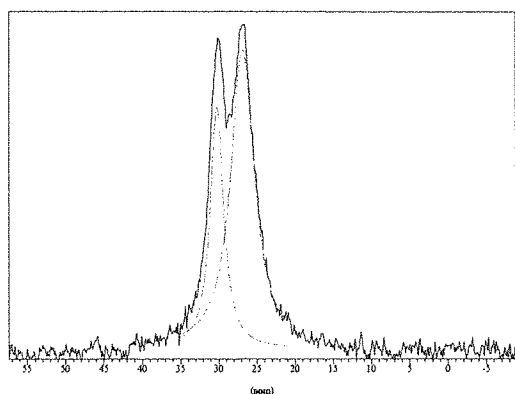
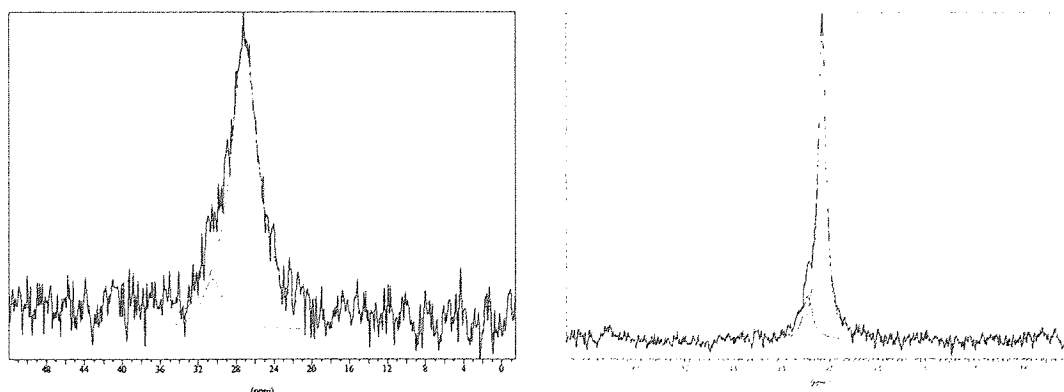


Table 27 ^{31}P MAS NMR Data of MIP's Stirred with *p*-Nitrophenyl Methylphosphonate for an Hour.

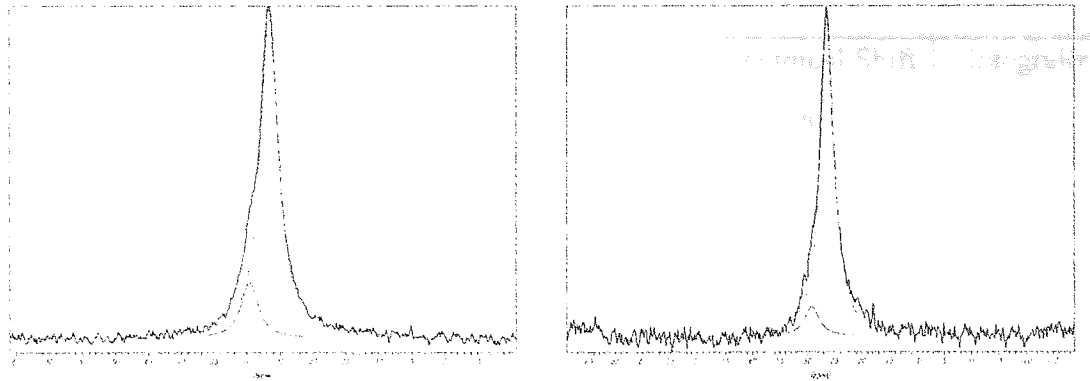
| Polymer | Chemical Shift (ppm) | Integral(rel.) | Chemical Shift (ppm) | Integral(rel.) |
|---|-------------------------|----------------|-------------------------|----------------|
| EDMA (Prepared with Template) | 30.48 | 32 | 26.95 | 68 |
| EDMA (Prepared without Template) | 29.93 | 14 | 26.80 | 86 |
| Acrylamide (Prepared with Template) | 29.82 | 19 | 26.76 | 81 |
| Acrylamide (Prepared without Template) | 29.27 | 15 | 26.15 | 85 |
| Methyl methacrylate (Prepared with Template) | 30.24 | 31 | 26.87 | 69 |
| Methyl methacrylate (Prepared without Template) | 29.63 | 35 | 26.55 | 65 |

Figure 93 ^{31}P MAS NMR Spectra of MIP's Stirred with *p*-Nitrophenyl Methylphosphonate for an Hour then Filtered.

a) EDMA – Prepared With and Without Template



b) Acrylamide – Prepared With and Without Template ~~with 2-Nitroethyl Methacrylate~~



c) Methyl-methacrylate – Prepared With and Without Template

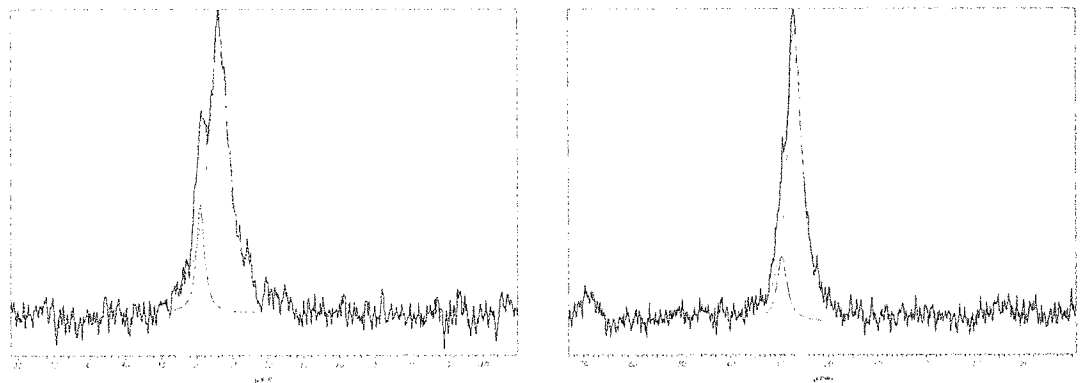


Table 28 ^{31}P MAS NMR Data of MIP's Stirred with *p*-Nitrophenyl Methylphosphonate for an Hour then Filtered.

| Polymer | Chemical Shift (ppm) | Integral(rel.) | Chemical Shift (ppm) | Integral(rel.) |
|---|----------------------|----------------|----------------------|----------------|
| EDMA (Prepared with Template) | 30.49 | 12 | 27.08 | 88 |
| EDMA (Prepared without Template) | 29.50 | 15 | 26.52 | 85 |
| Acrylamide (Prepared with Template) | 29.62 | 14 | 26.57 | 86 |
| Acrylamide (Prepared without Template) | 29.14 | 9 | 26.28 | 91 |
| Methyl methacrylate (Prepared with Template) | 29.48 | 13 | 26.89 | 87 |
| Methyl methacrylate (Prepared without Template) | 29.44 | 13 | 26.77 | 87 |

Comparison of the spectra for unfiltered polymers in which reintroduction of the template has taken place for 24 hours and 1 hour shows that in general less template is found associated with the polymer after 1 hour than after 24 hours. There was little difference between the spectra of filtered polymers stirred for 24 hours and 1 hour with the template molecule. The behaviour of all the polymer systems was similar.

It has been assumed from studies that measure the amount of template within the washings that all of this template is removed from imprinted cavities. This study suggests that up to 40 % of the template is to be found in large solvent pores upon polymerisation. It has also shown that it is possible to distinguish between template that is associated with the polymer and that which is simply precipitated onto the surface or within solvent pores, though the ^{31}P MAS NMR spectra are not sufficiently well resolved to distinguish between template associated within imprinted cavities and that which is simply associated with the polymer.

Chapter 6 Artificial Enzymes for the Oxy-Cope Rearrangement.

... However, although
... few enzymes that
...

6.0 Artificial Enzymes for the Oxy-Cope Rearrangement.

Enzymes are known which catalyse most classes of organic reactions.⁸ However, although pericyclic reactions play an important role in organic chemistry very few enzymes that catalyse the reactions have been found. Enzymes that catalyse the Claisen rearrangement are known but an enzyme to catalyse the oxy-Cope rearrangement has yet to be found. There has also recently been a claim for the isolation of the first Diels-Alderase.¹⁴¹

Clearly the scarcity of enzymes that are able to catalyse pericyclic reactions provide a good opportunity for the design of artificial enzymes that will catalyse these reactions. One approach to the design of artificial enzymes for pericyclic reactions has been the use of catalytic antibodies. This technique involves the generation of antibodies against a suitable transition state mimic. Antibodies which catalyse Diels-Alder reactions¹¹⁵ and the oxy-Cope rearrangement¹⁴² have been reported.

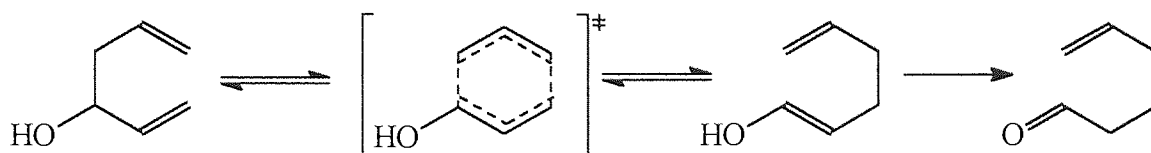
Since both the synthesis of catalytic antibodies and catalytic imprinted polymers rely on the use of transition state mimics, the mimics which have been used in the successful preparation of catalytic antibodies should also be suitable transition state mimics for the synthesis of catalytic imprinted polymers. This has been demonstrated by Mosbach et al¹⁰⁰ who successfully synthesised an imprinted polymer which gave a 270-fold increase in the rate of the Diels-Alder reaction between tetrachlorothiophene dioxide and maleic anhydride using a transition state mimic similar to one used by Hilvert¹¹⁵ in the preparation of antibodies which are Diels-Alder catalysts. To date no imprinted polymer which catalyses the oxy-Cope reaction has been reported.

Schultz et al¹⁴² have reported the use of cyclohexanol based compounds as transition state mimics for the oxy-Cope reaction in the successful preparation of catalytic antibodies for the oxy-Cope reaction. Since Mosbach had successfully synthesised an imprinted polymer for a Diels-Alder reaction, it seemed reasonable to suppose that polymers imprinted with cyclohexanol might catalyse the simplest oxy-Cope rearrangement, that of 1,5-hexadien-3-ol.

6.1 The Oxy-Cope Rearrangement.

The oxy-Cope rearrangement is an example of a [3,3]-sigmatropic rearrangement, see Figure 94.

Figure 94 The Oxy-Cope rearrangement.



Sigmatropic rearrangements, like all pericyclic reactions, take place in a concerted process via a cyclic transition state. The Cope and oxy-Cope rearrangements both have a chair-like six-membered transition state.¹⁴³ Although the Cope rearrangement is reversible, the oxy-Cope reaction is essentially irreversible. The [3,3]-sigmatropic rearrangement is reversible in both reactions but the product of the oxy-Cope rearrangement is an enol. In most cases the keto form has much greater stability than the enol form. Consequently the initially formed enol product is converted to the more stable keto form and the oxy-Cope rearrangement therefore effectively becomes irreversible.

The imprinted polymer catalyst for the Diels-Alder reaction reported by Mosbach was synthesised from ethyleneglycol dimethacrylate (EDMA) and methacrylic acid allowing hydrogen bonding to occur between the polymer and template. It was hoped that an EDMA based polymer imprinted with cyclohexanol, relying solely on the shape of the cavities, would be a catalyst for the oxy-Cope rearrangement of 1,5-hexadien-3-ol.

In contrast to most other molecules used as transition state mimics for imprinting, cyclohexanol is an inexpensive compound that is a liquid at room temperature. Two polymers were synthesised from EDMA, one containing 5 mol% cyclohexanol as the imprint molecule and one using cyclohexanol as both imprint molecule and porogen. The latter system should contain a very large number of active sites and might be a particularly effective catalyst. A control polymer was synthesised in the absence of the template molecule.

6.2 Oxy-Cope Rearrangement of 1,5-Hexadien-3-ol.

The oxy-Cope rearrangement of 1,5-hexadien-3-ol takes place readily at temperatures in excess of 300 °C¹⁴⁴. It was hoped that the use of imprinted polymers as catalysts would significantly decrease the temperature at which the reaction occurred. 1,5-hexadien-3-ol has a bp. of 132-133 °C¹⁴⁵ and the product 5-hexen-1-al has a bp. of 118-120 °C.¹⁴⁶ The reaction was monitored by gas chromatography.

Initially neat 1,5-hexadien-3-ol was heated by oil bath at 120 °C under a nitrogen atmosphere. Samples (0.5 µL) were analysed by GC. The trace showed a peak with a retention time of 2.567 minutes that corresponded to 1,5-hexadien-3-ol. After 8 hours, a shoulder with a longer retention time began to appear. As the product of the oxy-Cope rearrangement, 5-hexen-1-al, has a lower boiling point than 1,5-hexadien-3-ol this product should have a lower retention time than that found for 1,5-hexadien-3-ol. The GC trace of the product obtained after 8 hours showed no evidence of the product from the oxy-Cope rearrangement. This result was not unexpected as temperatures in excess of 300 °C are normally required for the oxy-Cope reaction to occur.

It is possible that the higher boiling product obtained in these experiments was a decomposition product of 1,5-hexadien-3-ol or residual cyclohexanol which had leached out of the polymer as this has a boiling point of 161 °C. Unfortunately, due to the minute amounts produced, it was not possible to determine what this product was.

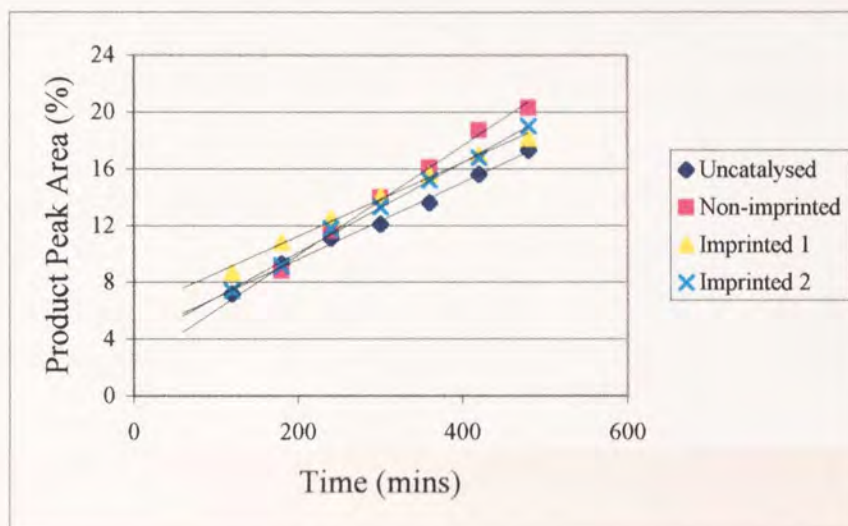
The polymer prepared using cyclohexanol as a porogen should be a more efficient catalyst than the other imprinted polymer and consequently was used in order to test whether any 5-hexen-3-ol could be formed in the presence of this polymer at 120 °C. The reaction was again monitored by GC and the only product detected by GC was the higher boiling material. The shoulder was not resolved, but the shape and increase in size appeared the same as in the uncatalysed reaction.

Although no product from the oxy-Cope reaction was observed when the reaction was carried out at 120 °C it was possible that the polymers might be active catalysts at higher temperatures. The relatively low boiling points of the starting materials and the products provided a problem. Although carrying out the reaction in sealed tubes appeared to be a possible solution, the need to withdraw samples in order to monitor the rate of reaction and to agitate the two phase mixture during the reaction precluded this as a viable technique. In an

attempt to study this reaction at higher temperatures, tetraethyleneglycol (b.p. 275-276 °C) was employed as a solvent and the reaction heated by an oil bath at 200 °C.

The experiment was carried out with no catalyst, with each of the two polymers prepared in the presence of the template and with the polymer which was prepared without template. Again no lower boiling point product appeared, but the peak at higher boiling point grew at a measurable rate. The results are shown in Figure 95.

Figure 95 Effect of Polymer on the Rate of Formation of the Higher Boiling Point Product.



The rates of reaction are shown in Table 29.

Table 29 Rates of Reaction for the Formation of the Higher Boiling Point Product.

| Experiment | Rate of reaction (min^{-1}) | R^2 |
|---------------|--|-------|
| No catalyst | 0.027 ± 0.002 | 0.994 |
| Non-imprinted | 0.039 ± 0.001 | 0.995 |
| Imprinted 1 | 0.026 ± 0.007 | 0.992 |
| Imprinted 2 | 0.032 ± 0.002 | 0.997 |

It can be seen from the results above that the rate of formation of the higher boiling point product is not significantly affected by the presence of polymer. Although the formation of 5-hexen-1-al was not observed in these reactions it is possible that at higher temperatures the catalysts may be active. The difficulty of monitoring this reaction at high temperatures has already been discussed. An alternative method for carrying out this reaction might be to pack

the polymers into GC columns and then vary the length of time the 1,5-hexadien-3-ol is in contact with the polymer by changing the flow rate of the carrier gas in the gas chromatograph. Unfortunately it was not possible to pursue this approach further during this work.

Chapter 7 Conclusions and Further Work.

to be used as a model for a

to be used as a model for a

7.0 Conclusions.

The aim of this project was the synthesis of a MIP that could be used as a model for a synthetic serine protease. Derivatives of L-histidine were investigated as models for the Asp-His couple found in the catalytic triad of serine proteases. It was found using molecular dynamics and ^1H NMR that in aqueous solution the most populated conformations of *N*-acetyl-L-histidine and the *N*-acetyl-L-histidine anion were those in which the carboxylate group and imidazole ring were gauche to each other. These conformations indicated that an interaction may be present and the N-H-O distances and angles obtained from the molecular modelling in the gas phase were of values that would allow hydrogen bonding to take place. This confirmed previous studies¹²¹ using ^1H NMR to calculate the mole fractions of the three conformations though this study indicated that steric factors were more important than had been thought.

The molecular modelling results gave promise that derivatives of L histidine might be good models for the Asp-His couple in the serine proteases. As the serine proteases are known to hydrolyse esters, imidazole, *N*-acetyl-L-histidine and two salts of *N*-acetyl-L-histidine were used as catalysts in the hydrolysis of *p*-nitrophenyl acetate in order to determine whether there was any interaction between the carboxylate group and the imidazole ring. It was found that in DMSO/H₂O 9:1 v/v solution that when using salts of *N*-acetyl-L-histidine there was indeed an interaction between the carboxylate group and the imidazole ring which increased the rate of reaction over that obtained for imidazole and the *N*-acetyl-L-histidine zwitterion. This showed that the carboxylate group increased the nucleophilicity of the imidazole ring. It was also found that the counterion of the salt had an effect, the sodium salt being a better catalyst than the tetra-*n*-butylammonium salt.

A new technique using ^{31}P MAS NMR spectroscopy to study the environment of the template molecule within imprinted polymers was designed. The technique was used on imprinted and non-imprinted polymers derived from EDMA, EDMA/methyl methacrylate and EDMA/acrylamide. This study showed that up to 40% of the template is to be found in large solvent pores upon polymerisation rather than within imprinted cavities. It was also shown that it is possible to distinguish between template that is associated with the polymer and that which is simply precipitated onto the surface or within solvent pores, though the ^{31}P MAS NMR cannot be resolved to distinguish between template associated within imprinted cavities and that which is simply associated with the polymer.

Attempts to determine whether the Asp-His couple was present within imprinted cavities in an imprinted polymer derived from *N*-methacryloyl-L-histidine were hindered by difficulties carrying out the kinetic studies. It was not possible to obtain consistent measurements and therefore not possible to calculate rates of reaction. The results did however show that the presence of imprinted cavities improved the rate of reaction for the polymer derived from *N*-methacryloyl-L-histidine in pH 8.0 buffer solution.

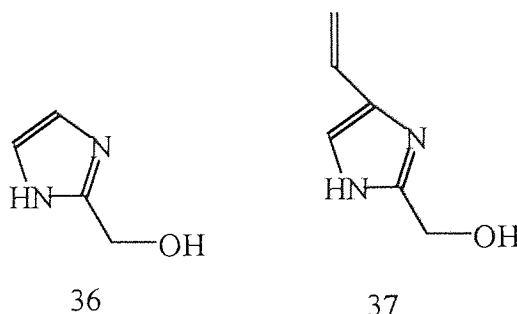
An investigation into the formation of an imprinted polymer to catalyse the oxy-Cope rearrangement was initially unsuccessful. Due to the extreme conditions needed for this reaction, it was not possible to synthesise the product of the rearrangement. The formation of a by-product which was formed, was not catalysed by the presence of an imprinted polymer.

7.1 Further Work.

There are three main areas that need to be studied further in order to continue with this work. The first is the design of a suitable method from which it is possible to obtain consistent values when studying the rate of hydrolysis of *p*-nitrophenyl acetate by MIP's. This is necessary due to the difficulties in reproducibility of the results obtained using the current method. The most promising method to solve this problem is the use of an HPLC column packed with the imprinted polymer and passing through solutions of *p*-nitrophenyl acetate at different rates. The inconsistency could also be overcome by the use of an improved filtration method.

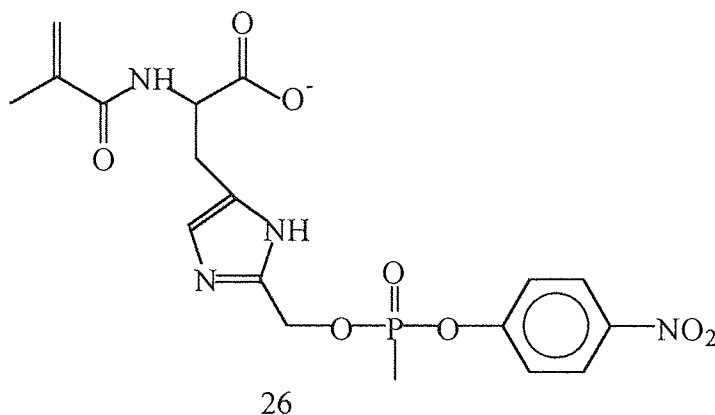
The second area that could be followed up is the formation of small molecules and polymers that contain the hydroxyl functional groups. It would be interesting to synthesise molecules that contain the imidazole and hydroxyl functional groups such as **36** and **37**, shown in Figure 96, in order to see if there is any interaction between these groups.

Figure 96 Potential Catalysts Containing an Imidazole Ring and Hydroxyl Group.



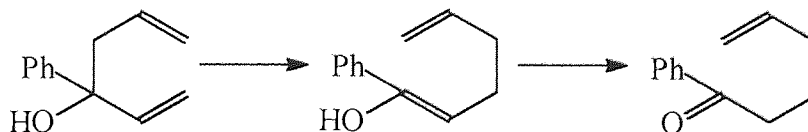
Eventually it could be possible to synthesise an MIP derived from L-histidine that incorporates these three functional groups into its imprinted cavity such as molecule **26**, shown in Figure 97, which may show catalytic ability for the hydrolysis of an ester approaching that shown by the enzyme.

Figure 97 Monomer for an Ester Hydrolysing MIP.



It would also be interesting to try and continue the work on pericyclic reactions as this has been shown to give good rate increases.¹⁰⁰ Though the oxy-Cope system used in this study, did not work, it is hoped that a system that does not require such harsh conditions for reaction to take place would offer more promising results. One such system is the following oxy-Cope rearrangement, see Figure 98.

Figure 98 Oxy-Cope Rearrangement.



This is a more promising oxy-Cope rearrangement as the intermediate product is stabilised by resonance.

Chapter 8 Experimental.

8.0 Experimental.

8.1 Reagents.

All reagents and solvents were used as supplied unless otherwise stated.

| Compound | RMM | MP/BP (°C) | Supplier |
|--|--------|------------|-----------|
| Acetone | 58.08 | 56.0 | Fisher |
| Acetonitrile, anhydrous | 41.05 | 81.6 | Fisher |
| <i>N</i> -Acetyl-L-histidine | 197.2 | 157-159 | Aldrich |
| <i>N</i> -Acetyl-L-phenylalanine | 207.23 | 171-173 | Aldrich |
| Acrylamide | 71.08 | 84-86 | Vickers |
| α,α' -Azobisisobutyronitrile | 164 | - | Aldrich |
| <i>n</i> -Butyllithium, 2.5M solution in Hexanes | 64.06 | - | Aldrich |
| Chloroform | 119.38 | 60.5-61.5 | Fisher |
| Dichloromethane | 84.93 | 40 | Fisher |
| Diethyl ether | 74.12 | 34.6 | Fisher |
| <i>N,N</i> -Dimethylformamide, anhydrous | 73.09 | 157.0 | Fisher |
| Dimethyl sulfoxide, anhydrous | 78.13 | 189 | Aldrich |
| Disodium phosphate | 141.96 | 770 | Aldrich |
| EDMA | 198.22 | 98-100 | Aldrich |
| Ethanol | 48.0 | 78.5 | Fisher |
| Ethyl acetate | 88.11 | 76.5-77.5 | Fisher |
| Hexane | 86.18 | 69 | Fisher |
| L-Histidine | 155.16 | 282 | Aldrich |
| Hydrochloric acid | 36.46 | - | Fisher |
| Imidazole | 68.08 | 89-91 | Aldrich |
| Imidazolecarboxaldehyde | 96.09 | 174-177 | Aldrich |
| Magnesium sulfate | 120.37 | - | Lancaster |
| Methacryloyl chloride | 104.54 | 95-96 | Lancaster |
| Methanol | 32.04 | 64.7 | Fisher |

| | | | |
|--|--------|---------|-----------|
| Methylimidazole | 82.11 | 46-48 | Aldrich |
| Methyl methacrylate | 100.12 | 100 | Aldrich |
| Methylphosphonic dichloride | 132.91 | 35-37 | Aldrich |
| (Methyl)triphenylphosphonium bromide | 357.24 | 230-234 | Lancaster |
| <i>p</i> -Nitrophenol | 139.11 | 113-115 | Aldrich |
| <i>p</i> -Nitrophenyl acetate | 181.15 | 77-79 | Aldrich |
| Phosphorous pentoxide | 283.89 | 340 | Aldrich |
| Potassium chloride | 74.56 | 770 | Aldrich |
| Potassium dihydrogen phosphate | 136.09 | 252 | Aldrich |
| Sodium bicarbonate | 84.01 | - | Lancaster |
| Sodium borohydride | 37.83 | 400 | Aldrich |
| Sodium hydride 60% dispersion in mineral oil | 24.00 | - | Avocado |
| Sodium hydroxide | 40.00 | 318 | Fisher |
| Tetra- <i>n</i> -butylammonium hydroxide 1.0M solution in methanol | 259.48 | - | Aldrich |
| Tetrahydrofuran, anhydrous | 72.11 | 67.0 | Fisher |
| Toluene, anhydrous | 92.14 | 110.6 | Fisher |
| Triethylamine | 101.19 | 88 | Aldrich |
| Trityl chloride | 278.78 | 110-112 | Lancaster |
| Water (HPLC grade) | 18.02 | 100 | Fisher |

8.2 Formation of pH 7.0, 7.6 and 8.0 Buffer Solutions.

The aqueous buffered solutions were formed using the method described in Geigy Scientific Tables.¹⁴⁷ Potassium dihydrogen phosphate (9.07 g, 67 mmol) was dissolved in HPLC grade H₂O (1 L) to form solution A. Disodium phosphate (11.87 g, 67 mmol) was dissolved in HPLC grade H₂O (1 L) to form solution B.

pH 7.0 buffered solution was formed by measuring 27.0 cm³ of solution A and 38.25 cm³ of solution B into a 250 cm³ volumetric flask and making up to 250 cm³ with HPLC grade H₂O. The ionic strength (μ) was made up to 0.1 with potassium chloride (1.87 g).

pH 7.6 buffered solution was formed by measuring 7.85 cm³ of solution A and 53.53 cm³ of solution B into a 250 cm³ volumetric flask and making up to 250 cm³ with HPLC grade H₂O.

The ionic strength (μ) was made up to 0.1 with potassium chloride (1.87 g).

pH 8.0 buffered solution was formed by measuring 2.25 cm³ of solution A and 58.00 cm³ of solution B into a 250 cm³ volumetric flask and making up to 250 cm³ with HPLC grade H₂O.

The ionic strength (μ) was made up to 0.1 with potassium chloride (1.87 g).

8.3 Methods of Analysis.

Infrared spectra were recorded on a Perkin Elmer 1710 Fourier Transform infrared Spectrometer. Solid samples were prepared as KBr discs, whilst liquids were prepared as thin films on sodium chloride plates.

NMR spectra were recorded on a Bruker AC300 spectrometer. ¹³C NMR spectra were recorded as Pendent spectra.

All ³¹P MAS NMR spectra were obtained using 121.5 Hz proton high power, MAS decoupling with a rotor speed of 6500 MHz and using 88 % phosphoric acid as reference.

UV absorbances were measured on a Perkin Elmer Lambda 12 UV/Vis spectrometer.

GC plots were run on a ATI Unicam 610 series Gas Chromatograph using a silica gel column.

8.4 Synthesis of Imidazole Derivatives.

8.4.1 Synthesis of 4(5)-vinylimidazole.

8.4.1.1 Synthesis of *N*-Trityl-4-imidazolecarboxaldehyde.

Imidazolecarboxaldehyde (0.48 g, 5 mmol) was stirred in anhydrous DMF (10 cm³). Trityl chloride (1.32 g, 6 mmol) was added, then triethylamine (1.7 cm³, 12 mmol) was slowly added dropwise. Upon addition of the triethylamine a white precipitate was formed. The mixture was left to stir overnight. After 12 hours the solution had become pink. The mixture was filtered and the solvent was reduced by evaporation to yield a pink solid. The solid was taken up in chloroform and hexane added dropwise to yield a white solid. The white solid was crystallised from chloroform/hexane, filtered and washed with hexane to yield white needle-like crystals of *N*-trityl-4-imidazolecarboxaldehyde (1.1 g, 65 %); mp 188-190 °C (Lit.¹⁴⁸ 189-192 °C); $\nu_{\max}/\text{cm}^{-1}$ 1490 (phenyl), 1610 (phenyl), 1690 (CO); δ_{H} (300MHz, CDCl₃) 7.1 (6H, d, *J* 4, (Aromatic -CH-), 7.4 (9H, s, (Aromatic -CH-)), 7.5 (1H, s, Im 5 - CH=), 7.6 (1H, s, Im 2 -CH-), 9.9 (1H, s, -CHO); δ_{C} (75MHz, CDCl₃) 126.7 (Im 5 -CH-), 127.9 (Aromatic -CH-), 128.4 (Aromatic -CH-), 140.6 (Im 2 -CH-), 140.9 (-C-(Ph₃)), 141.5 (=C-CHO), 186.5 (CHO).

8.4.1.2 Synthesis of 4-Vinyl-1-tritylimidazole.

The procedure followed was that described by Kokosa et al.¹²⁴ A 60 % dispersion of sodium hydride in oil (0.25 g, 10 mmol) was added to an oven dried three neck round bottom flask with a stir bar and was washed under N₂ with 3 portions of anhydrous hexane to remove the mineral oil. Under N₂, anhydrous DMSO (8.0 cm³) was added and the mixture heated at 75-80 °C for 1.5 hours. The mixture was cooled to 50 °C and (methyl)triphenylphosphonium bromide (3.57 g, 10 mmol) was added and the mixture stirred at 50 °C for 0.5 hours. *N*-trityl-4-imidazolecarboxaldehyde (0.169 g, 5 mmol) was added and the mixture stirred for 4.5 hours at 70 °C. After 4.5 hours the mixture was cooled to 50 °C and poured into H₂O (50 cm³) with stirring. The precipitate was filtered, washed with H₂O and dried under vacuum to yield a brown sticky solid. The solid was chromatographed on a silica gel column using chloroform as the liquid phase. The chloroform was evaporated to yield a white solid of 4-

vinyl-1-tritylimidazole (1.1 g, 65 %); mp 201-204°C (Lit.¹²⁴ 205-207 °C); $\nu_{\max}/\text{cm}^{-1}$ 1490 (phenyl), 1600 (phenyl), 1640 (C=C); δ_{H} (300MHz, CDCl_3) 5.1 (1H, d, J 11, -CH=CH₂), 5.8 (1H, d, J 17, -CH=CH₂), 6.5 (1H, dd, J 11, J 17, -CH=CH₂), 6.8 (1H, s, Im 5 -CH-), 7.1 (6H, s, Aromatic -CH-), 7.3 (9H, s, Aromatic -CH-), 7.4 (1H, s, Im 2 -CH-); δ_{C} (75MHz, CDCl_3) 112.1 (-CH=CH₂), 119.3 (-CH=CH₂), 128.6 (Im 5 -CH-), 139.1 (Im 2 -CH-), 139.5 (Im 4 -C=), 142.3 (-C-(Ph₃))

8.4.1.3 Synthesis of 4(5)-vinylimidazole.

The procedure followed was that described by Kokosa et al.¹²⁴ 4-vinyl-1-tritylimidazole (0.67 g, 2 mmol) was stirred in THF (2.5 cm³) and 6 M HCl (0.7 cm³, 4 mmol) was added and the solution refluxed for 2 hours. The solvent was then removed under vacuum at a temperature less than 45 °C. The resulting solid was stirred in H₂O, filtered and the aqueous phase basified with saturated sodium bicarbonate solution to pH7. The water was removed under vacuum at a temperature less than 45 °C and the resulting solid was stirred in chloroform for 24 hours. The chloroform was filtered and the solvent removed under vacuum at a temperature less than 45 °C to yield a yellow oil. Upon scratching, the oil started to crystallise, yielding yellow crystals of 4(5)-vinylimidazole (0.14 g, 74 %), mp 78-79 °C (Lit.¹²⁴ 80-82°C); $\nu_{\max}/\text{cm}^{-1}$; δ_{H} (300MHz, CDCl_3) 5.1 (1H, d, J 11, -CH=CH₂), 5.7 (1H, d, J 18, -CH=CH₂), 6.6 (1H, q, J 11, J 17, -CH=CH₂), 7.0 (1H, s, Im 5 -CH-), 7.6 (1H, s, Im 5 -CH-), 10.6 (1H, s, NH); δ_{C} (75MHz, CDCl_3) 112.8 (-CH=CH₂), 119.8 (Im 5 -CH-), 128.1 (Im 2 -CH-), 135.5 (Im 4 -C=), 135.8 (-CH=CH₂),

8.5 Synthesis of Amino-Acid Derivatives.

8.5.1 Synthesis of *N*-Methacryloyl-L-histidine.

The procedure followed was that described by Yoshihara et al.¹²³ Methacryloyl chloride (1.95 cm³, 20 mmol) in dichloromethane (8 cm³) was added dropwise to a solution of L-histidine (2.48 g, 16 mmol) and sodium hydroxide (0.8 g) in water (10 cm³) cooled in an ice bath. The mixture was then acidified to pH 2.0 using 6 M hydrochloric acid and extracted with ether (2x50 cm³). The aqueous layer was then adjusted to pH 5.0 with 2 M sodium hydroxide solution and the water was removed under vacuum, at a temperature no greater

than 40 °C. The resulting solid was shaken with ethanol, all insoluble material removed by filtration and the solution reduced under vacuum until a precipitate appeared. Excess acetone was added to this mixture and the white precipitate formed was filtered and dried over phosphorous pentoxide to yield *N*-methacryloyl-L-histidine (2.09 g, 59 %); $\nu_{\max}/\text{cm}^{-1}$ 3420 (NH), 1655 (CONH); δ_{H} (300MHz, CDCl_3) 1.7 (3H, s, $-\text{CH}_3$), 3.1 (2H, d, J 6, $-\text{CH}_2-$), 4.4 (1H, t, J 6, $-\text{CH}-$), 5.2 (1H, s, $-\text{C}=\text{CH}_2$), 5.5 (1H, s, $-\text{C}=\text{CH}_2$), 7.0 (1H, s, Im 5 $-\text{CH}=\text{}$), 8.3 (1H, s, -Im 2 $-\text{CH}=\text{}$); δ_{C} (75MHz, CDCl_3) 8.6 ($-\text{CH}_3$), 18.6 ($-\text{CH}_2-$), 44.9 ($-\text{CH}-$), 108.2 (Im 5 $-\text{CH}=\text{}$), 108.8 ($\text{C}=\text{CH}_2$), 122.5 (Im 4 $-\text{C}-$), 124.8 (Im 2 $-\text{CH}_2=\text{}$), 131.0 ($\text{C}=\text{CH}_2$), 160.4 ($\text{C}=\text{O}$), 166.0 (CO_2)

8.5.2 Synthesis of *N*-Acetyl-L-histidine Salts.

Sodium salt

N-acetyl-L-histidine (1.0 g, 5 mmol) was dissolved in an equimolar amount of 1.0 M sodium hydroxide solution. The solution was stirred overnight and the solvent removed under vacuum. Any residual water was removed using Dean and Stark apparatus. The resulting solid was stored over phosphorous pentoxide.

Tetra-*n*-butylammonium salt

The experiment above was repeated replacing the 1.0 M sodium hydroxide solution with 1.20 M tetra-*n*-butylammonium hydroxide in methanol solution.

8.5.3 Synthesis of *N*-Acetyl-L-phenylalanine Salts.

The experiment was repeated as in 8.5.2, but the *N*-acetyl-L-histidine was replaced with *N*-acetyl-L-phenylalanine.

8.6 Synthesis of Template Molecules.

8.6.1 Synthesis of *p*-Nitrophenyl Methylphosphonate.

The procedure followed was that described by Edwards et al.¹²⁵ Methylphosphonodichloride (5 g, 38 mmol) and *p*-nitrophenol (10 g, 72 mmol) were heated to 160 °C over a period of 3 hours and then kept at 160 °C for a further hour. After cooling to room temperature the black

oily mixture was then dissolved in toluene and decolourised with charcoal. The solution was filtered and the solvent reduced under vacuum. The resulting brown crystals were recrystallised from toluene/ether (50/50 v/v) to give pale brown crystals of crude bis(*p*-nitrophenyl)methylphosphonate 4.98 g.

Bis(*p*-nitrophenyl)methylphosphonate (2.5 g, 7 mmol) and sodium hydroxide (0.65 g) were dissolved in water (50 ml) and heated to reflux. The solution was then cooled and acidified to pH 3.5 with 6M hydrochloric acid then extracted with ether. The extractions were continued until thin layer chromatography showed no product in the aqueous phase. The ether was then dried with magnesium sulfate and the solvent removed under vacuum. Upon addition of excess ether a white precipitate formed which was filtered, washed with cold ether and recrystallised from ether/THF to yield pale needlelike crystals of *p*-nitrophenyl methylphosphonate (0.68 g, 47 %), mp 107-111 °C (Lit. 113-114 °C); $\nu_{\max}/\text{cm}^{-1}$; δ_{H} (300MHz, CDCl₃) 1.6 (3H, d, *J* 17, -CH₃), 7.3 (2H, d, *J* 8, Aromatic CH), 8.2 (2H, d, *J* 8, Aromatic CH); δ_{C} (75MHz, CDCl₃) 11.4 (d, -CH₃), 120.0 (Aromatic -CH-), 124.4 (Aromatic -CH-), 124.8 (Aromatic -C-), 155.0 (Aromatic -C-).

8.7 Polymer Synthesis.

The imprinted polymers were synthesised using the method of Yu and Mosbach.¹⁴⁹

8.7.1 Synthesis of an Acrylamide Based MIP.

Acrylamide (86 mg, 1 mmol), EDMA (0.95 cm³, 5 mmol), *p*-nitrophenyl methylphosphonate (55 mg, 0.25 mmol) and AIBN (10 mg) were dissolved in anhydrous acetonitrile (1.5 cm³). The solution was degassed in a sonic bath, bubbled with nitrogen for 5 minutes, heated in an oven at 60 °C for 72 hours. The polymer was ground and those particles retained by a 38 μm sieve were then washed with methanol using a Soxhlet extractor for 72 hours.

The synthesis was repeated without *p*-nitrophenyl methylphosphonate to form a non-imprinted analogue.

8.7.2 Synthesis of an EDMA Based MIP.

EDMA (0.95 cm³, 5 mmol), *p*-nitrophenyl methylphosphonate (55 mg, 0.25 mmol) and AIBN (10 mg) were dissolved in anhydrous acetonitrile (1.5 cm³). The solution was degassed in a sonic bath, bubbled with nitrogen for 5 minutes, heated in an oven at 60 °C for 72 hours. The polymer was ground and those particles retained by a 38 μm sieve were then washed with methanol using a Soxhlet extractor for 72 hours.

The synthesis was repeated without *p*-nitrophenyl methylphosphonate to form a non-imprinted analogue.

8.7.3 Synthesis of a Methyl Methacrylate Based MIP.

Methyl methacrylate (0.1 cm³, 1 mmol), EDMA (0.95 cm³, 5 mmol), *p*-nitrophenyl methylphosphonate (55 mg, 0.25 mmol) and AIBN (10 mg) were dissolved in anhydrous acetonitrile (1.5 cm³). The solution was degassed in a sonic bath, bubbled with nitrogen for 5 minutes, heated in an oven at 60 °C for 72 hours. The polymer was ground and those particles retained by a 38 μm sieve were then washed with methanol using a Soxhlet extractor for 72 hours.

The synthesis was repeated without *p*-nitrophenyl methylphosphonate to form a non-imprinted analogue.

8.7.4 Synthesis of an *N*-Methacryloyl-L-histidine Based MIP.

N-methacryloyl-L-histidine (0.22 g, 1 mmol), EDMA (0.95 cm³, 5 mmol), *p*-nitrophenyl methylphosphonate (55 mg, 0.25 mmol) and AIBN (10 mg) were dissolved in anhydrous DMSO (1.5 cm³). The solution was degassed in a sonic bath, bubbled with nitrogen for 5 minutes, heated in an oven at 60 °C for 72 hours. The polymer was ground and those particles retained by a 38 μm sieve were then washed with methanol using a Soxhlet extractor for 72 hours.

The synthesis was repeated without *p*-nitrophenyl methylphosphonate to form a non-imprinted analogue.

8.7.5 Synthesis of a 4(5)-vinylimidazole Based MIP.

4(5)-vinylimidazole (0.094 g, 1 mmol), EDMA (0.95 cm³, 5 mmol), *p*-nitrophenyl methylphosphonate (55 mg, 0.25 mmol) and AIBN (10 mg) were dissolved in anhydrous acetonitrile (1.5 cm³). The solution was degassed in a sonic bath, bubbled with nitrogen for 5 minutes, heated in an oven at 60 °C for 72 hours. The polymer was ground and those particles retained by a 38 µm sieve were then washed with methanol using a Soxhlet extractor for 72 hours.

The synthesis was repeated without *p*-nitrophenyl methylphosphonate to form a non-imprinted analogue.

8.7.6 Treatment of *N*-Methacryloyl-L-histidine Imprinted and Non-imprinted Polymers with Sodium Hydroxide and Tetra-*n*-butylammonium Hydroxide.

The *N*-methacryloyl-L-histidine imprinted polymer was synthesised using the method described in 8.7.4. The polymer was ground and those particles retained by a 38 µm sieve were washed for three days using a Soxhlet extractor. Imprinted polymer (1.9 g) was soaked for 24 hours in 1.11 M NaOH solution (1.4 cm³, 1.6 mmol). The polymer was then filtered and washed for three days using a Soxhlet extractor. This was repeated for the non-imprinted polymer.

The above experiment was also repeated soaking both imprinted and non-imprinted polymers in 1.20 M tetra-*n*-butylammonium hydroxide (1.3 cm³, 1.6 mmol).

8.8 Kinetic Studies.

8.8.1 Hydrolysis of *p*-Nitrophenyl Acetate.

A 0.04 M solution of *p*-nitrophenyl acetate in anhydrous DMSO was prepared. pH 8.0 buffer solution (3.00 cm³) was measured into both the reaction and background cells. All solutions were equilibrated at 25.0±0.1 °C for an hour. The background spectrum was run. 0.04 M *p*-nitrophenyl acetate solution (25 µL) was added to the reaction cell, the solution shaken, and the UV absorbance measured at 410 nm every minute for an hour.

The experiment was repeated using pH 7.6 and pH 8.0 buffered solutions

The experiment was repeated using DMSO/H₂O 9:1 v/v solution.

8.8.2 Hydrolysis of *p*-Nitrophenyl Acetate in Buffer Solution, Small Molecules as Catalyst.

A 0.04 M solution of *p*-nitrophenyl acetate in anhydrous DMSO was prepared. 1.50x10⁻³ M, 1.25x10⁻³ M, 1.00x10⁻³ M, 0.75x10⁻³ M and 0.50x10⁻³ M imidazole and *N*-acetyl-L-histidine solutions in pH 7.0, 7.6 and 8.0 buffer solutions were prepared. All solutions were equilibrated in a 25°C±0.1 °C water bath for an hour. 3.00 cm³ of pH 7.0 buffered solution was measured into the background cell. 3.00 cm³ of 1.50x10⁻³ M catalyst solution was measured into the reaction cell and a background spectrum was run at 410 nm. *p*-Nitrophenyl acetate solution (25 µL) was added to the reaction cell, shaken and the UV absorbance measured every minute at 410 nm for an hour. The reaction was repeated twice.

The above reaction was repeated with all concentrations of imidazole and *N*-acetyl-L-histidine solutions, at all pHs.

8.8.3 Hydrolysis of *p*-Nitrophenyl Acetate in a DMSO/H₂O 9:1 v/v Solution, Small Molecules as Catalyst.

A 0.04 M solution of *p*-nitrophenyl acetate in anhydrous DMSO was prepared. 1.50x10⁻³ M, 1.25x10⁻³ M, 1.00x10⁻³ M, 0.75x10⁻³ M and 0.50x10⁻³ M imidazole, *N*-acetyl-L-histidine, *N*-acetyl-L-histidine sodium salt and *N*-acetyl-L-histidine tetra-*n*-butylammonium salt solutions in DMSO/H₂O 9:1 v/v solution were prepared. All solutions were equilibrated in a 25.0±0.1 °C water bath for an hour. 3.00 cm³ of buffer was measured into the background cell. 3.00 cm³ of 1.50x10⁻³ M catalyst solution was measured into the reaction cell and a background spectrum was run at 410 nm. *p*-Nitrophenyl acetate solution (25 µL) was added to the reaction cell, shaken and the UV absorbance measured every minute at 410 nm for an hour. The reaction was repeated twice.

The above reaction was repeated with all concentrations of imidazole, *N*-acetyl-L-histidine, *N*-acetyl-L-histidine sodium salt and *N*-acetyl-L-histidine tetra-*n*-butylammonium salt solutions.

8.8.4 Hydrolysis of *p*-Nitrophenyl Acetate in pH 8.0 Buffer Solutions, MIP's as Catalyst.

A 0.04 M solution of *p*-nitrophenyl acetate in anhydrous DMSO was prepared. 4(5)-vinylimidazole based MIP (0.20 g) was weighed into a jacketed flask and pH 8.0 buffered solution (30 ml) was added. The polymer was soaked for 16 hours the mixture was then equilibrated at 25.0 ± 0.1 °C for an hour. The reaction was stirred and 0.015 M *p*-nitrophenyl acetate solution (250 μ L) was added. A 0.25 cm³ sample was taken every 6 minutes, filtered and the UV absorbance measured at 410 nm.

The above experiment was repeated with 0.16 g, 0.13 g, 0.10 g and 0.06 g of imprinted polymer and all masses of non-imprinted polymer.

The above experiment was repeated with 0.22 g, 0.18 g, 0.15 g, 0.11 g and 0.07 g of imprinted and non-imprinted *N*-methacryloyl-L-histidine based MIP.

8.8.5 Hydrolysis of *p*-Nitrophenyl Acetate in DMSO/H₂O 9:1 v/v Solution, MIP's as Catalyst.

A 0.04 M solution of *p*-nitrophenyl acetate in anhydrous DMSO was prepared. 4(5)-vinylimidazole based MIP (0.20 g) was weighed into a jacketed flask and DMSO/H₂O 9:1 v/v (30 ml) was added. The polymer was soaked for 16 hours the mixture was then equilibrated at 25.0 ± 0.1 °C for an hour. The reaction was stirred and 0.015 M *p*-nitrophenyl acetate solution (250 μ L) was added. A 0.25 cm³ sample was taken every 6 minutes, filtered and the UV absorbance measured at 424.8 nm.

The above experiment was repeated with 0.16 g, 0.13 g, 0.10 g and 0.06 g of imprinted polymer and all masses of non-imprinted polymer.

The above experiment was repeated with 0.22 g, 0.18 g, 0.15 g, 0.11 g and 0.07 g of imprinted and non-imprinted *N*-methacryloyl-L-histidine based MIP.

The above experiment was repeated with 0.22 g, 0.18 g, 0.15 g, 0.11 g and 0.07 g of imprinted and non-imprinted *N*-methacryloyl-L-histidine sodium salt based MIP.

The above experiment was repeated with 0.26 g, 0.21 g, 0.18 g, 0.13 g and 0.08 g of imprinted and non-imprinted *N*-methacryloyl-L-histidine tetra-*n*-butylammonium salt based MIP.

8.9 Study of the Conformations of *N*-Acetyl-L-histidine, *N*-Acetyl-L-phenylalanine and their Salts.

8.9.1 Association of *N*-Acetyl-L-histidine and its Salts.

Aqueous solutions of *N*-acetyl-L-histidine (0.45 M, 0.30 M, 0.15 M, and 0.05 M) were measured into a 1 mm pathlength cuvette and the UV spectra measured at 260 nm.

Aqueous solutions of *N*-acetyl-L-histidine sodium salt (0.45 M, 0.30 M, 0.15 M, and 0.05 M) were measured into a 1 mm pathlength cuvette and the UV spectra measured at 390.4 nm.

Aqueous solutions of *N*-acetyl-L-histidine tetra-*n*-butylammonium salt (0.45 M, 0.30 M, 0.15 M, and 0.05 M) were measured into a 1 mm pathlength cuvette and the UV spectra measured at 285 nm.

8.9.2 Association of *N*-Acetyl-L-phenylalanine and its Salts.

Aqueous solutions of *N*-acetyl-L-phenylalanine sodium salt (0.45 M, 0.30 M, 0.15 M and 0.05 M) were measured into a 1 mm pathlength cuvette and the UV spectra measured at 257.6 nm.

N-acetyl-L-phenylalanine and *N*-acetyl-L-phenylalanine tetra-*n*-butylammonium salt would not dissolve at the required concentrations.

8.10 Study of the Environment of the Template in MIP's using ^{31}P MAS NMR.

All ^{31}P MAS NMR spectra were obtained using 121.5 Hz proton high power, MAS decoupling with a rotor speed of 6500 MHz and using 88 % phosphoric acid as reference.

8.10.1 Study of the Environment of the Template in MIP using ^{31}P MAS NMR – Initial Imprinted Polymer.

Acrylamide based MIP was synthesised as in 8.7.1, but the polymer was not washed with methanol for 72 hrs. A ^{31}P MAS NMR spectra of imprinted acrylamide MIP (0.5 g) was obtained.

The above experiment was repeated using both the methyl methacrylate and EDMA imprinted polymers.

8.10.2 Study of the Environment of Template in MIP's using ^{31}P MAS NMR – Ground with *p*-Nitrophenyl Methylphosphonate.

Imprinted acrylamide polymer (0.5 g) and *p*-nitrophenyl methylphosphonate (25 mg) were ground up together and a ^{31}P MAS NMR spectra obtained. This experiment was repeated with non-imprinted acrylamide polymer (0.5 g).

The above experiment was repeated using both the methyl methacrylate and EDMA imprinted polymers.

8.10.3 Study of the Environment of Template in MIP's using ^{31}P MAS NMR – Stirred with *p*-Nitrophenyl Methylphosphonate for an Hour.

Imprinted acrylamide polymer (0.5 g) and *p*-nitrophenyl methylphosphonate (25 mg) were stirred together in acetonitrile (5.0 cm³) for 1 hour, the solvent evaporated in an oven at 60 °C and a ^{31}P MAS NMR Spectra obtained. This experiment was repeated with non-imprinted acrylamide polymer (0.5 g).

The above experiment was repeated using both the methyl methacrylate and EDMA imprinted polymers.

8.10.4 Study of the Environment of Template in MIP's using ^{31}P MAS NMR – Stirred with *p*-Nitrophenyl Methylphosphonate for Twenty-four Hours.

The experiment was carried out as in 8.10.3, but the mixture was stirred for 24 hours.

8.10.5 Study of the Environment of Template in MIP's using ^{31}P MAS NMR – Stirred with *p*-Nitrophenyl Methylphosphonate for an Hour and Filtered.

Imprinted acrylamide polymer (0.5 g) and *p*-nitrophenyl methylphosphonate (25 mg) were stirred together in acetonitrile (5 cm³) for 1 hour, the mixture filtered and a ^{31}P MAS NMR Spectra obtained. This experiment was repeated with non-imprinted acrylamide polymer (0.5 g).

The above experiment was repeated using both the methyl methacrylate and EDMA imprinted and non-imprinted polymers.

8.10.6 Study of the Environment of Template in MIP's using ^{31}P MAS NMR – Stirred with *p*-Nitrophenyl Methylphosphonate for Twenty-four Hours and Filtered.

The experiment was carried out as in 8.10.5, but the mixture was stirred for 24 hours.

8.11 Oxy-Cope Rearrangement.

8.11.1 Polymer Synthesis

EDMA (0.95 cm³, 5 mmol), cyclohexanol (0.026 cm³, 0.25 mmol) and AIBN (10 mg) were dissolved in acetonitrile (1.5 cm³), degassed in a sonic bath, bubbled with N₂ for 5 minutes and heated in an oven at 60 °C for 72 hours. The polymer was ground up and extracted with methanol for 72 hours – Imprinted 1.

The above method was repeated with no cyclohexanol (non-imprinted) and with the acetonitrile replaced with cyclohexanol (1.5 cm³) – Imprinted 2.

8.11.2 Catalysis.

1,5-hexadien-3-ol (0.5 cm³) was stirred in tetraethylene glycol dimethyl ether (3.0 cm³) at 200 °C under N₂. 5 µL samples were taken every 60 minutes for 8 hours and injected into a silica gel column at 100 °C.

The experiment was repeated in the presence of non-imprinted polymer (50 mg), imprinted polymer 1 (50 mg) and imprinted polymer 2 (50 mg).

8.12 Molecular Mechanics and Molecular Dynamics.

The molecular mechanics and molecular dynamics were carried out using Hyper Chem release 5.01 and using the AMBER forcefield.

8.12.1 Molecular Mechanics.

A random conformational search method was used to calculate the minimum energy conformations of N-acetyl-L-histidine and the two tautomers of its anion. Minima were assumed to have been reached when the gradient was below 0.01 kcal/Åmol. 5000

minimisations were carried out, with each conformation within 2.4 kcalmol^{-1} of the lowest energy conformation found at least 12 times.

8.12.2 Molecular Dynamics.

The lowest energy arrangements for each of the conformations I-III, see Figure 46, of N-acetyl-L-histidine and the two tautomers of its anion, obtained from molecular mechanics calculations were used for molecular dynamics simulations. The solute was placed within a periodic box filled with water molecules. The solvent alone was subject to energy minimization with the solute kept in its initial conformation. The solvent was evolved using molecular dynamics, by heating the system from 100-300 K over 1 ps then remaining at 300 K for 15 ps. The entire system was then minimized. The molecular dynamics calculations were then carried out. The system was heated from 100-300 K over 0.1 ps and then kept at 300 K for 50 ps with a data point recorded every 0.0025 ps. The $\alpha\beta$ and $\alpha\beta'$ dihedral angles were measured.

Appendices.

| | |
|-----|---------------------------|
| 8.1 | DMSO:H ₂ O 9:1 |
|-----|---------------------------|

Appendix 1 Hydrolysis of *p*-Nitrophenyl Acetate - No Catalyst.

| Time (s) | pH 7.0 | pH 7.6 | pH 8.0 | DMSO/H ₂ O 9:1 v/v |
|----------|---|-----------------------|-----------------------|----------------------------------|
| | <i>p</i> -Nitrophenol Concentration (M) | | | |
| 60 | 1.42x10 ⁻⁶ | 2.40x10 ⁻⁶ | 7.65x10 ⁻⁶ | 3.50x10 ⁻⁹ |
| 120 | 1.42x10 ⁻⁶ | 2.66x10 ⁻⁶ | 8.73x10 ⁻⁶ | 3.50x10 ⁻⁹ |
| 180 | 1.51x10 ⁻⁶ | 3.01x10 ⁻⁶ | 9.20x10 ⁻⁶ | 3.25x10 ⁻⁹ |
| 240 | 1.51x10 ⁻⁶ | 3.36x10 ⁻⁶ | 9.66x10 ⁻⁶ | 3.25x10 ⁻⁹ |
| 300 | 1.59x10 ⁻⁶ | 3.88x10 ⁻⁶ | 1.04x10 ⁻⁵ | 3.50x10 ⁻⁹ |
| 360 | 1.59x10 ⁻⁶ | 4.57x10 ⁻⁶ | 1.12x10 ⁻⁵ | 3.50x10 ⁻⁹ |
| 420 | 1.59x10 ⁻⁶ | 4.92x10 ⁻⁶ | 1.23x10 ⁻⁵ | 3.50x10 ⁻⁹ |
| 480 | 1.68x10 ⁻⁶ | 4.75x10 ⁻⁶ | 1.26x10 ⁻⁵ | 3.50x10 ⁻⁹ |
| 540 | 1.68x10 ⁻⁶ | 4.92x10 ⁻⁶ | 1.31x10 ⁻⁵ | 3.50x10 ⁻⁹ |
| 600 | 1.76x10 ⁻⁶ | 5.36x10 ⁻⁶ | 1.40x10 ⁻⁵ | 3.50x10 ⁻⁹ |
| 660 | 1.85x10 ⁻⁶ | 5.62x10 ⁻⁶ | 1.46x10 ⁻⁵ | 3.50x10 ⁻⁹ |
| 720 | 1.85x10 ⁻⁶ | 5.97x10 ⁻⁶ | 1.52x10 ⁻⁵ | 3.50x10 ⁻⁹ |
| 780 | 1.94x10 ⁻⁶ | 6.23x10 ⁻⁶ | 1.74x10 ⁻⁵ | 3.50x10 ⁻⁹ |
| 840 | 1.94x10 ⁻⁶ | 6.57x10 ⁻⁶ | 1.74x10 ⁻⁵ | 3.50x10 ⁻⁹ |
| 900 | 1.94x10 ⁻⁶ | 6.83x10 ⁻⁶ | 1.77x10 ⁻⁵ | 3.50x10 ⁻⁹ |
| 960 | 2.02x10 ⁻⁶ | 7.18x10 ⁻⁶ | 1.85x10 ⁻⁵ | 3.50x10 ⁻⁹ |
| 1020 | 2.02x10 ⁻⁶ | 7.53x10 ⁻⁶ | 2.02x10 ⁻⁵ | 3.50x10 ⁻⁹ |
| 1080 | 2.11x10 ⁻⁶ | 7.88x10 ⁻⁶ | 2.00x10 ⁻⁵ | 3.50x10 ⁻⁹ |
| 1140 | 2.11x10 ⁻⁶ | 8.23x10 ⁻⁶ | 2.14x10 ⁻⁵ | 3.50x10 ⁻⁹ |
| 1200 | 2.19x10 ⁻⁶ | 8.83x10 ⁻⁶ | 2.23x10 ⁻⁵ | 3.50x10 ⁻⁹ |

Appendix 2 Hydrolysis of *p*-Nitrophenyl Acetate – Small Molecules.

Hydrolysis of *p*-Nitrophenyl Acetate in Buffer Solution using Imidazole and *N*-Acetyl-L-histidine as Catalyst.

Imidazole pH 7.0.

| Time (s) | Catalyst Concentration (M) | | | | |
|----------|---|-----------------------|-----------------------|-----------------------|-----------------------|
| | 1.50x10 ⁻³ | 1.25x10 ⁻³ | 1.00x10 ⁻³ | 0.75x10 ⁻³ | 0.50x10 ⁻³ |
| | <i>p</i> -Nitrophenol Concentration (M) | | | | |
| 60 | 1.50x10 ⁻⁵ | 1.34x10 ⁻⁵ | 1.14x10 ⁻⁵ | 9.29x10 ⁻⁶ | 7.72x10 ⁻⁶ |
| 120 | 2.15x10 ⁻⁵ | 1.87x10 ⁻⁵ | 1.56x10 ⁻⁵ | 1.23x10 ⁻⁵ | 9.74x10 ⁻⁶ |
| 180 | 2.85x10 ⁻⁵ | 2.38x10 ⁻⁵ | 1.96x10 ⁻⁵ | 1.52x10 ⁻⁵ | 1.17x10 ⁻⁵ |
| 240 | 3.34x10 ⁻⁵ | 2.87x10 ⁻⁵ | 2.34x10 ⁻⁵ | 1.81x10 ⁻⁵ | 1.36x10 ⁻⁵ |
| 300 | 3.91x10 ⁻⁵ | 3.35x10 ⁻⁵ | 2.72x10 ⁻⁵ | 2.09x10 ⁻⁵ | 1.56x10 ⁻⁵ |
| 360 | 4.45x10 ⁻⁵ | 3.80x10 ⁻⁵ | 3.08x10 ⁻⁵ | 2.37x10 ⁻⁵ | 1.75x10 ⁻⁵ |
| 420 | 4.98x10 ⁻⁵ | 4.25x10 ⁻⁵ | 3.43x10 ⁻⁵ | 2.64x10 ⁻⁵ | 1.93x10 ⁻⁵ |
| 480 | 5.49x10 ⁻⁵ | 4.68x10 ⁻⁵ | 3.78x10 ⁻⁵ | 2.91x10 ⁻⁵ | 2.12x10 ⁻⁵ |
| 540 | 5.99x10 ⁻⁵ | 5.11x10 ⁻⁵ | 4.12x10 ⁻⁵ | 3.17x10 ⁻⁵ | 2.30x10 ⁻⁵ |
| 600 | 6.47x10 ⁻⁵ | 5.52x10 ⁻⁵ | 4.45x10 ⁻⁵ | 3.43x10 ⁻⁵ | 2.48x10 ⁻⁵ |
| 660 | 6.95x10 ⁻⁵ | 5.94x10 ⁻⁵ | 4.80x10 ⁻⁵ | 3.69x10 ⁻⁵ | 2.66x10 ⁻⁵ |
| 720 | 7.40x10 ⁻⁵ | 6.33x10 ⁻⁵ | 5.11x10 ⁻⁵ | 3.94x10 ⁻⁵ | 2.83x10 ⁻⁵ |
| 780 | 7.84x10 ⁻⁵ | 6.71x10 ⁻⁵ | 5.43x10 ⁻⁵ | 4.18x10 ⁻⁵ | 3.00x10 ⁻⁵ |
| 840 | 8.26x10 ⁻⁵ | 7.07x10 ⁻⁵ | 5.73x10 ⁻⁵ | 4.42x10 ⁻⁵ | 3.17x10 ⁻⁵ |
| 900 | 8.67x10 ⁻⁵ | 7.44x10 ⁻⁵ | 6.03x10 ⁻⁵ | 4.65x10 ⁻⁵ | 3.34x10 ⁻⁵ |
| 960 | 9.07x10 ⁻⁵ | 7.78x10 ⁻⁵ | 6.32x10 ⁻⁵ | 4.89x10 ⁻⁵ | 3.51x10 ⁻⁵ |
| 1020 | 9.45x10 ⁻⁵ | 8.13x10 ⁻⁵ | 6.61x10 ⁻⁵ | 5.11x10 ⁻⁵ | 3.68x10 ⁻⁵ |
| 1080 | 9.83x10 ⁻⁵ | 8.46x10 ⁻⁵ | 6.89x10 ⁻⁵ | 5.34x10 ⁻⁵ | 3.84x10 ⁻⁵ |
| 1140 | 1.02x10 ⁻⁴ | 8.78x10 ⁻⁵ | 7.16x10 ⁻⁵ | 5.56x10 ⁻⁵ | 3.99x10 ⁻⁵ |
| 1200 | 1.05x10 ⁻⁴ | 9.10x10 ⁻⁵ | 7.43x10 ⁻⁵ | 5.78x10 ⁻⁵ | 4.15x10 ⁻⁵ |
| 1260 | 1.09x10 ⁻⁴ | 9.43x10 ⁻⁵ | 7.71x10 ⁻⁵ | 6.00x10 ⁻⁵ | 4.31x10 ⁻⁵ |
| 1320 | 1.12x10 ⁻⁴ | 9.73x10 ⁻⁵ | 7.97x10 ⁻⁵ | 6.21x10 ⁻⁵ | 4.47x10 ⁻⁵ |
| 1380 | 1.16x10 ⁻⁴ | 1.00x10 ⁻⁴ | 8.22x10 ⁻⁵ | 6.42x10 ⁻⁵ | 4.62x10 ⁻⁵ |

| | | | | | |
|------|-----------------------|-----------------------|-----------------------|-----------------------|-----------------------|
| 1440 | 1.19×10^{-4} | 1.03×10^{-4} | 8.47×10^{-5} | 6.62×10^{-5} | 4.77×10^{-5} |
| 1500 | 1.22×10^{-4} | 1.06×10^{-4} | 8.71×10^{-5} | 6.82×10^{-5} | 4.92×10^{-5} |
| 1560 | 1.25×10^{-4} | 1.09×10^{-4} | 8.95×10^{-5} | 7.02×10^{-5} | 5.07×10^{-5} |
| 1620 | 1.27×10^{-4} | 1.11×10^{-4} | 9.18×10^{-5} | 7.22×10^{-5} | 5.21×10^{-5} |
| 1680 | 1.30×10^{-4} | 1.14×10^{-4} | 9.41×10^{-5} | 7.41×10^{-5} | 5.36×10^{-5} |
| 1740 | 1.33×10^{-4} | 1.16×10^{-4} | 9.63×10^{-5} | 7.60×10^{-5} | 5.50×10^{-5} |
| 1800 | 1.36×10^{-4} | 1.19×10^{-4} | 9.85×10^{-5} | 7.78×10^{-5} | 5.64×10^{-5} |
| 1860 | 1.38×10^{-4} | 1.21×10^{-4} | 1.01×10^{-4} | 7.97×10^{-5} | 5.78×10^{-5} |
| 1920 | 1.41×10^{-4} | 1.24×10^{-4} | 1.03×10^{-4} | 8.15×10^{-5} | 5.93×10^{-5} |
| 1980 | 1.43×10^{-4} | 1.26×10^{-4} | 1.05×10^{-4} | 8.33×10^{-5} | 6.06×10^{-5} |
| 2040 | 1.45×10^{-4} | 1.28×10^{-4} | 1.07×10^{-4} | 8.50×10^{-5} | 6.19×10^{-5} |
| 2100 | 1.48×10^{-4} | 1.30×10^{-4} | 1.09×10^{-4} | 8.67×10^{-5} | 6.33×10^{-5} |
| 2160 | 1.50×10^{-4} | 1.32×10^{-4} | 1.11×10^{-4} | 8.84×10^{-5} | 6.46×10^{-5} |
| 2220 | 1.52×10^{-4} | 1.35×10^{-4} | 1.13×10^{-4} | 9.01×10^{-5} | 6.59×10^{-5} |
| 2280 | 1.54×10^{-4} | 1.37×10^{-4} | 1.15×10^{-4} | 9.07×10^{-5} | 6.72×10^{-5} |
| 2340 | 1.56×10^{-4} | 1.39×10^{-4} | 1.17×10^{-4} | 9.33×10^{-5} | 6.85×10^{-5} |
| 2400 | 1.58×10^{-4} | 1.41×10^{-4} | 1.18×10^{-4} | 9.50×10^{-5} | 6.97×10^{-5} |
| 2460 | 1.60×10^{-4} | 1.43×10^{-4} | 1.20×10^{-4} | 9.57×10^{-5} | 7.11×10^{-5} |
| 2520 | 1.62×10^{-4} | 1.44×10^{-4} | 1.22×10^{-4} | 9.81×10^{-5} | 7.23×10^{-5} |
| 2580 | 1.64×10^{-4} | 1.46×10^{-4} | 1.24×10^{-4} | 9.97×10^{-5} | 7.35×10^{-5} |
| 2640 | 1.65×10^{-4} | 1.48×10^{-4} | 1.25×10^{-4} | 1.01×10^{-4} | 7.47×10^{-5} |
| 2700 | 1.67×10^{-4} | 1.50×10^{-4} | 1.27×10^{-4} | 1.03×10^{-4} | 7.59×10^{-5} |
| 2760 | 1.69×10^{-4} | 1.51×10^{-4} | 1.29×10^{-4} | 1.04×10^{-4} | 7.71×10^{-5} |
| 2820 | 1.70×10^{-4} | 1.53×10^{-4} | 1.30×10^{-4} | 1.06×10^{-4} | 7.82×10^{-5} |
| 2880 | 1.72×10^{-4} | 1.55×10^{-4} | 1.32×10^{-4} | 1.07×10^{-4} | 7.94×10^{-5} |
| 2940 | 1.73×10^{-4} | 1.56×10^{-4} | 1.33×10^{-4} | 1.08×10^{-4} | 8.06×10^{-5} |
| 3000 | 1.75×10^{-4} | 1.58×10^{-4} | 1.35×10^{-4} | 1.10×10^{-4} | 8.17×10^{-5} |
| 3060 | 1.77×10^{-4} | 1.59×10^{-4} | 1.36×10^{-4} | 1.11×10^{-4} | 8.28×10^{-5} |
| 3120 | 1.78×10^{-4} | 1.61×10^{-4} | 1.38×10^{-4} | 1.13×10^{-4} | 8.40×10^{-5} |
| 3180 | 1.79×10^{-4} | 1.62×10^{-4} | 1.39×10^{-4} | 1.14×10^{-4} | 8.51×10^{-5} |
| 3240 | 1.80×10^{-4} | 1.63×10^{-4} | 1.41×10^{-4} | 1.15×10^{-4} | 8.62×10^{-5} |
| 3300 | 1.82×10^{-4} | 1.65×10^{-4} | 1.42×10^{-4} | 1.17×10^{-4} | 8.73×10^{-5} |

| | | | | | |
|------|-----------------------|-----------------------|-----------------------|-----------------------|-----------------------|
| 3360 | 1.83×10^{-4} | 1.66×10^{-4} | 1.43×10^{-4} | 1.18×10^{-4} | 8.83×10^{-5} |
| 3420 | 1.85×10^{-4} | 1.68×10^{-4} | 1.45×10^{-4} | 1.19×10^{-4} | 8.94×10^{-5} |
| 3480 | 1.86×10^{-4} | 1.69×10^{-4} | 1.46×10^{-4} | 1.20×10^{-4} | 9.05×10^{-5} |
| 3540 | 1.87×10^{-4} | 1.70×10^{-4} | 1.47×10^{-4} | 1.22×10^{-4} | 9.15×10^{-5} |
| 3600 | 1.88×10^{-4} | 1.71×10^{-4} | 1.49×10^{-4} | 1.23×10^{-4} | 9.26×10^{-5} |

N-Acetyl-L-histidine pH 7.0.

| Time (s) | Catalyst Concentration (M) | | | | |
|----------|---|-----------------------|-----------------------|-----------------------|-----------------------|
| | 1.50x10 ⁻³ | 1.25x10 ⁻³ | 1.00x10 ⁻³ | 0.75x10 ⁻³ | 0.50x10 ⁻³ |
| | <i>p</i> -Nitrophenol Concentration (M) | | | | |
| 60 | 9.43x10 ⁻⁶ | 9.34x10 ⁻⁶ | 7.83x10 ⁻⁶ | 8.43x10 ⁻⁶ | 7.78x10 ⁻⁶ |
| 120 | 1.20x10 ⁻⁵ | 1.18x10 ⁻⁵ | 9.86x10 ⁻⁶ | 9.94x10 ⁻⁶ | 8.75x10 ⁻⁶ |
| 180 | 1.45x10 ⁻⁵ | 1.41x10 ⁻⁵ | 1.17x10 ⁻⁵ | 1.14x10 ⁻⁵ | 9.86x10 ⁻⁶ |
| 240 | 1.71x10 ⁻⁵ | 1.65x10 ⁻⁵ | 1.35x10 ⁻⁵ | 1.29x10 ⁻⁵ | 1.09x10 ⁻⁵ |
| 300 | 1.96x10 ⁻⁵ | 1.87x10 ⁻⁵ | 1.54x10 ⁻⁵ | 1.44x10 ⁻⁵ | 1.19x10 ⁻⁵ |
| 360 | 2.20x10 ⁻⁵ | 2.08x10 ⁻⁵ | 1.71x10 ⁻⁵ | 1.58x10 ⁻⁵ | 1.29x10 ⁻⁵ |
| 420 | 2.44x10 ⁻⁵ | 2.30x10 ⁻⁵ | 1.89x10 ⁻⁵ | 1.73x10 ⁻⁵ | 1.40x10 ⁻⁵ |
| 480 | 2.68x10 ⁻⁵ | 2.51x10 ⁻⁵ | 2.07x10 ⁻⁵ | 1.87x10 ⁻⁵ | 1.49x10 ⁻⁵ |
| 540 | 2.91x10 ⁻⁵ | 2.72x10 ⁻⁵ | 2.24x10 ⁻⁵ | 2.01x10 ⁻⁵ | 1.59x10 ⁻⁵ |
| 600 | 3.14x10 ⁻⁵ | 2.92x10 ⁻⁵ | 2.41x10 ⁻⁵ | 2.15x10 ⁻⁵ | 1.69x10 ⁻⁵ |
| 660 | 3.38x10 ⁻⁵ | 3.14x10 ⁻⁵ | 2.58x10 ⁻⁵ | 2.30x10 ⁻⁵ | 1.80x10 ⁻⁵ |
| 720 | 3.61x10 ⁻⁵ | 3.34x10 ⁻⁵ | 2.75x10 ⁻⁵ | 2.43x10 ⁻⁵ | 1.90x10 ⁻⁵ |
| 780 | 3.83x10 ⁻⁵ | 3.54x10 ⁻⁵ | 2.92x10 ⁻⁵ | 2.57x10 ⁻⁵ | 1.99x10 ⁻⁵ |
| 840 | 4.04x10 ⁻⁵ | 3.74x10 ⁻⁵ | 3.08x10 ⁻⁵ | 2.70x10 ⁻⁵ | 2.09x10 ⁻⁵ |
| 900 | 4.25x10 ⁻⁵ | 3.93x10 ⁻⁵ | 3.24x10 ⁻⁵ | 2.83x10 ⁻⁵ | 2.18x10 ⁻⁵ |
| 960 | 4.46x10 ⁻⁵ | 4.12x10 ⁻⁵ | 3.40x10 ⁻⁵ | 2.96x10 ⁻⁵ | 2.27x10 ⁻⁵ |
| 1020 | 4.67x10 ⁻⁵ | 4.30x10 ⁻⁵ | 3.56x10 ⁻⁵ | 3.11x10 ⁻⁵ | 2.37x10 ⁻⁵ |
| 1080 | 4.87x10 ⁻⁵ | 4.49x10 ⁻⁵ | 3.71x10 ⁻⁵ | 3.23x10 ⁻⁵ | 2.46x10 ⁻⁵ |
| 1140 | 5.07x10 ⁻⁵ | 4.67x10 ⁻⁵ | 3.87x10 ⁻⁵ | 3.36x10 ⁻⁵ | 2.56x10 ⁻⁵ |
| 1200 | 5.27x10 ⁻⁵ | 4.85x10 ⁻⁵ | 4.02x10 ⁻⁵ | 3.48x10 ⁻⁵ | 2.65x10 ⁻⁵ |
| 1260 | 5.47x10 ⁻⁵ | 5.04x10 ⁻⁵ | 4.18x10 ⁻⁵ | 3.61x10 ⁻⁵ | 2.75x10 ⁻⁵ |
| 1320 | 5.68x10 ⁻⁵ | 5.22x10 ⁻⁵ | 4.32x10 ⁻⁵ | 3.74x10 ⁻⁵ | 2.83x10 ⁻⁵ |
| 1380 | 5.86x10 ⁻⁵ | 5.39x10 ⁻⁵ | 4.47x10 ⁻⁵ | 3.86x10 ⁻⁵ | 2.93x10 ⁻⁵ |
| 1440 | 6.04x10 ⁻⁵ | 5.56x10 ⁻⁵ | 4.62x10 ⁻⁵ | 3.98x10 ⁻⁵ | 3.01x10 ⁻⁵ |
| 1500 | 6.22x10 ⁻⁵ | 5.73x10 ⁻⁵ | 4.7x10 ⁻⁵ | 4.11x10 ⁻⁵ | 3.10x10 ⁻⁵ |
| 1560 | 6.40x10 ⁻⁵ | 5.89x10 ⁻⁵ | 4.90x10 ⁻⁵ | 4.23x10 ⁻⁵ | 3.19x10 ⁻⁵ |
| 1620 | 6.59x10 ⁻⁵ | 6.06x10 ⁻⁵ | 5.05x10 ⁻⁵ | 4.35x10 ⁻⁵ | 3.28x10 ⁻⁵ |
| 1680 | 6.76x10 ⁻⁵ | 6.23x10 ⁻⁵ | 5.19x10 ⁻⁵ | 4.47x10 ⁻⁵ | 3.37x10 ⁻⁵ |

| | | | | | |
|------|-----------------------|-----------------------|-----------------------|-----------------------|-----------------------|
| 1740 | 6.93×10^{-5} | 6.39×10^{-5} | 5.32×10^{-5} | 4.58×10^{-5} | 3.45×10^{-5} |
| 1800 | 7.11×10^{-5} | 6.54×10^{-5} | 5.46×10^{-5} | 4.70×10^{-5} | 3.54×10^{-5} |
| 1860 | 7.28×10^{-5} | 6.70×10^{-5} | 5.60×10^{-5} | 4.82×10^{-5} | 3.63×10^{-5} |
| 1920 | 7.45×10^{-5} | 6.86×10^{-5} | 5.73×10^{-5} | 4.93×10^{-5} | 3.71×10^{-5} |
| 1980 | 7.61×10^{-5} | 7.01×10^{-5} | 5.86×10^{-5} | 5.04×10^{-5} | 3.80×10^{-5} |
| 2040 | 7.77×10^{-5} | 7.16×10^{-5} | 5.99×10^{-5} | 5.16×10^{-5} | 3.88×10^{-5} |
| 2100 | 7.94×10^{-5} | 7.30×10^{-5} | 6.12×10^{-5} | 5.27×10^{-5} | 3.97×10^{-5} |
| 2160 | 8.09×10^{-5} | 7.45×10^{-5} | 6.24×10^{-5} | 5.38×10^{-5} | 4.05×10^{-5} |
| 2220 | 8.25×10^{-5} | 7.59×10^{-5} | 6.38×10^{-5} | 5.49×10^{-5} | 4.13×10^{-5} |
| 2280 | 8.40×10^{-5} | 7.74×10^{-5} | 6.50×10^{-5} | 5.60×10^{-5} | 4.22×10^{-5} |
| 2340 | 8.55×10^{-5} | 7.88×10^{-5} | 6.62×10^{-5} | 5.70×10^{-5} | 4.30×10^{-5} |
| 2400 | 8.70×10^{-5} | 8.02×10^{-5} | 6.75×10^{-5} | 5.81×10^{-5} | 4.38×10^{-5} |
| 2460 | 8.85×10^{-5} | 8.16×10^{-5} | 6.87×10^{-5} | 5.92×10^{-5} | 4.45×10^{-5} |
| 2520 | 9.00×10^{-5} | 8.29×10^{-5} | 7.00×10^{-5} | 6.03×10^{-5} | 4.53×10^{-5} |
| 2580 | 9.14×10^{-5} | 8.44×10^{-5} | 7.12×10^{-5} | 6.13×10^{-5} | 4.61×10^{-5} |
| 2640 | 9.27×10^{-5} | 8.57×10^{-5} | 7.23×10^{-5} | 6.24×10^{-5} | 4.69×10^{-5} |
| 2700 | 9.41×10^{-5} | 8.70×10^{-5} | 7.35×10^{-5} | 6.34×10^{-5} | 4.77×10^{-5} |
| 2760 | 9.55×10^{-5} | 8.82×10^{-5} | 7.46×10^{-5} | 6.44×10^{-5} | 4.85×10^{-5} |
| 2820 | 9.68×10^{-5} | 8.95×10^{-5} | 7.58×10^{-5} | 6.54×10^{-5} | 4.93×10^{-5} |
| 2880 | 9.81×10^{-5} | 9.07×10^{-5} | 7.69×10^{-5} | 6.64×10^{-5} | 5.01×10^{-5} |
| 2940 | 9.94×10^{-5} | 9.20×10^{-5} | 7.80×10^{-5} | 6.74×10^{-5} | 5.08×10^{-5} |
| 3000 | 1.01×10^{-4} | 9.32×10^{-5} | 7.91×10^{-5} | 6.83×10^{-5} | 5.16×10^{-5} |
| 3060 | 1.02×10^{-4} | 9.46×10^{-5} | 8.03×10^{-5} | 6.94×10^{-5} | 5.24×10^{-5} |
| 3120 | 1.03×10^{-4} | 9.57×10^{-5} | 8.13×10^{-5} | 7.03×10^{-5} | 5.31×10^{-5} |
| 3180 | 1.05×10^{-4} | 9.69×10^{-5} | 8.24×10^{-5} | 7.13×10^{-5} | 5.39×10^{-5} |
| 3240 | 1.06×10^{-4} | 9.81×10^{-5} | 8.35×10^{-5} | 7.22×10^{-5} | 5.46×10^{-5} |
| 3300 | 1.07×10^{-4} | 9.92×10^{-5} | 8.45×10^{-5} | 7.32×10^{-5} | 5.54×10^{-5} |
| 3360 | 1.08×10^{-4} | 1.00×10^{-4} | 8.55×10^{-5} | 7.41×10^{-5} | 5.62×10^{-5} |
| 3420 | 1.09×10^{-4} | 1.01×10^{-4} | 8.66×10^{-5} | 7.51×10^{-5} | 5.69×10^{-5} |
| 3480 | 1.10×10^{-4} | 1.03×10^{-4} | 8.76×10^{-5} | 7.60×10^{-5} | 5.76×10^{-5} |
| 3540 | 1.12×10^{-4} | 1.04×10^{-4} | 8.86×10^{-5} | 7.70×10^{-5} | 5.83×10^{-5} |
| 3600 | 1.13×10^{-4} | 1.05×10^{-4} | 8.96×10^{-5} | 7.79×10^{-5} | 5.91×10^{-5} |

Imidazole pH 7.6.

| Time (s) | Catalyst Concentration (M) | | | | |
|----------|---|-----------------------|-----------------------|-----------------------|-----------------------|
| | 1.50x10 ⁻³ | 1.25x10 ⁻³ | 1.00x10 ⁻³ | 0.75x10 ⁻³ | 0.50x10 ⁻³ |
| | <i>p</i> -Nitrophenol Concentration (M) | | | | |
| 60 | 2.85x10 ⁻⁵ | 2.46x10 ⁻⁵ | 2.13x10 ⁻⁵ | 1.74x10 ⁻⁵ | 1.47x10 ⁻⁵ |
| 120 | 4.30x10 ⁻⁵ | 3.72x10 ⁻⁵ | 3.12x10 ⁻⁵ | 2.50x10 ⁻⁵ | 1.99x10 ⁻⁵ |
| 180 | 5.67x10 ⁻⁵ | 4.89x10 ⁻⁵ | 4.07x10 ⁻⁵ | 3.23x10 ⁻⁵ | 2.49x10 ⁻⁵ |
| 240 | 6.97x10 ⁻⁵ | 6.02x10 ⁻⁵ | 4.99x10 ⁻⁵ | 3.93x10 ⁻⁵ | 2.98x10 ⁻⁵ |
| 300 | 8.19x10 ⁻⁵ | 7.10x10 ⁻⁵ | 5.87x10 ⁻⁵ | 4.61x10 ⁻⁵ | 3.45x10 ⁻⁵ |
| 360 | 9.36x10 ⁻⁵ | 8.12x10 ⁻⁵ | 6.72x10 ⁻⁵ | 5.28x10 ⁻⁵ | 3.91x10 ⁻⁵ |
| 420 | 1.05x10 ⁻⁴ | 9.10x10 ⁻⁵ | 7.54x10 ⁻⁵ | 5.92x10 ⁻⁵ | 4.36x10 ⁻⁵ |
| 480 | 1.15x10 ⁻⁴ | 1.00x10 ⁻⁴ | 8.19x10 ⁻⁵ | 6.55x10 ⁻⁵ | 4.81x10 ⁻⁵ |
| 540 | 1.25x10 ⁻⁴ | 1.09x10 ⁻⁴ | 9.10x10 ⁻⁵ | 7.16x10 ⁻⁵ | 5.24x10 ⁻⁵ |
| 600 | 1.35x10 ⁻⁴ | 1.18x10 ⁻⁴ | 9.84x10 ⁻⁵ | 7.75x10 ⁻⁵ | 5.67x10 ⁻⁵ |
| 660 | 1.44x10 ⁻⁴ | 1.27x10 ⁻⁴ | 1.06x10 ⁻⁴ | 8.36x10 ⁻⁵ | 6.11x10 ⁻⁵ |
| 720 | 1.53x10 ⁻⁴ | 1.35x10 ⁻⁴ | 1.13x10 ⁻⁴ | 8.92x10 ⁻⁵ | 6.51x10 ⁻⁵ |
| 780 | 1.61x10 ⁻⁴ | 1.42x10 ⁻⁴ | 1.19x10 ⁻⁴ | 9.47x10 ⁻⁵ | 6.92x10 ⁻⁵ |
| 840 | 1.69x10 ⁻⁴ | 1.50x10 ⁻⁴ | 1.26x10 ⁻⁴ | 1.00x10 ⁻⁴ | 7.31x10 ⁻⁵ |
| 900 | 1.76x10 ⁻⁴ | 1.57x10 ⁻⁴ | 1.32x10 ⁻⁴ | 1.05x10 ⁻⁴ | 7.70x10 ⁻⁵ |
| 960 | 1.83x10 ⁻⁴ | 1.64x10 ⁻⁴ | 1.38x10 ⁻⁴ | 1.10x10 ⁻⁴ | 8.07x10 ⁻⁵ |
| 1020 | 1.90x10 ⁻⁴ | 1.70x10 ⁻⁴ | 1.44x10 ⁻⁴ | 1.15x10 ⁻⁴ | 8.45x10 ⁻⁵ |
| 1080 | 1.96x10 ⁻⁴ | 1.76x10 ⁻⁴ | 1.50x10 ⁻⁴ | 1.20x10 ⁻⁴ | 8.81x10 ⁻⁵ |
| 1140 | 2.02x10 ⁻⁴ | 1.82x10 ⁻⁴ | 1.55x10 ⁻⁴ | 1.25x10 ⁻⁴ | 9.17x10 ⁻⁵ |
| 1200 | 2.07x10 ⁻⁴ | 1.87x10 ⁻⁴ | 1.60x10 ⁻⁴ | 1.29x10 ⁻⁴ | 9.53x10 ⁻⁵ |
| 1260 | 2.12x10 ⁻⁴ | 1.93x10 ⁻⁴ | 1.66x10 ⁻⁴ | 1.34x10 ⁻⁴ | 9.90x10 ⁻⁵ |
| 1320 | 2.17x10 ⁻⁴ | 1.98x10 ⁻⁴ | 1.70x10 ⁻⁴ | 1.39x10 ⁻⁴ | 1.02x10 ⁻⁴ |
| 1380 | 2.21x10 ⁻⁴ | 2.02x10 ⁻⁴ | 1.75x10 ⁻⁴ | 1.43x10 ⁻⁴ | 1.06x10 ⁻⁴ |
| 1440 | 2.25x10 ⁻⁴ | 2.07x10 ⁻⁴ | 1.79x10 ⁻⁴ | 1.47x10 ⁻⁴ | 1.09x10 ⁻⁴ |
| 1500 | 2.29x10 ⁻⁴ | 2.11x10 ⁻⁴ | 1.84x10 ⁻⁴ | 1.51x10 ⁻⁴ | 1.12x10 ⁻⁴ |
| 1560 | 2.32x10 ⁻⁴ | 2.15x10 ⁻⁴ | 1.88x10 ⁻⁴ | 1.55x10 ⁻⁴ | 1.15x10 ⁻⁴ |
| 1620 | 2.35x10 ⁻⁴ | 2.19x10 ⁻⁴ | 1.92x10 ⁻⁴ | 1.59x10 ⁻⁴ | 1.19x10 ⁻⁴ |
| 1680 | 2.38x10 ⁻⁴ | 2.22x10 ⁻⁴ | 1.96x10 ⁻⁴ | 1.62x10 ⁻⁴ | 1.22x10 ⁻⁴ |

| | | | | | |
|------|-----------------------|-----------------------|-----------------------|-----------------------|-----------------------|
| 1740 | 2.41×10^{-4} | 2.25×10^{-4} | 1.99×10^{-4} | 1.66×10^{-4} | 1.25×10^{-4} |
| 1800 | 2.44×10^{-4} | 2.28×10^{-4} | 2.03×10^{-4} | 1.70×10^{-4} | 1.28×10^{-4} |
| 1860 | 2.46×10^{-4} | 2.31×10^{-4} | 2.07×10^{-4} | 1.73×10^{-4} | 1.31×10^{-4} |
| 1920 | 2.47×10^{-4} | 2.34×10^{-4} | 2.10×10^{-4} | 1.77×10^{-4} | 1.34×10^{-4} |
| 1980 | 2.49×10^{-4} | 2.36×10^{-4} | 2.13×10^{-4} | 1.80×10^{-4} | 1.36×10^{-4} |
| 2040 | 2.51×10^{-4} | 2.39×10^{-4} | 2.16×10^{-4} | 1.83×10^{-4} | 1.39×10^{-4} |
| 2100 | 2.52×10^{-4} | 2.41×10^{-4} | 2.19×10^{-4} | 1.86×10^{-4} | 1.42×10^{-4} |
| 2160 | 2.54×10^{-4} | 2.43×10^{-4} | 2.21×10^{-4} | 1.89×10^{-4} | 1.45×10^{-4} |
| 2220 | 2.54×10^{-4} | 2.44×10^{-4} | 2.24×10^{-4} | 1.92×10^{-4} | 1.47×10^{-4} |
| 2280 | 2.56×10^{-4} | 2.47×10^{-4} | 2.26×10^{-4} | 1.95×10^{-4} | 1.50×10^{-4} |
| 2340 | 2.57×10^{-4} | 2.47×10^{-4} | 2.29×10^{-4} | 1.97×10^{-4} | 1.52×10^{-4} |
| 2400 | 2.58×10^{-4} | 2.49×10^{-4} | 2.31×10^{-4} | 2.00×10^{-4} | 1.55×10^{-4} |
| 2460 | 2.59×10^{-4} | 2.51×10^{-4} | 2.33×10^{-4} | 2.03×10^{-4} | 1.58×10^{-4} |
| 2520 | 2.60×10^{-4} | 2.52×10^{-4} | 2.34×10^{-4} | 2.05×10^{-4} | 1.60×10^{-4} |
| 2580 | 2.60×10^{-4} | 2.53×10^{-4} | 2.36×10^{-4} | 2.08×10^{-4} | 1.62×10^{-4} |
| 2640 | 2.60×10^{-4} | 2.54×10^{-4} | 2.38×10^{-4} | 2.10×10^{-4} | 1.65×10^{-4} |
| 2700 | 2.61×10^{-4} | 2.54×10^{-4} | 2.40×10^{-4} | 2.12×10^{-4} | 1.67×10^{-4} |
| 2760 | 2.61×10^{-4} | 2.55×10^{-4} | 2.41×10^{-4} | 2.14×10^{-4} | 1.69×10^{-4} |
| 2820 | 2.63×10^{-4} | 2.57×10^{-4} | 2.43×10^{-4} | 2.16×10^{-4} | 1.72×10^{-4} |
| 2880 | 2.62×10^{-4} | 2.57×10^{-4} | 2.44×10^{-4} | 2.18×10^{-4} | 1.74×10^{-4} |
| 2940 | 2.63×10^{-4} | 2.59×10^{-4} | 2.45×10^{-4} | 2.20×10^{-4} | 1.76×10^{-4} |
| 3000 | 2.63×10^{-4} | 2.58×10^{-4} | 2.47×10^{-4} | 2.22×10^{-4} | 1.78×10^{-4} |
| 3060 | 2.64×10^{-4} | 2.59×10^{-4} | 2.49×10^{-4} | 2.24×10^{-4} | 1.80×10^{-4} |
| 3120 | 2.64×10^{-4} | 2.59×10^{-4} | 2.49×10^{-4} | 2.26×10^{-4} | 1.82×10^{-4} |
| 3180 | 2.65×10^{-4} | 2.60×10^{-4} | 2.49×10^{-4} | 2.28×10^{-4} | 1.84×10^{-4} |
| 3240 | 2.64×10^{-4} | 2.60×10^{-4} | 2.51×10^{-4} | 2.29×10^{-4} | 1.86×10^{-4} |
| 3300 | 2.65×10^{-4} | 2.62×10^{-4} | 2.51×10^{-4} | 2.31×10^{-4} | 1.88×10^{-4} |
| 3360 | 2.65×10^{-4} | 2.61×10^{-4} | 2.53×10^{-4} | 2.32×10^{-4} | 1.90×10^{-4} |
| 3420 | 2.66×10^{-4} | 2.62×10^{-4} | 2.53×10^{-4} | 2.34×10^{-4} | 1.92×10^{-4} |
| 3480 | 2.67×10^{-4} | 2.62×10^{-4} | 2.53×10^{-4} | 2.35×10^{-4} | 1.94×10^{-4} |
| 3540 | 2.65×10^{-4} | 2.62×10^{-4} | 2.55×10^{-4} | 2.36×10^{-4} | 1.96×10^{-4} |
| 3600 | 2.67×10^{-4} | 2.64×10^{-4} | 2.56×10^{-4} | 2.38×10^{-4} | 1.97×10^{-4} |

N-Acetyl-L-histidine pH7.6.

| Time (s) | Catalyst Concentration (M) | | | | |
|----------|---|-----------------------|-----------------------|------------------------|-----------------------|
| | 1.50x10 ⁻³ | 1.25x10 ⁻³ | 1.00x10 ⁻³ | 0.75x10 ⁻³ | 0.50x10 ⁻³ |
| | <i>p</i> -Nitrophenol Concentration (M) | | | | |
| 60 | 1.80x10 ⁻⁵ | 1.65x10 ⁻⁵ | 1.56x10 ⁻⁵ | 1.43x10 ⁻⁵ | 1.28x10 ⁻⁵ |
| 120 | 2.57x10 ⁻⁵ | 2.30x10 ⁻⁵ | 2.12x10 ⁻⁵ | 1.88x10 ⁻⁵ | 1.60x10 ⁻⁵ |
| 180 | 3.31x10 ⁻⁵ | 2.94x10 ⁻⁵ | 2.66x10 ⁻⁵ | 2.31x10 ⁻⁵ | 1.90x10 ⁻⁵ |
| 240 | 4.01x10 ⁻⁵ | 3.55x10 ⁻⁵ | 3.19x10 ⁻⁵ | 2.74x10 ⁻⁵ | 2.20x10 ⁻⁵ |
| 300 | 4.70x10 ⁻⁵ | 4.15x10 ⁻⁵ | 3.70x10 ⁻⁵ | 3.14x10 ⁻⁵ | 2.50x10 ⁻⁵ |
| 360 | 5.37x10 ⁻⁵ | 4.73x10 ⁻⁵ | 4.20x10 ⁻⁵ | 3.55x10 ⁻⁵ | 2.80x10 ⁻⁵ |
| 420 | 6.02x10 ⁻⁵ | 5.29x10 ⁻⁵ | 4.69x10 ⁻⁵ | 3.95x10 ⁻⁵ | 3.08x10 ⁻⁵ |
| 480 | 6.65x10 ⁻⁵ | 5.84x10 ⁻⁵ | 5.16x10 ⁻⁵ | 4.34 x10 ⁻⁵ | 3.37x10 ⁻⁵ |
| 540 | 7.26x10 ⁻⁵ | 6.38x10 ⁻⁵ | 5.63x10 ⁻⁵ | 4.72x10 ⁻⁵ | 3.65x10 ⁻⁵ |
| 600 | 7.86x10 ⁻⁵ | 6.91x10 ⁻⁵ | 6.09x10 ⁻⁵ | 5.10x10 ⁻⁵ | 3.95x10 ⁻⁵ |
| 660 | 8.48x10 ⁻⁵ | 7.45x10 ⁻⁵ | 6.56x10 ⁻⁵ | 5.49x10 ⁻⁵ | 4.22x10 ⁻⁵ |
| 720 | 9.04x10 ⁻⁵ | 7.96x10 ⁻⁵ | 7.00x10 ⁻⁵ | 5.85x10 ⁻⁵ | 4.48x10 ⁻⁵ |
| 780 | 9.59x10 ⁻⁵ | 8.45x10 ⁻⁵ | 7.43x10 ⁻⁵ | 6.21x10 ⁻⁵ | 4.75x10 ⁻⁵ |
| 840 | 1.01x10 ⁻⁴ | 8.93x10 ⁻⁵ | 7.85x10 ⁻⁵ | 6.57x10 ⁻⁵ | 5.03x10 ⁻⁵ |
| 900 | 1.07x10 ⁻⁴ | 9.40x10 ⁻⁵ | 8.26x10 ⁻⁵ | 6.92x10 ⁻⁵ | 5.30x10 ⁻⁵ |
| 960 | 1.12x10 ⁻⁴ | 9.86x10 ⁻⁵ | 8.67x10 ⁻⁵ | 7.26x10 ⁻⁵ | 5.55x10 ⁻⁵ |
| 1020 | 1.17x10 ⁻⁴ | 1.03x10 ⁻⁴ | 9.07x10 ⁻⁵ | 7.60x10 ⁻⁵ | 5.81x10 ⁻⁵ |
| 1080 | 1.21x10 ⁻⁴ | 1.07x10 ⁻⁴ | 9.46x10 ⁻⁵ | 7.93x10 ⁻⁵ | 6.06x10 ⁻⁵ |
| 1140 | 1.26x10 ⁻⁴ | 1.12x10 ⁻⁴ | 9.85x10 ⁻⁵ | 8.25x10 ⁻⁵ | 6.30x10 ⁻⁵ |
| 1200 | 1.31x10 ⁻⁴ | 1.16x10 ⁻⁴ | 1.02x10 ⁻⁴ | 8.58x10 ⁻⁵ | 6.56x10 ⁻⁵ |
| 1260 | 1.35x10 ⁻⁴ | 1.20x10 ⁻⁴ | 1.06x10 ⁻⁴ | 8.92x10 ⁻⁵ | 6.81x10 ⁻⁵ |
| 1320 | 1.40x10 ⁻⁴ | 1.24x10 ⁻⁴ | 1.10x10 ⁻⁴ | 9.23x10 ⁻⁵ | 7.04x10 ⁻⁵ |
| 1380 | 1.44x10 ⁻⁴ | 1.28x10 ⁻⁴ | 1.13x10 ⁻⁴ | 9.55x10 ⁻⁵ | 7.29x10 ⁻⁵ |
| 1440 | 1.48x10 ⁻⁴ | 1.32x10 ⁻⁴ | 1.17x10 ⁻⁴ | 9.86x10 ⁻⁵ | 7.51x10 ⁻⁵ |
| 1500 | 1.52x10 ⁻⁴ | 1.36x10 ⁻⁴ | 1.20x10 ⁻⁴ | 1.02x10 ⁻⁴ | 7.74x10 ⁻⁵ |
| 1560 | 1.56x10 ⁻⁴ | 1.39x10 ⁻⁴ | 1.24x10 ⁻⁴ | 1.05x10 ⁻⁴ | 7.96x10 ⁻⁵ |
| 1620 | 1.60x10 ⁻⁴ | 1.43x10 ⁻⁴ | 1.27x10 ⁻⁴ | 1.07x10 ⁻⁴ | 8.20x10 ⁻⁵ |
| 1680 | 1.64x10 ⁻⁴ | 1.46x10 ⁻⁴ | 1.30x10 ⁻⁴ | 1.10x10 ⁻⁴ | 8.44x10 ⁻⁵ |

| | | | | | |
|------|-----------------------|-----------------------|-----------------------|-----------------------|-----------------------|
| 1740 | 1.67×10^{-4} | 1.50×10^{-4} | 1.33×10^{-4} | 1.13×10^{-4} | 8.68×10^{-5} |
| 1800 | 1.71×10^{-4} | 1.53×10^{-4} | 1.36×10^{-4} | 1.16×10^{-4} | 8.90×10^{-5} |
| 1860 | 1.74×10^{-4} | 1.57×10^{-4} | 1.40×10^{-4} | 1.19×10^{-4} | 9.13×10^{-5} |
| 1920 | 1.77×10^{-4} | 1.60×10^{-4} | 1.43×10^{-4} | 1.21×10^{-4} | 9.33×10^{-5} |
| 1980 | 1.81×10^{-4} | 1.63×10^{-4} | 1.46×10^{-4} | 1.24×10^{-4} | 9.54×10^{-5} |
| 2040 | 1.84×10^{-4} | 1.66×10^{-4} | 1.48×10^{-4} | 1.27×10^{-4} | 9.76×10^{-5} |
| 2100 | 1.86×10^{-4} | 1.69×10^{-4} | 1.51×10^{-4} | 1.29×10^{-4} | 9.97×10^{-5} |
| 2160 | 1.90×10^{-4} | 1.72×10^{-4} | 1.54×10^{-4} | 1.32×10^{-4} | 1.02×10^{-4} |
| 2220 | 1.92×10^{-4} | 1.75×10^{-4} | 1.57×10^{-4} | 1.34×10^{-4} | 1.04×10^{-4} |
| 2280 | 1.95×10^{-4} | 1.77×10^{-4} | 1.59×10^{-4} | 1.37×10^{-4} | 1.06×10^{-4} |
| 2340 | 1.98×10^{-4} | 1.80×10^{-4} | 1.62×10^{-4} | 1.39×10^{-4} | 1.08×10^{-4} |
| 2400 | 2.00×10^{-4} | 1.83×10^{-4} | 1.64×10^{-4} | 1.42×10^{-4} | 1.10×10^{-4} |
| 2460 | 2.03×10^{-4} | 1.85×10^{-4} | 1.67×10^{-4} | 1.44×10^{-4} | 1.12×10^{-4} |
| 2520 | 2.05×10^{-4} | 1.88×10^{-4} | 1.70×10^{-4} | 1.46×10^{-4} | 1.14×10^{-4} |
| 2580 | 2.07×10^{-4} | 1.90×10^{-4} | 1.72×10^{-4} | 1.49×10^{-4} | 1.15×10^{-4} |
| 2640 | 2.10×10^{-4} | 1.92×10^{-4} | 1.74×10^{-4} | 1.51×10^{-4} | 1.17×10^{-4} |
| 2700 | 2.12×10^{-4} | 1.94×10^{-4} | 1.77×10^{-4} | 1.53×10^{-4} | 1.19×10^{-4} |
| 2760 | 2.13×10^{-4} | 1.97×10^{-4} | 1.79×10^{-4} | 1.55×10^{-4} | 1.21×10^{-4} |
| 2820 | 2.16×10^{-4} | 1.99×10^{-4} | 1.81×10^{-4} | 1.57×10^{-4} | 1.23×10^{-4} |
| 2880 | 2.18×10^{-4} | 2.01×10^{-4} | 1.83×10^{-4} | 1.60×10^{-4} | 1.25×10^{-4} |
| 2940 | 2.20×10^{-4} | 2.03×10^{-4} | 1.85×10^{-4} | 1.62×10^{-4} | 1.27×10^{-4} |
| 3000 | 2.21×10^{-4} | 2.05×10^{-4} | 1.87×10^{-4} | 1.64×10^{-4} | 1.28×10^{-4} |
| 3060 | 2.23×10^{-4} | 2.07×10^{-4} | 1.90×10^{-4} | 1.66×10^{-4} | 1.30×10^{-4} |
| 3120 | 2.24×10^{-4} | 2.09×10^{-4} | 1.91×10^{-4} | 1.68×10^{-4} | 1.32×10^{-4} |
| 3180 | 2.27×10^{-4} | 2.11×10^{-4} | 1.93×10^{-4} | 1.70×10^{-4} | 1.33×10^{-4} |
| 3240 | 2.28×10^{-4} | 2.13×10^{-4} | 1.95×10^{-4} | 1.72×10^{-4} | 1.35×10^{-4} |
| 3300 | 2.30×10^{-4} | 2.14×10^{-4} | 1.97×10^{-4} | 1.74×10^{-4} | 1.37×10^{-4} |
| 3360 | 2.31×10^{-4} | 2.16×10^{-4} | 1.99×10^{-4} | 1.75×10^{-4} | 1.38×10^{-4} |
| 3420 | 2.32×10^{-4} | 2.18×10^{-4} | 2.01×10^{-4} | 1.77×10^{-4} | 1.40×10^{-4} |
| 3480 | 2.34×10^{-4} | 2.19×10^{-4} | 2.02×10^{-4} | 1.79×10^{-4} | 1.42×10^{-4} |
| 3540 | 2.34×10^{-4} | 2.21×10^{-4} | 2.04×10^{-4} | 1.81×10^{-4} | 1.44×10^{-4} |
| 3600 | 2.37×10^{-4} | 2.22×10^{-4} | 2.06×10^{-4} | 1.83×10^{-4} | 1.45×10^{-4} |

Imidazole pH 8.0.

| Time (s) | Catalyst Concentration (M) | | | | |
|----------|---|-----------------------|-----------------------|-----------------------|------------------------|
| | 1.50x10 ⁻³ | 1.25x10 ⁻³ | 1.00x10 ⁻³ | 0.75x10 ⁻³ | 0.50x10 ⁻³ |
| | <i>p</i> -Nitrophenol Concentration (M) | | | | |
| 60 | 6.96x10 ⁻⁵ | 6.23x10 ⁻⁵ | 5.35x10 ⁻⁵ | 4.44x10 ⁻⁵ | 3.25x10 ⁻⁵ |
| 120 | 1.12x10 ⁻⁴ | 9.82x10 ⁻⁵ | 8.34x10 ⁻⁵ | 6.77x10 ⁻⁵ | 4.81x10 ⁻⁵ |
| 180 | 1.52x10 ⁻⁴ | 1.32x10 ⁻⁴ | 1.12x10 ⁻⁴ | 8.99x10 ⁻⁵ | 6.30x10 ⁻⁵ |
| 240 | 1.89x10 ⁻⁴ | 1.64x10 ⁻⁴ | 1.39x10 ⁻⁴ | 1.11x10 ⁻⁴ | 7.77x10 ⁻⁵ |
| 300 | 2.23x10 ⁻⁴ | 1.94x10 ⁻⁴ | 1.64x10 ⁻⁴ | 1.32x10 ⁻⁴ | 9.19x10 ⁻⁵ |
| 360 | 2.54x10 ⁻⁴ | 2.23x10 ⁻⁴ | 1.89x10 ⁻⁴ | 1.51x10 ⁻⁴ | 1.06x10 ⁻⁴ |
| 420 | 2.84x10 ⁻⁴ | 2.49x10 ⁻⁴ | 2.12x10 ⁻⁴ | 1.70x10 ⁻⁴ | 1.19x10 ⁻⁴ |
| 480 | 3.10x10 ⁻⁴ | 2.74x10 ⁻⁴ | 2.34x10 ⁻⁴ | 1.88x10 ⁻⁴ | 1.32x10 ⁻⁴ |
| 540 | 3.35x10 ⁻⁴ | 2.97x10 ⁻⁴ | 2.54x10 ⁻⁴ | 2.05x10 ⁻⁴ | 1.45x10 ⁻⁴ |
| 600 | 3.57x10 ⁻⁴ | 3.18x10 ⁻⁴ | 2.74x10 ⁻⁴ | 2.22x10 ⁻⁴ | 1.57x10 ⁻⁴ |
| 660 | 3.76x10 ⁻⁴ | 3.38x10 ⁻⁴ | 2.93x10 ⁻⁴ | 2.38x10 ⁻⁴ | 1.70x10 ⁻⁴ |
| 720 | 3.93x10 ⁻⁴ | 3.56x10 ⁻⁴ | 3.10x10 ⁻⁴ | 2.53x10 ⁻⁴ | 1.82x10 ⁻⁴ |
| 780 | 4.08x10 ⁻⁴ | 3.73x10 ⁻⁴ | 3.27x10 ⁻⁴ | 2.68x10 ⁻⁴ | 1.93x10 ⁻⁴ |
| 840 | 4.21x10 ⁻⁴ | 3.88x10 ⁻⁴ | 3.42x10 ⁻⁴ | 2.82x10 ⁻⁴ | 2.04x10 ⁻⁴ |
| 900 | 4.32x10 ⁻⁴ | 3.99x10 ⁻⁴ | 3.56x10 ⁻⁴ | 2.96x10 ⁻⁴ | 2.15x10 ⁻⁴ |
| 960 | 4.39x10 ⁻⁴ | 4.10x10 ⁻⁴ | 3.69x10 ⁻⁴ | 3.08x10 ⁻⁴ | 2.26x10 ⁻⁴ |
| 1020 | 4.45x10 ⁻⁴ | 4.20x10 ⁻⁴ | 3.81x10 ⁻⁴ | 3.21x10 ⁻⁴ | 2.36x10 ⁻⁴ |
| 1080 | 4.52x10 ⁻⁴ | 4.29x10 ⁻⁴ | 3.93x10 ⁻⁴ | 3.32x10 ⁻⁴ | 2.46x10 ⁻⁴ |
| 1140 | 4.58x10 ⁻⁴ | 4.38x10 ⁻⁴ | 4.03x10 ⁻⁴ | 3.43x10 ⁻⁴ | 2.56x10 ⁻⁴ |
| 1200 | 4.65x10 ⁻⁴ | 4.43x10 ⁻⁴ | 4.10x10 ⁻⁴ | 3.54x10 ⁻⁴ | 2.65x10 ⁻⁴ |
| 1260 | 4.67x10 ⁻⁴ | 4.47x10 ⁻⁴ | 4.18x10 ⁻⁴ | 3.64x10 ⁻⁴ | 2.75x10 ⁻⁴ |
| 1320 | 4.66x10 ⁻⁴ | 4.51x10 ⁻⁴ | 4.27x10 ⁻⁴ | 3.73x10 ⁻⁴ | 2.84x10 ⁻⁴ |
| 1380 | 4.66x10 ⁻⁴ | 4.56x10 ⁻⁴ | 4.33x10 ⁻⁴ | 3.82x10 ⁻⁴ | 2.92x10 ⁻⁴ |
| 1440 | 4.71x10 ⁻⁴ | 4.61x10 ⁻⁴ | 4.40x10 ⁻⁴ | 3.90x10 ⁻⁴ | 3.01x10 ⁻⁴ |
| 1500 | 4.72x10 ⁻⁴ | 4.65x10 ⁻⁴ | 4.42x10 ⁻⁴ | 3.96x10 ⁻⁴ | 3.09x10 ⁻⁴ |
| 1560 | 4.75x10 ⁻⁴ | 4.64x10 ⁻⁴ | 4.45x10 ⁻⁴ | 4.04x10 ⁻⁴ | 3.17x10 ⁻⁴ |
| 1620 | 4.74x10 ⁻⁴ | 4.64x10 ⁻⁴ | 4.51x10 ⁻⁴ | 4.10x10 ⁻⁴ | 3.25x10 ⁻⁴ |
| 1680 | 4.72x10 ⁻⁴ | 4.69x10 ⁻⁴ | 4.55x10 ⁻⁴ | 4.18x10 ⁻⁴ | 3.32 x10 ⁻⁴ |

| | | | | | |
|------|-----------------------|-----------------------|-----------------------|-----------------------|-----------------------|
| 1740 | 4.76x10 ⁻⁴ | 4.68x10 ⁻⁴ | 4.61x10 ⁻⁴ | 4.22x10 ⁻⁴ | 3.38x10 ⁻⁴ |
| 1800 | 4.76x10 ⁻⁴ | 4.74x10 ⁻⁴ | 4.61x10 ⁻⁴ | 4.25x10 ⁻⁴ | 3.46x10 ⁻⁴ |
| 1860 | 4.78x10 ⁻⁴ | 4.76x10 ⁻⁴ | 4.62x10 ⁻⁴ | 4.31x10 ⁻⁴ | 3.53x10 ⁻⁴ |
| 1920 | 4.79x10 ⁻⁴ | 4.73x10 ⁻⁴ | 4.63x10 ⁻⁴ | 4.35x10 ⁻⁴ | 3.59x10 ⁻⁴ |
| 1980 | 4.77x10 ⁻⁴ | 4.72x10 ⁻⁴ | 4.66x10 ⁻⁴ | 4.40x10 ⁻⁴ | 3.66x10 ⁻⁴ |
| 2040 | 4.76x10 ⁻⁴ | 4.74x10 ⁻⁴ | 4.69x10 ⁻⁴ | 4.45x10 ⁻⁴ | 3.71x10 ⁻⁴ |
| 2100 | 4.78x10 ⁻⁴ | 4.77x10 ⁻⁴ | 4.71x10 ⁻⁴ | 4.46x10 ⁻⁴ | 3.76x10 ⁻⁴ |
| 2160 | 4.79x10 ⁻⁴ | 4.77x10 ⁻⁴ | 4.71x10 ⁻⁴ | 4.47x10 ⁻⁴ | 3.83x10 ⁻⁴ |
| 2220 | 4.82x10 ⁻⁴ | 4.76x10 ⁻⁴ | 4.68x10 ⁻⁴ | 4.52x10 ⁻⁴ | 3.87x10 ⁻⁴ |
| 2280 | 4.76x10 ⁻⁴ | 4.73x10 ⁻⁴ | 4.72x10 ⁻⁴ | 4.53x10 ⁻⁴ | 3.93x10 ⁻⁴ |
| 2340 | 4.76x10 ⁻⁴ | 4.79x10 ⁻⁴ | 4.73x10 ⁻⁴ | 4.60x10 ⁻⁴ | 3.98x10 ⁻⁴ |
| 2400 | 4.81x10 ⁻⁴ | 4.76x10 ⁻⁴ | 4.76x10 ⁻⁴ | 4.58x10 ⁻⁴ | 4.01x10 ⁻⁴ |
| 2460 | 4.80x10 ⁻⁴ | 4.78x10 ⁻⁴ | 4.78x10 ⁻⁴ | 4.60x10 ⁻⁴ | 4.06x10 ⁻⁴ |
| 2520 | 4.82x10 ⁻⁴ | 4.79x10 ⁻⁴ | 4.73x10 ⁻⁴ | 4.61x10 ⁻⁴ | 4.10x10 ⁻⁴ |
| 2580 | 4.82x10 ⁻⁴ | 4.76x10 ⁻⁴ | 4.73x10 ⁻⁴ | 4.63x10 ⁻⁴ | 4.14x10 ⁻⁴ |
| 2640 | 4.80x10 ⁻⁴ | 4.74x10 ⁻⁴ | 4.75x10 ⁻⁴ | 4.65x10 ⁻⁴ | 4.20x10 ⁻⁴ |
| 2700 | 4.77x10 ⁻⁴ | 4.78x10 ⁻⁴ | 4.76x10 ⁻⁴ | 4.69x10 ⁻⁴ | 4.22x10 ⁻⁴ |
| 2760 | 4.81x10 ⁻⁴ | 4.79x10 ⁻⁴ | 4.81x10 ⁻⁴ | 4.68x10 ⁻⁴ | 4.23x10 ⁻⁴ |
| 2820 | 4.81x10 ⁻⁴ | 4.79x10 ⁻⁴ | 4.77x10 ⁻⁴ | 4.64x10 ⁻⁴ | 4.28x10 ⁻⁴ |
| 2880 | 4.84x10 ⁻⁴ | 4.77x10 ⁻⁴ | 4.74x10 ⁻⁴ | 4.70x10 ⁻⁴ | 4.30x10 ⁻⁴ |
| 2940 | 4.79x10 ⁻⁴ | 4.73x10 ⁻⁴ | 4.77x10 ⁻⁴ | 4.68x10 ⁻⁴ | 4.36x10 ⁻⁴ |
| 3000 | 4.76x10 ⁻⁴ | 4.77x10 ⁻⁴ | 4.76x10 ⁻⁴ | 4.75x10 ⁻⁴ | 4.36x10 ⁻⁴ |
| 3060 | 4.78x10 ⁻⁴ | 4.85x10 ⁻⁴ | 4.79x10 ⁻⁴ | 4.75x10 ⁻⁴ | 4.39x10 ⁻⁴ |
| 3120 | 4.79x10 ⁻⁴ | 4.86x10 ⁻⁴ | 4.81x10 ⁻⁴ | 4.71x10 ⁻⁴ | 4.40x10 ⁻⁴ |
| 3180 | 4.80x10 ⁻⁴ | 4.83x10 ⁻⁴ | 4.77x10 ⁻⁴ | 4.71x10 ⁻⁴ | 4.44x10 ⁻⁴ |
| 3240 | 4.83x10 ⁻⁴ | 4.81x10 ⁻⁴ | 4.76x10 ⁻⁴ | 4.75x10 ⁻⁴ | 4.45x10 ⁻⁴ |
| 3300 | 4.78x10 ⁻⁴ | 4.77x10 ⁻⁴ | 4.79x10 ⁻⁴ | 4.74x10 ⁻⁴ | 4.50x10 ⁻⁴ |
| 3360 | 4.77x10 ⁻⁴ | 4.80x10 ⁻⁴ | 4.77x10 ⁻⁴ | 4.78x10 ⁻⁴ | 4.50x10 ⁻⁴ |
| 3420 | 4.78x10 ⁻⁴ | 4.81x10 ⁻⁴ | 4.81x10 ⁻⁴ | 4.75x10 ⁻⁴ | 4.48x10 ⁻⁴ |
| 3480 | 4.80x10 ⁻⁴ | 4.85x10 ⁻⁴ | 4.80x10 ⁻⁴ | 4.73x10 ⁻⁴ | 4.53x10 ⁻⁴ |
| 3540 | 4.85x10 ⁻⁴ | 4.85x10 ⁻⁴ | 4.74x10 ⁻⁴ | 4.76x10 ⁻⁴ | 4.53x10 ⁻⁴ |
| 3600 | 4.84x10 ⁻⁴ | 4.80x10 ⁻⁴ | 4.79x10 ⁻⁴ | 4.77x10 ⁻⁴ | 4.59x10 ⁻⁴ |

N-Acetyl-L-histidine pH 8.0.

| Time (s) | Catalyst Concentration (M) | | | | |
|----------|---|-----------------------|-----------------------|-----------------------|-----------------------|
| | 1.50x10 ⁻³ | 1.25x10 ⁻³ | 1.00x10 ⁻³ | 0.75x10 ⁻³ | 0.50x10 ⁻³ |
| | <i>p</i> -Nitrophenol Concentration (M) | | | | |
| 60 | 3.84x10 ⁻⁵ | 3.39x10 ⁻⁵ | 3.19x10 ⁻⁵ | 2.98x10 ⁻⁵ | 2.57x10 ⁻⁵ |
| 120 | 5.59x10 ⁻⁵ | 4.87x10 ⁻⁵ | 4.43x10 ⁻⁵ | 4.01x10 ⁻⁵ | 3.32x10 ⁻⁵ |
| 180 | 7.26x10 ⁻⁵ | 6.29x10 ⁻⁵ | 5.64x10 ⁻⁵ | 5.00x10 ⁻⁵ | 4.06x10 ⁻⁵ |
| 240 | 8.86x10 ⁻⁵ | 7.67x10 ⁻⁵ | 6.81x10 ⁻⁵ | 5.96x10 ⁻⁵ | 4.78x10 ⁻⁵ |
| 300 | 1.04x10 ⁻⁴ | 9.00x10 ⁻⁵ | 7.96x10 ⁻⁵ | 6.90x10 ⁻⁵ | 5.48x10 ⁻⁵ |
| 360 | 1.19x10 ⁻⁴ | 1.03x10 ⁻⁴ | 9.08x10 ⁻⁵ | 7.83x10 ⁻⁵ | 6.16x10 ⁻⁵ |
| 420 | 1.34x10 ⁻⁴ | 1.16x10 ⁻⁴ | 1.02x10 ⁻⁴ | 8.73x10 ⁻⁵ | 6.84x10 ⁻⁵ |
| 480 | 1.48x10 ⁻⁴ | 1.28x10 ⁻⁴ | 1.12x10 ⁻⁴ | 9.61x10 ⁻⁵ | 7.50x10 ⁻⁵ |
| 540 | 1.61x10 ⁻⁴ | 1.40x10 ⁻⁴ | 1.23x10 ⁻⁴ | 1.05x10 ⁻⁴ | 8.15x10 ⁻⁵ |
| 600 | 1.75x10 ⁻⁴ | 1.51x10 ⁻⁴ | 1.33x10 ⁻⁴ | 1.13x10 ⁻⁴ | 8.80x10 ⁻⁵ |
| 660 | 1.88x10 ⁻⁴ | 1.63x10 ⁻⁴ | 1.40x10 ⁻⁴ | 1.22x10 ⁻⁴ | 9.47x10 ⁻⁵ |
| 720 | 2.00x10 ⁻⁴ | 1.74x10 ⁻⁴ | 1.53x10 ⁻⁴ | 1.30x10 ⁻⁴ | 1.01x10 ⁻⁴ |
| 780 | 2.12x10 ⁻⁴ | 1.85x10 ⁻⁴ | 1.63x10 ⁻⁴ | 1.38x10 ⁻⁴ | 1.07x10 ⁻⁴ |
| 840 | 2.24x10 ⁻⁴ | 1.95x10 ⁻⁴ | 1.72x10 ⁻⁴ | 1.46x10 ⁻⁴ | 1.13x10 ⁻⁴ |
| 900 | 2.35x10 ⁻⁴ | 2.05x10 ⁻⁴ | 1.81x10 ⁻⁴ | 1.54x10 ⁻⁴ | 1.19x10 ⁻⁴ |
| 960 | 2.46x10 ⁻⁴ | 2.15x10 ⁻⁴ | 1.90x10 ⁻⁴ | 1.61x10 ⁻⁴ | 1.25x10 ⁻⁴ |
| 1020 | 2.57x10 ⁻⁴ | 2.25x10 ⁻⁴ | 1.99x10 ⁻⁴ | 1.69x10 ⁻⁴ | 1.31x10 ⁻⁴ |
| 1080 | 2.67x10 ⁻⁴ | 2.34x10 ⁻⁴ | 2.07x10 ⁻⁴ | 1.76x10 ⁻⁴ | 1.37x10 ⁻⁴ |
| 1140 | 2.77x10 ⁻⁴ | 2.44x10 ⁻⁴ | 2.15x10 ⁻⁴ | 1.83x10 ⁻⁴ | 1.42x10 ⁻⁴ |
| 1200 | 2.87x10 ⁻⁴ | 2.53x10 ⁻⁴ | 2.24x10 ⁻⁴ | 1.90x10 ⁻⁴ | 1.48x10 ⁻⁴ |
| 1260 | 2.97x10 ⁻⁴ | 2.62x10 ⁻⁴ | 2.32x10 ⁻⁴ | 1.98x10 ⁻⁴ | 1.54x10 ⁻⁴ |
| 1320 | 3.06x10 ⁻⁴ | 2.70x10 ⁻⁴ | 2.40x10 ⁻⁴ | 2.04x10 ⁻⁴ | 1.59x10 ⁻⁴ |
| 1380 | 3.15x10 ⁻⁴ | 2.78x10 ⁻⁴ | 2.47x10 ⁻⁴ | 2.11x10 ⁻⁴ | 1.65x10 ⁻⁴ |
| 1440 | 3.23x10 ⁻⁴ | 2.86x10 ⁻⁴ | 2.55x10 ⁻⁴ | 2.18x10 ⁻⁴ | 1.70x10 ⁻⁴ |
| 1500 | 3.31x10 ⁻⁴ | 2.94x10 ⁻⁴ | 2.62x10 ⁻⁴ | 2.24x10 ⁻⁴ | 1.75x10 ⁻⁴ |
| 1560 | 3.38x10 ⁻⁴ | 3.01x10 ⁻⁴ | 2.69x10 ⁻⁴ | 2.31x10 ⁻⁴ | 1.80x10 ⁻⁴ |
| 1620 | 3.46x10 ⁻⁴ | 3.09x10 ⁻⁴ | 2.76x10 ⁻⁴ | 2.37x10 ⁻⁴ | 1.85x10 ⁻⁴ |
| 1680 | 3.53x10 ⁻⁴ | 3.16x10 ⁻⁴ | 2.83x10 ⁻⁴ | 2.43x10 ⁻⁴ | 1.90x10 ⁻⁴ |

| | | | | | |
|------|-----------------------|-----------------------|-----------------------|-----------------------|-----------------------|
| 1740 | 3.60×10^{-4} | 3.22×10^{-4} | 2.90×10^{-4} | 2.49×10^{-4} | 1.95×10^{-4} |
| 1800 | 3.66×10^{-4} | 3.29×10^{-4} | 2.96×10^{-4} | 2.55×10^{-4} | 2.00×10^{-4} |
| 1860 | 3.72×10^{-4} | 3.36×10^{-4} | 3.03×10^{-4} | 2.61×10^{-4} | 2.05×10^{-4} |
| 1920 | 3.78×10^{-4} | 3.42×10^{-4} | 3.09×10^{-4} | 2.67×10^{-4} | 2.10×10^{-4} |
| 1980 | 3.85×10^{-4} | 3.48×10^{-4} | 3.15×10^{-4} | 2.72×10^{-4} | 2.15×10^{-4} |
| 2040 | 3.90×10^{-4} | 3.54×10^{-4} | 3.20×10^{-4} | 2.78×10^{-4} | 2.20×10^{-4} |
| 2100 | 3.95×10^{-4} | 3.59×10^{-4} | 3.26×10^{-4} | 2.83×10^{-4} | 2.24×10^{-4} |
| 2160 | 3.99×10^{-4} | 3.64×10^{-4} | 3.32×10^{-4} | 2.89×10^{-4} | 2.29×10^{-4} |
| 2220 | 4.04×10^{-4} | 3.70×10^{-4} | 3.37×10^{-4} | 2.94×10^{-4} | 2.33×10^{-4} |
| 2280 | 4.08×10^{-4} | 3.75×10^{-4} | 3.42×10^{-4} | 2.99×10^{-4} | 2.38×10^{-4} |
| 2340 | 4.13×10^{-4} | 3.78×10^{-4} | 3.47×10^{-4} | 3.04×10^{-4} | 2.42×10^{-4} |
| 2400 | 4.16×10^{-4} | 3.84×10^{-4} | 3.52×10^{-4} | 3.09×10^{-4} | 2.46×10^{-4} |
| 2460 | 4.20×10^{-4} | 3.89×10^{-4} | 3.57×10^{-4} | 3.14×10^{-4} | 2.51×10^{-4} |
| 2520 | 4.24×10^{-4} | 3.93×10^{-4} | 3.62×10^{-4} | 3.19×10^{-4} | 2.55×10^{-4} |
| 2580 | 4.26×10^{-4} | 3.98×10^{-4} | 3.67×10^{-4} | 3.23×10^{-4} | 2.59×10^{-4} |
| 2640 | 4.30×10^{-4} | 4.01×10^{-4} | 3.71×10^{-4} | 3.27×10^{-4} | 2.63×10^{-4} |
| 2700 | 4.33×10^{-4} | 4.04×10^{-4} | 3.75×10^{-4} | 3.32×10^{-4} | 2.67×10^{-4} |
| 2760 | 4.36×10^{-4} | 4.08×10^{-4} | 3.79×10^{-4} | 3.36×10^{-4} | 2.71×10^{-4} |
| 2820 | 4.37×10^{-4} | 4.12×10^{-4} | 3.83×10^{-4} | 3.40×10^{-4} | 2.75×10^{-4} |
| 2880 | 4.39×10^{-4} | 4.15×10^{-4} | 3.87×10^{-4} | 3.44×10^{-4} | 2.79×10^{-4} |
| 2940 | 4.43×10^{-4} | 4.18×10^{-4} | 3.90×10^{-4} | 3.48×10^{-4} | 2.83×10^{-4} |
| 3000 | 4.47×10^{-4} | 4.21×10^{-4} | 3.93×10^{-4} | 3.52×10^{-4} | 2.87×10^{-4} |
| 3060 | 4.48×10^{-4} | 4.24×10^{-4} | 3.98×10^{-4} | 3.56×10^{-4} | 2.91×10^{-4} |
| 3120 | 4.50×10^{-4} | 4.26×10^{-4} | 4.01×10^{-4} | 3.61×10^{-4} | 2.95×10^{-4} |
| 3180 | 4.50×10^{-4} | 4.28×10^{-4} | 4.05×10^{-4} | 3.64×10^{-4} | 2.98×10^{-4} |
| 3240 | 4.52×10^{-4} | 4.33×10^{-4} | 4.07×10^{-4} | 3.68×10^{-4} | 3.02×10^{-4} |
| 3300 | 4.54×10^{-4} | 4.34×10^{-4} | 4.10×10^{-4} | 3.71×10^{-4} | 3.05×10^{-4} |
| 3360 | 4.56×10^{-4} | 4.35×10^{-4} | 4.12×10^{-4} | 3.74×10^{-4} | 3.09×10^{-4} |
| 3420 | 4.56×10^{-4} | 4.38×10^{-4} | 4.15×10^{-4} | 3.78×10^{-4} | 3.12×10^{-4} |
| 3480 | 4.57×10^{-4} | 4.39×10^{-4} | 4.18×10^{-4} | 3.81×10^{-4} | 3.15×10^{-4} |
| 3540 | 4.59×10^{-4} | 4.41×10^{-4} | 4.21×10^{-4} | 3.84×10^{-4} | 3.19×10^{-4} |
| 3600 | 4.59×10^{-4} | 4.43×10^{-4} | 4.26×10^{-4} | 3.87×10^{-4} | 3.22×10^{-4} |

Hydrolysis of *p*-Nitrophenyl Acetate in DMSO/H₂O 9:1 v/v Solution, Small Molecules

Catalyst.

Imidazole.

| Time (s) | Catalyst Concentration (M) | | | | |
|----------|---|-----------------------|-----------------------|-----------------------|-----------------------|
| | 1.50x10 ⁻³ | 1.25x10 ⁻³ | 1.00x10 ⁻³ | 0.75x10 ⁻³ | 0.50x10 ⁻³ |
| | <i>p</i> -Nitrophenol Concentration (M) | | | | |
| 60 | 3.83x10 ⁻⁷ | 5.43x10 ⁻⁷ | 3.83x10 ⁻⁷ | 3.04x10 ⁻⁷ | 2.24x10 ⁻⁷ |
| 120 | 5.43x10 ⁻⁷ | 7.02x10 ⁻⁷ | 4.63x10 ⁻⁷ | 3.83x10 ⁻⁷ | 2.64x10 ⁻⁷ |
| 180 | 6.62x10 ⁻⁷ | 8.62x10 ⁻⁷ | 5.83x10 ⁻⁷ | 4.23x10 ⁻⁷ | 3.04x10 ⁻⁷ |
| 240 | 9.02x10 ⁻⁷ | 1.02x10 ⁻⁶ | 7.02x10 ⁻⁷ | 5.43x10 ⁻⁷ | 3.83x10 ⁻⁷ |
| 300 | 1.06x10 ⁻⁶ | 1.14x10 ⁻⁶ | 7.82x10 ⁻⁷ | 5.83x10 ⁻⁷ | 4.23x10 ⁻⁷ |
| 360 | 1.14x10 ⁻⁶ | 1.30x10 ⁻⁶ | 9.02x10 ⁻⁷ | 7.02x10 ⁻⁷ | 4.63x10 ⁻⁷ |
| 420 | 1.34x10 ⁻⁶ | 1.42x10 ⁻⁶ | 9.81x10 ⁻⁷ | 7.42x10 ⁻⁷ | 5.43x10 ⁻⁷ |
| 480 | 1.50x10 ⁻⁶ | 1.54x10 ⁻⁶ | 1.06x10 ⁻⁶ | 8.22x10 ⁻⁷ | 5.83x10 ⁻⁷ |
| 540 | 1.62x10 ⁻⁶ | 1.70x10 ⁻⁶ | 1.18x10 ⁻⁶ | 9.02x10 ⁻⁷ | 6.23x10 ⁻⁷ |
| 600 | 1.78x10 ⁻⁶ | 1.82x10 ⁻⁶ | 1.26x10 ⁻⁶ | 9.81x10 ⁻⁷ | 6.62x10 ⁻⁷ |
| 660 | 1.90x10 ⁻⁶ | 1.94x10 ⁻⁶ | 1.38x10 ⁻⁶ | 1.02x10 ⁻⁶ | 7.02x10 ⁻⁷ |
| 720 | 2.06x10 ⁻⁶ | 2.06x10 ⁻⁶ | 1.42x10 ⁻⁶ | 1.06x10 ⁻⁶ | 7.42x10 ⁻⁷ |
| 780 | 2.18x10 ⁻⁶ | 2.14x10 ⁻⁶ | 1.54x10 ⁻⁶ | 1.14x10 ⁻⁶ | 7.82x10 ⁻⁷ |
| 840 | 2.30x10 ⁻⁶ | 2.30x10 ⁻⁶ | 1.62x10 ⁻⁶ | 1.22x10 ⁻⁶ | 8.62x10 ⁻⁷ |
| 900 | 2.42x10 ⁻⁶ | 2.42x10 ⁻⁶ | 1.70x10 ⁻⁶ | 1.30x10 ⁻⁶ | 9.02x10 ⁻⁷ |
| 960 | 2.58x10 ⁻⁶ | 2.54x10 ⁻⁶ | 1.78x10 ⁻⁶ | 1.38x10 ⁻⁶ | 9.41x10 ⁻⁷ |
| 1020 | 2.66x10 ⁻⁶ | 2.66x10 ⁻⁶ | 1.90x10 ⁻⁶ | 1.42x10 ⁻⁶ | 9.81x10 ⁻⁷ |
| 1080 | 2.81x10 ⁻⁶ | 2.73x10 ⁻⁶ | 1.98x10 ⁻⁶ | 1.50x10 ⁻⁶ | 1.02x10 ⁻⁶ |
| 1140 | 2.89x10 ⁻⁶ | 2.85x10 ⁻⁶ | 2.06x10 ⁻⁶ | 1.58x10 ⁻⁶ | 1.06x10 ⁻⁶ |
| 1200 | 3.05x10 ⁻⁶ | 2.97x10 ⁻⁶ | 2.14x10 ⁻⁶ | 1.62x10 ⁻⁶ | 1.14x10 ⁻⁶ |
| 1260 | 3.13x10 ⁻⁶ | 3.05x10 ⁻⁶ | 2.22x10 ⁻⁶ | 1.66x10 ⁻⁶ | 1.18x10 ⁻⁶ |
| 1320 | 3.25x10 ⁻⁶ | 3.17x10 ⁻⁶ | 2.30x10 ⁻⁶ | 1.74x10 ⁻⁶ | 1.22x10 ⁻⁶ |
| 1380 | 3.41x10 ⁻⁶ | 3.29x10 ⁻⁶ | 2.38x10 ⁻⁶ | 1.82x10 ⁻⁶ | 1.26x10 ⁻⁶ |
| 1440 | 3.49x10 ⁻⁶ | 3.37x10 ⁻⁶ | 2.42x10 ⁻⁶ | 1.86x10 ⁻⁶ | 1.30x10 ⁻⁶ |
| 1500 | 3.57x10 ⁻⁶ | 3.45x10 ⁻⁶ | 2.54x10 ⁻⁶ | 1.90x10 ⁻⁶ | 1.34x10 ⁻⁶ |
| 1560 | 3.69x10 ⁻⁶ | 3.53x10 ⁻⁶ | 2.58x10 ⁻⁶ | 1.98x10 ⁻⁶ | 1.38x10 ⁻⁶ |

| | | | | | |
|------|-----------------------|-----------------------|-----------------------|-----------------------|-----------------------|
| 1620 | 3.81×10^{-6} | 3.65×10^{-6} | 2.66×10^{-6} | 2.02×10^{-6} | 1.42×10^{-6} |
| 1680 | 3.89×10^{-6} | 3.73×10^{-6} | 2.70×10^{-6} | 2.06×10^{-6} | 1.46×10^{-6} |
| 1740 | 3.97×10^{-6} | 3.85×10^{-6} | 2.77×10^{-6} | 2.14×10^{-6} | 1.50×10^{-6} |
| 1800 | 4.05×10^{-6} | 3.93×10^{-6} | 2.85×10^{-6} | 2.18×10^{-6} | 1.54×10^{-6} |
| 1860 | 4.21×10^{-6} | 4.01×10^{-6} | 2.93×10^{-6} | 2.26×10^{-6} | 1.58×10^{-6} |
| 1920 | 4.29×10^{-6} | 4.09×10^{-6} | 3.01×10^{-6} | 2.30×10^{-6} | 1.62×10^{-6} |
| 1980 | 4.37×10^{-6} | 4.21×10^{-6} | 3.05×10^{-6} | 2.34×10^{-6} | 1.66×10^{-6} |
| 2040 | 4.49×10^{-6} | 4.29×10^{-6} | 3.13×10^{-6} | 2.42×10^{-6} | 1.70×10^{-6} |
| 2100 | 4.57×10^{-6} | 4.37×10^{-6} | 3.21×10^{-6} | 2.46×10^{-6} | 1.78×10^{-6} |
| 2160 | 4.65×10^{-6} | 4.45×10^{-6} | 3.29×10^{-6} | 2.54×10^{-6} | 1.78×10^{-6} |
| 2220 | 4.73×10^{-6} | 4.53×10^{-6} | 3.37×10^{-6} | 2.58×10^{-6} | 1.78×10^{-6} |
| 2280 | 4.81×10^{-6} | 4.61×10^{-6} | 3.37×10^{-6} | 2.62×10^{-6} | 1.86×10^{-6} |
| 2340 | 4.89×10^{-6} | 4.69×10^{-6} | 3.45×10^{-6} | 2.70×10^{-6} | 1.86×10^{-6} |
| 2400 | 4.97×10^{-6} | 4.77×10^{-6} | 3.53×10^{-6} | 2.70×10^{-6} | 1.90×10^{-6} |
| 2460 | 5.05×10^{-6} | 4.85×10^{-6} | 3.61×10^{-6} | 2.77×10^{-6} | 1.94×10^{-6} |
| 2520 | 5.13×10^{-6} | 4.93×10^{-6} | 3.69×10^{-6} | 2.81×10^{-6} | 1.98×10^{-6} |
| 2580 | 5.21×10^{-6} | 5.01×10^{-6} | 3.69×10^{-6} | 2.85×10^{-6} | 2.02×10^{-6} |
| 2640 | 5.29×10^{-6} | 5.09×10^{-6} | 3.77×10^{-6} | 2.93×10^{-6} | 2.06×10^{-6} |
| 2700 | 5.37×10^{-6} | 5.17×10^{-6} | 3.85×10^{-6} | 2.93×10^{-6} | 2.10×10^{-6} |
| 2760 | 5.45×10^{-6} | 5.21×10^{-6} | 3.89×10^{-6} | 3.01×10^{-6} | 2.14×10^{-6} |
| 2820 | 5.52×10^{-6} | 5.29×10^{-6} | 3.93×10^{-6} | 3.09×10^{-6} | 2.18×10^{-6} |
| 2880 | 5.60×10^{-6} | 5.33×10^{-6} | 4.01×10^{-6} | 3.09×10^{-6} | 2.22×10^{-6} |
| 2940 | 5.68×10^{-6} | 5.41×10^{-6} | 4.05×10^{-6} | 3.17×10^{-6} | 2.22×10^{-6} |
| 3000 | 5.76×10^{-6} | 5.49×10^{-6} | 4.13×10^{-6} | 3.17×10^{-6} | 2.26×10^{-6} |
| 3060 | 5.84×10^{-6} | 5.56×10^{-6} | 4.17×10^{-6} | 3.25×10^{-6} | 2.30×10^{-6} |
| 3120 | 5.92×10^{-6} | 5.64×10^{-6} | 4.21×10^{-6} | 3.29×10^{-6} | 2.34×10^{-6} |
| 3180 | 6.00×10^{-6} | 5.68×10^{-6} | 4.29×10^{-6} | 3.33×10^{-6} | 2.38×10^{-6} |
| 3240 | 6.04×10^{-6} | 5.76×10^{-6} | 4.37×10^{-6} | 3.37×10^{-6} | 2.42×10^{-6} |
| 3300 | 6.12×10^{-6} | 5.84×10^{-6} | 4.37×10^{-6} | 3.41×10^{-6} | 2.42×10^{-6} |
| 3360 | 6.20×10^{-6} | 5.88×10^{-6} | 4.45×10^{-6} | 3.45×10^{-6} | 2.46×10^{-6} |
| 3420 | 6.28×10^{-6} | 5.96×10^{-6} | 4.49×10^{-6} | 3.53×10^{-6} | 2.50×10^{-6} |
| 3480 | 6.32×10^{-6} | 6.00×10^{-6} | 4.57×10^{-6} | 3.53×10^{-6} | 2.54×10^{-6} |

| | | | | | |
|------|-----------------------|-----------------------|-----------------------|-----------------------|-----------------------|
| 3540 | 6.40×10^{-6} | 6.08×10^{-6} | 4.61×10^{-6} | 3.61×10^{-6} | 2.58×10^{-6} |
| 3600 | 6.44×10^{-6} | 6.16×10^{-6} | 4.65×10^{-6} | 3.61×10^{-6} | 2.58×10^{-6} |

N-Acetyl-L-histidine.

| Time (s) | Catalyst Concentration (M) | | | | |
|----------|---|-----------------------|-----------------------|-----------------------|-----------------------|
| | 1.50x10 ⁻³ | 1.25x10 ⁻³ | 1.00x10 ⁻³ | 0.75x10 ⁻³ | 0.50x10 ⁻³ |
| | <i>p</i> -Nitrophenol Concentration (M) | | | | |
| 60 | 1.03x10 ⁻⁵ | 1.02x10 ⁻⁵ | 1.03x10 ⁻⁵ | 1.01x10 ⁻⁵ | 1.00x10 ⁻⁵ |
| 120 | 1.04x10 ⁻⁵ | 1.04x10 ⁻⁵ | 1.04x10 ⁻⁵ | 1.01x10 ⁻⁵ | 1.01x10 ⁻⁵ |
| 180 | 1.05x10 ⁻⁵ | 1.05x10 ⁻⁵ | 1.04x10 ⁻⁵ | 1.02x10 ⁻⁵ | 1.02x10 ⁻⁵ |
| 240 | 1.07x10 ⁻⁵ | 1.06x10 ⁻⁵ | 1.05x10 ⁻⁵ | 1.03x10 ⁻⁵ | 1.03x10 ⁻⁵ |
| 300 | 1.08x10 ⁻⁵ | 1.06x10 ⁻⁵ | 1.06x10 ⁻⁵ | 1.04x10 ⁻⁵ | 1.03x10 ⁻⁵ |
| 360 | 1.09x10 ⁻⁵ | 1.07x10 ⁻⁵ | 1.07x10 ⁻⁵ | 1.04x10 ⁻⁵ | 1.03x10 ⁻⁵ |
| 420 | 1.10x10 ⁻⁵ | 1.08x10 ⁻⁵ | 1.07x10 ⁻⁵ | 1.05x10 ⁻⁵ | 1.04x10 ⁻⁵ |
| 480 | 1.11x10 ⁻⁵ | 1.10x10 ⁻⁵ | 1.08x10 ⁻⁵ | 1.05x10 ⁻⁵ | 1.04x10 ⁻⁵ |
| 540 | 1.13x10 ⁻⁵ | 1.11x10 ⁻⁵ | 1.09x10 ⁻⁵ | 1.06x10 ⁻⁵ | 1.05x10 ⁻⁵ |
| 600 | 1.14x10 ⁻⁵ | 1.11x10 ⁻⁵ | 1.10x10 ⁻⁵ | 1.07x10 ⁻⁵ | 1.06x10 ⁻⁵ |
| 660 | 1.15x10 ⁻⁵ | 1.13x10 ⁻⁵ | 1.11x10 ⁻⁵ | 1.08x10 ⁻⁵ | 1.06x10 ⁻⁵ |
| 720 | 1.17x10 ⁻⁵ | 1.14x10 ⁻⁵ | 1.12x10 ⁻⁵ | 1.08x10 ⁻⁵ | 1.07x10 ⁻⁵ |
| 780 | 1.18x10 ⁻⁵ | 1.15x10 ⁻⁵ | 1.13x10 ⁻⁵ | 1.09x10 ⁻⁵ | 1.07x10 ⁻⁵ |
| 840 | 1.19x10 ⁻⁵ | 1.16x10 ⁻⁵ | 1.13x10 ⁻⁵ | 1.10x10 ⁻⁵ | 1.07x10 ⁻⁵ |
| 900 | 1.20x10 ⁻⁵ | 1.17x10 ⁻⁵ | 1.14x10 ⁻⁵ | 1.10x10 ⁻⁵ | 1.08x10 ⁻⁵ |
| 960 | 1.21x10 ⁻⁵ | 1.18x10 ⁻⁵ | 1.15x10 ⁻⁵ | 1.11x10 ⁻⁵ | 1.09x10 ⁻⁵ |
| 1020 | 1.23x10 ⁻⁵ | 1.19x10 ⁻⁵ | 1.16x10 ⁻⁵ | 1.11x10 ⁻⁵ | 1.09x10 ⁻⁵ |
| 1080 | 1.24x10 ⁻⁵ | 1.20x10 ⁻⁵ | 1.17x10 ⁻⁵ | 1.12x10 ⁻⁵ | 1.10x10 ⁻⁵ |
| 1140 | 1.25x10 ⁻⁵ | 1.21x10 ⁻⁵ | 1.18x10 ⁻⁵ | 1.13x10 ⁻⁵ | 1.10x10 ⁻⁵ |
| 1200 | 1.26x10 ⁻⁵ | 1.22x10 ⁻⁵ | 1.19x10 ⁻⁵ | 1.13x10 ⁻⁵ | 1.10x10 ⁻⁵ |
| 1260 | 1.28x10 ⁻⁵ | 1.23x10 ⁻⁵ | 1.19x10 ⁻⁵ | 1.14x10 ⁻⁵ | 1.11x10 ⁻⁵ |
| 1320 | 1.29x10 ⁻⁵ | 1.24x10 ⁻⁵ | 1.20x10 ⁻⁵ | 1.15x10 ⁻⁵ | 1.11x10 ⁻⁵ |
| 1380 | 1.30x10 ⁻⁵ | 1.25x10 ⁻⁵ | 1.21x10 ⁻⁵ | 1.15x10 ⁻⁵ | 1.12x10 ⁻⁵ |
| 1440 | 1.31x10 ⁻⁵ | 1.27x10 ⁻⁵ | 1.22x10 ⁻⁵ | 1.16x10 ⁻⁵ | 1.13x10 ⁻⁵ |
| 1500 | 1.33x10 ⁻⁵ | 1.27x10 ⁻⁵ | 1.23x10 ⁻⁵ | 1.17x10 ⁻⁵ | 1.13x10 ⁻⁵ |
| 1560 | 1.34x10 ⁻⁵ | 1.28x10 ⁻⁵ | 1.24x10 ⁻⁵ | 1.18x10 ⁻⁵ | 1.14x10 ⁻⁵ |
| 1620 | 1.35x10 ⁻⁵ | 1.29x10 ⁻⁵ | 1.25x10 ⁻⁵ | 1.18x10 ⁻⁵ | 1.15x10 ⁻⁵ |
| 1680 | 1.36x10 ⁻⁵ | 1.30x10 ⁻⁵ | 1.25x10 ⁻⁵ | 1.19x10 ⁻⁵ | 1.15x10 ⁻⁵ |

| | | | | | |
|------|-----------------------|-----------------------|-----------------------|-----------------------|-----------------------|
| 1740 | 1.38×10^{-5} | 1.32×10^{-5} | 1.26×10^{-5} | 1.20×10^{-5} | 1.15×10^{-5} |
| 1800 | 1.38×10^{-5} | 1.33×10^{-5} | 1.27×10^{-5} | 1.20×10^{-5} | 1.16×10^{-5} |
| 1860 | 1.40×10^{-5} | 1.34×10^{-5} | 1.28×10^{-5} | 1.21×10^{-5} | 1.16×10^{-5} |
| 1920 | 1.41×10^{-5} | 1.35×10^{-5} | 1.29×10^{-5} | 1.21×10^{-5} | 1.17×10^{-5} |
| 1980 | 1.42×10^{-5} | 1.36×10^{-5} | 1.29×10^{-5} | 1.22×10^{-5} | 1.18×10^{-5} |
| 2040 | 1.44×10^{-5} | 1.37×10^{-5} | 1.30×10^{-5} | 1.23×10^{-5} | 1.18×10^{-5} |
| 2100 | 1.45×10^{-5} | 1.38×10^{-5} | 1.31×10^{-5} | 1.23×10^{-5} | 1.18×10^{-5} |
| 2160 | 1.46×10^{-5} | 1.39×10^{-5} | 1.32×10^{-5} | 1.24×10^{-5} | 1.19×10^{-5} |
| 2220 | 1.47×10^{-5} | 1.40×10^{-5} | 1.33×10^{-5} | 1.25×10^{-5} | 1.19×10^{-5} |
| 2280 | 1.48×10^{-5} | 1.41×10^{-5} | 1.34×10^{-5} | 1.26×10^{-5} | 1.20×10^{-5} |
| 2340 | 1.49×10^{-5} | 1.42×10^{-5} | 1.34×10^{-5} | 1.26×10^{-5} | 1.20×10^{-5} |
| 2400 | 1.51×10^{-5} | 1.43×10^{-5} | 1.35×10^{-5} | 1.27×10^{-5} | 1.21×10^{-5} |
| 2460 | 1.52×10^{-5} | 1.44×10^{-5} | 1.36×10^{-5} | 1.27×10^{-5} | 1.21×10^{-5} |
| 2520 | 1.53×10^{-5} | 1.45×10^{-5} | 1.37×10^{-5} | 1.28×10^{-5} | 1.22×10^{-5} |
| 2580 | 1.54×10^{-5} | 1.46×10^{-5} | 1.38×10^{-5} | 1.28×10^{-5} | 1.23×10^{-5} |
| 2640 | 1.55×10^{-5} | 1.47×10^{-5} | 1.38×10^{-5} | 1.30×10^{-5} | 1.23×10^{-5} |
| 2700 | 1.56×10^{-5} | 1.48×10^{-5} | 1.39×10^{-5} | 1.30×10^{-5} | 1.24×10^{-5} |
| 2760 | 1.58×10^{-5} | 1.49×10^{-5} | 1.40×10^{-5} | 1.30×10^{-5} | 1.24×10^{-5} |
| 2820 | 1.59×10^{-5} | 1.50×10^{-5} | 1.41×10^{-5} | 1.31×10^{-5} | 1.24×10^{-5} |
| 2880 | 1.60×10^{-5} | 1.51×10^{-5} | 1.42×10^{-5} | 1.32×10^{-5} | 1.25×10^{-5} |
| 2940 | 1.61×10^{-5} | 1.52×10^{-5} | 1.43×10^{-5} | 1.33×10^{-5} | 1.25×10^{-5} |
| 3000 | 1.62×10^{-5} | 1.53×10^{-5} | 1.43×10^{-5} | 1.33×10^{-5} | 1.25×10^{-5} |
| 3060 | 1.64×10^{-5} | 1.54×10^{-5} | 1.44×10^{-5} | 1.34×10^{-5} | 1.26×10^{-5} |
| 3120 | 1.65×10^{-5} | 1.55×10^{-5} | 1.45×10^{-5} | 1.34×10^{-5} | 1.27×10^{-5} |
| 3180 | 1.66×10^{-5} | 1.56×10^{-5} | 1.45×10^{-5} | 1.35×10^{-5} | 1.27×10^{-5} |
| 3240 | 1.67×10^{-5} | 1.57×10^{-5} | 1.46×10^{-5} | 1.36×10^{-5} | 1.28×10^{-5} |
| 3300 | 1.68×10^{-5} | 1.58×10^{-5} | 1.47×10^{-5} | 1.37×10^{-5} | 1.28×10^{-5} |
| 3360 | 1.69×10^{-5} | 1.59×10^{-5} | 1.48×10^{-5} | 1.37×10^{-5} | 1.29×10^{-5} |
| 3420 | 1.70×10^{-5} | 1.60×10^{-5} | 1.49×10^{-5} | 1.38×10^{-5} | 1.29×10^{-5} |
| 3480 | 1.72×10^{-5} | 1.61×10^{-5} | 1.50×10^{-5} | 1.38×10^{-5} | 1.30×10^{-5} |
| 3540 | 1.73×10^{-5} | 1.62×10^{-5} | 1.51×10^{-5} | 1.39×10^{-5} | 1.30×10^{-5} |
| 3600 | 1.74×10^{-5} | 1.63×10^{-5} | 1.52×10^{-5} | 1.40×10^{-5} | 1.31×10^{-5} |

N-Acetyl-L-histidine Sodium Salt.

| Time (s) | Catalyst Concentration (M) | | | | |
|----------|---|-----------------------|-----------------------|-----------------------|-----------------------|
| | 1.50x10 ⁻³ | 1.25x10 ⁻³ | 1.00x10 ⁻³ | 0.75x10 ⁻³ | 0.50x10 ⁻³ |
| | <i>p</i> -Nitrophenol Concentration (M) | | | | |
| 60 | 1.13x10 ⁻⁵ | 1.05x10 ⁻⁵ | 1.03x10 ⁻⁵ | 1.05x10 ⁻⁵ | 9.67x10 ⁻⁶ |
| 120 | 1.24x10 ⁻⁵ | 1.14x10 ⁻⁵ | 1.10x10 ⁻⁵ | 1.10x10 ⁻⁵ | 9.93x10 ⁻⁶ |
| 180 | 1.34x10 ⁻⁵ | 1.21x10 ⁻⁵ | 1.16x10 ⁻⁵ | 1.14x10 ⁻⁵ | 1.02x10 ⁻⁵ |
| 240 | 1.45x10 ⁻⁵ | 1.29x10 ⁻⁵ | 1.23x10 ⁻⁵ | 1.19x10 ⁻⁵ | 1.05x10 ⁻⁵ |
| 300 | 1.55x10 ⁻⁵ | 1.37x10 ⁻⁵ | 1.29x10 ⁻⁵ | 1.23x10 ⁻⁵ | 1.08x10 ⁻⁵ |
| 360 | 1.65x10 ⁻⁵ | 1.44x10 ⁻⁵ | 1.36x10 ⁻⁵ | 1.27x10 ⁻⁵ | 1.11x10 ⁻⁵ |
| 420 | 1.74x10 ⁻⁵ | 1.52x10 ⁻⁵ | 1.42x10 ⁻⁵ | 1.32x10 ⁻⁵ | 1.13x10 ⁻⁵ |
| 480 | 1.83x10 ⁻⁵ | 1.59x10 ⁻⁵ | 1.48x10 ⁻⁵ | 1.36x10 ⁻⁵ | 1.16x10 ⁻⁵ |
| 540 | 1.93x10 ⁻⁵ | 1.66x10 ⁻⁵ | 1.54x10 ⁻⁵ | 1.40x10 ⁻⁵ | 1.19x10 ⁻⁵ |
| 600 | 2.02x10 ⁻⁵ | 1.73x10 ⁻⁵ | 1.60x10 ⁻⁵ | 1.44x10 ⁻⁵ | 1.21x10 ⁻⁵ |
| 660 | 2.11x10 ⁻⁵ | 1.80x10 ⁻⁵ | 1.66x10 ⁻⁵ | 1.48x10 ⁻⁵ | 1.24x10 ⁻⁵ |
| 720 | 2.20x10 ⁻⁵ | 1.87x10 ⁻⁵ | 1.72x10 ⁻⁵ | 1.52x10 ⁻⁵ | 1.27x10 ⁻⁵ |
| 780 | 2.29x10 ⁻⁵ | 1.94x10 ⁻⁵ | 1.78x10 ⁻⁵ | 1.56x10 ⁻⁵ | 1.29x10 ⁻⁵ |
| 840 | 2.37x10 ⁻⁵ | 2.00x10 ⁻⁵ | 1.84x10 ⁻⁵ | 1.60x10 ⁻⁵ | 1.32x10 ⁻⁵ |
| 900 | 2.46x10 ⁻⁵ | 2.07x10 ⁻⁵ | 1.89x10 ⁻⁵ | 1.64x10 ⁻⁵ | 1.34x10 ⁻⁵ |
| 960 | 2.54x10 ⁻⁵ | 2.13x10 ⁻⁵ | 1.95x10 ⁻⁵ | 1.68x10 ⁻⁵ | 1.37x10 ⁻⁵ |
| 1020 | 2.62x10 ⁻⁵ | 2.20x10 ⁻⁵ | 2.00x10 ⁻⁵ | 1.72x10 ⁻⁵ | 1.39x10 ⁻⁵ |
| 1080 | 2.70x10 ⁻⁵ | 2.26x10 ⁻⁵ | 2.05x10 ⁻⁵ | 1.76x10 ⁻⁵ | 1.41x10 ⁻⁵ |
| 1140 | 2.78x10 ⁻⁵ | 2.32x10 ⁻⁵ | 2.11x10 ⁻⁵ | 1.79x10 ⁻⁵ | 1.44x10 ⁻⁵ |
| 1200 | 2.86x10 ⁻⁵ | 2.38x10 ⁻⁵ | 2.16x10 ⁻⁵ | 1.83x10 ⁻⁵ | 1.46x10 ⁻⁵ |
| 1260 | 2.94x10 ⁻⁵ | 2.44x10 ⁻⁵ | 2.21x10 ⁻⁵ | 1.86x10 ⁻⁵ | 1.49x10 ⁻⁵ |
| 1320 | 3.01x10 ⁻⁵ | 2.50x10 ⁻⁵ | 2.26x10 ⁻⁵ | 1.90x10 ⁻⁵ | 1.51x10 ⁻⁵ |
| 1380 | 3.09x10 ⁻⁵ | 2.56x10 ⁻⁵ | 2.31x10 ⁻⁵ | 1.94x10 ⁻⁵ | 1.53x10 ⁻⁵ |
| 1440 | 3.16x10 ⁻⁵ | 2.62x10 ⁻⁵ | 2.36x10 ⁻⁵ | 1.97x10 ⁻⁵ | 1.55x10 ⁻⁵ |
| 1500 | 3.23x10 ⁻⁵ | 2.67x10 ⁻⁵ | 2.41x10 ⁻⁵ | 2.01x10 ⁻⁵ | 1.58x10 ⁻⁵ |
| 1560 | 3.30x10 ⁻⁵ | 2.73x10 ⁻⁵ | 2.46x10 ⁻⁵ | 2.04x10 ⁻⁵ | 1.60x10 ⁻⁵ |
| 1620 | 3.37x10 ⁻⁵ | 2.78x10 ⁻⁵ | 2.51x10 ⁻⁵ | 2.07x10 ⁻⁵ | 1.62x10 ⁻⁵ |
| 1680 | 3.44x10 ⁻⁵ | 2.83x10 ⁻⁵ | 2.56x10 ⁻⁵ | 2.11x10 ⁻⁵ | 1.64x10 ⁻⁵ |

| | | | | | |
|------|-----------------------|-----------------------|-----------------------|-----------------------|-----------------------|
| 1740 | 3.50×10^{-5} | 2.89×10^{-5} | 2.60×10^{-5} | 2.14×10^{-5} | 1.66×10^{-5} |
| 1800 | 3.57×10^{-5} | 2.94×10^{-5} | 2.65×10^{-5} | 2.17×10^{-5} | 1.69×10^{-5} |
| 1860 | 3.64×10^{-5} | 2.99×10^{-5} | 2.69×10^{-5} | 2.21×10^{-5} | 1.71×10^{-5} |
| 1920 | 3.70×10^{-5} | 3.05×10^{-5} | 2.74×10^{-5} | 2.24×10^{-5} | 1.73×10^{-5} |
| 1980 | 3.77×10^{-5} | 3.10×10^{-5} | 2.78×10^{-5} | 2.27×10^{-5} | 1.75×10^{-5} |
| 2040 | 3.83×10^{-5} | 3.14×10^{-5} | 2.83×10^{-5} | 2.30×10^{-5} | 1.77×10^{-5} |
| 2100 | 3.89×10^{-5} | 3.19×10^{-5} | 2.87×10^{-5} | 2.33×10^{-5} | 1.79×10^{-5} |
| 2160 | 3.94×10^{-5} | 3.24×10^{-5} | 2.91×10^{-5} | 2.36×10^{-5} | 1.81×10^{-5} |
| 2220 | 4.01×10^{-5} | 3.29×10^{-5} | 2.95×10^{-5} | 2.39×10^{-5} | 1.83×10^{-5} |
| 2280 | 4.06×10^{-5} | 3.34×10^{-5} | 3.00×10^{-5} | 2.42×10^{-5} | 1.85×10^{-5} |
| 2340 | 4.12×10^{-5} | 3.38×10^{-5} | 3.04×10^{-5} | 2.45×10^{-5} | 1.87×10^{-5} |
| 2400 | 4.18×10^{-5} | 3.43×10^{-5} | 3.08×10^{-5} | 2.48×10^{-5} | 1.89×10^{-5} |
| 2460 | 4.24×10^{-5} | 3.48×10^{-5} | 3.12×10^{-5} | 2.51×10^{-5} | 1.91×10^{-5} |
| 2520 | 4.29×10^{-5} | 3.52×10^{-5} | 3.16×10^{-5} | 2.54×10^{-5} | 1.93×10^{-5} |
| 2580 | 4.35×10^{-5} | 3.57×10^{-5} | 3.20×10^{-5} | 2.57×10^{-5} | 1.95×10^{-5} |
| 2640 | 4.40×10^{-5} | 3.61×10^{-5} | 3.24×10^{-5} | 2.59×10^{-5} | 1.97×10^{-5} |
| 2700 | 4.46×10^{-5} | 3.65×10^{-5} | 3.28×10^{-5} | 2.62×10^{-5} | 1.99×10^{-5} |
| 2760 | 4.51×10^{-5} | 3.69×10^{-5} | 3.31×10^{-5} | 2.65×10^{-5} | 2.00×10^{-5} |
| 2820 | 4.55×10^{-5} | 3.74×10^{-5} | 3.35×10^{-5} | 2.68×10^{-5} | 2.02×10^{-5} |
| 2880 | 4.61×10^{-5} | 3.78×10^{-5} | 3.38×10^{-5} | 2.70×10^{-5} | 2.04×10^{-5} |
| 2940 | 4.66×10^{-5} | 3.82×10^{-5} | 3.42×10^{-5} | 2.73×10^{-5} | 2.06×10^{-5} |
| 3000 | 4.71×10^{-5} | 3.86×10^{-5} | 3.46×10^{-5} | 2.76×10^{-5} | 2.08×10^{-5} |
| 3060 | 4.76×10^{-5} | 3.90×10^{-5} | 3.49×10^{-5} | 2.78×10^{-5} | 2.10×10^{-5} |
| 3120 | 4.80×10^{-5} | 3.94×10^{-5} | 3.53×10^{-5} | 2.81×10^{-5} | 2.11×10^{-5} |
| 3180 | 4.85×10^{-5} | 3.98×10^{-5} | 3.56×10^{-5} | 2.84×10^{-5} | 2.13×10^{-5} |
| 3240 | 4.90×10^{-5} | 4.02×10^{-5} | 3.60×10^{-5} | 2.86×10^{-5} | 2.15×10^{-5} |
| 3300 | 4.95×10^{-5} | 4.05×10^{-5} | 3.63×10^{-5} | 2.89×10^{-5} | 2.17×10^{-5} |
| 3360 | 5.00×10^{-5} | 4.09×10^{-5} | 3.67×10^{-5} | 2.91×10^{-5} | 2.18×10^{-5} |
| 3420 | 5.03×10^{-5} | 4.12×10^{-5} | 3.70×10^{-5} | 2.94×10^{-5} | 2.20×10^{-5} |
| 3480 | 5.07×10^{-5} | 4.16×10^{-5} | 3.73×10^{-5} | 2.96×10^{-5} | 2.22×10^{-5} |
| 3540 | 5.12×10^{-5} | 4.20×10^{-5} | 3.76×10^{-5} | 2.99×10^{-5} | 2.24×10^{-5} |
| 3600 | 5.16×10^{-5} | 4.24×10^{-5} | 3.79×10^{-5} | 3.01×10^{-5} | 2.25×10^{-5} |

***N*-Acetyl-L-histidine Tetra-*n*-butylammonium Salt.**

| Time (s) | Catalyst Concentration (M) | | | | |
|----------|---|-----------------------|-----------------------|-----------------------|-----------------------|
| | 1.50x10 ⁻³ | 1.25x10 ⁻³ | 1.00x10 ⁻³ | 0.75x10 ⁻³ | 0.50x10 ⁻³ |
| | <i>p</i> -Nitrophenol Concentration (M) | | | | |
| 60 | 1.84x10 ⁻⁶ | 1.75x10 ⁻⁶ | 1.60x10 ⁻⁶ | 1.90x10 ⁻⁶ | 1.53x10 ⁻⁶ |
| 120 | 2.71x10 ⁻⁶ | 2.44x10 ⁻⁶ | 2.10x10 ⁻⁶ | 2.28x10 ⁻⁶ | 1.80x10 ⁻⁶ |
| 180 | 3.54x10 ⁻⁶ | 3.13x10 ⁻⁶ | 2.64x10 ⁻⁶ | 2.68x10 ⁻⁶ | 2.06x10 ⁻⁶ |
| 240 | 4.37x10 ⁻⁶ | 3.83x10 ⁻⁶ | 3.14x10 ⁻⁶ | 3.07x10 ⁻⁶ | 2.32x10 ⁻⁶ |
| 300 | 5.21x10 ⁻⁶ | 4.52x10 ⁻⁶ | 3.64x10 ⁻⁶ | 3.43x10 ⁻⁶ | 2.56x10 ⁻⁶ |
| 360 | 6.03x10 ⁻⁶ | 5.18x10 ⁻⁶ | 4.13x10 ⁻⁶ | 3.80x10 ⁻⁶ | 2.81x10 ⁻⁶ |
| 420 | 6.83x10 ⁻⁶ | 5.83x10 ⁻⁶ | 4.62x10 ⁻⁶ | 4.17x10 ⁻⁶ | 3.06x10 ⁻⁶ |
| 480 | 7.62x10 ⁻⁶ | 6.46x10 ⁻⁶ | 5.12x10 ⁻⁶ | 4.53x10 ⁻⁶ | 3.31x10 ⁻⁶ |
| 540 | 8.38x10 ⁻⁶ | 7.10x10 ⁻⁶ | 5.59x10 ⁻⁶ | 4.89x10 ⁻⁶ | 3.56x10 ⁻⁶ |
| 600 | 9.14x10 ⁻⁶ | 7.72x10 ⁻⁶ | 6.06x10 ⁻⁶ | 5.23x10 ⁻⁶ | 3.81x10 ⁻⁶ |
| 660 | 9.94x10 ⁻⁶ | 8.37x10 ⁻⁶ | 6.54x10 ⁻⁶ | 5.59x10 ⁻⁶ | 4.06x10 ⁻⁶ |
| 720 | 1.07x10 ⁻⁵ | 8.97x10 ⁻⁶ | 7.03x10 ⁻⁶ | 5.93x10 ⁻⁶ | 4.29x10 ⁻⁶ |
| 780 | 1.14x10 ⁻⁵ | 9.55x10 ⁻⁶ | 7.47x10 ⁻⁶ | 6.28x10 ⁻⁶ | 4.51x10 ⁻⁶ |
| 840 | 1.21x10 ⁻⁵ | 1.02x10 ⁻⁵ | 7.91x10 ⁻⁶ | 6.61x10 ⁻⁶ | 4.75x10 ⁻⁶ |
| 900 | 1.28x10 ⁻⁵ | 1.07x10 ⁻⁵ | 8.35x10 ⁻⁶ | 6.93x10 ⁻⁶ | 4.99x10 ⁻⁶ |
| 960 | 1.35x10 ⁻⁵ | 1.13x10 ⁻⁵ | 8.80x10 ⁻⁶ | 7.28x10 ⁻⁶ | 5.21x10 ⁻⁶ |
| 1020 | 1.42x10 ⁻⁵ | 1.18x10 ⁻⁵ | 9.22x10 ⁻⁶ | 7.60x10 ⁻⁶ | 5.43x10 ⁻⁶ |
| 1080 | 1.48x10 ⁻⁵ | 1.24x10 ⁻⁵ | 9.65x10 ⁻⁶ | 7.91x10 ⁻⁶ | 5.65x10 ⁻⁶ |
| 1140 | 1.54x10 ⁻⁵ | 1.29x10 ⁻⁵ | 1.01x10 ⁻⁵ | 8.21x10 ⁻⁶ | 5.87x10 ⁻⁶ |
| 1200 | 1.61x10 ⁻⁵ | 1.34x10 ⁻⁵ | 1.05x10 ⁻⁵ | 8.53x10 ⁻⁶ | 6.08x10 ⁻⁶ |
| 1260 | 1.67x10 ⁻⁵ | 1.40x10 ⁻⁵ | 1.09x10 ⁻⁵ | 8.85x10 ⁻⁶ | 6.31x10 ⁻⁶ |
| 1320 | 1.73x10 ⁻⁵ | 1.45x10 ⁻⁵ | 1.13x10 ⁻⁵ | 9.16x10 ⁻⁶ | 6.51x10 ⁻⁶ |
| 1380 | 1.80x10 ⁻⁵ | 1.50x10 ⁻⁵ | 1.17x10 ⁻⁵ | 9.45x10 ⁻⁶ | 6.72x10 ⁻⁶ |
| 1440 | 1.85x10 ⁻⁵ | 1.55x10 ⁻⁵ | 1.21x10 ⁻⁵ | 9.77x10 ⁻⁶ | 6.92x10 ⁻⁶ |
| 1500 | 1.91x10 ⁻⁵ | 1.60x10 ⁻⁵ | 1.25x10 ⁻⁵ | 1.01x10 ⁻⁵ | 7.13x10 ⁻⁶ |
| 1560 | 1.97x10 ⁻⁵ | 1.65x10 ⁻⁵ | 1.29x10 ⁻⁵ | 1.03x10 ⁻⁵ | 7.33x10 ⁻⁶ |
| 1620 | 2.03x10 ⁻⁵ | 1.70x10 ⁻⁵ | 1.32x10 ⁻⁵ | 1.06x10 ⁻⁵ | 7.53x10 ⁻⁶ |
| 1680 | 2.08x10 ⁻⁵ | 1.74x10 ⁻⁵ | 1.36x10 ⁻⁵ | 1.09x10 ⁻⁵ | 7.73x10 ⁻⁶ |

| | | | | | |
|------|-----------------------|-----------------------|-----------------------|-----------------------|-----------------------|
| 1740 | 2.14×10^{-5} | 1.79×10^{-5} | 1.40×10^{-5} | 1.12×10^{-5} | 7.93×10^{-6} |
| 1800 | 2.19×10^{-5} | 1.84×10^{-5} | 1.43×10^{-5} | 1.15×10^{-5} | 8.12×10^{-6} |
| 1860 | 2.25×10^{-5} | 1.88×10^{-5} | 1.47×10^{-5} | 1.18×10^{-5} | 8.32×10^{-6} |
| 1920 | 2.30×10^{-5} | 1.93×10^{-5} | 1.51×10^{-5} | 1.20×10^{-5} | 8.52×10^{-6} |
| 1980 | 2.35×10^{-5} | 1.97×10^{-5} | 1.54×10^{-5} | 1.23×10^{-5} | 8.72×10^{-6} |
| 2040 | 2.40×10^{-5} | 2.01×10^{-5} | 1.58×10^{-5} | 1.26×10^{-5} | 8.89×10^{-6} |
| 2100 | 2.45×10^{-5} | 2.06×10^{-5} | 1.61×10^{-5} | 1.29×10^{-5} | 9.08×10^{-6} |
| 2160 | 2.50×10^{-5} | 2.10×10^{-5} | 1.64×10^{-5} | 1.31×10^{-5} | 9.26×10^{-6} |
| 2220 | 2.55×10^{-5} | 2.14×10^{-5} | 1.68×10^{-5} | 1.34×10^{-5} | 9.44×10^{-6} |
| 2280 | 2.60×10^{-5} | 2.18×10^{-5} | 1.71×10^{-5} | 1.36×10^{-5} | 9.62×10^{-6} |
| 2340 | 2.65×10^{-5} | 2.22×10^{-5} | 1.74×10^{-5} | 1.39×10^{-5} | 9.80×10^{-6} |
| 2400 | 2.70×10^{-5} | 2.26×10^{-5} | 1.77×10^{-5} | 1.41×10^{-5} | 9.97×10^{-6} |
| 2460 | 2.74×10^{-5} | 2.30×10^{-5} | 1.81×10^{-5} | 1.44×10^{-5} | 1.02×10^{-5} |
| 2520 | 2.79×10^{-5} | 2.34×10^{-5} | 1.84×10^{-5} | 1.46×10^{-5} | 1.03×10^{-5} |
| 2580 | 2.83×10^{-5} | 2.38×10^{-5} | 1.87×10^{-5} | 1.49×10^{-5} | 1.05×10^{-5} |
| 2640 | 2.88×10^{-5} | 2.42×10^{-5} | 1.90×10^{-5} | 1.51×10^{-5} | 1.07×10^{-5} |
| 2700 | 2.92×10^{-5} | 2.46×10^{-5} | 1.93×10^{-5} | 1.53×10^{-5} | 1.08×10^{-5} |
| 2760 | 2.96×10^{-5} | 2.50×10^{-5} | 1.96×10^{-5} | 1.56×10^{-5} | 1.10×10^{-5} |
| 2820 | 3.01×10^{-5} | 2.53×10^{-5} | 1.99×10^{-5} | 1.58×10^{-5} | 1.12×10^{-5} |
| 2880 | 3.05×10^{-5} | 2.57×10^{-5} | 2.02×10^{-5} | 1.61×10^{-5} | 1.13×10^{-5} |
| 2940 | 3.09×10^{-5} | 2.60×10^{-5} | 2.05×10^{-5} | 1.63×10^{-5} | 1.15×10^{-5} |
| 3000 | 3.13×10^{-5} | 2.64×10^{-5} | 2.08×10^{-5} | 1.65×10^{-5} | 1.17×10^{-5} |
| 3060 | 3.17×10^{-5} | 2.67×10^{-5} | 2.11×10^{-5} | 1.67×10^{-5} | 1.18×10^{-5} |
| 3120 | 3.21×10^{-5} | 2.71×10^{-5} | 2.14×10^{-5} | 1.70×10^{-5} | 1.20×10^{-5} |
| 3180 | 3.25×10^{-5} | 2.74×10^{-5} | 2.17×10^{-5} | 1.72×10^{-5} | 1.21×10^{-5} |
| 3240 | 3.29×10^{-5} | 2.78×10^{-5} | 2.20×10^{-5} | 1.74×10^{-5} | 1.23×10^{-5} |
| 3300 | 3.32×10^{-5} | 2.81×10^{-5} | 2.22×10^{-5} | 1.76×10^{-5} | 1.25×10^{-5} |
| 3360 | 3.36×10^{-5} | 2.84×10^{-5} | 2.25×10^{-5} | 1.79×10^{-5} | 1.26×10^{-5} |
| 3420 | 3.40×10^{-5} | 2.88×10^{-5} | 2.28×10^{-5} | 1.81×10^{-5} | 1.28×10^{-5} |
| 3480 | 3.44×10^{-5} | 2.91×10^{-5} | 2.30×10^{-5} | 1.83×10^{-5} | 1.29×10^{-5} |
| 3540 | 3.47×10^{-5} | 2.94×10^{-5} | 2.33×10^{-5} | 1.85×10^{-5} | 1.31×10^{-5} |
| 3600 | 3.51×10^{-5} | 2.97×10^{-5} | 2.36×10^{-5} | 1.87×10^{-5} | 1.32×10^{-5} |

Appendix 3 Hydrolysis of *p*-Nitrophenyl Acetate – MIP's.

Hydrolysis of *p*-Nitrophenyl Acetate in pH 8.0 Buffer Solutions using MIP's as Catalyst.

Vinylimidazole – Imprinted.

| Time (s) | Number of Catalytic Groups (mol) | | | | |
|----------|----------------------------------|-----------------------|-----------------------|-----------------------|-----------------------|
| | 4.50×10^{-5} | 3.75×10^{-5} | 3.00×10^{-5} | 2.25×10^{-5} | 1.50×10^{-5} |
| | Absorbance | | | | |
| 360 | 0.040 | 0.030 | 0.023 | 0.018 | 0.027 |
| 720 | 0.069 | 0.050 | 0.043 | 0.036 | 0.032 |
| 1080 | 0.089 | 0.069 | 0.065 | 0.057 | 0.064 |
| 1440 | 0.109 | 0.098 | 0.084 | 0.072 | 0.069 |
| 1800 | 0.115 | 0.102 | 0.099 | 0.083 | 0.086 |
| 2160 | 0.118 | 0.103 | 0.108 | 0.097 | 0.086 |
| 2520 | 0.119 | 0.123 | 0.121 | 0.103 | 0.105 |
| 2880 | 0.117 | 0.116 | 0.124 | 0.111 | 0.110 |
| 3240 | 0.113 | 0.118 | 0.132 | 0.118 | 0.123 |
| 3600 | 0.116 | 0.115 | 0.125 | 0.114 | 0.115 |

Vinylimidazole – Non-imprinted.

| Time (s) | Number of Catalytic Groups (mol) | | | | |
|----------|----------------------------------|-----------------------|-----------------------|-----------------------|-----------------------|
| | 4.50×10^{-5} | 3.75×10^{-5} | 3.00×10^{-5} | 2.25×10^{-5} | 1.50×10^{-5} |
| | Absorbance | | | | |
| 360 | 0.043 | 0.044 | 0.025 | 0.022 | 0.034 |
| 720 | 0.066 | 0.078 | 0.045 | 0.042 | 0.052 |
| 1080 | 0.067 | 0.081 | 0.078 | 0.065 | 0.076 |
| 1440 | 0.085 | 0.101 | 0.078 | 0.094 | 0.09 |
| 1800 | 0.102 | 0.103 | 0.098 | 0.109 | 0.097 |
| 2160 | 0.111 | 0.103 | 0.116 | 0.129 | 0.112 |
| 2520 | 0.105 | 0.109 | 0.114 | 0.16 | 0.117 |
| 2880 | 0.111 | 0.115 | 0.114 | 0.128 | 0.128 |
| 3240 | 0.116 | 0.112 | 0.117 | 0.136 | 0.133 |
| 3600 | 0.110 | 0.112 | 0.112 | 0.148 | 0.125 |

N-Methacryloyl-L-histidine – Imprinted

| Time (s) | Number of Catalytic Groups (mol) | | | | |
|----------|----------------------------------|-----------------------|-----------------------|-----------------------|-----------------------|
| | 4.50×10^{-5} | 3.75×10^{-5} | 3.00×10^{-5} | 2.25×10^{-5} | 1.50×10^{-5} |
| | Absorbance | | | | |
| 360 | 0.047 | 0.058 | 0.055 | 0.06 | 0.046 |
| 720 | 0.056 | 0.059 | 0.069 | 0.075 | 0.056 |
| 1080 | 0.079 | 0.085 | 0.083 | 0.088 | 0.075 |
| 1440 | 0.098 | 0.101 | 0.095 | 0.098 | 0.082 |
| 1800 | 0.107 | 0.122 | 0.111 | 0.110 | 0.097 |
| 2160 | 0.098 | 0.117 | 0.113 | 0.112 | 0.111 |
| 2520 | 0.146 | 0.112 | 0.11 | 0.121 | 0.116 |
| 2880 | 0.119 | 0.125 | 0.129 | 0.123 | 0.120 |
| 3240 | 0.102 | 0.098 | 0.147 | 0.127 | 0.131 |
| 3600 | 0.094 | 0.104 | 0.141 | 0.145 | 0.136 |

N-Methacryloyl-L-histidine – Non-imprinted

| Time (s) | Number of Catalytic Groups (mol) | | | | |
|----------|----------------------------------|-----------------------|-----------------------|-----------------------|-----------------------|
| | 4.50×10^{-5} | 3.75×10^{-5} | 3.00×10^{-5} | 2.25×10^{-5} | 1.50×10^{-5} |
| | Absorbance | | | | |
| 360 | 0.028 | 0.020 | 0.015 | 0.028 | 0.017 |
| 720 | 0.039 | 0.024 | 0.022 | 0.042 | 0.036 |
| 1080 | 0.048 | 0.038 | 0.041 | 0.042 | 0.052 |
| 1440 | 0.057 | 0.042 | 0.053 | 0.048 | 0.048 |
| 1800 | 0.062 | 0.032 | 0.035 | 0.069 | 0.052 |
| 2160 | 0.088 | 0.055 | 0.045 | 0.065 | 0.064 |
| 2520 | 0.05 | 0.057 | 0.063 | 0.073 | 0.072 |
| 2880 | 0.055 | 0.054 | 0.065 | 0.073 | 0.077 |
| 3240 | 0.106 | 0.053 | 0.052 | 0.105 | 0.081 |
| 3600 | 0.051 | 0.054 | 0.065 | 0.084 | 0.099 |

Hydrolysis of *p*-Nitrophenyl Acetate in DMSO/H₂O 9:1 v/v Solution using MIP's as Catalyst.**4(5)-vinylimidazole – Imprinted.**

| Time (s) | Number of Catalytic Groups (mol) | | | | |
|----------|----------------------------------|-----------------------|-----------------------|-----------------------|-----------------------|
| | 4.50×10^{-5} | 3.75×10^{-5} | 3.00×10^{-5} | 2.25×10^{-5} | 1.50×10^{-5} |
| | Absorbance | | | | |
| 360 | 0.010 | 0.014 | 0.017 | 0.007 | 0.003 |
| 720 | 0.019 | 0.025 | 0.017 | 0.008 | 0.000 |
| 1080 | 0.027 | 0.030 | 0.023 | 0.008 | 0.002 |
| 1440 | 0.038 | 0.030 | 0.028 | 0.016 | 0.010 |
| 1800 | 0.040 | 0.026 | 0.032 | 0.022 | 0.009 |
| 2160 | 0.047 | 0.043 | 0.036 | 0.016 | 0.010 |
| 2520 | 0.047 | 0.047 | 0.038 | 0.020 | 0.017 |
| 2880 | 0.060 | 0.056 | 0.040 | 0.031 | 0.015 |
| 3240 | 0.059 | 0.068 | 0.042 | 0.014 | 0.018 |
| 3600 | 0.077 | 0.074 | 0.045 | 0.032 | 0.021 |

4(5)-vinylimidazole – Non-imprinted.

| Time (s) | Number of Catalytic Groups (mol) | | | | |
|----------|----------------------------------|-----------------------|-----------------------|-----------------------|-----------------------|
| | 4.50×10^{-5} | 3.75×10^{-5} | 3.00×10^{-5} | 2.25×10^{-5} | 1.50×10^{-5} |
| | Absorbance | | | | |
| 360 | 0.012 | 0.008 | 0.009 | 0.006 | 0.000 |
| 720 | 0.013 | 0.014 | 0.005 | 0.005 | 0.000 |
| 1080 | 0.020 | 0.022 | 0.011 | 0.009 | 0.005 |
| 1440 | 0.020 | 0.024 | 0.013 | 0.010 | 0.011 |
| 1800 | 0.030 | 0.028 | 0.018 | 0.009 | 0.004 |
| 2160 | 0.035 | 0.028 | 0.020 | 0.021 | 0.002 |
| 2520 | 0.035 | 0.03 | 0.020 | 0.019 | 0.001 |
| 2880 | 0.042 | 0.041 | 0.025 | 0.020 | 0.014 |
| 3240 | 0.046 | 0.047 | 0.024 | 0.021 | 0.018 |
| 3600 | 0.051 | 0.045 | 0.025 | 0.023 | 0.013 |

N-Methacryloyl-L-histidine – Imprinted.

| Time (s) | Number of Catalytic Groups (mol) | | | | |
|----------|----------------------------------|-----------------------|-----------------------|-----------------------|-----------------------|
| | 4.50×10^{-5} | 3.75×10^{-5} | 3.00×10^{-5} | 2.25×10^{-5} | 1.50×10^{-5} |
| | Absorbance | | | | |
| 360 | 0.013 | 0.009 | 0.011 | 0.013 | 0.005 |
| 720 | 0.016 | 0.014 | 0.014 | 0.016 | 0.008 |
| 1080 | 0.024 | 0.017 | 0.017 | 0.022 | 0.010 |
| 1440 | 0.021 | 0.020 | 0.023 | 0.030 | 0.012 |
| 1800 | 0.036 | 0.023 | 0.026 | 0.025 | 0.014 |
| 2160 | 0.028 | 0.024 | 0.029 | 0.023 | 0.016 |
| 2520 | 0.034 | 0.033 | 0.03 | 0.028 | 0.018 |
| 2880 | 0.038 | 0.035 | 0.032 | 0.030 | 0.020 |
| 3240 | 0.043 | 0.037 | 0.036 | 0.033 | 0.023 |
| 3600 | 0.048 | 0.041 | 0.039 | 0.039 | 0.024 |

***N*-Methacryloyl-L-histidine – Non-imprinted. Treated with Sodium Hydroxide.**

| Time (s) | Number of Catalytic Groups (mol) | | | | |
|----------|----------------------------------|-----------------------|-----------------------|-----------------------|-----------------------|
| | 4.50×10^{-5} | 3.75×10^{-5} | 3.00×10^{-5} | 2.25×10^{-5} | 1.50×10^{-5} |
| | Absorbance | | | | |
| 360 | 0.010 | 0.007 | 0.011 | 0.011 | 0.004 |
| 720 | 0.014 | 0.009 | 0.012 | 0.016 | 0.004 |
| 1080 | 0.017 | 0.012 | 0.013 | 0.017 | 0.006 |
| 1440 | 0.023 | 0.014 | 0.017 | 0.018 | 0.008 |
| 1800 | 0.027 | 0.019 | 0.016 | 0.015 | 0.011 |
| 2160 | 0.033 | 0.022 | 0.020 | 0.019 | 0.008 |
| 2520 | 0.037 | 0.022 | 0.022 | 0.019 | 0.010 |
| 2880 | 0.039 | 0.019 | 0.023 | 0.03 | 0.015 |
| 3240 | 0.041 | 0.027 | 0.028 | 0.023 | 0.014 |
| 3600 | 0.046 | 0.028 | 0.031 | 0.027 | 0.014 |

***N*-Methacryloyl-L-histidine – Imprinted – Treated with Sodium Hydroxide.**

| Time (s) | Number of Catalytic Groups (mol) | | | | |
|----------|----------------------------------|-----------------------|-----------------------|-----------------------|-----------------------|
| | 4.50×10^{-5} | 3.75×10^{-5} | 3.00×10^{-5} | 2.25×10^{-5} | 1.50×10^{-5} |
| | Absorbance | | | | |
| 360 | 0.006 | 0.006 | 0.006 | 0.006 | 0.006 |
| 720 | 0.007 | 0.006 | 0.010 | 0.008 | 0.006 |
| 1080 | 0.006 | 0.007 | 0.005 | 0.010 | 0.009 |
| 1440 | 0.007 | 0.012 | 0.013 | 0.008 | 0.008 |
| 1800 | 0.012 | 0.012 | 0.011 | 0.009 | 0.007 |
| 2160 | 0.013 | 0.015 | 0.007 | 0.009 | 0.008 |
| 2520 | 0.012 | 0.013 | 0.012 | 0.014 | 0.009 |
| 2880 | 0.016 | 0.018 | 0.015 | 0.012 | 0.008 |
| 3240 | 0.019 | 0.014 | 0.013 | 0.014 | 0.009 |
| 3600 | 0.018 | 0.013 | 0.018 | 0.014 | 0.009 |

***N*-Methacryloyl-L-histidine– Non-imprinted – Treated with Sodium Hydroxide.**

| Time (s) | Number of Catalytic Groups (mol) | | | | |
|----------|----------------------------------|-----------------------|-----------------------|-----------------------|-----------------------|
| | 4.50×10^{-5} | 3.75×10^{-5} | 3.00×10^{-5} | 2.25×10^{-5} | 1.50×10^{-5} |
| | Absorbance | | | | |
| 360 | 0.003 | 0.008 | 0.017 | 0.000 | 0.008 |
| 720 | 0.006 | 0.017 | 0.011 | 0.001 | 0.003 |
| 1080 | 0.016 | 0.018 | 0.019 | 0.003 | 0.010 |
| 1440 | 0.015 | 0.022 | 0.018 | 0.002 | 0.011 |
| 1800 | 0.019 | 0.022 | 0.023 | 0.004 | 0.011 |
| 2160 | 0.019 | 0.023 | 0.029 | 0.006 | 0.011 |
| 2520 | 0.044 | 0.030 | 0.031 | 0.011 | 0.011 |
| 2880 | 0.034 | 0.027 | 0.023 | 0.015 | 0.013 |
| 3240 | 0.036 | 0.033 | 0.033 | 0.012 | 0.012 |
| 3600 | 0.042 | 0.027 | 0.026 | 0.011 | 0.016 |

***N*-Methacryloyl-L-histidine – Imprinted – Treated with Tetra-*n*-butylammonium Hydroxide.**

| Time (s) | Number of Catalytic Groups (mol) | | | | |
|----------|----------------------------------|-----------------------|-----------------------|-----------------------|-----------------------|
| | 4.50×10^{-5} | 3.75×10^{-5} | 3.00×10^{-5} | 2.25×10^{-5} | 1.50×10^{-5} |
| | Absorbance | | | | |
| 360 | 0.006 | 0.007 | 0.007 | 0.010 | 0.006 |
| 720 | 0.010 | 0.009 | 0.012 | 0.004 | 0.007 |
| 1080 | 0.014 | 0.008 | 0.009 | 0.006 | 0.008 |
| 1440 | 0.018 | 0.010 | 0.010 | 0.009 | 0.014 |
| 1800 | 0.024 | 0.012 | 0.014 | 0.012 | 0.008 |
| 2160 | 0.023 | 0.015 | 0.017 | 0.013 | 0.010 |
| 2520 | 0.020 | 0.018 | 0.018 | 0.010 | 0.011 |
| 2880 | 0.026 | 0.019 | 0.019 | 0.017 | 0.013 |
| 3240 | 0.024 | 0.017 | 0.021 | 0.020 | 0.016 |
| 3600 | 0.030 | 0.020 | 0.023 | 0.022 | 0.015 |

***N*-Methacryloyl-L-histidine– Non-imprinted - Treated with Tetra-*n*-butylammonium Hydroxide.**

| Time (s) | Number of Catalytic Groups (mol) | | | | |
|----------|----------------------------------|-----------------------|-----------------------|-----------------------|-----------------------|
| | 4.50×10^{-5} | 3.75×10^{-5} | 3.00×10^{-5} | 2.25×10^{-5} | 1.50×10^{-5} |
| | Absorbance | | | | |
| 360 | 0.015 | 0.011 | 0.005 | 0.003 | 0.006 |
| 720 | 0.019 | 0.010 | 0.008 | 0.013 | 0.013 |
| 1080 | 0.022 | 0.013 | 0.013 | 0.015 | 0.014 |
| 1440 | 0.031 | 0.018 | 0.014 | 0.016 | 0.018 |
| 1800 | 0.032 | 0.02 | 0.017 | 0.020 | 0.014 |
| 2160 | 0.035 | 0.027 | 0.021 | 0.020 | 0.016 |
| 2520 | 0.043 | 0.029 | 0.024 | 0.020 | 0.017 |
| 2880 | 0.042 | 0.037 | 0.029 | 0.024 | 0.019 |
| 3240 | 0.057 | 0.037 | 0.036 | 0.035 | 0.021 |
| 3600 | 0.060 | 0.047 | 0.038 | 0.036 | 0.022 |

Appendix 4 The oxy-Cope Rearrangement.

Catalysis of the Oxy-Cope Rearrangement.

| Time (mins) | Catalyst | | | |
|-------------|-------------------|---------------|-------------|-------------|
| | No catalyst | Non-imprinted | Imprinted 1 | Imprinted 2 |
| | % of product peak | | | |
| 60 | - | - | - | - |
| 120 | 7.2 | - | 8.7 | 7.4 |
| 180 | 9.3 | 8.8 | 10.8 | 9.2 |
| 240 | 11.1 | 11.6 | 12.5 | 11.8 |
| 300 | 12.1 | 14.0 | 14.1 | 13.3 |
| 360 | 13.6 | 16.1 | 15.6 | 15.2 |
| 420 | 15.6 | 18.7 | 17.0 | 16.8 |
| 480 | 17.3 | 20.3 | 18.1 | 19.0 |

References.

Perspective. Acc. Chem. Res.

- 1 F.M. Menger, Enzyme Reactivity from an Organic Perspective, *Acc. Chem. Res.*, 1993, **26**, 206-212.
- 2 C.J. Sih, E. Abushanab and J.B. Jones, Biochemical Procedures in Organic Synthesis, *Ann. Rep. Med. Chem.*, 1977, **12**, 298-308.
- 3 H.M. Sweers and C-H. Wong, Enzyme-Catalysed Regioselective Deacylation of Protected Sugars in Carbohydrate Synthesis, *J. Am. Chem. Soc.*, 1986, **108**, 6421-6422.
- 4 *Enzyme Reactions in Organic Media*, Eds., A.M.P. Koskinen and A.M. Klibanov, Blackie Academic & Professional, London, 1996.
- 5 E. Fischer, Einfluss der Configuration auf die Wirkung der Enzyme, *Ber. Dtsch. Chem. Ges.*, 1894, **27**, 2985-2993.
- 6 D.E. Koshland, Jr and K.E. Neet, The Catalytic and Regulatory Properties of Enzymes, *Ann. Rev. Biochem.*, 1968, **37**, 359-405.
- 7 H.E Avery, *Basic Reaction Kinetics and Mechanisms*, The Macmillan Press Ltd, London, 1974, 127.
- 8 K. Faber, *Biotransformations in Organic Chemistry*, Springer, London, 1995, 18.
- 9 A. Fersht, *Enzyme Structure and Mechanism*, W.H. Freeman and Company, Reading, 1977, 18.
- 10 D.M. Blow, J.J. Birktoft and B.S. Hartley, Role of a Buried Acid Group in the Mechanism of Action of Chymotrypsin, *Nature*, 1969, **221**, 337-340.

- 11 M.W. Hunkapiller, S.H. Smallcombe, D.R. Whitaker and J.H. Richards, Carbon Nuclear Magnetic Resonance Studies of the Histidine Residue in α -Lytic Protease. Implications for the Catalytic Mechanism of Serine Proteases, *Biochemistry*, 1973, **12**, 4732-4743.
- 12 W.W. Bachovchin and J.D. Roberts, Nitrogen-15 Nuclear Magnetic Resonance Spectroscopy. The State of Histidine in the Catalytic Triad of α -Lytic Protease. Implications for the Charge-Relay Mechanism of Peptide-Bond Cleavage by Serine Proteases, *J. Am. Chem. Soc.*, 1978, **100**, 8041-8047.
- 13 P.A. Frey, S.A. Whitt and J.B. Tobin, A Low-Barrier Hydrogen Bond in the Catalytic Triad of Serine Proteases, *Science*, 1994, **264**, 1927-1930.
- 14 C.L. Perrin and J.B. Nielson, Asymmetry of Hydrogen Bonds in Solutions of Monoanions of Dicarboxylic Acids, *J. Am. Chem. Soc.*, 1997, **119**, 12734-12741.
- 15 A. Warshel, A. Papazyan and P.A. Kollman, On Low-Barrier Hydrogen Bonds and Enzyme Catalysis, *Science*, 1995, **269**, 102-103.
- 16 C.D. Hubbard and T.S. Shoupe, Mechanisms of Acylation of Chymotrypsin by Phenyl Esters of Benzoic Acid and Acetic Acid, *J. Biol. Chem.*, 1977, **252**, 1633-1638.
- 17 D.M. Quinn, J.P. Elrod, R. Ardis, P. Friesen and R.L. Schowen, Protonic Reorganisation in Catalysis by Serine Proteases: Acylation by Small Substrates, *J. Am. Chem. Soc.*, 1980, **102**, 5358-5365.
- 18 D.W. Christianson and R.S. Alexander, Carboxylate-Histidine-Zinc Interactions in Protein Structure and Function, *J. Am. Chem. Soc.*, 1989, **111**, 6412-6419.
- 19 P.A. Karplus, E.F. Pai and G.E. Schulz, A Crystallographic Study of the Glutathione Binding Site of Glutathione Reductase at 0.3-nm Resolution, *Eur. J. Biochem.*, 1989, **178**, 693-703.

- 20 B.W. Dijkstra, J. Drenth and K.H. Kalk, Active Site and Catalytic Mechanism of Phospholipase A₂, *Nature*, 1981, **289**, 604-606.
- 21 J.J. Birkofit and L.J. Banaszak, The Presence of a Histidine-Aspartic Acid Pair in the Active Site of 2-Hydroxyacid Dehydrogenases, *J. Biol.Chem.*, 1983, **258**, 472-482.
- 22 D. Suck, A. Lahm and C. Oefner, Structure Refined to 2Å of a Nicked DNA Octanucleotide Complex with Dnase I, *Nature*, 1988, **332**, 464-468.
- 23 J. Kraut, Serine Proteases: Structure and Mechanism of Catalysis, *Ann. Rev. Biochem.*, 1977, **46**, 331-358.
- 24 T.A. Steitz and R.G. Shulman, Crystallographic and NMR-Studies of the Serine Proteases, *Ann. Rev. Biophys. Bioeng.*, 1982, **11**, 419-444.
- 25 G.A. Rogers and T.C. Bruice, Synthesis and Evaluation of a Model for the So-Called "Charge-Relay" System of the Serine Esterases, *J. Am. Chem. Soc.*, 1974, **96**, 2473-2481.
- 26 K. I. Skorey, V. Somayaji, and R. S. Brown, Direct O-Acylation of Small Molecules Containing CO₂⁻---HN – HO Units by a Distorted Amide: Enhancement of Amine Basicity by a Pendant Carboxylate in a Serine Protease Mimic, *J. Am. Chem. Soc.* 1989, **111**, 1445-1452.
- 27 S.C. Zimmerman, J.S. Korthals, and K.D. Cramer, Syn and Anti-Oriented Imidazole Carboxylates as models for the Histidine-Aspartate Couple in Serine Proteases and Other Enzymes, *Tetrahedron*, 1991, **47**, 2649-2660.
- 28 R.C. Van Etten, J.F. Sebastien, G.A. Clowes and M.L. Bender, Acceleration of Phenyl Ester Cleavage by Cycloamyloses. A Model for Enzymatic Specificity, *J. Am. Chem. Soc.*, 1967, **69**, 3242-3253.

- 29 V.T. D'Souza, K. Hanabusa, T. O'Leary, R.C. Gadwood and M.L. Bender, Synthesis and Evaluation of a Miniature Organic Model of Chymotrypsin, *Biochem. Biophys. Res. Commun.*, 1985, **129**, 727-732.
- 30 C.G. Overberger, J.C. Salamone and S. Yaroslasky, Cooperative Effects in the Esterolytic Action of Synthetic Macromolecules Containing Imidazole and Hydroxyl Functions, *J. Am. Chem. Soc.*, 1967, **89**, 6231-6236.
- 31 T. Kunitake and Y. Okahata, Multifunctional Hydrolytic Catalyses. 7. Cooperative Catalysis of the Hydrolysis of Phenyl Esters by a Copolymer of N-Methylacrylohydroxamic Acid and 4-Vinylimidazole, *J. Am. Chem. Soc.*, 1976, **98**, 7793-7799.
- 32 A.N. Sarwal, E.O. Adigun, R.A. Stephani and A. Kapoor, Synthesis and Catalytic Activity of Poly-L-Histidyl-L-Aspartyl-L-Seryl-Glycine, *Journal of Pharmaceutical Sciences*, 1982, **71**, 1380-1383.
- 33 K.W. Hahn, W.A. Klis and J.M. Stewart, Design and Synthesis of a Peptide Having Chymotrypsin-Like Esterase Activity, *Science*, 1990, **248**, 1544-1547.
- 34 Y.N. Belokon, V.I. Tararov, T.F. Savel'eva, O.L. Lependina, G.I. Timofeyeva and V.M. Belikov, Biomimetic Approach to the Design of a Pyridoxal Enzyme Model, 2, Cyclopolymerisation as a New Method of Constructing Polymers with Defined Arrangement of Functional Groups in the Chain, *Makromol. Chem.*, 1982, **183**, 1921-1934.
- 35 G. Wulff, Molecular Imprinting in Cross-Linked Materials with the Aid of Molecular Templates – A Way Towards Artificial Antibodies, *Angew. Chem. Int. Ed. Engl.*, 1995, **34**, 1812-1832.
- 36 G. Wulff, W. Vesper, R. Grobe-Einsler and A. Sarhan, Enzyme-Analogue Built Polymers, 5: On the Specificity Distribution of Chiral Cavities Prepared in Synthetic Polymers, *Makromol. Chem.*, 1977, **178**, 2817-2825.

- 37 G. Wulff and M. Minarik, Template Imprinted Polymers for HPLC Separation of Racemates, *J. Liq. Chromatogr.*, 1990, **13**, 2987-3000.
- 38 B. Sellergren, M. Lepistö, and K. Mosbach, Highly Enantioselective and Substrate-Selective Polymers Obtained by Molecular Imprinting Utilising Noncovalent Interactions. NMR and Chromatographic Studies on the Nature of Recognition, *J. Am. Chem. Soc.*, 1988, **110**, 5853-5860.
- 39 G. Wulff, I. Schulze, K. Zabrocki and W. Vesper, Über enzymanalog gebaute Polymere, 11: Bindungsstellen im Polymer mit unterschiedlicher Zahl der Haftgruppen, *Makromol.Chem.*, 1980, **181**, 531-544.
- 40 A. Sarhan and M.A. El-Zahab, Racemic Resolution of Mandelic Acid on Polymers with Chiral Cavities, 2: Enzyme-Analogue Stereospecific Conversion of Configuration, *Makromol. Chem., Rapid Commun.*, 1987, **8**, 555-561.
- 41 O. Ramström, I.A. Nicholls and K. Mosbach, Synthetic Peptide Receptor Mimics: Highly Stereoselective Recognition in Non-covalent Molecularly Imprinted Polymers, *Tetrahedron: Asymmetry*, 1994, **5**, 649-656.
- 42 S. Mallik, S.D. Plunkett, P.K. Dhal, R.D. Johnson, D. Pack, D. Schnek and F.H. Arnold, Towards Materials for the Specific Recognition and Separation of Proteins, *New. J. Chem.*, 1994, **18**, 299-304.
- 43 D.R. Schnek, D.W. Pack, D.Y. Sasaki and F.H. Arnold, Specific Protein Attachment to Artificial Membranes Via Coordination to Lipid-Bound Copper(II), *Langmuir*, 1994, **10**, 2382-2388.
- 44 K.J. Shea, D.A. Spivak and B. Sellergren, Polymer Complements to Nucleotide Bases. Selective Binding of Adenine Derivatives to Imprinted Polymers, *J. Am. Chem. Soc.*, 1993, **115**, 3368-3369.

- 45 H. Bünemann, N. Dattagupta, H.J. Schuetz and W. Müller, Synthesis and Properties of Acrylamide-Substituted Base Pair Specific Dyes for Deoxyribonucleic Acid Template Mediated Synthesis of Dye Polymers, *Biochemistry*, 1981, **20**, 2864-2874.
- 46 G. Vlatakis, L.I. Andersson, R. Müller and K. Mosbach, Drug Assay using Antibody Mimics made by Molecular Imprinting, *Nature*, 1993, **361**, 645-647.
- 47 S.E. Byström, A. Börje and B. Akermark, Selective Reduction of Steroid 3- and 17-Ketones Using LiAlH_4 Activated Template Polymers, *J. Am. Chem. Soc.*, 1993, **115**, 2081-2083.
- 48 M.J. Whitcombe, M.E. Rodriguez, P. Villar and E.N. Vulfson, A New Method for the Introduction of Recognition Site Functionality into Polymers Prepared by Molecular Imprinting: Synthesis and Characterisation of Polymeric Receptors for Cholesterol, *J. Am. Chem. Soc.*, 1995, **117**, 7105-7111.
- 49 M. Lepistö and B. Sellergren, Discrimination between Amino Acid Amide Conformers by Imprinted Polymers, *J. Org. Chem.*, 1989, **54**, 6010-6012.
- 50 L. Fischer, R. Müller, B. Ekberg and K. Mosbach, Direct Enantioseparation of β -Adrenergic Blockers Using a Chiral Stationary Phase Prepared by Molecular Imprinting, *J. Am. Chem. Soc.*, 1991, **113**, 9358-9360.
- 51 M. Kempe and K. Mosbach, Separation of Amino Acids, Peptides and Proteins on Molecularly Imprinted Stationary Phases, *J. Chromatogr.*, 1995, **691**, 317-323.
- 52 G. Wulff, B. Heide and G. Helfmeier, Molecular Recognition through the Exact Placement of Functional Groups on Rigid Matrices via a Template Approach, *J. Am. Chem. Soc.*, 1986, **108**, 1089-1091.
- 53 K.J. Shea and D.Y. Sasaki, An Analysis of Small-Molecule Binding to Functionalised Synthetic Polymers by ^{13}C CP/MAS NMR and FTIR Spectroscopy, *J. Am. Chem. Soc.*, 1991, **113**, 4109-4120.

- 54 G. Wulff and I. Schulze, Directed Cooperativity and Site Separation of Mercapto Groups in Synthetic Polymers, *Angew. Chem. Int. Ed. Engl.*, 1978, **17**, 537-538.
- 55 R. Arshady and K. Mosbach, Synthesis of Substrate-selective Polymers by Host-Guest Polymerisation, *Makromol. Chem. Rapid Commun.*, 1981, **182**, 687-692.
- 56 I.R. Dunkin, J. Lenfeld and D.C. Sherrington, Molecular Imprinting of Flat Polycondensed Aromatic Molecules in Macroporous Polymers, *Polymer*, 1993, **34**, 77-84.
- 57 P.K. Dhal and F. H. Arnold, Template-Mediated Synthesis of Metal-Complexing Polymers for Molecular Recognition, *J. Am. Chem. Soc.*, 1991 **113**, 7417-7418.
- 58 P.K. Dhal and F.H. Arnold, Metal-Coordination Interactions in the Template-Mediated Synthesis of Substrate-Selective Polymers: Recognition of Bis(imidazole) Substrates by Copper(II) Iminodiacetate Containing Polymers, *Macromolecules*, 1992, **25**, 7051-7059.
- 59 K. Ohkubo, Y. Urata, S. Hirota, Y. Honda and T. Sagawa, Homogeneous and Heterogeneous Esterolytic Catalyses of Imidazole-Containing Polymers Prepared by Molecular Imprinting of a Transition State Analog, *J. Mol. Catal.*, 1994, **87**, L21-L24.
- 60 K. Ohkubo, Y. Urata, S. Hirota, Y. Honda, Y. Fujishita and T. Sagawa, Homogeneous Esterolytic Catalysis of a Polymer Prepared by Molecular Imprinting of a Transition State Analog, *J. Mol. Catal.*, 1994, **93**, 189-193.
- 61 K.J. Shea and E.A. Thompson, Template Synthesis of Macromolecules. Selective Functionalisation of an Organic Polymer, *J. Org. Chem.*, 1978, **43**, 4253-4255.
- 62 L.I. Andersson and K. Mosbach, Molecular Imprinting of the Coenzyme-Substrate Analogue N-Pyridoxyl-L-phenylalaninamide, *Makromol. Chem., Rapid Commun.*, 1989, **10**, 491-495.

- 63 K. Haupt and K. Mosbach, Molecularly Imprinted Polymers and Their use in Biomimetic Sensors, *Chem. Rev.*, 2000, **100**, 2495-2504. *Sensors, Sens. Actuators B*.
- 64 F.L. Dickert, P. Forth, P. Lieberzeit and M. Tortschanoff, Molecular Imprinting in Chemical Sensing – Detection of Aromatic and Halogenated Hydrocarbons as well as Polar Solvent Vapors, *Fresenius' J. Anal. Chem.*, 1998, **360**, 759.
- 65 F.L. Dickert, M. Tortschanoff, W.E. Bulst and G. Fiscerauer, Molecularly Imprinted Sensor Layers for the Detection of Polycyclic Aromatic Hydrocarbons, *Anal. Chem.*, 1999, **71**, 4559-4563.
- 66 B. Jakoby, G.M. Ismail, M.P. Byfield and M.J. Vellekoop, A Novel Molecularly Imprinted Thin Film Applied to a Love Wave Gas Sensor, *Sens. Actuators A*, 1999, **76**, 93-97.
- 67 F.L. Dickert and S. Thierer, Molecularly Imprinted Polymers for Optochemical Sensors, *Adv. Mater.*, 1996, **8**, 987-990.
- 68 K. Haupt, K. Noworyta and W. Kutner, Imprinted Polymer-based Enantioselective Acoustic Sensor using Quartz Crystal Microbalance, *Anal. Commun.*, 1999, **36**, 391-393.
- 69 C. Malitesta, I. Losito and P.G. Zambonin, Molecularly Imprinted Electrosynthesised Polymers: New Materials for Biomimetic Sensors, *Anal. Chem.*, 1999, **71**, 1366-1370.
- 70 H.S. Ji, S. McNiven, K. Ikebukuro and I. Karube, Selective Piezoelectric Odor Sensors using Molecularly Imprinted Polymers, *Anal. Chim. Acta*, 1999, **390**, 93-100.
- 71 S.A. Piletsky, E.V. Piletskaya, A.V. Elgersma, K. Yano and I. Karube, Atrazine Sensing by Molecularly Imprinted Membranes, *Biosens. Bioelectron.*, 1995, **10**, 959-964.

- 72 D. Kriz, M. Kempe and K. Mosbach, Introduction of Molecularly Imprinted Polymers as Recognition Elements in Conductometric Chemical Sensors, *Sens. Actuators B*, 1996, **33**, 178-181.
- 73 S.A. Piletsky, E.V. Piletskaya, T.L. Panasyuk, A.V. El'skaya, R. Levi, I. Karube and G. Wulff, Imprinted Membranes for Sensor Technology: Opposite Behavior of Covalently and Noncovalently Imprinted Membranes, *Macromolecules*, 1998, **31**, 2137-2140.
- 74 T.A. Sergeyeva, S.A. Piletsky, A.A. Brovko, E.A. Slinchenko, L.M. Sergeeva, T.L. Panasyuk and A.V. El'skaya, Conductimetric Sensor for Atrazine Detection based on Molecularly Imprinted Polymer Membranes, *Analyst*, 1999, **124**, 331-334.
- 75 S.A. Piletsky, Y.P. Parhometz, N.V. Lavryk, T.L. Panasyuk and A.V. Elskaya, Sensors for Low Weight Organic-Molecules Based on Molecular Imprinting Technique, *Sens. Actuators B*, 1994, **18-19**, 629-631.
- 76 S.A. Piletsky, E.V. Piletskaya, K. Yano, A. Kugimaya, A.V. Elgersma, R. Levi, U. Kahlow, T. Takeuchi, I. Karube, T.J. Panasyuk and A.V. Elskaya, A Biomimetic Receptor System for Sialic Acid Based on Molecular Imprinting, *Anal. Lett.*, 1996, **29**, 157-170.
- 77 D. Kriz, O. Ramstrom, A. Svensson and K. Mosbach, Introducing Biomimetic Sensors based on Molecularly Imprinted Polymers as Recognition Elements, *Anal. Chem.*, 1995, **67**, 2142-2144.
- 78 K. Haupt, A.G. Mayes and K. Mosbach, Herbicide Assay using an Imprinted Polymer based System Analogous to Competitive Fluoroimmunoassays, *Anal. Chem.*, 1998, **70**, 3936-3939.
- 79 K. Haupt, Molecularly Imprinted Sorbent Assays and the use of Non-related Probes, *React. Funct. Polym.*, 1999, **41**, 125-131.

- 80 S.A. Piletsky, E. Terpetschnik, H.S. Andersson, I.A. Nicholls and O.S. Wolfbeis, Application of Non-specific Fluorescent Dyes for Monitoring Enantioselective Ligand Binding to Molecularly Imprinted Polymers, *Fresenius' J. Anal. Chem.*, 1999, **364**, 512-516.
- 81 R. Levi, S. McNiven, S.A. Piletsky, S.H. Cheong, K. Yano and I. Karube, Optical Detection of Chloramphenicol using Molecularly Imprinted Polymers, *Anal. Chem.*, 1997, **69**, 2017-2021.
- 82 S. Kroger, A.P.F. Turner, K. Mosbach and K. Haupt, Imprinted Polymer Based Sensor System for Herbicides using Differential-pulse Voltammetry on Screen Printed Electrodes, *Anal. Chem.*, 1999, **71**, 3698-3702.
- 83 G.H. Chen, Z.B. Guan, C.T. Chen, L.T. Fu, V. Sundaresan and F.H. Arnold, A Glucose-sensing Polymer, *Nat. Biotechnol.*, 1997, **15**, 354-357.
- 84 P. Turkewitsch, B. Wandelt, G.D. Darling and W.S. Powell, Fluorescent Functional Recognition Sites through Molecular Imprinting. A Polymer-based Fluorescent Chemosensor for Aqueous camp, *Anal. Chem.*, 1998, **70**, 2025-2030.
- 85 J. Matsui, Y. Tachibana and T. Takeuchi, Molecularly Imprinted Receptor having Metalloporphyrin-based Signalling Binding Site, *Anal. Commun.*, 1998, **35**, 225-227.
- 86 A.L. Jenkins, O.M. Uy and G.M. Murray, Polymer-based Lanthanide Luminescent Sensor for Detection of the Hydrolysis Product of the Nerve Agent Soman in Water, *Anal. Chem.*, 1999, **71**, 373-378.
- 87 S. Marx-Tibbon and I. Willner, Imprinted Polymers: A Light-regulated Medium for Transport of Amino Acids, *J. Chem. Soc., Chem. Commun.*, 1994, 1261-1262.
- 88 J.H.G Steinke, I.R. Dunkin and D.C. Sherrington, Molecularly Imprinted Anisotropic Polymer Monoliths, *Macromolecules*, 1996, **29**, 407-415.

- 89 A. Leonhardt and K. Mosbach, Enzyme-Mimicking Polymers Exhibiting Specific Substrate Binding and Catalytic Functions, *React. Polym.*, 1987, **6**, 285-290.
- 90 B. Sellergren and K.J. Shea, Enantioselective Ester Hydrolysis Catalysed by Imprinted Polymers, *Tetrahedron: Asymmetry*, 1994, **5**, 1403-1406.
- 91 B. Sellergren, R.N. Karmalkar and K.J. Shea, Enantioselective Ester Hydrolysis Catalysed by Imprinted Polymers. 2, *J. Org. Chem.*, 2000, **65**, 4009-4027.
- 92 K. Ohkubo, Y. Funakoshi, Y. Urata, S. Hirota, S. Usui and T. Sagawa, High Esterolytic Activity of a Novel Water-soluble Polymer Catalyst Imprinted by a Transition-state Analogue, *J. Chem. Soc., Chem. Commun.*, 1995, 2143-2144.
- 93 K. Ohkubo, Y. Urata, S. Hirota, Y. Funakoshi, T. Sagawa, S. Usui and K. Yoshinaga, Catalytic Activities of Novel L-Histidyl Group-Introduced Polymers Imprinted by a Transition State Analog in the Hydrolysis of Amino Acid Esters, *J. Mol. Catal. A, Chem.*, 1995, **101**, L111-L114.
- 94 R.N. Karmalkar, M.G. Kulkarni and R.A. Mashelkar, Molecularly Imprinted Hydrogels Exhibit Chymotrypsin-like Activity, *Macromolecules*, 1996, **29**, 1366-1368.
- 95 D.K. Robinson and K. Mosbach, Molecular Imprinting of a Transition State Analogue Leads to a Polymer Exhibiting Esterolytic Activity, *J. Chem. Soc., Chem. Commun.*, 1989, 969-970.
- 96 R. Müller, L.I. Andersson and K. Mosbach, Molecularly Imprinted Polymers Facilitating a β -Elimination Reaction, *Makromol. Chem., Rapid Commun.*, 1993, **14**, 637-641.
- 97 O. Brüggeman, Catalytically Active Polymers Obtained by Molecular Imprinting and Their Application in Chemical Reaction Engineering, *Biomol. Eng.*, 2001, **18**, 1-7

- 98 J.V. Beach and K.J. Shea, Designed Catalysts. A Synthetic Network Polymer That Catalyses the Dehydrofluorination of 4-Fluoro-4-(*p*-nitrophenyl)butan-2-one, *J. Am. Chem. Soc.*, 1994, **116**, 379-380.
- 99 J. Matsui, I.A. Nicholls, I. Karube and K. Mosbach, Carbon-Carbon Bond Formation Using Substrate Selective Catalytic Polymers Prepared by Molecular Imprinting: An Artificial Class II Aldolase, *J. Org. Chem.*, 1996, **61**, 5414-5417.
- 100 X. Liu and K. Mosbach, Studies Towards a Tailor-Made Catalyst for the Diels-Alder Reaction using the Technique of Molecular Imprinting, *Macromol. Rapid Commun.*, 1997, **18**, 609-615.
- 101 G. Wulff, T. Gross and R. Schönfeld, Enzyme Models Based on Molecularly Imprinted Polymers with Strong Esterase Activity, *Angew. Chem. Int. Ed. Engl.* 1997, **36**, 1962-1965.
- 102 X. Liu and K. Mosbach, Catalysis of Benzisoxazole Isomerisation by Molecularly Imprinted Polymers, *Macromol. Rapid Commun.*, 1998, **19**, 671-674.
- 103 T. Yamazaki, E. Yilmaz, K. Mosbach and K. Sode, Towards the use of Molecularly Imprinted Polymers Containing Imidazoles and Bivalent Metal Complexes for the Detection and Degradation of Organophosphotriester Pesticides, *Anal. Chim. Acta*, 2001, **435**, 209-214.
- 104 K. Polborn and K. Severin, Molecular Imprinting with an Organometallic Transition State Analogue, *Chem. Commun.*, 1999, **24**, 2481-2482.
- 105 P. Gamez, B. Dunjic, C. Pinel and M. Lemaire, "Molecular Imprinting Effect" in the Synthesis of Immobilized Rhodium Complex Catalyst (IRC cat), *Tetrahedron Lett.*, 1995, **36**, 8779-8782.
- 106 A. Katz and M.E. Davis, Molecular Imprinting of Bulk, Microporous Silica, *Nature*, 2000, **403**, 286-289.

- 107 Y. Kawanami, T. Yunoki, A. Nakamura, K. Fujii, K. Umamo, H. Yamauchi and K. Masuda, Imprinted Polymer Catalysts for the Hydrolysis of *p*-Nitrophenyl Acetate, *J. Mol. Catal. A – Chem.*, 1999, **145**, 107-110.
- 108 G. Köhler and C. Milstein, Continuous Cultures of Fused Cells Secreting Antibody of Predefined Specificity, *Nature*, 1975, **256**, 495-497.
- 109 P.G. Schultz, Catalytic Antibodies, *Angew. Chem. Int. Ed. Eng.*, 1989, **28**, 1283-1295.
- 110 B. Holmquist, Characterisation of the “Microprotease” from *Bacillus cereus*. A Zinc Neutral Endopeptidase, *Biochemistry*, 1977, **16**, 4591-4594.
- 111 L.H. Weaver, W.R. Kester and B.W. Matthews, A Chrystallographic Study of the Complex of Phosphoramidon with Thermolysin. A model for the Presumed Catalytic Transition State and for the Binding of Extended Substrates, *J. Mol. Biol.*, 1977, **114**, 119-132.
- 112 G. E. Lienhard, Enzymatic Catalysis and Transition-State Theory. Transition-State Analogs show that Catalysis is due to Tighter Binding of Transition States than of Substrates, *Science*, 1973, **180**, 149-154.
- 113 S.J. Pollack, J.W. Jacobs and P.G. Schultz, Selective Chemical Catalysis by an Antibody, *Science*, 1986, **234**, 1570-1573.
- 114 A. Tramontano, K.D. Janda and R.A. Lerner, Catalytic Antibodies, *Science*, 1986, **234**, 1566-1570.
- 115 D. Hilvert, K.W. Hill, K.D. Nared and M-T.M. Auditor, Antibody Catalysis of a Diels-Alder Reaction, *J. Am. Chem. Soc.*, 1989, **111**, 9261-9262.
- 116 A.C. Braisted and P.G. Schultz, An Antibody-Catalysed Bimolecular Diels-Alder Reaction, *J. Am. Chem. Soc.*, 1990, **112**, 7430-7431.

- 117 K. Ohkubo, Y. Urata, Y. Honda, Y. Nakashima and K. Yoshinaga, Preparation and Catalytic Property of L-Histidyl Group-introduced, Cross-Linked Poly(ethyleneimine)s Imprinted by a Transition State Analogue of an Esterolysis Reaction, *Polymer*, 1994, **35**, 5372-5374.
- 118 C. Gitler and A. Ochoa-Solano, Nonpolar Contributions to the Rate of Nucleophilic Displacements of *p*-Nitrophenyl Esters in Micelles, *J. Am. Chem. Soc.*, 1968, **90**, 5004-5009.
- 119 Y. Ihara, Stereoselective Micellar Catalysis. Reactions of Amino-acid Ester Derivatives with N-Acyl-L-histidine in Micelles, *J. Chem. Soc., Perkin Trans. 2*, 1980, 1483-1487.
- 120 Y. Ihara, M. Nango, Y. Kimura and N. Kuroki, Multifunctional Micellar Catalysis as a Model of Enzyme Action, *J. Am. Chem. Soc.*, 1983, **105**, 1252-1255.
- 121 R.J. Weinkam and E.C. Jorgensen, Rotamer Stability of Histidine and Histidine Derivatives, *J. Am. Chem. Soc.*, 1973, **95**, 6084-6090.
- 122 H. Komber, NMR Conformational Study of the Neutralisation of *meso*- and *rac*-Dimethyl- and 2,3-Diethylsuccinic Acids in Aqueous Solution, *J. Chem. Soc. Perkin Trans. 2*, 1995, 1923-1927.
- 123 Y. Okuda, M. Yoshihara and T. Maeshima, Stereoselective Differentiation in Heterogeneous Methanolysis of Amino Acid Nitrophenyl Esters by Powdered Poly(N-methacryloyl-L-histidine), *Makromol. Chem., Rapid Commun.*, 1987, **8**, 579-582.
- 124 J.M. Kokosa, R.A. Szafasz, and E. Tagupa, Practical Multigram Synthesis for 4(5)-Vinylimidazole, *J. Org. Chem.* 1983, **48**, 3605-3607.

- 125 E.J. Behrman, M.J. Biallas, H.J. Brass, J.O. Edwards, and M. Isaks, Reactions of Phosphonic Acid Esters with Nucleophiles. I. Hydrolysis, *J. Org. Chem.*, 1970, **35**, 3063-3069.
- 126 W.G. Espersen and R. Bruce Martin, Carboxyl Carbon-13-Proton Three-Bond Coupling Constants as an Indicator of Conformation, *J. Phys. Chem.*, 1976, **80**, 741-745.
- 127 J. R. Cavanaugh and B. P. Dailey, Proton Chemical Shifts for the Alkyl Derivatives, *J. Chem. Phys.*, 1961, **34**, 1099-1107.
- 128 G. Del Re, B. Pullman, and T. Yonezawa, Electronic Structure of the α -Amino Acids of Proteins, I. Charge Distributions and Proton Chemical Shifts, *Biochim. Biophys. Acta*, 1963, **75**, 153-182.
- 129 G.C. Pimentel and A.L. McClellan, *The Hydrogen Bond*, W.H. Freeman and Company, London, 1960, 287.
- 130 A.R. Leach, *Molecular Modelling: Principles and Applications*, Addison Wesley Longman Limited, Harlow, 1996, 326.
- 131 H. Neuvonen and K. Neuvonen, Investigation of the Applicability of *cis*-Urocanic Acid as a Model for the Catalytic Asp-His Dyad in the Active Site of Serine Proteases based on ^1H NMR Hydrogen Bonding Studies and Spectroscopic pK_a Measurements, *J. Chem. Soc., Perkin Trans. 2*, 1998, 1665-1670.
- 132 W.H. Cruickshank and H. Kaplan, Properties of the Histidine Residues of Indole-Chymotrypsin, *Biochem. J.*, 1975, **147**, 411-416.
- 133 A.R. Quirt, J.R. Lyerla, Jr, I.R. Peat, J.S. Cohen, W.F. Reynolds and M.H. Freedman, Carbon-13 Nuclear Magnetic Resonance Titration Shifts in Amino Acids, *J. Am. Chem. Soc.*, 1974, **96**, 570-574.

- 134 F.G. Bordwell, Equilibrium Acidities in Dimethyl Sulfoxide Solution, *Acc. Chem. Res.*, 1988, **21**, 456-463.
- 135 A.R. Fersht, D.M. Blow and J. Fastrez, Leaving Group Specificity in the Chymotrypsin-Catalysed Hydrolysis of Peptides. A Stereochemical Interpretation, *Biochemistry*, 1973, **12**, 2035-2041.
- 136 J. Svenson and I.A. Nicholls, On the Thermal and Chemical Stability of Molecularly Imprinted Polymers, *Anal. Chim. Acta*, 2001, **435**, 19-24.
- 137 S.S. Milojkovic, D. Kostoski, J.J. Comor and J.M. Nedeljkovic, Radiation Induced Synthesis of Molecularly Imprinted Polymers, *Polymer*, 1997, **38**, 2853-2855.
- 138 P. Sajonz, M. Kele, G. Zhong, B. Sellergren and G. Guiochon, Study of the Thermodynamics and Mass Transfer Kinetics of Two Enantiomers on a Polymeric Imprinted Stationary Phase, *J. Chromatogr. A*, 1998, **810**, 1-17.
- 139 R.J. Umpleby II, S.C. Baxter, M. Bode, J.K. Berch Jr., R.N. Shah and K.D. Shimizu, Application of the Freundlich Adsorption Isotherm in the Characterisation of Molecularly Imprinted Polymers, *Anal. Chim. Acta*, 2001, **435**, 35-42.
- 140 R.J. Abraham, J. Fisher and P. Loftus, *Introduction to NMR Spectroscopy*, Wiley, Chichester, 1988, 13.
- 141 S. Laschat, Pericyclic Reactions in Biological Systems-Does Nature Know About the Diels-Alder Reaction?, *Angew. Chem. Int. Ed. Engl.*, 1996, **35**, 289-291.
- 142 H.D. Ulrich, E. Mundorff, B.D. Santarsiero, E.M. Driggers, R.C. Stevens and P.G. Schultz, The Interplay Between Binding Energy and Catalysis in the Evolution of a Catalytic Antibody, *Science*, 1997, **389**, 271-275.
- 143 J. March, *Advanced Organic Chemistry, Reactions, Mechanisms and Structure*, Wiley Interscience, Chichester, 1992, 1130.